4. SITE 659[1]

Shipboard Scientific Party[2]

HOLE 659A

Date occupied: 9 March 1986, 0930 UTC

Date departed: 11 March 1986, 0530 UTC

Time on hole: 43.5 hr

Position: 18°04.63′N, 21°01.57′W

Water depth (sea level; corrected m, echo-sounding): 3069.8

Water depth (rig floor; corrected m, echo-sounding): 3080.3

Bottom felt (rig floor; m, drill pipe measurement): 3081.7

Distance between rig floor and sea level (m): 10.5

Total depth (rig floor, m): 3355.5

Penetration (m): 273.8

Number of cores (including cores with no recovery): 29

Total length of cored section (m): 273.8

Total core recovered (m): 174.5

Core recovery (%): 70.8

Oldest sediment cored:
Depth (mbsf): 273.8
Nature: blue grayish clay, barren
Age: latest Oligocene
Measured velocity (km/s): 1.730

HOLE 659B

Date occupied: 11 March 1986, 0905 UTC

Date departed: 12 March 1986, 0945 UTC

Time on hole: 24.5 hr

Position: 18°04.63′N, 21°01.57′W

Water depth (sea level; corrected m, echo-sounding): 3069.8

Water depth (rig floor; corrected m, echo-sounding): 3080.3

Bottom felt (rig floor; m, drill pipe measurement): 3083.9

Distance between rig floor and sea level (m): 10.5

Total depth (rig floor, m): 3286

Penetration (m): 202.1

Number of cores (including cores with no recovery): 22

Total length of cored section (m): 202.1

Total core recovered (m): 163.9

Core recovery (%): 81.0

Oldest sediment cored:
Depth (mbsf): 202.1
Nature: blue clay
Age: late Miocene, older than NN10
Measured velocity (km/s): 1.530

HOLE 659C

Date occupied: 12 March 1986, 1115 UTC

Date departed: 13 March 1986, 0600 UTC

Time on hole: 17.75 hr

Position: 18°04.63′N, 21°01.57′W

Water depth (sea level; corrected m, echo-sounding): 3069.8

Water depth (rig floor; corrected m, echo-sounding): 3080.3

Bottom felt (rig floor; m, drill pipe measurement): 3081.0

Distance between rig floor and sea level (m): 10.5

Total depth (rig floor, m): 3277

Penetration (m): 196.0

Number of cores (including cores with no recovery): 8

Total length of cored section (m): 76.0

Total core recovered (m): 72.48

Core recovery (%): 95.4

Oldest sediment cored:
Depth (mbsf): 196.0
Nature: brown silt-bearing nannofossil ooze
Age: NN10 (late Miocene)

Principal results: Site 659 (18°04.63′N, 21°01.57′W) is located near Site 368 on top of the smooth Cape Verde Plateau near the east Atlantic continental margin. The upper part of the seismic record at this site is finely laminated, almost transparent, with a thick series of stronger seismic layering underneath. Among three companion sites (Sites 657, 658, and 659) where we were investigating Neogene paleoceanography and paleoclimate off northwest Africa, we chose this location as a "non-upwelling," low-productivity reference site to recover a complete late Neogene pelagic section at the relatively shallow water depth of 3071.2 m. Our primary objectives were to monitor advection of cold water by the Canary Current and advection of Saharan dust; this site is located below the Saharan Air Layer near the Intertropical Convergence Zone during northern summer.

[1] Ruddiman, W., Sarnthein, M., Baldauf, J., et al., 1988. *Proc., Init. Repts. (Pt. A), ODP*, 108.

[2] William Ruddiman (Co-Chief Scientist), Lamont-Doherty Geological Observatory, Palisades, NY 10964; Michael Sarnthein (Co-Chief Scientist), Geologisch-Paläontologisches Institut, Universität Kiel, Olshausenstrasse 40, D-2300 Kiel, Federal Republic of Germany; Jack Baldauf, ODP Staff Scientist, Ocean Drilling Program, Texas A&M University, College Station, TX 77843; Jan Backman, Department of Geology, University of Stockholm, S-106 91 Stockholm, Sweden; Jan Bloemendal, Graduate School of Oceanography, University of Rhode Island, Narragansett, RI 02882-1197; William Curry, Woods Hole Oceanographic Institution, Woods Hole, MA 02543; Paul Farrimond, School of Chemistry, University of Bristol, Cantocks Close, Bristol BS8 1TS, United Kingdom; Jean Claude Faugeres, Laboratoire de Géologie-Océanographie, Université de Bordeaux I, Avenue des Facultés Talence 33405, France; Thomas Janacek, Lamont-Doherty Geological Observatory, Palisades, NY 10964; Yuzo Katsura, Institute of Geosciences, University of Tsukuba, Ibaraki 305, Japan; Hélène Manivit, Laboratoire de Stratigraphie des Continents et Océans, (UA 319) Université Paris VI, 4 Place Jussieu, 75230 Paris Cedex, France; James Mazzullo, Department of Geology, Texas A&M University, College Station, TX 77843; Jürgen Mienert, Geologisch-Paläontologisches Institut, Universität Kiel, Olshausenstrasse 40, D-2300 Kiel, Federal Republic of Germany, and Woods Hole Oceanographic Institution, Woods Hole, MA 02543; Edward Pokras, Lamont-Doherty Geological Observatory, Palisades, NY 10964; Maureen Raymo, Lamont-Doherty Geological Observatory, Palisades, NY 10964; Peter Schultheiss, Institute of Oceanographic Sciences, Brook Road, Wormley, Godalming, Surrey GU8 5UG, United Kingdom; Rüdiger Stein, Geologisch-Paläontologisches Institut, Universität Giessen, Senckenbergstrasse 3, 6300 Giessen, Federal Republic of Germany; Lisa Tauxe, Scripps Institution of Oceanography, La Jolla, CA 92093; Jean-Pierre Valet, Centre des Faibles Radioactivités, CNRS, Avenue de la Terrasse, 91190 Gif-sur-Yvette, France; Philip Weaver, Institute of Oceanographic Sciences, Brook Road, Wormley, Godalming, Surrey GU8 5UG, United Kingdom; Hisato Yasuda, Department of Geology, Kochi University, Kochi 780, Japan.

From Holes 659A, 659B, and 659C we recovered a total of 50 advanced-piston-cores (APC) and 9 extended-core-barrel (XCB) cores to total depths of 273.8, 202.1, and 196.0 meters below seafloor (mbsf), respectively. Holes 659A and 659B were cored continuously; Hole 659C was spot-cored from 0–38.0, 100.0–119.0, and 177.0–196.0 mbsf (Table 1).

The Neogene sediment section at Site 659 comprises two major lithologic units, each of which has two subunits (Fig. 1). All units and subunits have good-to-excellent biostratigraphic time control, despite substantial carbonate dissolution in the lower subunits and good magnetostratigraphy for the last 3 m.y. Continuous magnetic-susceptibility and *P*-wave-velocity curves enabled us to establish a nearly complete composite-depth (c.d.) section of the three holes. We used composite depths for defining boundaries between the lithologic units to resolve apparently disparate depth values below seafloor (bsf) in the three holes drilled at Site 659.

Unit I (0–166 mbsf c.d.) consists of upper Miocene through Holocene pelagic sediment cycles of light gray foraminifer-nannofossil ooze and whitish nannofossil ooze, with minor amounts of silt and clay. Subunit IA (0–55.3 mbsf c.d.) consists of upper Pliocene through upper Pleistocene (0–2.0 Ma) large-amplitude cycles of foraminifer-nannofossil ooze and foraminifer-bearing nannofossil ooze. Subunit IB (55.3–166 mbsf c.d.) is upper Miocene through Pliocene (2.0–7.0 Ma) silt and foraminifer-bearing nannofossil ooze and is distinguished from the overlying subunit by a uniformly higher carbonate content (Fig. 20). Subunit IIA (166–200 mbsf c.d.) is upper Miocene (7.0–11.2 Ma) cycles of light gray nannofossil ooze and yellowish brown silty nannofossil ooze. Subunit IIB (200.0–273.8 mbsf) is lower to

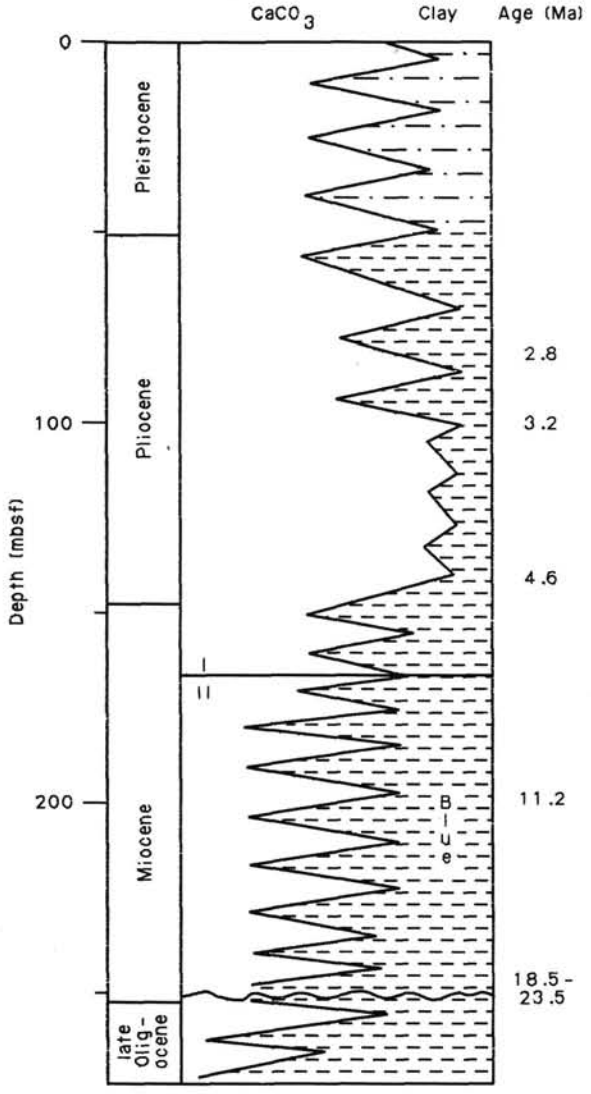

Figure 1. Lithostratigraphic and biostratigraphic summary of Site 659. Schematic $CaCO_3$ cycles show general range of $CaCO_3$ fluctuations. I and II are lithologic units.

Table 1. ODP coring summary for Site 659.

Core no.	Date (March 1986)	Time (UTC)	Depth (mbsf)	Length cored (m)	Length recovered (m)	Recovery (%)
Hole 659A						
1H	9	1702	0–7.8	7.8	7.8	100.0
2H	9	1820	7.8–17.3	9.5	6.9	72.5
3H	9	1902	17.3–26.8	9.5	9.1	95.6
4H	9	1958	26.8–36.3	9.5	5.6	58.4
5H	9	2106	36.3–45.8	9.5	8.5	89.2
6H	9	2207	45.8–55.3	9.5	0.0	0.0
7H	9	2257	55.3–64.8	9.5	9.6	101.0
8H	10	0004	64.8–74.3	9.5	8.6	90.4
9H	10	0114	74.3–83.8	9.5	8.3	87.6
10H	10	0230	83.8–93.3	9.5	8.6	90.9
11H	10	0322	93.3–102.8	9.5	7.9	82.9
12H	10	0410	102.8–112.3	9.5	1.6	16.8
13H	10	0612	112.3–121.8	9.5	9.5	99.5
14H	10	0715	121.8–131.3	9.5	8.3	87.1
15H	10	0805	131.3–140.8	9.5	7.3	76.6
16H	10	0850	140.8–150.3	9.5	8.2	86.0
17H	10	0945	150.3–159.8	9.5	7.9	83.1
18H	10	1040	159.8–169.3	9.5	0.0	0.0
19H	10	1200	169.3–178.8	9.5	0.0	0.0
20H	10	1253	178.8–188.3	9.5	9.7	102.0
21X	10	1457	188.3–197.8	9.5	4.5	47.6
22X	10	1620	197.8–207.3	9.5	6.7	70.9
23X	10	1743	207.3–216.8	9.5	8.4	88.5
24X	10	1915	216.8–226.3	9.5	2.7	28.2
25X	10	2031	226.3–235.8	9.5	7.9	82.6
26X	10	2202	235.8–245.3	9.5	0.0	0.0
27X	10	2340	245.3–254.8	9.5	9.7	102.0
28X	11	0125	254.8–264.3	9.5	0.5	5.1
29X	11	0340	264.3–273.8	9.5	1.3	13.6
Hole 659B						
1H	11	0920	0–6.6	6.6	6.6	99.2
2H	11	1015	6.6–16.1	9.5	0.0	0.0
3H	11	1110	16.1–25.6	9.5	0.0	0.0
4H	11	1222	25.6–35.1	9.5	9.5	100.0
5H	11	1835	35.1–44.6	9.5	8.6	90.1
6H	11	1557	44.6–54.1	9.5	9.4	98.4
7H	11	1710	54.1–63.6	9.5	9.5	99.9
8H	11	1814	63.6–73.1	9.5	9.6	100.0
9H	11	1900	73.1–82.6	9.5	3.8	40.2
10H	11	1948	82.6–88.1	5.5	9.5	172.0
11H	11	2053	88.1–97.6	9.5	8.7	91.2
12H	11	2142	97.6–107.1	9.5	9.1	95.2
13H	11	2234	107.1–116.6	9.5	3.9	40.5
14H	11	2338	116.6–126.1	9.5	8.6	90.0
15H	12	0025	126.1–135.6	9.5	9.6	100.0
16H	12	0105	135.6–145.1	9.5	9.6	101.0
17H	12	0215	145.1–154.6	9.5	9.3	98.1
18H	12	0306	154.6–164.1	9.5	9.7	102.0
19H	12	0354	164.1–173.6	9.5	9.1	95.6
20H	12	0505	173.6–183.1	9.5	5.6	58.6
21H	12	0610	183.1–192.6	9.5	7.7	81.0
22H	12	0725	192.6–202.1	9.5	6.8	71.6
Hole 659C						
1H	12	1209	0.0–9.5	9.5	9.5	100.0
2H	12	1311	9.5–19.0	9.5	9.3	97.9
3H	12	1359	19.0–28.5	9.5	9.6	101.0
4H	12	1450	28.5–38.0	9.5	9.3	97.6
5H	12	1800	100.0–109.5	9.5	9.1	95.5
6H	12	1920	109.5–119.0	9.5	8.8	92.9
7H	12	2302	177.0–186.5	9.5	8.1	84.9
8H	12	2350	186.5–196.0	9.5	8.8	92.9

H = hydraulic piston. X = extended-core barrel. UTC = Universal Time Coordinated.

middle Miocene (11.2–~24 Ma) cycles of the same composition as Subunit IIA but with distinct greenish/bluish colors, stronger variations of $CaCO_3$, and a volcanic ash layer at 233 mbsf.

Deposition rates varied from 30 m/m.y. during the last 4.6 m.y. to 13 m/m.y. from 4.6 to 9.0 Ma. These rates were 4 m/m.y. from 9.0 to 14.4 Ma and 6 or 8 m/m.y. from 14.4 Ma to a hiatus from ?18.5 to 23.5 Ma. Rates from the hiatus to the base of the hole (just below the Oligocene/Miocene boundary) are about 11 m/m.y.

Our major achievement at Site 659 was the recovery of a complete fossil-bearing middle to upper Miocene pelagic sediment section for calcareous biostratigraphy. This profile represents a time interval for which few continuous stratigraphic sections previously were available.

In addition, initial shipboard investigations provided important preliminary results about the paleoceanography and paleoclimate of the Pliocene-Pleistocene. Planktonic foraminifers (common *Neogloboquadrina pachyderma*) record the onset of enhanced cold-water advection by the Canary Eastern Boundary Current at about 2.8 Ma, i.e., slightly preceding the initiation of major Northern Hemisphere glaciation (2.5 Ma). Higher-amplitude carbonate cycles with a duration of 20,000–100,000 yr began somewhat earlier—around 3.2 Ma. Dust-borne silt and clay particles occur throughout most of the section but become more frequent during the last 2 m.y. This may reflect an increased dust flux, since the sedimentation rates do not decrease across this boundary. Finally, the striking change of sediment color during ongoing sedimentation at about 11 Ma and the change in sedimentation rates and $CaCO_3$ dissolution at 4.6 Ma may signify major events of deep-water oceanography. The younger event also is observed at neighboring sites (Sites 657, 660, and 661).

BACKGROUND AND SCIENTIFIC OBJECTIVES

Site 659 (target Site MAU-4; 18°04.63′N, 21°01.57′W; 3071.2 m water depth) lies on the smooth top of the Cape Verde Rise near DSDP Site 368 and away from turbidite fans (Figs. 2 and 3). The Cape Verde Rise is the result of a broad uplift related to early Neogene volcanic and tectonic activity (Lancelot, Seibold, et al., 1978). Site 659 was proposed as a "non-upwelling" reference site from among three sites (Sites 657, 658, and 659) chosen along the eastern Atlantic continental margin to obtain a detailed sedimentary record of the history of surface-water and deep-water oceanography in the eastern North Atlantic and of atmospheric circulation in low latitudes during the Neogene (for more detail see Site 657 chapter, this volume).

From the sediment record at DSDP Site 368 (Lancelot, Seibold, et al., 1978), which sampled the Neogene only with spot rotary cores, we inferred that Site 659 would provide a well-preserved continuous record of pelagic carbonate sediments deposited at medium-high rates of 20–30 m/m.y. down to the middle Miocene and at a lower rate of 10 m/m.y. down to the Oligocene/Miocene boundary. In addition to continuous standard nannofossil and foraminifer biostratigraphy, we expected to establish continuous stratigraphic control with oxygen- and carbon-stable isotopes and with siliceous fossils from both high and low latitudes in the Miocene.

Site 659 lies under the distal Canary Current and directly under the main stream of the Saharan Air Layer (see Fig. 4, Site 657 chapter, this volume). Thus, this site records the input of a major proportion of eolian sediments from North Africa (Sarnthein et al., 1982; Stein and Sarnthein, 1984). The site was expected to provide an excellent opportunity for the following studies:

1. To obtain a detailed Neogene paleoceanographic record of the Canary Eastern Boundary Current system 350 km down-

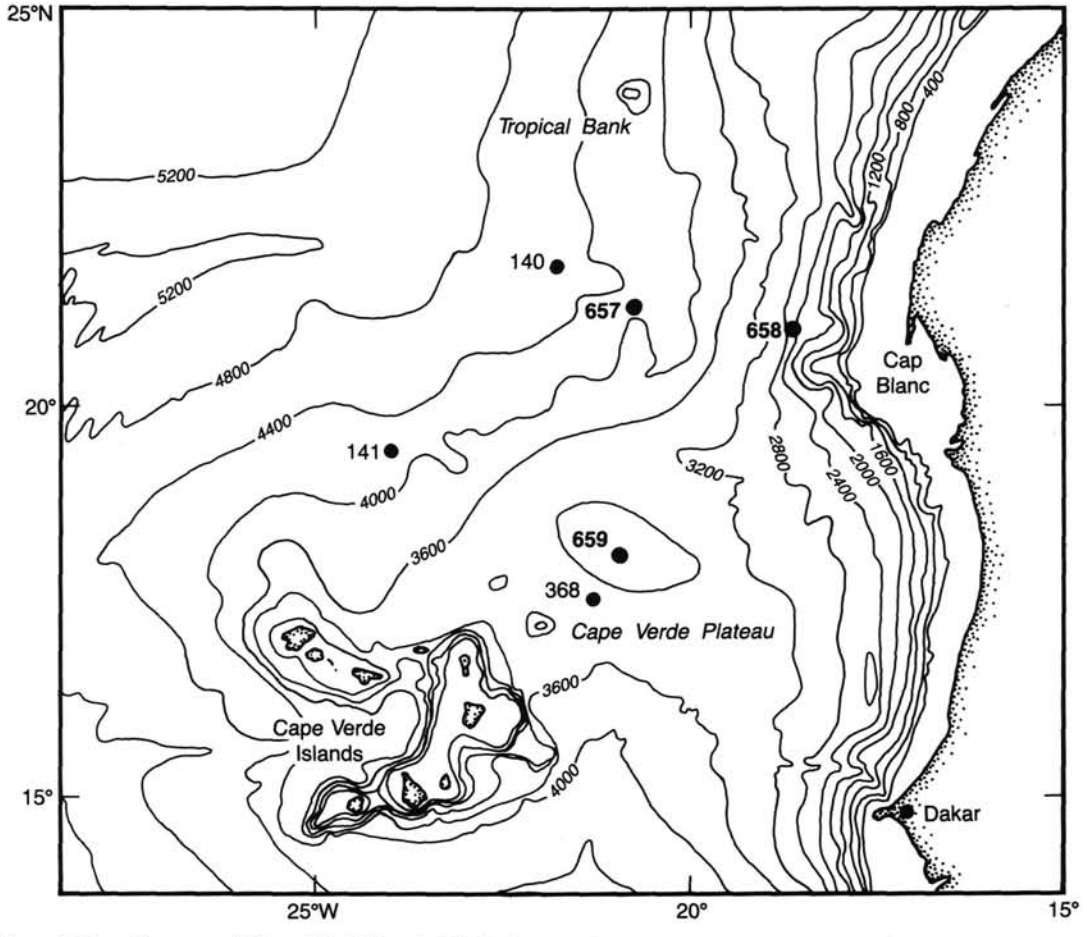

Figure 2. Location map of Sites 659, 657, and 658. Bathymetry from Uchupi (1971).

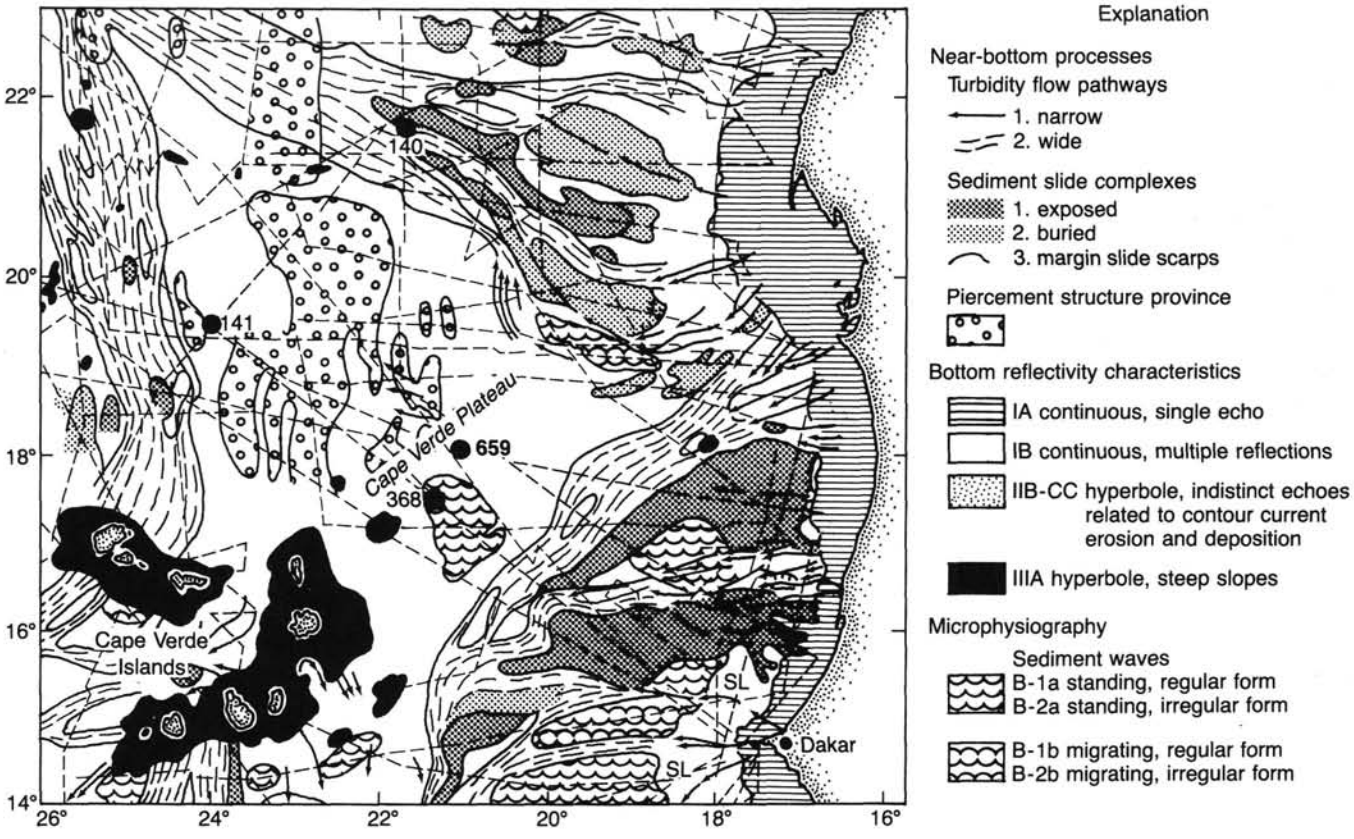

Figure 3. Microphysiography and 3.5-kHz seismic character of the Cape Verde Plateau near Site 659 (from Jacobi and Hayes, 1982).

stream of Site 657, away from influences of coastal upwelling, and to monitor the warming history toward the equator of the surface-water masses between the two sites.

2. To recover a well-preserved (late) Neogene (and particularly late Miocene) standard stratigraphic record for carbon- and oxygen-stable isotopes and for calcareous and siliceous plankton from subtropical latitudes in the northern Atlantic.

3. To study variations of carbonate dissolution and benthic-carbon isotopes for monitoring deep-water paleoceanography within the long-term uppermost range of vertical lysocline fluctuations (see Fig. 5, Site 657 chapter, this volume).

4. To determine the late Neogene history of eolian sedimentation from the Saharan Air Layer for measuring the history of midtropospheric zonal circulation as an indicator of the northward advance of the Intertropical Convergence Zone during northern summer.

Geologic Setting

Like DSDP Site 368, ODP Site 659 was selected on the basis of *Meteor* cruise seismic line 25/1971-B1 (but lying 70 km farther northeast), on a juncture of *Valdivia* cruise line 10-11, *GLOMAR Challenger* line Leg 41 parallel to the *Meteor* line, GEOTROPEX'85 records, and *Vema* cruise line 30-14 (Fig. 4). During the approach to Site 659, *JOIDES Resolution* obtained a water-gun seismic record and a 3.5-kHz echogram between Points 1 and 2 across the site position.

On the *Meteor* line, the top 0.25-s two-way traveltime of the seismic records is characterized by an almost transparent series of perfectly parallel, finely laminated, faint reflectors with a single, more prominent reflector at 0.07 s (Fig. 5). The clearly layered seismic structure of the record continues below 0.25-s traveltime but with much stronger reflectors. Lancelot, Seibold, et al. (1978) correlated the upper seismic unit with 200 m of nannofossil marls and oozes and the lower seismic unit with silty clays from the lower Miocene.

OPERATIONS

From Site 658, we steamed 15 hr southwest to Site 659 (target Site MAU-4), the survey area of *Meteor* cruise 25/1971, *Valdivia* cruise 10-II, *Vema* cruise 30-14, *Polarstern* cruise ANT IV/1b (GEOTROPEX'85), and *GLOMAR Challenger* Leg 41 on 20 March 1975. (All times are expressed as UTC, Universal Time Coordinated, formerly GMT, Greenwich Mean Time.)

On 9 March 1986, 0700–1045, we obtained an additional pre-site survey line when the *JOIDES Resolution* was run 5.5 kt from Point 1 to Point 2, and we dropped a beacon at 0845 while crossing the proposed site position (Fig. 4; Table 2). The survey deployed the 80-in.^{3} water guns, a 3.5-kHz sub-bottom profiler, and a magnetometer. After the ship turned at Point 2, the survey gear was retrieved. By 1045 the ship had stopped over the beacon, and the drill string was run into the hole. The Global Positioning System provided excellent positioning during that time.

The mud line for Hole 659A was established by drill pipe at 3071.2 m. The first APC core was brought on deck at 1702 on 9 March, and coring continued uneventfully for 20 APC cores (Table 1). We changed to XCB coring at 1253 on 10 March and continued coring in Hole 659A until Core 108-659A-29X came on deck from 273.8 mbsf at 0340 on 11 March. At this depth, core recovery had been greatly reduced and consisted of fossil-barren clay. The mud line of Hole 659A was cleared at 0530 and a 30-m offset to Hole 659B was finished at 0905.

The first core from Hole 659B came on deck at 0920 on 11 March, and coring continued successfully for 22 APC cores un-

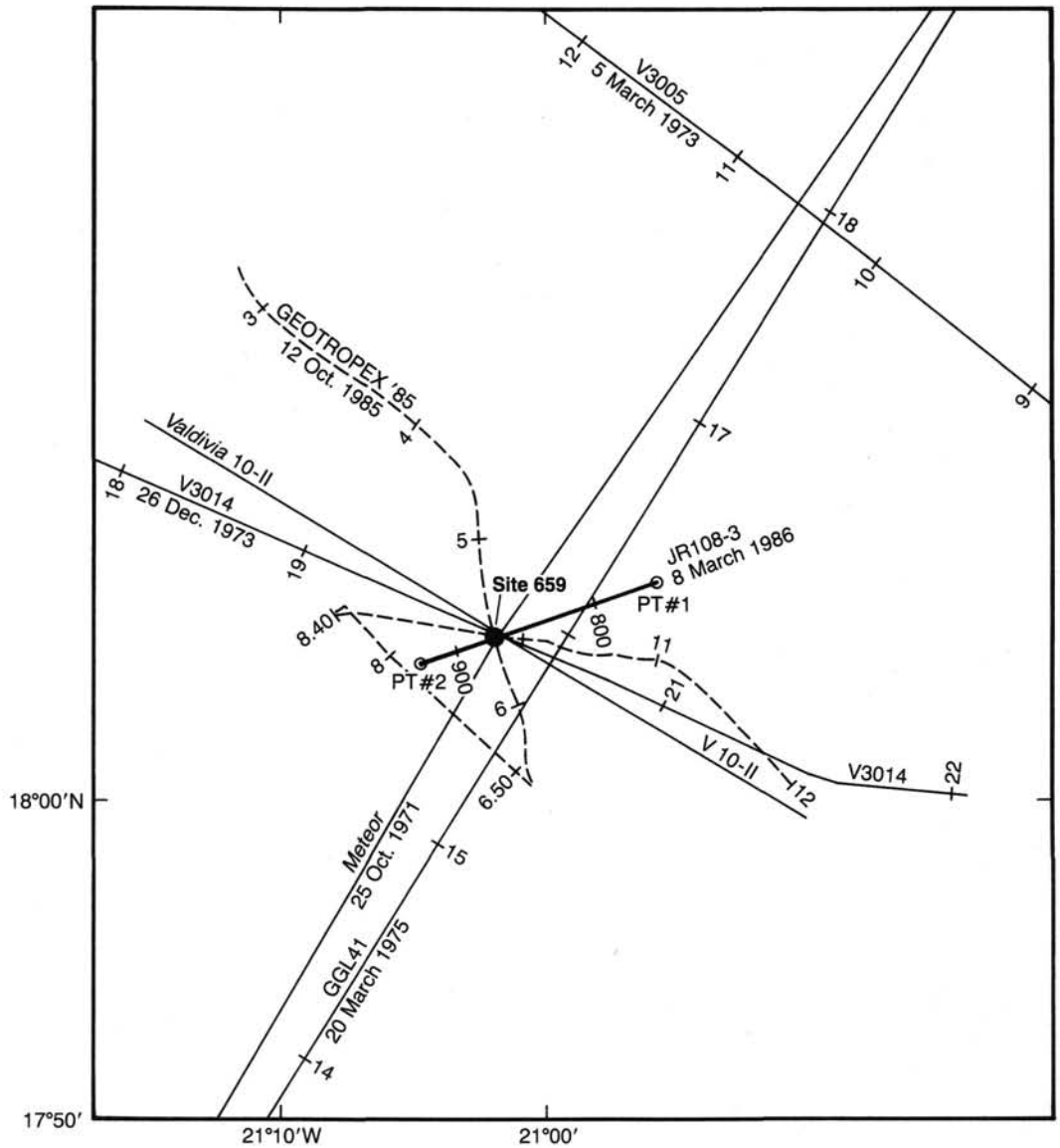

Figure 4. Seismic track lines near Site 659.

til 0725 on 12 March (Table 1). We tripped out of Hole 659B and finished a 15-m offset to Hole 659C at 1115 on 12 March. The first of eight APC cores from Hole 659C was brought on deck at 1209, and the last core (total depth, 196.0 mbsf) was on deck at 2350. We continuously cored the intervals from 0–37.5, 100–119, and 177–196 mbsf and washed down from 37.5 to 100 mbsf and from 119 to 177 mbsf, because coring in Hole 659C was intended to retrieve those intervals lost owing to contorted and incomplete core recovery in Holes 659A and 659B. We began tripping out of the hole at 0000, brought the drill string on deck, and headed south to Site 660 (target Site SLR-1) at 0600 on 13 March 1986.

After the coring device was fine-tuned, APC core recovery steadily increased from 70.8% in Hole 659A to 81% in Hole 659B and to 95.4% in Hole 659C. Core contortion was minor and usually restricted to the uppermost 20–50 cm of a core. Continuous downcore sound-velocity and susceptibility logs provided an excellent tool for between-hole correlations to verify coring of a complete record at this multihole site. A core-orientation tool was applied to Cores 108-659A-3H through -659A-5H, -659A-8H, and -659A-14H, but it did not work.

LITHOSTRATIGRAPHY AND SEDIMENTOLOGY

Introduction

Two major lithological units are recognized at Site 659; both are characterized by cyclic changes in sediment composition and color (Figs. 6 and 7). Unit I consists of interbedded nannofossil ooze and foraminifer-nannofossil ooze (Subunit IA) or foraminifer-bearing nannofossil ooze (Subunit IB), with minor amounts of silt and clay. The measured carbonate content varies from 40% to 90%. Unit II consists of interbedded nannofossil ooze and silt-bearing to silty nannofossil ooze. Carbonate concentration varies from about 20% to 70%. Unit II is subdivided into two subunits on the basis of a distinct color change from yellowish brown (Subunit IIA) to blue green (Subunit IIB).

Unit I

	Hole 659A	*Hole 659B*	*Hole 659C*
Cores:	1H to 17H	1H to 18H	1H to 6H
Depth (mbsf):	0 to 159.8	0 to 164.1	0 to 119.0
Age:	early Pliocene to Holocene	early Pliocene to Holocene	early Pliocene to Holocene

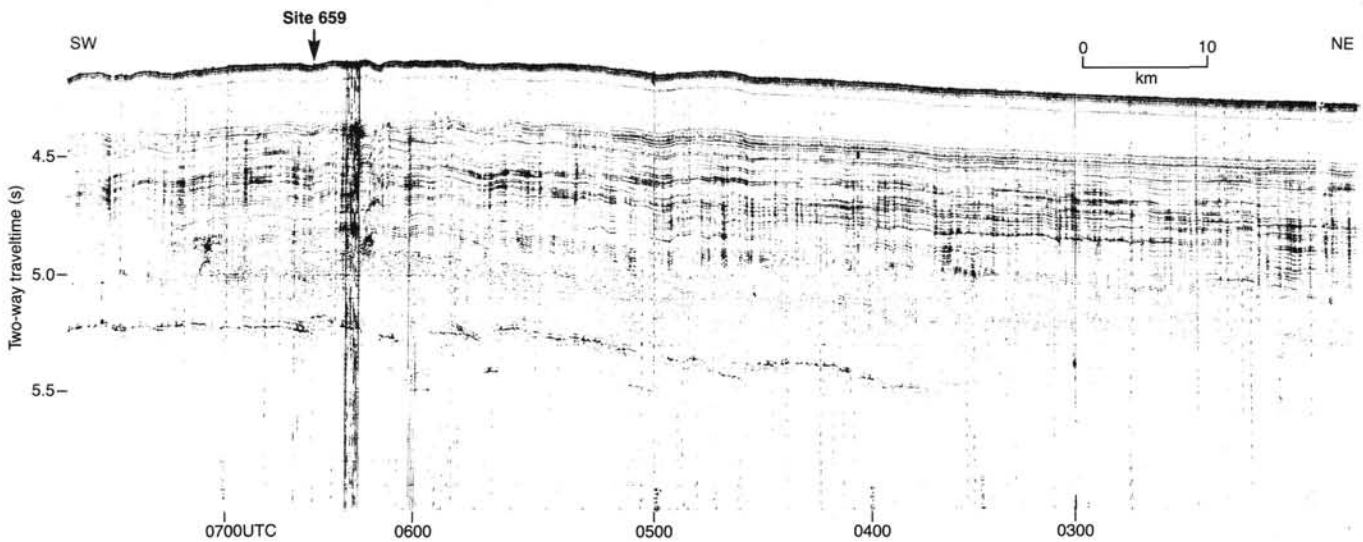

Figure 5. *Meteor* cruise 25/1971 seismic-reflection record near Site 659 across the Cape Verde Rise.

Table 2. Positions of site-survey turning points.

Point no.	Location
1	18°6.35′N; 20°56.3′W
2	18°3.70′N; 21°4.25′W

Unit I is subdivided into two subunits defined by the varying abundance of foraminifers (Figs. 6 and 7):

	Hole 659A	*Hole 659B*	*Hole 659C*
Subunit IA			
Cores:	1H to 6H	1H to 6H	1H to 4H
Depth (mbsf):	0 to 55.3	0 to 54.1	0 to 38.0
Subunit IB			
Cores:	7H to 17H	7H to 18H	5H and 6H
Depth (mbsf):	55.3 to 159.8	54.1 to 164.1	100.0 to 119.0

Subunit IA is characterized by alternating beds of white to light gray (in Core 108-659C-1H, pale brown) nannofossil ooze to foraminifer-bearing nannofossil ooze, and light greenish gray to light olive (in Core 108-659C-1H, light brownish gray) foraminifer-nannofossil ooze. The thicknesses of color cycles range between 40 and 110 cm. Both sediment types contain minor amounts of silt and clay. The measured carbonate values vary from 41% to 83%. Thin (1- to 3-mm-thick) pale green laminae of muddy foraminifer-nannofossil ooze with traces of volcanic glass are rare to common. Pyrite(?) is scattered throughout the entire subunit. In general, the sediment is slightly to moderately bioturbated (e.g., well-preserved large *Zoophycus* in 108-659A-2H-4, 0–42 cm).

Subunit IB is characterized by interbedded white to light gray nannofossil ooze and light greenish gray foraminifer-bearing and/or silt-bearing nannofossil ooze. The thicknesses of the color cycles range between 25 and 140 cm. The measured carbonate content varies from 36% to 90%, with higher values concentrated in the lower half of the subunit (Fig. 6). As in Subunit IA, thin greenish laminae of muddy foraminifer-nannofossil ooze with traces of volcanic glass and pyrite(?) also occur in Subunit IB. Thin graded beds of quartzose silty sand to muddy nannofossil ooze are recorded in Hole 659A, Sections 108-659A-10H-2 and -659A-14H-3, and in Hole 659B, Sections 108-659B-7H-4, -659B-8H-2, -659B-10H-5, -659B-12H-4, -659B-14H-5, and -659B-15H-7. In general, the sediments are slightly to moderately bioturbated.

Unit II

	Hole 659A	*Hole 659B*	*Hole 659C*
Cores:	[a]20H to 29X	19H to 22H	7H and 8H
Depth (mbsf):	178.8 to 273.8	164.1 to 202.1	177.0 to 196.0
Age:	Miocene	Miocene	Miocene

[a] No sediment was recovered from Cores 108-659A-18H and -659A-19H (159.8 to 178.8 mbsf).

Unit II is separated from Unit I by its higher content of siliciclastic components and its lower carbonate content (Fig. 6). On the basis of a distinct color change, Unit II is subdivided into two subunits:

	Hole 659A	*Hole 659B*	*Hole 659C*
Subunit IIA			
Cores:	20H to 22X-4, 96 cm	19H to 22X-5, 5 cm	7H and 8H
Depth (mbsf):	178.8 to 203.3	164.1 to 198.7	177.0 to 196.0
Subunit IIB			
Cores:	22X-4, 96 cm, to 29X	22H-5, 5 cm, to 22,CC	—
Depth (mbsf):	203.3 to 273.8	198.7 to 202.1	—

Subunit IIA is composed of interbedded light greenish to light gray nannofossil ooze to yellowish brown silt-bearing to silty nannofossil ooze. The thicknesses of the color cycles range between 20 and 60 cm. The measured carbonate value varies from 70% (light gray sediments) to about 20% (brownish sediments). (Note: The latter sediment type is classified as ooze in smear-slide description, but it is apparent that the clay-sized siliciclastic components have been distinctly underestimated.) Sediments of Subunit IIA are slightly to moderately bioturbated.

The sediment composition of Subunit IIB is similar to that of Subunit IIA, with interbedded nannofossil ooze and silt-bearing to silty nannofossil ooze dominating. The thicknesses of the color cycles range between 15 and 90 cm. The measured carbonate value varies from about 10% to 70%. However, Subunit IIB distinctly differs in color, with yellowish/brownish hues

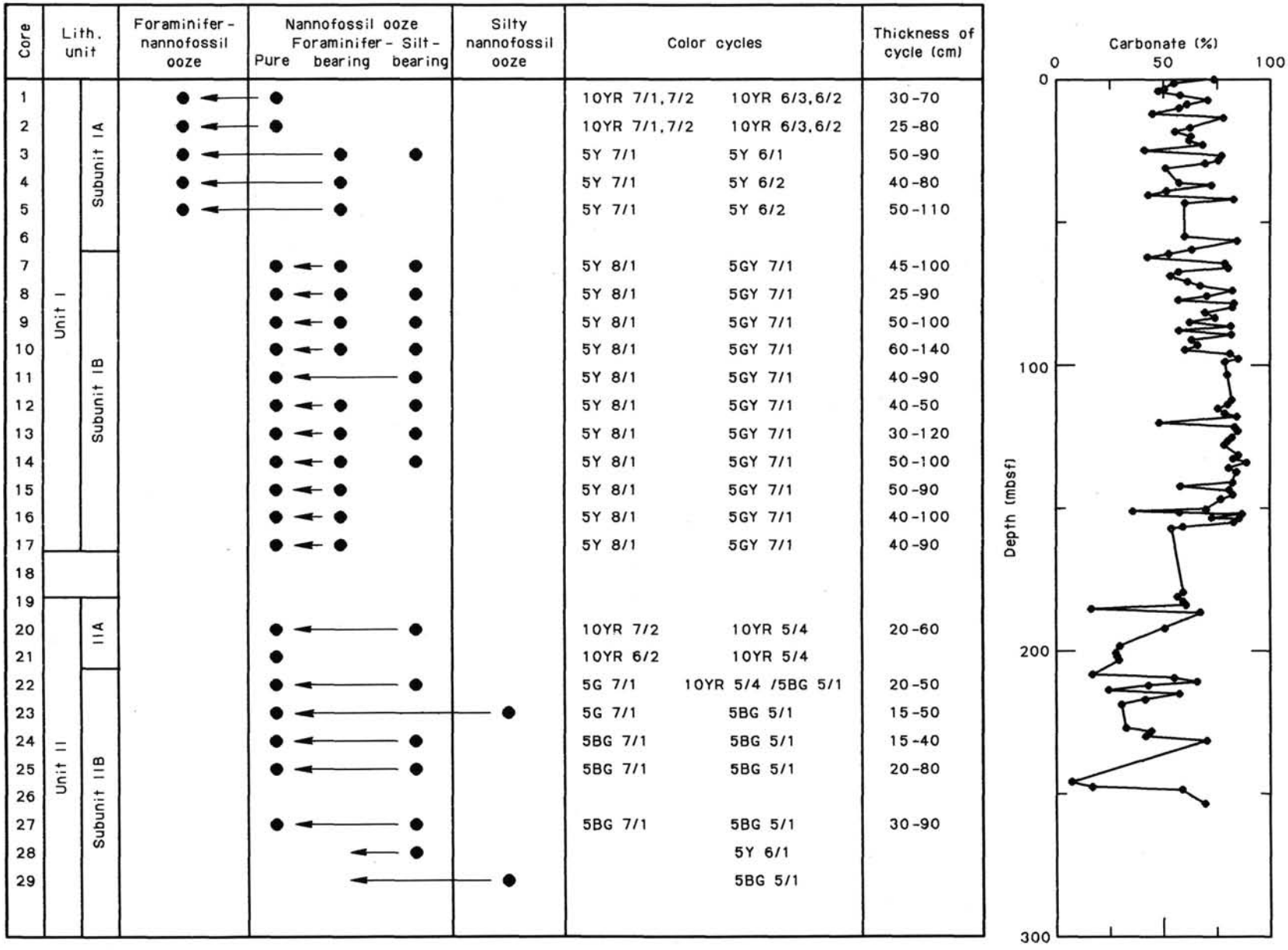

Figure 6. Dominant facies (based on smear-slide estimates) and colors of alternating sediment sequences, thicknesses of cycles, and carbonate contents at Site 659A. Black circles mark cores with beds of quartzose silty sand grading to muddy nannofossil ooze.

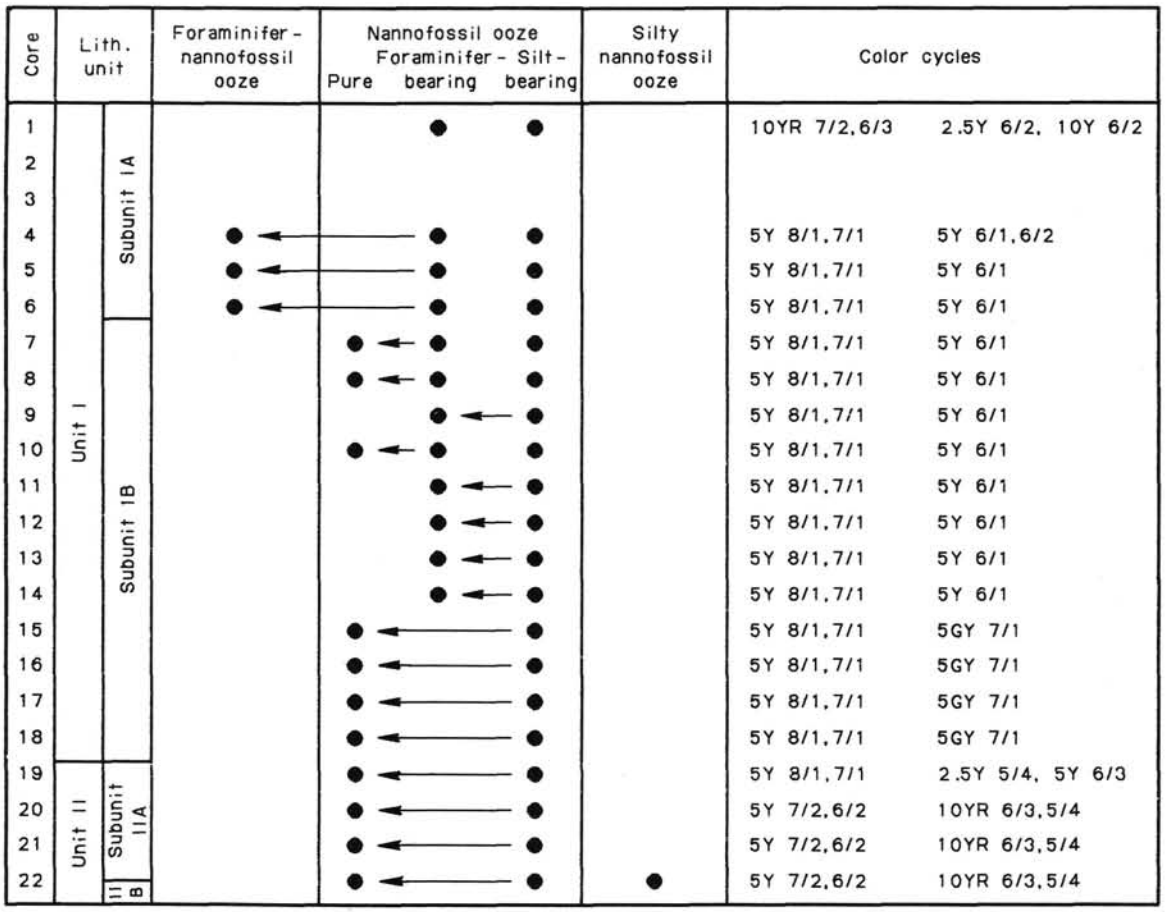

Figure 7. Dominant facies (based on smear-slide estimates) and colors of alternating sediment sequences. Black circles mark cores with grading beds of quartzose silty sand grading to muddy nannofossil ooze.

in Subunit IIA and greenish/bluish ones in Subunit IIB. A distinct volcanic ash layer occurs at Site 659A, Core 108-659A-25X-5, 70 cm (i.e., at 233 mbsf).

Depositional Environment

An almost 275-m-thick sequence of pelagic and hemipelagic sediments was recovered at Site 659. The most obvious characteristic of these sediments is their cyclicity: light gray to white carbonate-rich sediments alternate with greenish gray, brownish, or greenish blue carbonate-poor sediments. The thicknesses of these cycles are greater in Unit I (30–140 cm) than in Unit II (15–90 cm) (Fig. 6). However, considering that the sedimentation rates are distinctly higher in Unit I than in Unit II (i.e., about 30 m/m.y. and 10 m/m.y., respectively; see "Sediment-Accumulation Rates" section, this chapter), the periods of these cycles may be similar in both units. These short-term fluctuations in sediment composition represent time intervals of about 10,000 to 90,000 yr, which are on the order of the Milankovitch-type climatic cycles. In Unit I (i.e., during the last 5 m.y.), these cycles may have been caused by both an increased (eolian) supply of siliclastic matter, which dilutes the carbonate pelagics, and by $CaCO_3$ dissolution. In Unit II (i.e., during the Miocene), the carbonate-poor intervals may have resulted mainly from increased carbonate dissolution, a conclusion supported by the distinctly decreased sedimentation rates (see "Sediment-Accumulation Rates" section, this chapter) and by the observed dissolution of planktonic foraminifers (see "Biostratigraphy" section, this chapter).

Although the color of sediments in Subunit IIA (brownish/yellowish) and Subunit IIB (greenish/bluish) is distinctly different, no origin for this difference could be determined in smear-slide counts and carbonate measurements. Changes in redox conditions may have caused the different colors, but further detailed sedimentological and geochemical analyses are required.

The volcanic ash layer recorded at Site 659A, Core 108-659A-25X-5, is of early Miocene age. At the same time interval, ash layers also occur in the sediments of the nearby DSDP Site 368 and are interpreted as resulting from eruptive volcanic activity on the Cape Verde Islands that reached maximum levels during the early Miocene (Lancelot, Seibold, et al., 1978).

BIOSTRATIGRAPHY

Introduction

Three holes were cored at Site 659, located in a water depth of 3071.2 m. Hole 659A was cored to a depth of 273.8 mbsf, Hole 659B to a depth of 202.1 mbsf, and Hole 659C to a depth of 196.0 mbsf. Whereas Holes 659A and 659B were cored continuously, only specific stratigraphic intervals (0–38.0, 100.0–119.0, and 177.0–196.0 mbsf) were cored in Hole 659C. The sediments range in age from latest Oligocene through Holocene. Figures 8 through 10 show age and zonal assignments of the cores recovered at Site 659.

Calcareous nannofossils and planktonic foraminifers are abundant and well-preserved throughout most of the Pliocene and Pleistocene. The abundance and preservation of Miocene placo-

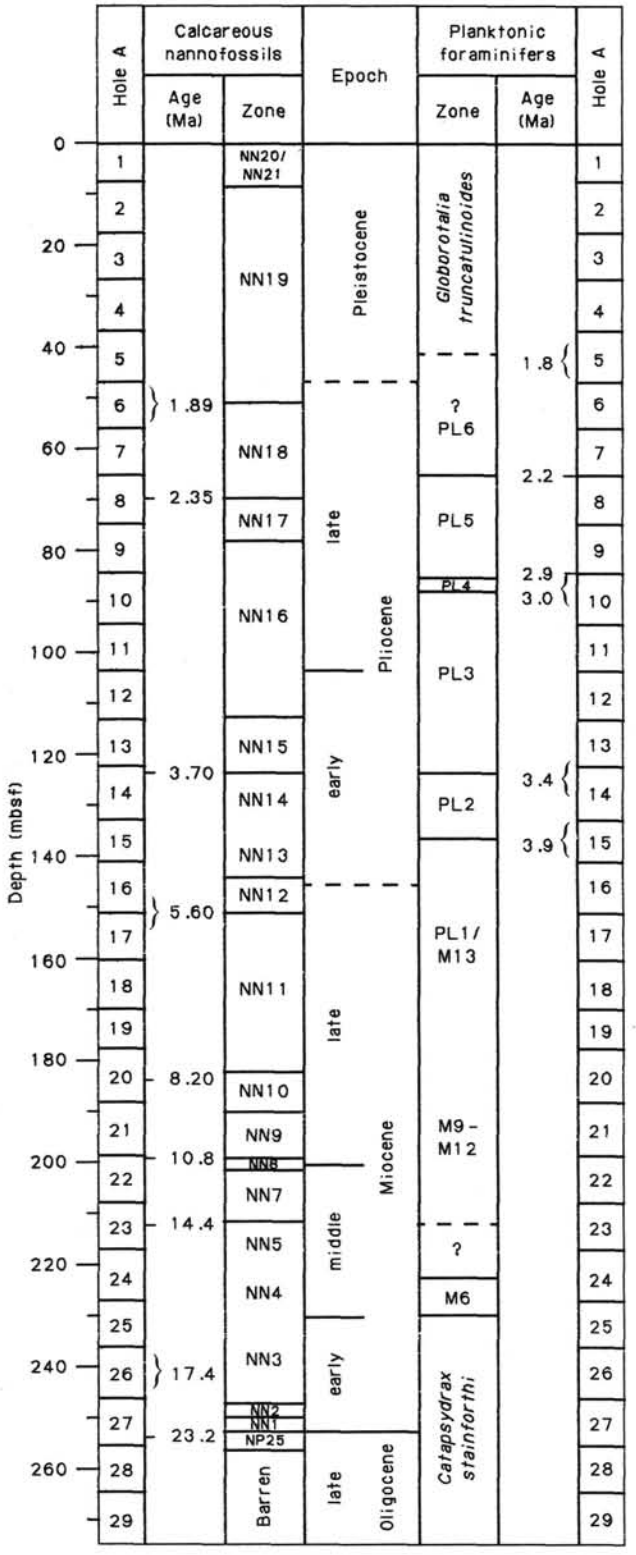

Figure 8. Zonal assignments for cores recovered from Hole 659A.

liths and planktonic foraminifers vary. The lower Miocene assemblages exhibit greater dissolution and calcite overgrowths on the discoasters.

The diatom flora at Site 659 is extremely sparse. Neritic and freshwater diatom species outnumber pelagic marine species.

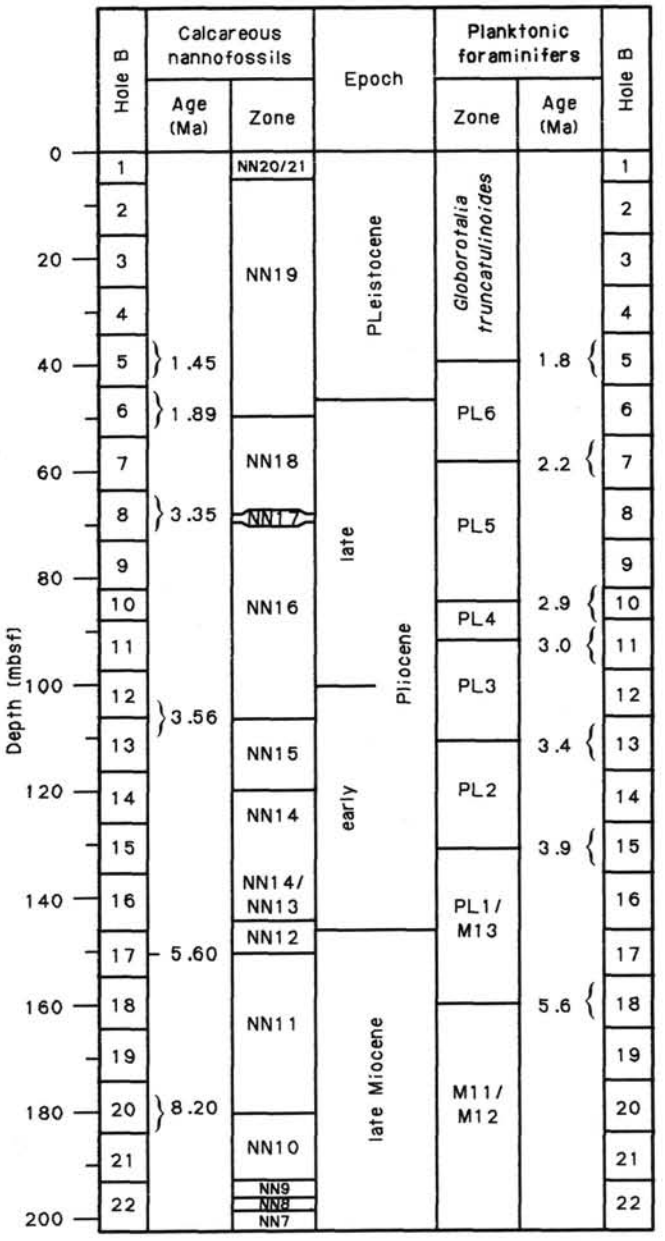

Figure 9. Zonal assignments for cores recovered from Hole 659B.

Preservation in these samples was invariably poor, and no stratigraphically useful species were observed. Benthic foraminifers are rare to common and well preserved in the upper Pliocene and Pleistocene. A few specimens having poor preservation occur in the Miocene and lower Pliocene.

Calcareous Nannofossils

Calcareous nannofossils are abundant and well-preserved throughout most of the Pliocene and Pleistocene. In general, the preservational states of Miocene placolith assemblages vary as a function of lithology: the bluish clays of the lower to middle Miocene contain severely dissolved placoliths and the white nannofossil oozes of the uppermost Miocene much less dissolved assemblages. Discoasters are generally well preserved, with the exception of overgrowths on the lower Miocene *Discoaster deflandrei* assemblages.

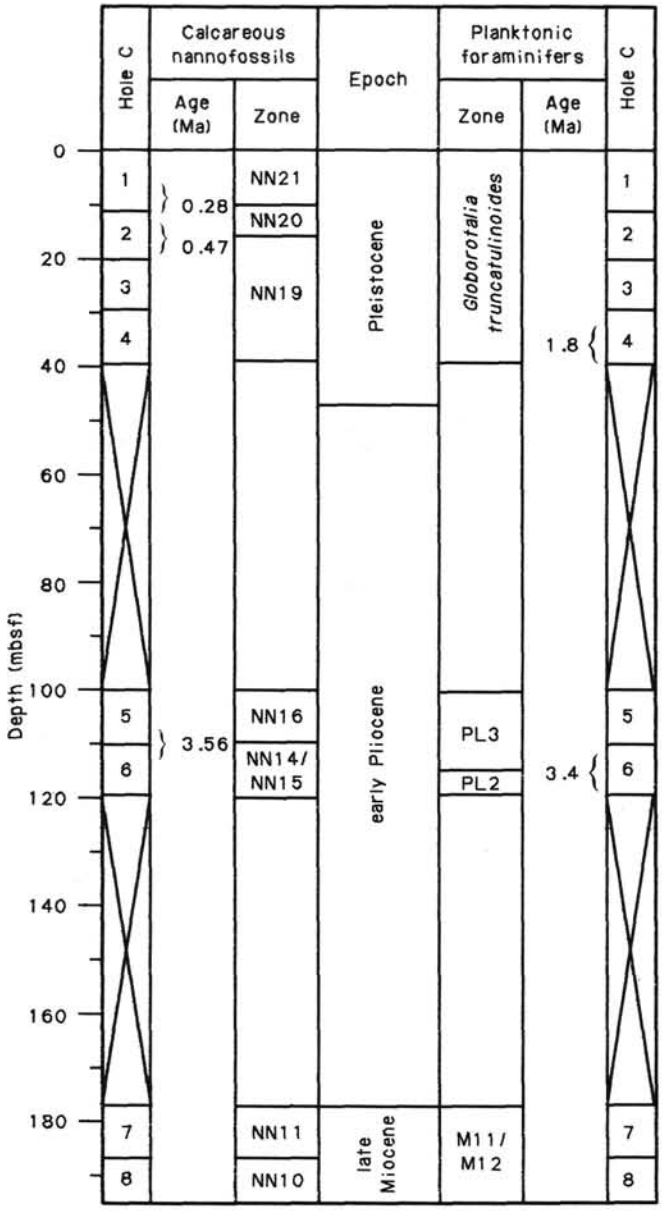

Figure 10. Zonal assignments for cores recovered from Hole 659C.

Pleistocene

The Pleistocene assemblages of Site 659 are virtually identical to those at Sites 657 and 658, with abundant gephyrocapsids and common to few *Coccolithus pelagicus, Calcidiscus leptoporus*, and *Helicosphaera carteri*. The first occurrence (FO) of *Emiliania huxleyi* and last occurrences of *Pseudoemiliania lacunosa* and *Helicosphaera sellii* were investigated in detail in Hole 659C. *Emiliania huxleyi* is more abundant than gephyrocapsids in Section 108-659C-1H-1 and has its FO in Section 108-659C-1H-6. Section 108-659C-2H-5 contains the last occurrence (LO) of *P. lacunosa*, whereas the LO of *H. sellii* was observed in Section 108-659C-4H-5. *Calcidiscus macintyrei* disappears within Core 108-659B-5H. Samples 108-659A-8H, CC and -659A-7H-1, 5 cm, indicate that both *C. macintyrei* and *Discoaster brouweri* disappear within Core 108-659A-6H, which had no recovery.

Pliocene

The Pliocene assemblages are generally more diverse than those of the Pleistocene. The dominant group is the small reticulofenestrids. Toward the basal Pliocene and the uppermost Miocene, the very small (about 1–2 μm) species *Reticulofenestra minuta* shows distinct blooms and may outnumber the sum of all other taxa by as much as one order of magnitude.

The high abundance interval of *Discoaster triradiatus*, relative to *D. brouweri*, was observed between Samples 108-659A-7H-1, 5 cm, and -659A-7H-4, 5 cm, but not in Section 108-659A-7H-5. In Hole 659B, this acme interval occurred between Sections 108-659B-6H-6 and -659B-7H-3. *Discoaster pentaradiatus* provided a more easily recognized disappearance than that of *Discoaster surculus*. A consistent occurrence of *D. pentaradiatus* was observed in Sample 108-659A-8H-5, 5 cm, but not one section higher. In Hole 659B, *D. pentaradiatus* has its LO in Section 108-659B-8H-3, and *Discoaster tamalis* disappears in Section 108-659B-9H-3. The latter event occurred at the boundary between Cores 108-659A-9H and -659A-10H in Hole 659A.

Sphenoliths survived slightly longer than *Reticulofenestra pseudoumbilica*. Investigation of Core 108-659C-5H suggests that sphenoliths (*Sphenolithus abies* and *Sphenolithus neoabies*) continued to exist 1.6–3.9 m above the range of *R. pseudoumbilica*, which at the established sedimentation rate of 30 m/m.y. corresponds to a time interval of about 0.05 to 0.13 m.y. The disappearance of *R. pseudoumbilica* occurred in Section 108-659B-12H-5 of Hole 659B and at the Core 108-659A-12H-13H boundary in Hole 659A.

Amaurolithids were not common at Site 659. Because they are even less numerous toward the end of their range, the upper limit of the range of nonbirefringent ceratoliths (*Amaurolithus tricorniculatus, Amaurolithus delicatus*, and *Amaurolithus primus*) has restricted biostratigraphic value. Consequently, recognition of the boundary between Zones NN14 and NN15 often involves a high degree of uncertainty. In Hole 659A, the disappearence of amaurolithids tentatively is placed in Section 108-659A-14H-2. In Hole 659B, members of this genus were observed in Sample 108-659B-14H, CC but not in Sample 108-659B-13H, CC.

Discoaster asymmetricus is common between the last occurrences of *R. pseudoumbilica* and *D. tamalis*, but seems consistently to be rare below the LO of *R. pseudoumbilica*. This implies that the boundary between Zones NN14 and NN13 is based on a vague species event, namely the FO of *D. asymmetricus*. No reliable observation of *D. asymmetricus* was made below the upper range of the amaurolithids.

Low abundances and severe diagenetic overgrowth of calcite on specimens of *Ceratolithus rugosus*, whose FO defines base Zone NN13, cause problems with precise recognition of the NN12/NN13 boundary. This species event tentatively is identified in the upper part of Core 108-659A-16H. The extinction of *Triquetrorhabdulus rugosus*, which occurs between Samples 108-659A-16H-5, 80 cm, and -659A-16H-4, 80 cm, may prove to represent a good auxiliary marker for subdivision of the basal Pliocene.

Miocene

A complete middle to upper Miocene sequence was cored at Site 659, although its sedimentation rates are lower than those in the Pliocene-Pleistocene sequence. Most of the lower Miocene is represented by a hiatus spanning the interval from upper NN3 to basal NN2. The Oligocene/Miocene boundary was recognized in the lowermost part of the nannofossil-bearing sediment of Hole 659A. Hole 659B was cored to approximately the middle to upper Miocene boundary. Two cores of Hole 659C represent the upper Miocene. Discoasters are abundant throughout the Miocene sediments. Placolith assemblages are dominated by reticulofenestrids in the middle to upper Miocene and by *Cyclicargolithus floridanus* in the lower Miocene.

The extinction of *Discoaster quinqueramus* was determined to within 65 cm in Hole 659B and in the lower half of Section

108-659B-17H-3. The FO of *Amaurolithus* spp. was observed in Section 108-659B-20H-1. *Amaurolithus amplificus* and *A. delicatus* are the most common amaurolithid species in Core 108-659B-19H, although they must be considered rare to few in relation to the total assemblage. The LO of *A. amplificus* was observed in Section 108-659B-19H-2. In Hole 659A, *D. quinqueramus* disappears at about the boundary between Cores 108-659A-16H and -659A-17H.

Numerous intermediate forms between *D. quinqueramus* and *Discoaster berggrenii* were observed in the lower part of the range of the former species, and these two morphotypes are not separated here. Nevertheless, they appear in Section 108-659A-20H-3, and between the base of Core 108-659B-20H (5.6-m recovery) and Sample 108-659B-21H-1, 130 cm. Core 108-659A-21X was characterized by moderate recovery (4.5 m) and severe disturbance. Core 108-659B-21H contains a typical NN10 discoaster assemblage (e.g., *Discoaster bellus, D. loeblichii*, and *D. neohamatus*). The LO of *Discoaster bollii* was observed in Section 108-659B-21H-5. Neither *Catinaster* spp. nor *Discoaster hamatus* were observed in Core 108-659B-21H.

Sample 108-659B-22H-1, 30 cm, represents Zone NN9, and contains *D. hamatus* and *Catinaster calyculus*, but no *Catinaster coalitus*. This last species was present together with *D. hamatus* in Sample 108-659B-22H-2, 132 cm, but without *C. calyculus*. *Discoaster hamatus* was not found in Sample 108-659B-22H-3, 132 cm, which thus represents a biostratigraphic position shortly below the base of Zone NN9. *Catinaster coalitus* has its FO (base of Zone NN8) between Samples 108-659B-22H-5, 6 cm, and -659B-22H-4, 120 cm. Core 108-659B-22H was the final core of Hole 659B. Sample 108-659B-22H, CC showed a poorly preserved assemblage without *Coccolithus miopelagicus* and *C. floridanus*. The few specimens of *Reticulofenestra umbilicus* indicate slight reworking from upper Eocene or lower Oligocene sources.

An undisturbed sample taken from Section 108-659A-21X-3 of Hole 659A contained *C. calyculus, C. coalitus*, and *D. hamatus* (Zone NN9). Of these three species, only *C. coalitus* was present in Sample 108-659A-22X-1, 136 cm, which thus represents Zone NN8. *Catinaster* spp. were not observed in Sample 108-659A-22X-2, 146 cm, or below this level. Rare to few *Discoaster kugleri* were observed throughout Core 108-659A-22X, indicating Zone NN7, whereas *C. floridanus* was absent. The large species *Coccolithus miopelagicus* disappears between Samples 108-659A-22X-3, 75 cm, and -659A-22X-4, 145 cm. Investigation of Sample 108-659A-22X-3, 146 cm, did not yield conclusively a precise LO of *C. miopelagicus*.

Cyclicargolithus floridanus shows a distinct LO between Samples 108-659A-23X-3, 140 cm, and -659A-23X-4, 114 cm, and the LO of *Sphenolithus heteromorphus* was observed between the latter sample and Sample 108-659A-23X-5, 110 cm. *Sphenolithus heteromorphus* was abundant throughout Cores 108-659A-24X and -659A-25X. Rare *Helicosphaera ampliaperta* was observed in Sample 108-659A-25X, CC. This species is rare in open-ocean environments, and its absence in Core 108-659A-24X and most of Core 108-659A-25X does not necessarily imply that most of Zone NN4 is missing. Sample 108-659A-25X, CC contains the last *Sphenolithus moriformis* s.s.

Core 108-659A-26X had no recovery. However, investigation of a small piece of sediment attached to the bottom of the core liner showed few *Sphenolithus belemnos* together with abundant *Discoaster deflandrei* and *C. floridanus*, common *C. pelagicus*, few *Coronocyclus nitescens* and *S. moriformis*, and rare *Triquetrorhabdulus milowii*. Thus, this sample indicates Zone NN3. *Discoaster druggii* was a rare assemblage component in Sample 108-659A-27X-1, 140 cm, but was not seen below that level, which probably indicates proximity to the boundary between Zones NN1 and NN2.

Dictyococcites bisectus and *Triquetrorhabdulus carinatus* were observed in Samples 108-659A-27X, CC and -659A-27X-6, 138 cm, suggesting uppermost Oligocene. The absence of *D. bisectus* in Sample 108-659A-27X-5, 80 cm, and above this sample suggests that the Oligocene/Miocene boundary can be located in the lower part of Core 108-659A-27X.

Planktonic Foraminifers

Planktonic foraminifers were abundant and well preserved throughout the Pliocene and Pleistocene. Through the upper Miocene, they were less common and less well preserved and in the lower to middle Miocene, preservation was variable, with some samples having common, moderately well-preserved specimens while others were barren. The fauna is slightly more diverse than at Sites 657 and 658, although *Neogloboquadrina pachyderma*, a relatively cool-water species, is still common. Warm-water influences are indicated by *Globigerinoides ruber*, *Globigerina decoraperta*, and *Globigerinoides obliquus*.

The *Globorotalia truncatulinoides* Zone was present in Cores 108-659A-1H through -659A-4H, -659B-1H through -659B-4H, and -659C-1H through -659C-4H. Sample 108-659A-5H, CC contained neither *G. truncatulinoides* nor *G. obliquus* and could not be dated. *Globorotalia bulloides, G. inflata, G. ruber*, and *N. pachyderma* (dextral) are all common in this zone and indicate cool, subtropical temperatures, which suggests the influence of the cool Canary Current.

The late Pliocene (Zones PL3 to PL6) contains common *G. ruber, Globorotalia puncticulata, G. decoraperta, G. obliquus*, and *Neogloboquadrina dutertrei*, with *N. pachyderma* common only in Zones PL5 and PL6. The base of Zone PL6 lies between Samples 108-659A-7H, CC and -659A-8H-1, 86 cm, and between Samples 108-659B-6H, CC and -659B-7H, CC. The FO of *G. inflata*, dated at 2.1 Ma (Weaver and Clement, 1986), is in Core 659B-6H, but could not be determined in Hole 659A because of no recovery from Core 108-659A-6H. The base of Zone PL5, determined by the extinction of *Dentogloboquadrina altispira*, is found between Samples 108-659A-9H, CC and -659A-10H-1, 101 cm, in Hole 659A, and between Samples 108-659B-9H, CC and -659B-10H, CC in Hole 659B. Zone PL4 is a short zone with its base between Samples 108-659A-10H-3, 70 cm, and -659A-10-5, 70 cm, and between Samples 108-659B-10, CC and -659B-11H, CC. The base of Zone PL3 is inferred from the LO of *Globorotalia margaritae* and lies between 108-659A-13H, CC and -659A-14H-3, 74 cm, in Hole 659A, and between 108-659B-12H, CC and -659B-13H, CC in Hole 659B.

The early Pliocene contains increased numbers of dextral and sinistral *Neogloboquadrina* spp., including *N. pachyderma, N. humerosa, N. acostaensis*, and *N. continuosa*, together with common *Globigerina decoraperta*. The base of Zone PL2 is defined from the LO of *G. nepenthes* and lies between 108-659A-14H, CC and -659A-15H, CC in Hole 659A, and between 108-659B-14H, CC and -659B-15H, CC in Hole 659B; however, this species is very rare in Zone PL1 at this site. The base of the Pliocene was defined by Berggren et al. (1985) at the LO of *Globoquadrina dehiscens*. However, this species is absent in the uppermost Miocene at this site; thus, Pliocene Zone PL1 and Miocene Zone M13 cannot be distinguished.

The base of Zone M13 is defined by the FO of *G. margaritae*, which lies between 108-659A-17H, CC and -659A-20H-3, 104 cm, in Hole 659A and between 108-659B-18H, CC and -659B-17H, CC in Hole 659B. Preservation also changes at this level, with upper Miocene samples containing fewer specimens and poorer preservation. The fauna of this interval contains common *Sphaeroidinellopsis seminulina, G. nepenthes*, and *Globoquadrina venezuelana*. The absence of *Globorotalia conomiozea* at this site precludes a distinction between Zones M11 and M12; however, Cores 108-659B-18H through -659B-21H contain

N. acostaensis, which places them above the base of Zone M11. Cores 108-659A-20H and -659A-21H and Core 108-659B-22H contain *G. nepenthes* but no *N. acostaensis* and, thus, belong to Zones M9 or M10. Sample 108-659A-22H, CC contains *G. nepenthes* and *Sphaeroidinellopsis multioba*, and Sample 108-659A-23H, CC is barren. The exact FO of *G. nepenthes* could not be determined.

Drilling of Hole 659A continued into lower to middle Miocene sediments, but only two samples contained foraminifers. Sample 108-659A-24H, CC contains *Praeorbulina sicana, Praeorbulina glomerosa curva*, and *Globorotalia fohsi peripheroronda*, placing it in the middle Miocene M6 Zone of Berggren et al. (1983) or the *Praeorbulina glomerosa* Zone of Bolli and Saunders (1985). Sample 108-659A-25H, CC contains *Catapsydrax dissimilis* and *G. fohsi peripheroronda*, placing it in the early Miocene *Catapsydrax stainforthi* Zone of Bolli and Saunders (1985).

Benthic Foraminifers

Except for Samples 108-659A-28X, CC and -659A-29X, CC, benthic foraminifers occur in all core-catcher samples examined from Hole 659A. Core-catcher Samples 108-659A-1H through -659A-9H contain rare to common and well-preserved specimens. Whereas Samples 108-659A-1H, CC through -659A-8H, CC contain an assemblage with low diversity, Sample 108-659A-9H, CC contains a highly diverse assemblage. Characteristic species include *Melonis pompilioides, M. barleeanus, Oridorsalis tener, Planulina wuellerstorfi, Pyrgo murrhina, Siphouvigerina proboscidea, Uvigerina peregrina, Cibicidoides kullenbergi, Eggerella bradyi, Dentalina* spp., *Lagena* spp., and *Quinqueloculina* sp. In addition, Sample 108-659A-9H, CC includes several specimens of *Pleurostomella* spp., *Bolivina* sp., *Francesista advena*, and *Orthomorphina himerensis*. This assemblage indicates middle bathyal to abyssal depths. In the interval between Cores 108-659A-10H and -659A-13H, benthic foraminifers are few and poorly preserved; this is especially true for Samples 108-659A-23H and -659A-27H. The faunal appearance may be influenced by selective dissolution. No specimens were observed in Sample 108-659A-29X, CC.

The FO of *Hoeglundina elegans* is recognized in Sample 108-659A-3H, CC (0.9 Ma). This age is older than that for the western North Atlantic (0.13 Ma) given by Schnitker (1979). The LO of *O. himerensis* is found in Sample 108-659A-9H, CC (late Pliocene). The estimated age of this event at Site 659 is similar to its age in the Indian Ocean (Boltovskoy, 1978). *Bulimina rostrata* disappears stratigraphically above Core 108-659A-15H.

Diatoms

The diatom flora at Site 659 was extremely sparse. Diatoms were few or rare in Samples 108-659A-1H, CC through -659A-4H, CC, -659B-1H, CC, and -659C-1H, CC through -659C-3H, CC, with neritic and freshwater diatoms outnumbering pelagic marine species. Preservation in these samples was invariably poor, and no stratigraphically useful species were observed. All other core-catcher samples were barren, except for Samples 108-659A-7H, CC, -659A-12H, CC, -659A-15H, CC, -659B-8H, CC, and -659B-9H, CC, which contained very rare specimens.

PALEOMAGNETISM

Magnetostratigraphy

Operating methods for Site 659 were similar to those used at previous sites. We made continuous measurements of core Sections 108-659A-3H through -659A-8H, all cores from Hole 659B, and Cores 108-659C-2H through -659C-4H. Continuous core measurements from the upper 45 m proved useful for polarity determinations, as illustrated by the Brunhes/Matuyama transition record shown in Figure 11. Even at this young age, however, the reversed inclinations are too shallow and more scattered than normal inclinations, indicating that an overprint is not removed completely by 50 Oe, the ODP limit for core sections. Below about 45 m, the overprint completely masks the original direction, and continuous core measurements were virtually useless. We illustrate this in Figure 12 by plotting the continuous data vs. discrete-sample data. Discrete samples were demagnetized to 200 Oe and clearly indicate negative inclinations, whereas continuous measurements, demagnetized to 50 Oe, are extremely scattered and do not suggest reversed directions. In view of these results, we feel that the ODP limit of 50 Oe should be raised to 150 Oe for archive halves. Under present guidelines, utility of the continuous method is severely hampered and, generally, is limited to the Pleistocene.

At previous sites, continuous measurements were conducted on unsplit cores. We noticed that occasionally cores were impossible to measure and attributed this to very strong magnetization. By measuring archive halves at Site 659, we determined that magnetization was not always too strong for our equipment. We were faced with a mystery, which was solved by attempting to measure a core liner filled with seawater. This produced the same effect as measuring whole cores. Therefore, we surmise that whole-core sections may have a continuous film of seawater between the sediment and the liner, producing a conduction layer. The interaction of a conducting cylinder with a trapped field apparently produces a magnetic moment strong enough to send magnetometer sensors off the scale. Until the field trapped in the magnetometer can be released, such induced moments may be common. We have, therefore, measured only archive halves from this site.

To obtain reliable magnetostratigraphy for sediments deeper than 45 m, we found it necessary to take subsamples. We measured from one to three discrete samples per core section. At least one sample per core was completely demagnetized. Owing to the variability of magnetic properties among samples, each sample was subjected to several demagnetization steps. Hence, we made approximately 1500 measurements on samples recovered at Site 659. Data were selected from these samples using the same criteria as at previous sites. Our selected data are plotted in Figures 13 through 16.

Inclination data from Hole 659A are shown in Figure 13. Inclinations from the upper 100 m generally agree with those expected for the location of this site. Below about 100 m, the data are extremely scattered and cannot be considered reliable.

In an attempt to improve data quality, we tried a different sampling technique for cores from Hole 659B. In Hole 659A, samples were taken by pressing 1-in.- × 1-in.- × 3/4-in.-sample boxes into the split face of the working half of the core. In Hole 659B, samples were taken by inserting a stainless steel 3/4-in.-square tube into the sediment and then extruding the sample into plastic boxes with a plastic plunger.

Data from 659B are shown in Figure 14. All inclinations steeper than 60° are indicated by dots in the upper part of the figure and have been eliminated in the lower part of the figure. Data from Hole 659B clearly are less reliable than those from Hole 659A. Particularly disappointing are results from below 100 m, shown in the lower part of Figure 14. Data from Holes 659A and 659B above 100 m are combined in Figure 15 for composite stratigraphy. We can correlate these data to the time scale with some confidence.

Returning to the first sampling technique, we sampled Cores 108-659C-5H through -659C-8H of Hole 659C at a rate of one sample per section. Our results are shown in Figure 16 and seem of exceptional quality. The inclinations agree with those expected, and results can be correlated to the time scale. The part from 100 to 120 mbsf continues from the A-B composite section in Figure 15. The part from 175 to 195 mbsf can be correlated

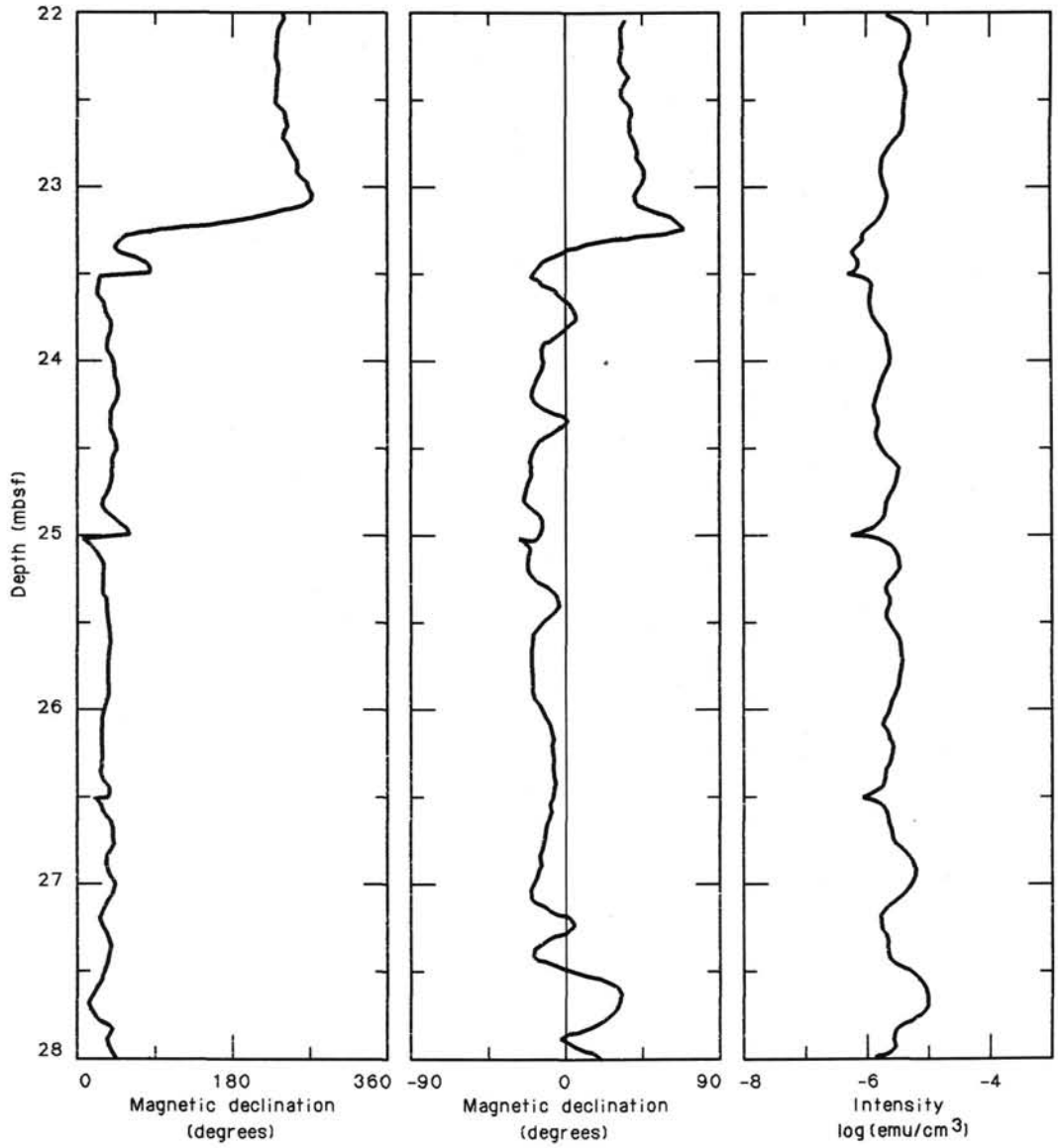

Figure 11. Results of the Brunhes-Matuyama transition obtained from measuring the archive-half section of Core 108-659C-3H in Hole 659C.

only tentatively using nannofossil data. Ironically, if Hole 659C had been cored continuously, our records would have been superb. We still are puzzled by the failure of the samples from Hole 659B and are not convinced completely that the blame lies with the sampling technique, although we certainly hope so. We will attempt to sample the cores again using our first technique to establish whether the problem is coring disturbance or sampling technique. Perhaps post-cruise data will improve our results.

Magnetic Susceptibility

We measured whole-core-volume magnetic susceptibility at 3-cm intervals for all suitable cores from Holes 659A, 659B, and 659C. Susceptibility values generally are less than 20×10^{-6} cgs in Unit I, but average around 40×10^{-6} cgs in Unit II (Cores 20H, 19H, and 7H and below in Holes 659A, 659B, and 659C). This increase probably reflects increased carbonate dissolution during the Miocene, causing a concentration of magnetic material relative to other sedimentary components. Susceptibility shows a sharp reduction—to less than 20×10^{-6} at around 200 mbsf in Hole 659A (Cores 108-659A-22X and below), corresponding to Subunit IIB, which otherwise is differentiated from Subunit IIA only by color.

Superimposed on these general trends of susceptibility variation are relatively high frequency fluctuations that probably reflect changes in the concentration of terrigenous components on time scales of around 10^4 to 10^5 years. Sharply defined susceptibility peaks in Cores 108-659A-4H and -659B-4H, -659A-10H and -659B-10H, -659B-12H, and -659C-4H and -659C-5H probably are volcanic ash layers.

High-resolution correlation of susceptibility features throughout the recovered intervals in Holes 659A, 659B, and 659C is possible. Figure 17 shows a typical example.

SEDIMENT-ACCUMULATION RATES

Sediment-accumulation rates in Hole 659A were established using 33 chronostratigraphic events (Table 3). The resulting curves (Figs. 18 and 19) suggest continuous deposition from approximately the latest early Miocene to the Holocene. A hiatus encompasses almost the entire early Miocene and is underlain by

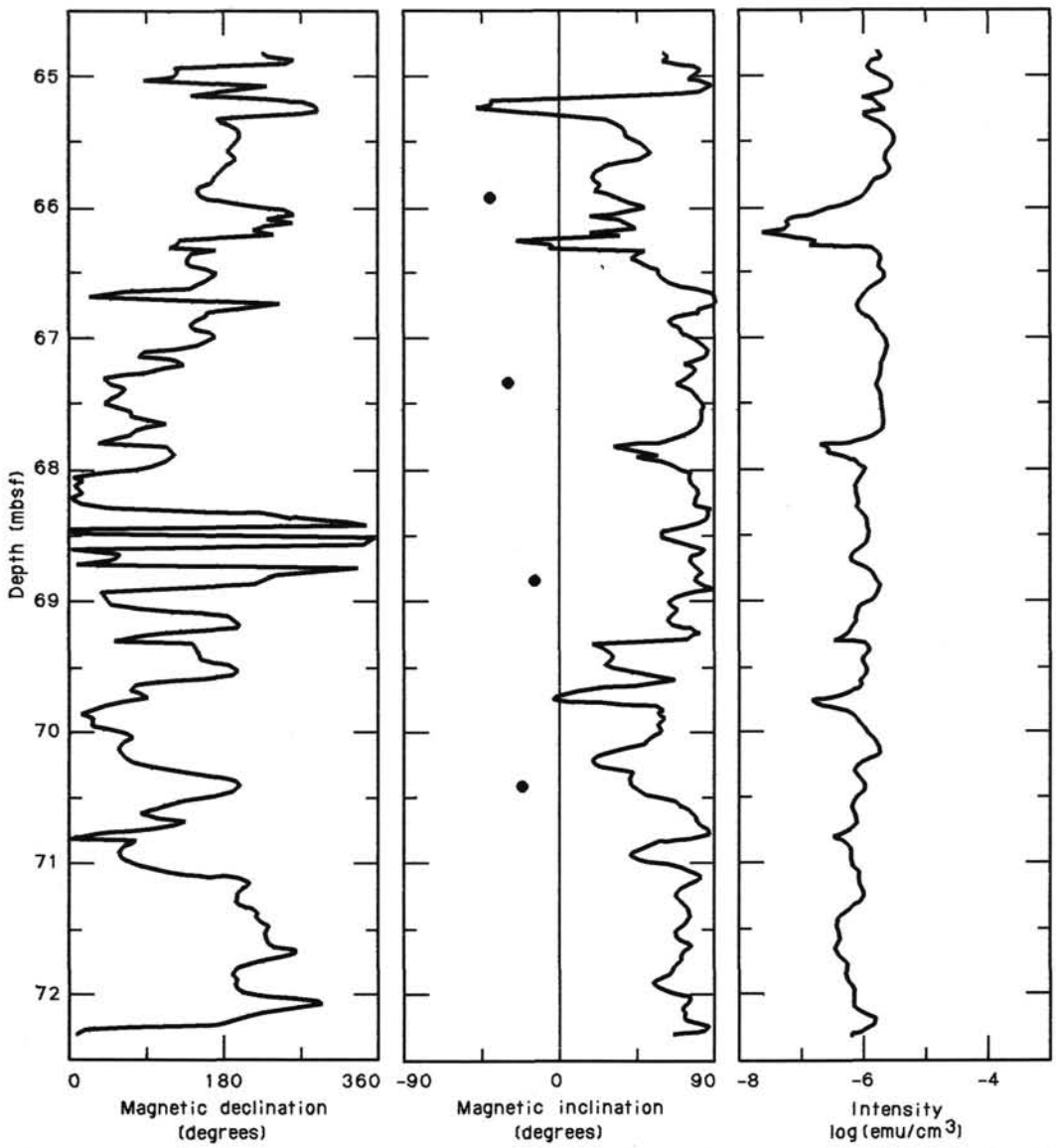

Figure 12. Companion data obtained from continuous-core measurements after 50 Oe demagnetization and results of a single sample demagnetized to 200 Oe. Differences are caused by the presence of a secondary component not completely removed by 50 Oe demagnetization.

continuous deposition across the Oligocene/Miocene boundary. The stratigraphic classification of the two deepest cores (Cores 108-659A-28X and -659A-29X) is unknown because no microfossils were found.

Calculated sedimentation rates are highly variable, with the highest rate (30 m/m.y.) in the Pliocene-Pliestocene and the lowest rate (4 m/m.y.) in the middle Miocene. To establish the sedimentation rates, we used only data from Hole 659A.

A major difference in reliability exists between the age estimates of Pliocene-Pleistocene and Miocene marker fossils. Because the Pliocene-Pleistocene biostratigraphic markers have been correlated directly to the magnetostratigraphic polarity scale, they are considered well controlled. Direct correlations of Miocene species events to the polarity scale are rare. Thus, although the biostratigraphic order of the Miocene species events are well known, their estimated ages should be regarded with caution.

Only two of the 16 Pliocene-Pleistocene control points have age-depth positions significantly off the suggested age-depth curve: the last occurrences of *Globorotalia margaritae* and *Globigerina nepenthes*. The former species is known to be diachronous in the North Atlantic (Weaver and Clement, 1986), and the latter species was extremely rare toward the end of its observed range. Neither event is considered reliable enough to change the age-depth curve in the lower Pliocene interval.

The FO of *G. nepenthes* has a quoted age of 11.3 Ma (Berggren et al., 1985), but this datum appears anomalous at Site 659. Poore (1984) found this species in sediment zoned as N8, which correlates to nannofossil Zone NN5 (approximately 15 Ma). This age compares better with other data at the site, and the FO of *G. nepenthes* should be regarded as unreliably correlated to the paleomagnetic polarity scale.

Two possible sedimentation rates (6 and 8 m/m.y., respectively; Fig. 18) are suggested for the interval between 14.4 Ma and the early Miocene hiatus (about 18.0 Ma). Berggren et al. (1985) acknowledged the difficulties for establishing accurate correlations between nannofossil and planktonic-foraminifer species events during early Miocene time. The discrepant age-depth positions of the early Miocene control points, the FO of *Discoas-*

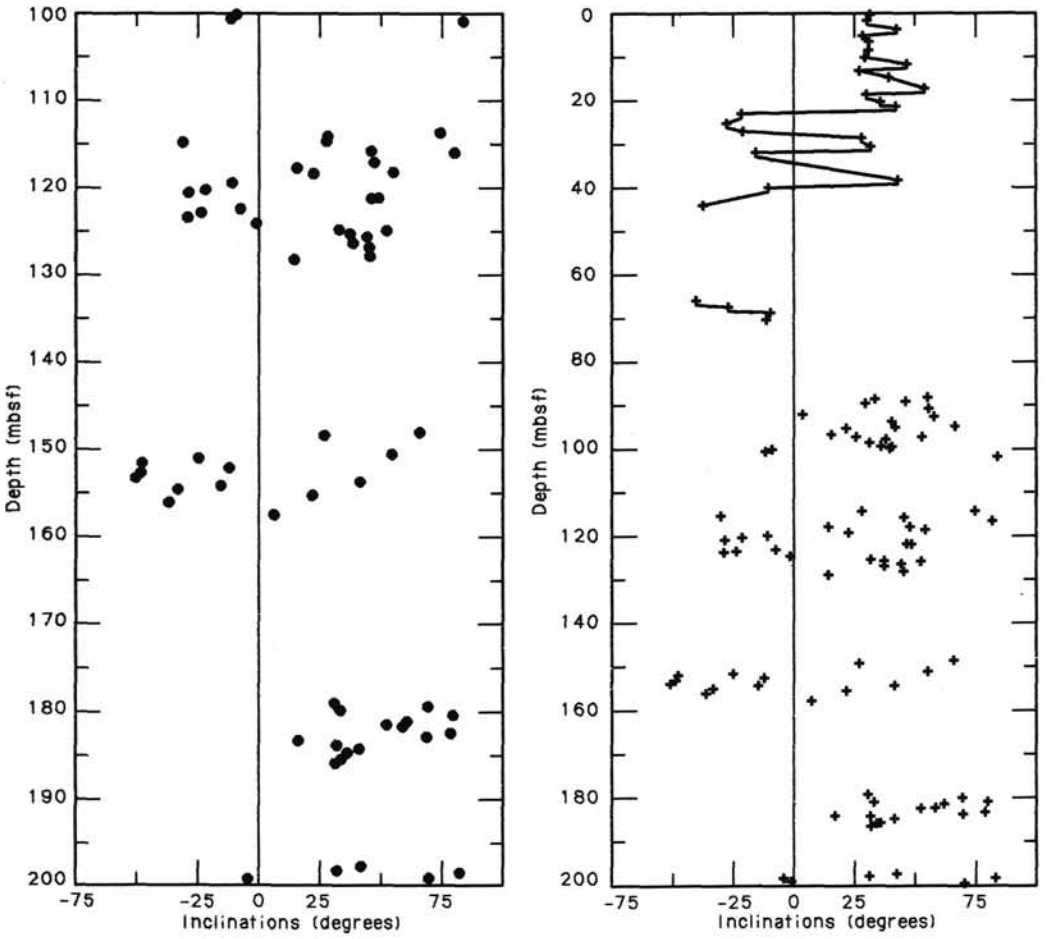

Figure 13. Inclination data from Hole 659A. Data obtained below 100 mbsf and plotted in the lower part of the figure are extremely scattered.

ter druggii and the LO of *Discoaster bisectus*, probably reflect these difficulties. The early Miocene hiatus thus may span a time interval of either 5 or 3.5 m.y.

INORGANIC GEOCHEMISTRY

Interstitial-water samples were squeezed from six sediment samples taken routinely from approximately every 50 m in Hole 659A (Cores 108-659A-21X and -659A-27X) and Hole 659B (Cores 108-659B-1H, -659B-6H, -659B-11H, and -659B-16H). Values for pH and alkalinity were measured in conjunction, using a Metrohm 605 pH-meter, followed by titration with 0.1N HCl. Salinities were measured using an optical refractometer, and chlorinities determined by titration with silver nitrate to a potassium chromate end point. Calcium, magnesium, and sulfate analyses were performed by ion chromatography using a Dionex 2120i instrument. Results from these analyses are presented in Table 4.

ORGANIC GEOCHEMISTRY

At Site 659, Hole 659A, 113 physical-properties samples were used to determine carbonate contents. Of these, 34 samples from throughout the sequence also were analyzed for total organic carbon (TOC). Carbonate analyses of 32 samples from Hole 659B were performed in an attempt to fill in the parts of the section not recovered from Hole 659A; composite depth was used to account for a change of several meters between Holes 659A and 659B.

Organic and Inorganic Carbon

Inorganic-carbon (IC) contents were measured on the Coulometrics Carbon Dioxide Coulometer, while total-carbon (TC) values were determined using the Perkin Elmer 240C Elemental Analyzer. TOC values were calculated by difference. Analytical methods are discussed, and data given in the Appendix (this volume).

All TOC values determined for Hole 659A are very low (generally $<0.1\%$), with the highest recorded value being 0.38% from Core 108-659A-2H. In fact, for many of the sediments analyzed, the IC values obtained are slightly higher (by up to 0.2% absolute) than the TC values. In these samples, the TOC values were assumed to be 0%.

According to carbonate content, the sediment sequence at Site 659 may be divided into two distinct parts (Fig. 20), corresponding to lithologic Units I and II (see "Lithostratigraphy and Sedimentology" section, this chapter). The boundary between these two units lies within the unrecovered part of the sequence between Cores 108-659A-17H and -659A-20H. Unit I is characterized by quasiperiodic variations in carbonate content from 40% to 90%, with values generally higher in the lower part of the unit. Unit II is poorer in carbonate content, with high-amplitude variations between 7% and 70% $CaCO_3$.

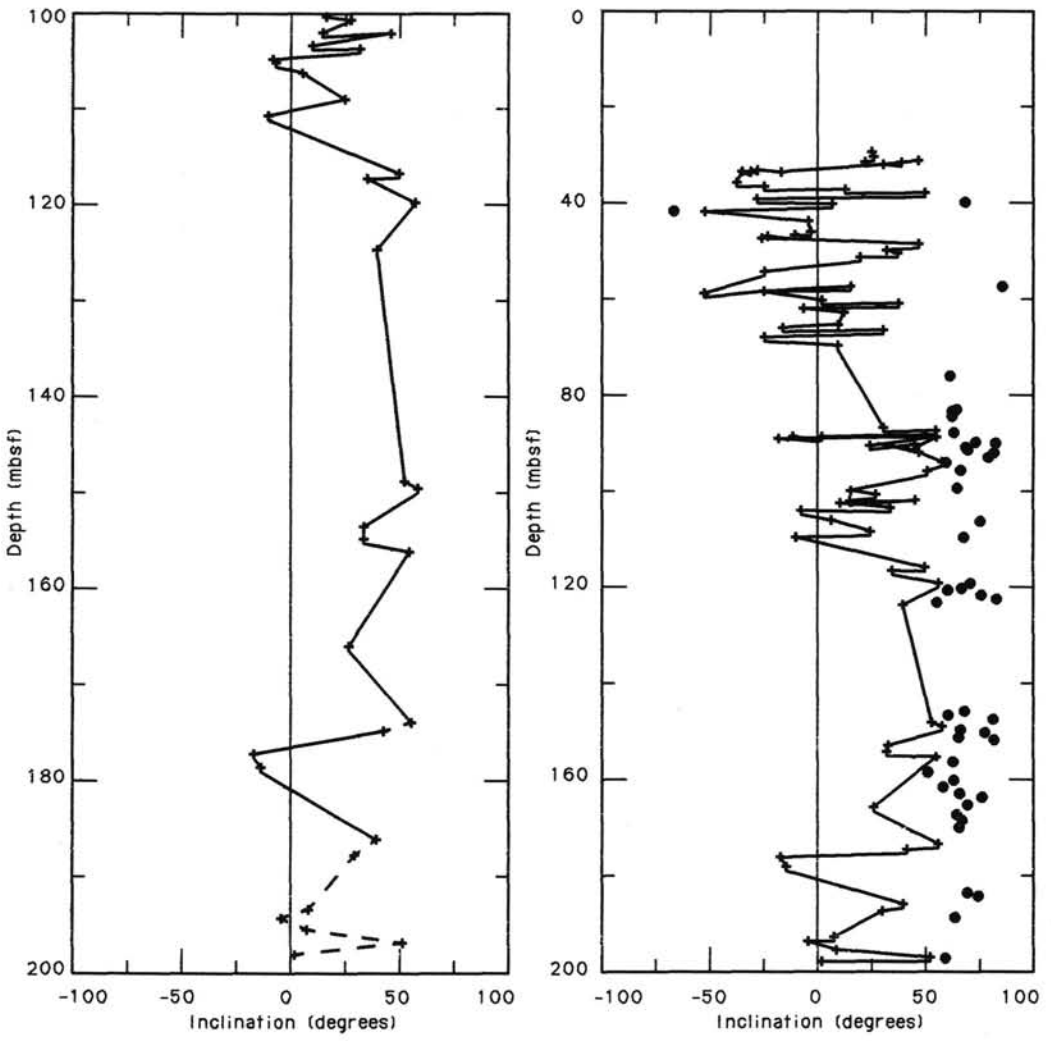

Figure 14. Inclination variations from Hole 659B. In the upper part of the figure, inclinations steeper than 60° are indicated by dots; inclinations have been removed in the lower part of the figure.

Discussion

The sediments at Site 659 are characterized by low TOC contents (<0.4%) typical of open-marine environments (e.g., Müller et al., 1983). The lower average carbonate content of Unit II may be explained by dissolution, obvious signs of which were noted during microscopic study of foraminifers (see "Biostratigraphy" section, this chapter). Further evidence can be found from sedimentation rates that are considerably higher in the carbonate-rich upper part of the sequence (Unit I; "Sediment-Accumulation Rates" section, this chapter).

PHYSICAL PROPERTIES

The techniques used for shipboard physical-properties measurements at Site 659 are outlined in the "Introduction and Explanatory Notes" (this volume). Tables 5 through 8 show the index-properties, vane-shear-strength, and compressional-wave-velocity (*P*-wave-logger) data for Holes 659A and 659B. Only GRAPE and PWL measurements were performed for Hole 659C. Most data for Holes 659A and 659B are presented graphically in Figures 21 through 27 (the calcium carbonate profile is shown in Figure 25 for comparison with other properties). None of the data presented in this section were screened for bad data points.

Wet-bulk density increases steadily from a near-surface value of 1.48 g/cm^3 to values around 1.8 g/cm^3 at a depth of 200 mbsf. Sample volumes (and, hence, some of the index properties) for Hole 659B were calculated using wet and dry weights and an assumed average grain density of 2.66 g/cm^3. The measured grain densities from Hole 659A averaged 2.65 g/cm^3 (Fig. 25). The carbonate content (Fig. 25) fluctuates between 40% and 90% down to a depth of 160 mbsf. Below this level, it fluctuates between 10% and 70%.

Hand-held "Torvane" shear-strength measurements were performed on cores from Site 659 (Fig. 26). Values do not exceed 40 kPa down to a depth of 160 mbsf but increase rapidly below this depth in the clay-rich lithologies, with values exceeding 100 kPa.

Downhole temperature was measured in Cores 108-659B-4H, -659B-14H, and -659B-17H (26–35, 117–126, and 146–155 mbsf, respectively) from Hole 659B. Shipboard thermal-conductivity measurements were conducted using these same cores. Attempted downhole-temperature measurements for Cores 108-659B-11H and -659B-18H were unsuccessful. The cause was probably a poor connection between the battery and the temperature re-

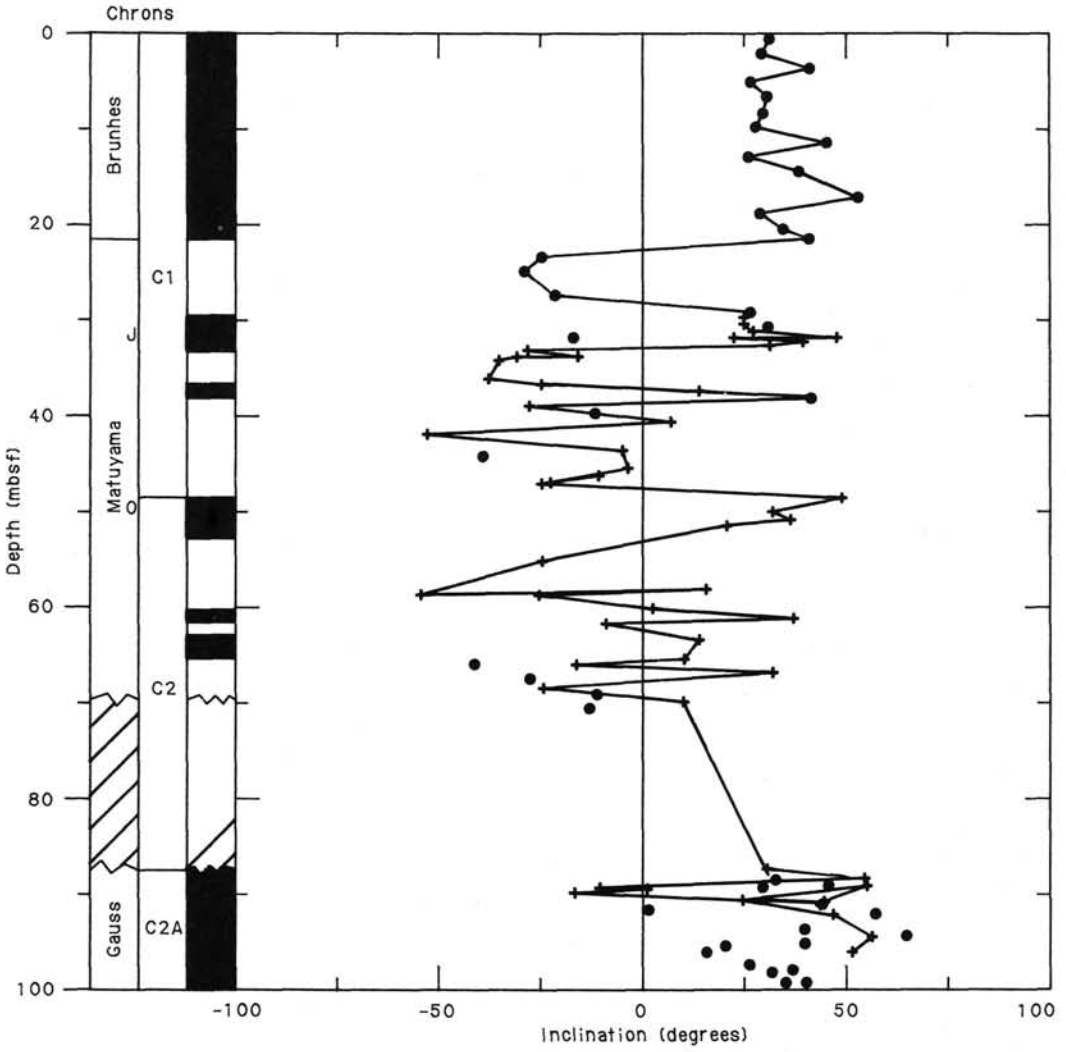

Figure 15. Composite inclination records from Holes 659A and 659B. Correlation of polarity intervals with the geomagnetic time scale is given in the left of the figure.

corder in the cutting shoe. Measured thermal conductivities vary between 0.956 and 1.289 W/m/°C. Maximum values occur in Core 108-659B-17H.

The *P*-wave logger (PWL) worked well for most of the cores recovered at this site. In Figure 27, a selected number of data points have been plotted to show the overall trend and range of the velocity fluctuations at different depths. In Figure 28, the PWL record for Core 108-659B-19H is used to illustrate the detailed "signature" that can be obtained from a high-quality core. For comparison, the velocity profile for the same core is shown with a sampling interval of about 1.5 m (typical of most velocity profiles obtained using the Hamilton Frame). The complete PWL records can be used to correlate Holes 659A and 659B to a precision of a few centimeters. All whole-core sections were logged continuously using the GRAPE.

SEISMIC STRATIGRAPHY

Several seismic-reflection profiles (air-gun, water-gun, 3.5-, and 12-kHz) were recorded at Site 659 (see "Background and Scientific Objectives" section, this chapter). The 20- to 500-Hz seismic record of *JOIDES Resolution* is characterized by three different units (Fig. 29 and Table 9). Seismic unit 1 extends to 0.13 s (approximately 100 m) below seafloor (bsf) and consists of five to six equally spaced reflectors that gradually fade out between reflectors 4 and 5. Seismic unit 2, at 0.13–0.31 sbsf, is transparent in the profile of Figure 29 but contains a faint lamination on the *Meteor* cruise record 25/1971 (Fig. 5). Seismic unit 3 begins with a reflector at 0.31 sbsf at Site 659 and contains several more or less distinct reflectors. Five km farther east northeast along the same profile, another stratigraphically higher reflector of this unit is intercalated at 0.29 s (Fig. 29). The upper boundary of seismic unit 3 thus appears to be slightly time transgressive.

The source of some of these reflectors was determined from (1) known *P*-wave velocities (see "Physical Properties" section, this chapter) and (2) various features or irregularities observed in the lithologic and stratigraphic evidence ("Lithostratigraphy and Sedimentology," "Biostratigraphy," and "Paleomagnetism" sections, this chapter) matching the seismic record. Details of our seismic correlation are summarized in Table 9.

The reflectors of seismic unit 1 do not correlate directly with the closely spaced carbonate cycles found in lithologic Subunits IA and (upper) IB (Fig. 20). Rather, they are the result of seismic-wave interference with impedance contrasts associated with these carbonate cycles. The transparent seismic unit 2 comprises both lithologic Subunits (lower) IB, IIA, and (upper) IIB. The

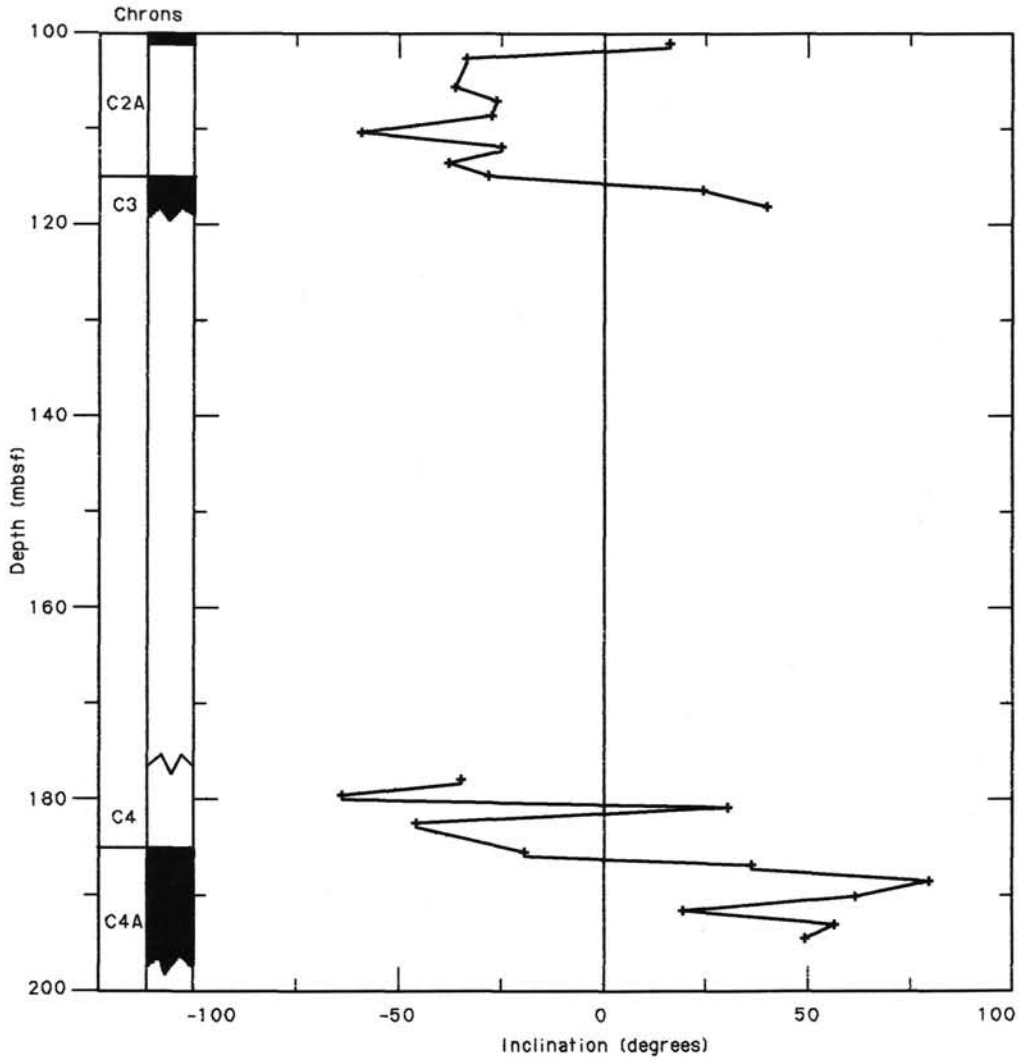

Figure 16. Inclination records obtained from Hole 659C correlated with the polarity time scale.

reflector at 0.31 sbsf (top of seismic unit 3) can be correlated with the 5-m.y. hiatus determined for the early Miocene (Fig. 18) at approximately 247 mbsf. The existence of a hiatus also can explain the time-transgressive character of the top of seismic unit 3. Finally, the reflector at 0.336 sbsf, with its rather transparent section below, may match the decrease of carbonate to 0% near the Oligocene/Miocene boundary.

COMPOSITE-DEPTH SECTION

At Site 659, three parallel holes were drilled with staggered core depths to obtain a complete pelagic sediment record. Holes 659A and 659B were cored completely down to about 200 mbsf. Hole 659C was spot-cored only in those intervals where sediments were lost because of incomplete and contorted core recovery in Holes 659A and 659B. The recovered lithologic units are essentially identical in the three holes (see "Lithostratigraphy and Sedimentology" section, this chapter). We succeeded in correlating the profiles of interbedded nannofossil ooze and silt-bearing nannofossil ooze for the three holes in perfect detail by comparing continuous magnetic-susceptibility curves, which show marked short-term cyclic fluctuations (see "Paleomagnetism" section, this chapter). Analogous results were achieved by comparing continuous *P*-wave-logging curves for the same cores (see "Physical Properties" section, this chapter).

The nominal depth below seafloor (based on the drilling record) of susceptibility-curve features generally is offset by as much as 4 m upward in Hole 659B vs. Holes 659A and 659C. The direction of displacement occasionally changes downhole (Fig. 30). Because most gains and losses of core length are tied to breaks between succeeding cores, we regard them as artifacts related to coring and to the ODP conventions for recording depths.

In Table 10, we correlated core depths for the three holes to arrive at a complete and uncontorted composite-depth section. The following criteria and rationales define our procedure:

1. The tops of Cores 108-659A-1H and -659C-1H were repositioned 0.25 m lower with respect to Hole 659B, based on a slightly more complete sediment record recovered in the uppermost part of Core 659B-1H.

2. We chose Hole 659A as the major reference unit for assembling a composite-depth section because this hole posed the least problems with the definition of nominal penetration depths. Points in the undisturbed parts of sediment cores that approxi-

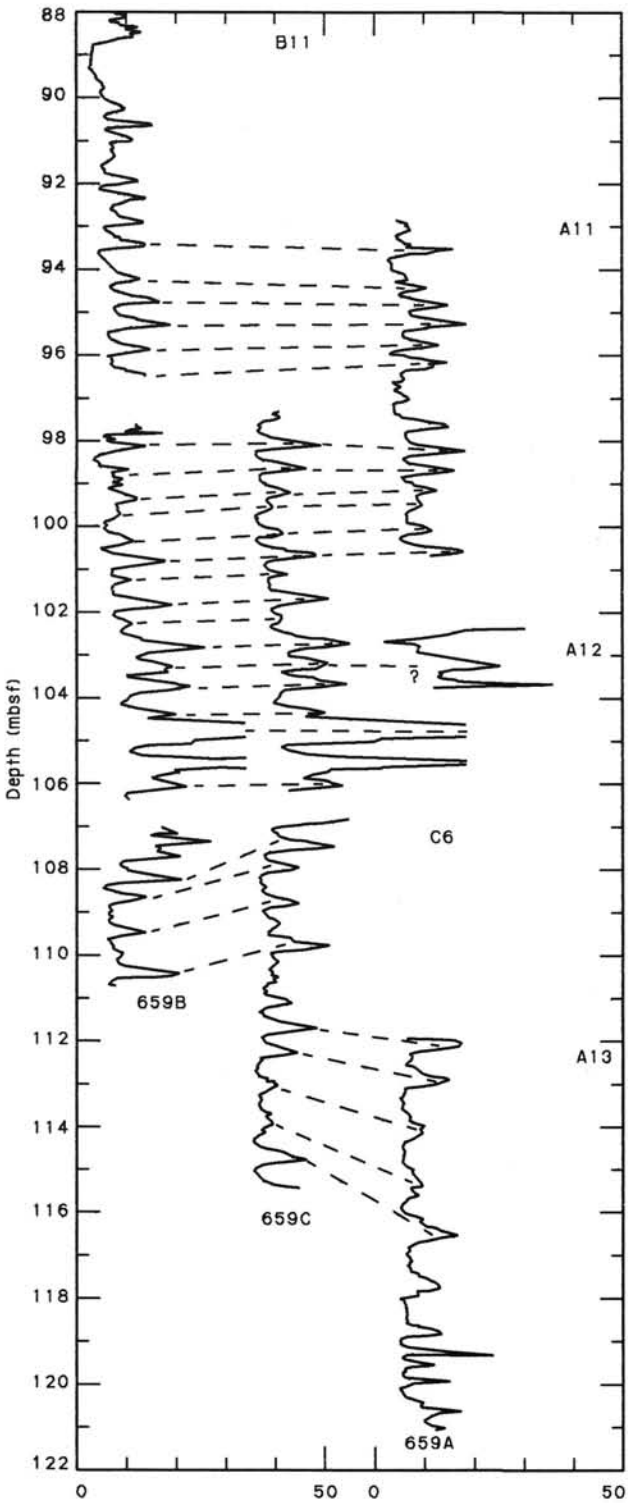

Figure 17. Correlation of susceptibility features among Holes 659A, 659B, and 659C.

mate the upper and lower boundaries of these cores were used as switch points to generate a continuous "pathway" of between-hole correlation.

3. Apparent gains in core length for Cores 108-659C-2H and -659C-4H relative to Cores 108-659A-2H and -659A-4H may be the result of a flowing in, as evidenced by the contorted structures near the upper core end (see "Barrel Sheets," this chapter).

4. Based on the correlation of susceptibility curves, the nominal penetration depths of Core 108-659B-10H were readjusted upward by 4.4 m. This adjustment also eliminated an equally long overlapping of core length between Cores 108-659B-10H and -659B-11H and enabled us to fill in a major gap in core recovery between Cores 108-659B-9H and -659B-10H. From these adjustments, we learned that about 5 m of sediment was recored in the top of Core 108-659B-10H. This was sediment that had fallen out of Core 108-659B-9H into the hole.

5. Our correlations and adjustments led to an almost complete overlapping of sections of "good core" among the three holes down to a composite depth of about 204 mbsf (about 11 Ma), except for minor composite-depth sections of 47.5–49.0, 175.0–175.5, and 193.5–195.0 mbsf.

This composite-depth section (Table 10 and Fig. 30) shows how voids and contorted sections in cores with poor recovery can be bypassed successfully by sampling companion holes.

Table 3. Depth and age estimates of biostratigraphic and magnetostratigraphic indicators used to establish accumulation rates for Hole 659A.

	Datum	Depth (mbsf)	Age (Ma)
	Brunhes/Matuyama	22.8–22.8	0.73
	Matuyama/Jaramillo	28.6–28.6	0.91
	Jaramillo/Matuyama	31.0–31.1	0.98
LO	*Calcidiscus macintyrei*	45.8–55.3	1.45
LO	*Discoaster brouweri*	45.8–55.3	1.89
FO	*D. triradiatus* acme	59.8–61.3	2.07
LO	*Globorotalia miocenica*	64.8–65.6	2.20
LO	*Discoaster pentaradiatus*	69.3–70.8	2.35
LO	*D. tamalis*	81.8–83.8	2.65
LO	*Dentogloboquadrina altispira*	83.8–84.8	2.90
LO	*Sphaeroidinellopsis semulina*	87.5–90.5	3.00
LO	*Globorotalia margaritae*	121.8–125.5	3.40
LO	*Reticulofenestra pseudoumbilica*	104.1–112.4	3.56
LO	*Amaurolithus* spp.	123.3–124.8	3.70
LO	*Globigerina nepenthes*	131.3–140.8	3.90
FO	*Ceratolithus rugosus*	136.4–143.1	4.60
LO	*Discoaster quinqueramus*	148.8–151.1	5.60
FO	*D. quinqueramus*	182.6–184.8	8.20
LO	*D. bollii*	184.1–188.3	8.30
LO	*Catinaster calyculus*	188.3–191.7	8.75
LO	*Discoaster hamatus*	188.3–191.7	8.85
LO	*Catinaster coalitus*	188.3–191.7	9.00
FO	*D. hamatus*	191.7–199.1	10.00
FO	*C. coalitus*	199.1–200.7	10.80
FO	*G. nepenthes*	207.3–216.8	11.30
LO	*Sphenolithus heteromorphus*	212.9–214.4	14.40
top	*Praeorbulina glomerosa* Zone	219.5–219.5	14.90
base	*P. glomerosa* Zone	219.5–219.5	16.50
FO	*S. heteromorphus*	235.8–245.3	17.10
LO	*Sphenolithus belemnos*	235.8–245.3	17.40
	Catapsydrax dissimulus present	235.8–235.8	17.60
FO	*Discoaster drugii*	246.7–248.6	23.20
LO	*D. bisectus*	252.1–254.1	23.70

LO = last occurrence; FO = first occurrence.

REFERENCES

Berggren, W. A., Aubrey, M. P., and Hamilton, N., 1983. Neogene magnetobiostratigraphy of Deep Sea Drilling Project Site 516 (Rio Grande Rise, South Atlantic). *In* Barker, P. F., Carlson, R. L., Johnson, D. A., et al., *Init. Repts. DSDP*, 72: Washington (U.S. Govt. Printing Office), 675–713.

Berggren, W. A., Kent, D. V., and Van Couvering, J. H., 1985. Neogene geochronology and chronostratigraphy. *In* Snelling, N. J. (Ed.), *The Chronology of the Geophysical Record*: London (Blackwell Scientific Publications), 211–259.

Bolli, H. M., and Saunders, J. B., 1985. Oligocene to Holocene low latitude planktic foraminifera. *In* Bolli, H. M., Saunders, J. B., and

Perch-Nielsen, K. (Eds.), *Plankton Stratigraphy*: Cambridge (Cambridge Univ. Press), 165–262.
Boltovskoy, E., 1978. Late Cenozoic benthonic foraminifera of the Ninetyeast Ridge (Indian Ocean). *Mar. Geol.*, 26:139–175.
Jacobi, R., and Hayes, D., 1982. Bathymetry, microphysiography and reflectivity characteristics of the west African margin between Sierra Leone and Mauritania. *In* von Rad, U., Hinz, K., Sarnthein, M., and Seibold, E. (Eds.), *Geology of the Northwest African Continental Margin*: Berlin-Heidelberg (Springer-Verlag), 182–212.
Lancelot, Y., Seibold, E., et al., 1978. Site 368: Cape Verde Rise. *In* Lancelot, Y., Seibold, E., et al., *Init. Repts. DSDP*, 41: Washington (U.S. Govt. Printing Office), 233–254.
Müller, P., Erlenkeuser, H., and von Grafenstein, R., 1983. Glacial-interglacial cycles in oceanic productivity inferred from organic carbon contents in eastern North Atlantic sediment cores. *In* Thiede, J., and Suess, E. (Eds.), *Coastal Upwelling: Its Sediment Record*, Pt. B: New York (Plenum Press), 365–398.
Poore, R. Z., Tauxe, L., Percival, S. F., LaBrecque, J. L., Wright, R., Petersen, N. P., Smith, C. C., Tucker, P., and Hsü, K. J., 1984. Late Cretaceous-Cenozoic magnetostratigraphic and biostratigraphic correlations for the South Atlantic Ocean, DSDP Leg 73. *In* Hsü, K. J., LaBrecque, J. L., et al., *Init. Repts. DSDP*, 73: Washington (U.S. Govt. Printing Office), 645–655.
Sarnthein, M., Thiede, J., Pflaumann, U., et al., 1982. Atmospheric and oceanic circulation patterns off northwest Africa during the past 25 million years. *In* von Rad, U., Hinz, K., Sarnthein, M., and Seibold, E. (Eds.), *Geology of the Northwest African Continental Margin*: Berlin-Heidelberg (Springer-Verlag), 545–604.
Schnitker, D., 1979. The deep waters of the western North Atlantic during the past 24,000 years, and the re-initiation of the Western Boundary Undercurrent. *Mar. Micropaleontol.*, 4:265–280.
Stein, R., and Sarnthein, M., 1984. Late Neogene events of atmospheric and oceanic circulation offshore northwest Africa: high resolution record from deep-sea sediments. *Palaeoecology of Africa*, 16:9–36.
Uchupi, E., 1971. Bathymetric atlas of the Atlantic, Caribbean, and Gulf of Mexico. Woods Hole Oceanographic Institution, ref. no. 71-72, unpubl. manuscript.
Weaver, P.P.E., and Clement, B. M., 1986. Synchroneity of Pliocene planktonic foraminiferal datums in the North Atlantic. *Mar. Micropaleontol.*, 295–307.

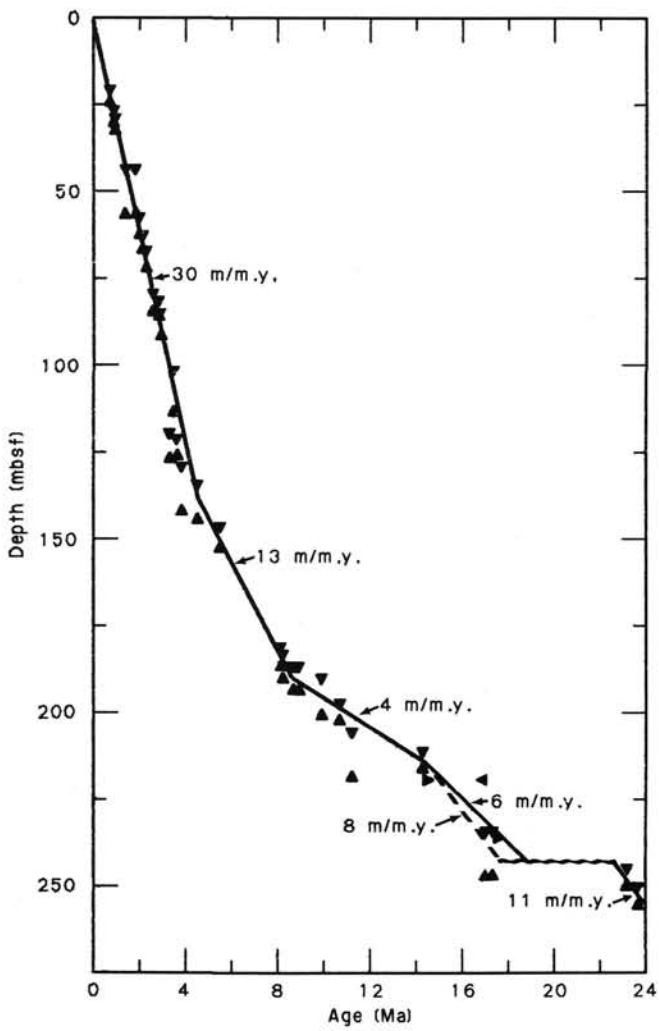

Figure 18. Graphic presentation of sediment-accumulation rates in Hole 659A.

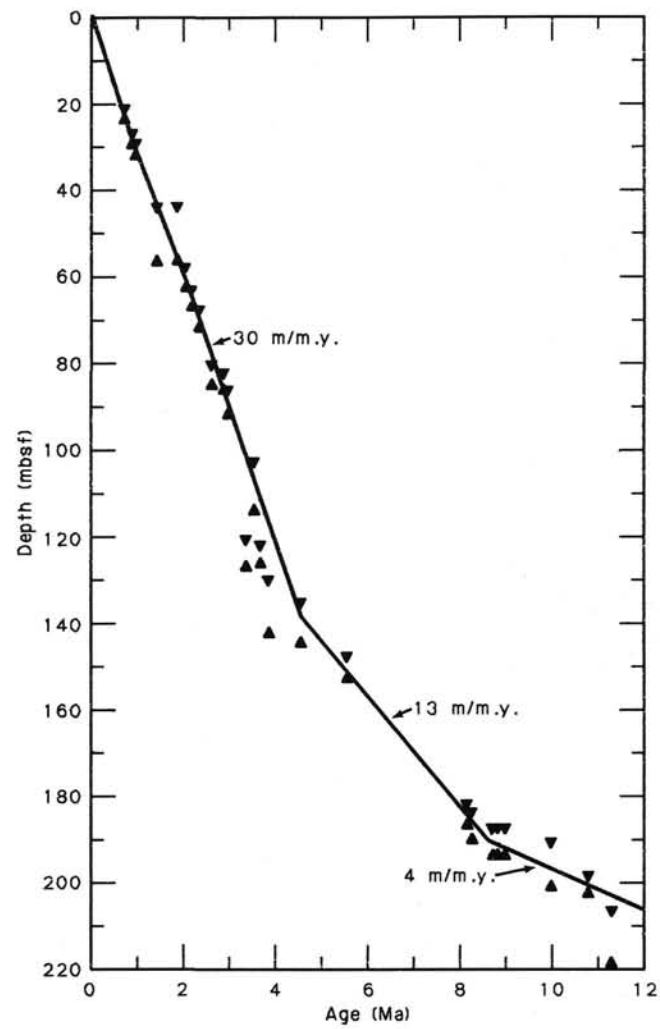

Figure 19. Graphic presentation of sediment-accumulation rates in the upper 220 m of Hole 659A.

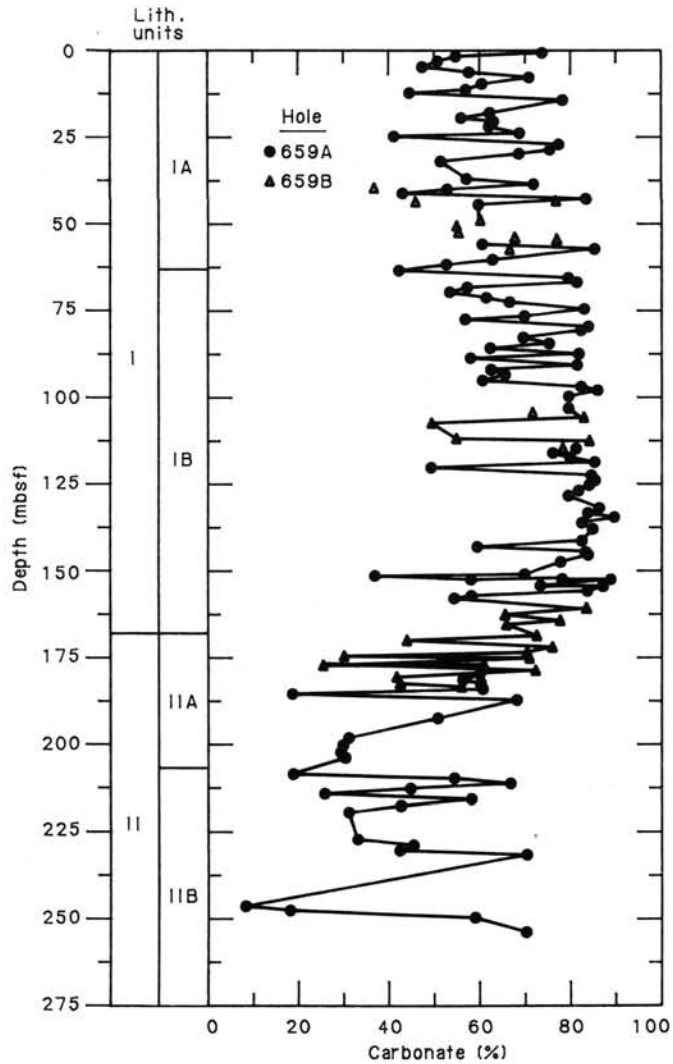

Figure 20. Carbonate curve for Site 659. Values from Hole 659B fill in gaps for core recovery at Hole 659A.

Table 4. Results of inorganic-geochemical analyses conducted for Site 659.

Hole/core/ section	pH	Alkalinity (mmol/L)	Salinity (‰)	Chlorinity (mmol/L)	SO^{2-} (mmol/L)	Mg^{2+} (mmol/L)	Ca^{2+} (mmol/L)
B-1H-3	7.45	3.48	34.3	562	26.0	47.4	10.87
B-6H-4	7.70	3.90	33.9	557	16.4	46.0	[a]low
B-11H-3	7.60	3.98	33.7	599	7.8	35.4	low
B-16H-5	7.78	3.78	33.8	604	1.5	32.6	low
A-21X-2	7.64	2.07	34.2	600	12.0	39.5	low
A-27X-4	7.52	2.17	43.8	637	4.4	36.2	12.80

[a] Ca^{2+} cannot be detected in standards containing 7.24 mmol/L.

Table 5. Index-properties data for Hole 659A.

Core/ section	Interval (cm)	Depth (mbsf)	Grain density (g/cm^3)	Wet-water contents (%)	Dry-water contents (%)	Wet-bulk density (g/cm^3)	Dry-bulk density (g/cm^3)	Porosity (%)
108-659A-1-1	56	0.56	2.78	82.13	108.89	1.46	0.75	75.00
108-659A-1-2	56	2.06	2.63	91.89	107.84	1.45	0.74	73.74
108-659A-1-3	56	3.56	2.33	48.18	92.97	1.44	0.79	68.19
108-659A-1-4	56	5.06	2.56	53.39	114.84	1.42	0.70	74.45
108-659A-1-5	56	6.56	2.61	45.16	82.34	1.93	0.89	67.98
108-659A-2-1	56	8.36	2.61	45.01	81.85	1.53	0.89	67.92
108-659A-2-2	56	9.86	2.46	48.40	93.79	1.46	0.83	69.54
108-659A-2-3	56	11.36	2.56	42.24	73.14	1.56	0.97	64.93
108-659A-2-4	56	12.86	2.50	52.54	110.71	1.42	0.72	73.34
108-659A-2-5	56	14.36	2.59	44.05	78.72	1.54	0.91	66.85
108-659A-3-1	60	17.90	2.64	43.98	78.50	1.55	0.94	67.21
108-659A-3-2	56	19.36	2.50	47.54	90.64	1.48	0.86	69.16
108-659A-3-3	56	20.86	2.54	45.15	82.33	1.52	0.88	67.39
108-659A-3-4	56	22.36	2.96	45.30	82.83	1.52	0.88	67.93
108-659A-3-5	56	23.86	2.50	44.07	78.79	1.52	0.90	66.05
108-659A-3-6	56	25.36	2.63	44.52	80.25	1.55	0.91	67.65
108-659A-4-1	56	27.36	2.53	43.05	75.58	1.54	0.93	65.40
108-659A-4-2	56	28.84	2.55	42.35	73.45	1.56	0.95	64.92
108-659A-4-3	56	30.34	2.69	43.87	78.15	1.57	0.92	67.82
108-659A-4-4	56	31.84	2.58	45.26	82.67	1.52	0.88	67.85
108-659A-5-1	56	36.86	2.56	43.65	77.47	1.54	0.92	66.23
108-659A-5-2	56	38.36	2.54	43.66	77.50	1.54	0.92	66.05
108-659A-5-3	56	39.86	2.56	41.26	70.24	1.58	0.97	64.04
108-659A-5-4	56	41.36	2.53	41.20	70.06	1.57	0.97	63.64
108-659A-5-5	56	42.86	2.09	54.54	119.96	1.33	0.66	71.39
108-659A-5-6	56	44.36	2.68	42.69	74.50	1.58	0.96	66.38
108-659A-7-1	56	55.86	2.54	40.11	66.98	1.59	1.00	62.72
108-659A-7-2	56	57.34	2.59	41.77	71.72	1.58	0.97	64.74
108-659A-7-3	56	58.84	2.56	38.32	62.14	1.62	1.05	61.12
108-659A-7-4	56	60.34	2.44	38.99	63.91	1.58	1.03	60.68
108-659A-7-5	56	61.84	2.59	37.40	59.75	1.64	1.07	60.47
108-659A-7-6	56	63.34	2.52	35.97	56.17	1.65	1.10	58.29
108-659A-8-1	59	65.39	2.60	45.01	81.86	1.53	0.89	67.82
108-659A-8-2	56	66.58	2.57	43.43	76.76	1.55	0.92	66.11
108-659A-8-3	56	68.08	2.65	42.44	73.73	1.58	0.95	65.91
108-659A-8-4	56	69.58	2.59	43.38	76.60	1.55	0.93	66.24
108-659A-8-5	56	71.08	2.61	41.12	69.82	1.59	0.98	64.27
108-659A-8-6	56	72.58	2.58	40.92	69.27	1.59	0.99	63.88
108-659A-9-1	56	74.86	2.78	44.52	80.24	1.57	0.91	68.80
108-659A-9-2	56	76.36	2.65	42.51	73.93	1.58	0.94	65.92
108-659A-9-3	56	77.86	2.78	34.10	51.74	1.75	1.13	56.70
108-659A-9-4	56	79.36	2.61	44.11	78.92	1.55	0.90	67.11
108-659A-9-5	56	80.86	2.64	43.18	75.98	1.57	0.94	66.47
108-659A-9-6	56	82.36	2.70	40.00	66.67	1.63	1.02	63.99
108-659A-10-1	56	84.36	2.60	41.98	72.37	1.57	0.95	65.02
108-659A-10-2	56	85.83	2.69	39.37	64.93	1.63	1.03	63.28
108-659A-10-3	56	87.33	2.58	43.82	78.00	1.54	0.90	66.56
108-659A-10-4	56	88.83	2.66	37.99	61.26	1.65	1.07	61.72
108-659A-10-5	56	90.33	2.66	43.48	76.93	1.57	0.92	66.92
108-659A-10-6	56	91.83	2.52	37.89	60.99	1.62	1.06	60.33
108-659A-11-1	56	93.86	2.62	40.43	67.87	1.60	1.00	63.70
108-659A-11-2	56	95.28	2.26	39.49	65.26	1.53	1.03	59.37
108-659A-11-3	56	96.76	2.66	42.57	74.13	1.58	0.94	66.10
108-659A-11-4	56	98.06	2.63	42.54	74.03	1.57	0.94	65.82
108-659A-11-5	56	99.56	2.67	41.99	72.38	1.59	0.96	65.62
108-659A-12-1	56	103.22	2.61	33.81	51.08	1.71	1.17	56.83
108-659A-13-1	56	112.86	2.74	42.26	73.18	1.60	0.97	66.46
108-659A-13-2	56	114.36	2.54	38.87	63.59	1.61	1.02	61.45
108-659A-13-3	56	115.86	2.56	40.56	68.23	1.59	1.00	63.33
108-659A-13-4	56	117.36	2.63	39.73	65.93	1.62	1.03	63.18
108-659A-13-5	56	118.86	2.70	41.22	70.11	1.61	0.98	65.17
108-659A-13-6	68	120.19	2.60	33.84	51.14	1.71	1.17	56.78
108-659A-14-1	56	122.36	2.76	41.10	69.77	1.62	1.01	65.57
108-659A-14-2	56	123.86	2.71	41.17	69.99	1.61	0.99	65.22
108-659A-14-3	56	125.36	2.63	40.96	69.38	1.60	0.99	64.29
108-659A-14-4	56	126.86	2.63	36.73	58.04	1.67	1.11	60.17
108-659A-14-5	56	128.36	2.61	36.84	63.51	1.63	1.04	62.08
108-659A-15-1	56	131.86	2.86	37.64	60.35	1.70	1.10	63.03
108-659A-15-2	56	133.32	2.64	37.80	60.76	1.65	1.09	61.32
108-659A-15-3	56	134.78	2.70	38.11	61.56	1.66	1.06	62.16
108-659A-15-4	56	136.28	2.65	36.79	58.21	1.67	1.09	60.35
108-659A-15-5	56	137.78	2.68	38.65	63.01	1.64	1.05	62.48
108-659A-16-1	60	141.40	2.70	37.70	60.52	1.67	1.07	61.73
108-659A-16-2	56	142.86	2.66	32.74	48.68	1.74	1.20	56.09
108-659A-16-3	56	144.36	2.70	40.42	67.84	1.62	1.00	64.39
108-659A-16-4	56	145.86	2.63	37.85	60.89	1.65	1.07	61.27

Table 5 (continued).

Core/ section	Interval (cm)	Depth (mbsf)	Grain density (g/cm^3)	Wet-water contents (%)	Dry-water contents (%)	Wet-bulk density (g/cm^3)	Dry-bulk density (g/cm^3)	Porosity (%)
108-659A-16-5	56	147.36	2.61	37.71	60.53	1.64	1.07	60.98
108-659A-17-1	56	150.86	2.58	36.88	58.43	1.65	1.11	59.86
108-659A-17-2	56	152.23	2.63	37.92	61.08	1.65	1.07	61.35
108-659A-17-3	56	153.68	2.53	37.98	61.24	1.62	1.05	60.45
108-659A-17-4	56	155.18	2.64	37.72	60.56	1.65	1.06	61.21
108-659A-17-5	56	156.68	2.67	33.18	49.66	1.74	1.21	56.66
108-659A-20-1	55	179.35	2.56	32.03	47.13	1.73	1.25	54.39
108-659A-20-2	56	180.86	2.66	31.91	46.86	1.76	1.22	55.18
108-659A-20-3	56	182.36	2.62	29.81	42.47	1.78	1.29	52.32
108-659A-20-4	56	183.86	2.65	30.53	43.94	1.78	1.27	53.44
108-659A-20-5	56	185.36	2.63	24.83	33.03	1.89	1.49	46.17
108-659A-20-6	56	186.86	2.60	33.08	49.44	1.72	1.20	55.90
108-659A-21-3	85	192.05	2.70	30.22	43.31	1.80	1.34	53.52
108-659A-22-1	56	198.36	2.54	31.80	46.64	1.72	1.25	53.90
108-659A-22-2	56	199.86	2.64	29.40	41.64	1.80	1.31	52.05
108-659A-22-3	56	201.36	2.62	28.48	39.83	1.81	1.36	50.72
108-659A-22-4	56	202.86	2.49	27.90	38.70	1.78	1.33	48.76
108-659A-23-1	65	207.95	2.65	25.92	34.99	1.87	1.42	47.75
108-659A-23-2	65	209.43	2.66	28.07	39.03	1.83	1.34	50.62
108-659A-23-3	76	211.04	2.71	28.18	39.24	1.85	1.37	51.14
108-659A-23-4	56	212.34	2.60	29.55	41.94	1.78	1.32	51.86
108-659A-23-5	74	213.74	2.66	29.06	40.97	1.81	1.35	51.84
108-659A-23-6	36	214.86	2.57	30.47	43.83	1.76	1.27	52.62
108-659A-24-1	51	217.31	2.69	30.38	43.63	1.80	1.31	53.64
108-659A-24-2	71	218.92	2.69	29.80	42.46	1.81	1.31	52.95

Table 6. Index-properties data for Hole 659B.

Core/ section	Interval (cm)	Depth (mbsf)	Wet-water content (%)	Dry-water content (%)	Porosity (%)	Wet-bulk density (g/cm^3)	Dry-bulk density (g/cm^3)	Vane shear strength (kPa)
108-659B-1-1	56	0.56	40.74	154.74	79.15	1.36	0.55	0.00
108-659B-1-2	56	2.06	30.82	103.35	72.07	1.48	0.74	2.00
108-659B-1-3	56	3.56	49.13	96.60	70.73	1.50	0.78	24.00
108-659B-1-4	56	4.96	31.24	105.08	72.39	1.47	0.73	10.00
108-659B-4-1	56	26.16	44.97	81.72	67.27	1.56	0.87	28.00
108-659B-4-2	56	27.66	42.18	72.96	64.79	1.60	0.93	21.00
108-659B-4-3	56	29.16	43.57	77.22	66.04	1.58	0.90	19.00
108-659B-4-4	56	30.66	44.95	81.65	67.25	1.56	0.87	22.00
108-659B-4-5	56	32.16	43.93	78.35	66.36	1.57	0.89	21.00
108-659B-4-6	56	33.66	37.78	60.73	60.60	1.67	1.04	30.00
108-659B-5-1	56	35.66	47.41	90.16	69.33	1.52	0.81	20.00
108-659B-5-2	56	37.16	43.49	76.95	65.97	1.88	0.90	17.60
108-659B-5-3	56	38.66	42.11	72.75	64.73	1.60	0.93	28.50
108-659B-5-4	56	40.16	43.02	75.81	65.55	1.58	0.91	31.50
108-659B-5-5	56	41.36	40.75	68.78	63.47	1.62	0.97	39.50
108-659B-5-6	56	42.86	46.92	88.39	68.92	1.53	0.82	20.00
108-659B-6-1	56	45.16	56.87	131.88	76.53	1.41	0.62	22.50
108-659B-6-2	56	46.66	34.06	117.69	74.51	1.44	0.68	34.00
108-659B-6-3	56	48.16	49.25	97.03	70.82	1.50	0.77	32.00
108-659B-6-4	56	49.66	49.79	99.16	71.26	1.49	0.76	29.00
108-659B-6-5	56	51.06	47.34	89.91	69.27	1.52	0.81	25.50
108-659B-6-6	56	52.56	46.32	86.29	68.42	1.54	0.84	38.00
108-659B-7-1	56	54.66	39.69	65.82	62.46	1.63	0.99	10.50
108-659B-7-2	11	55.61	37.36	59.64	60.18	1.67	1.06	28.00
108-659B-7-3	56	57.56	37.35	59.63	60.17	1.67	1.06	34.50
108-659B-7-4	56	59.06	34.64	53.00	57.37	1.72	1.13	31.50
108-659B-7-5	56	60.56	35.95	56.13	56.75	1.70	1.09	25.00
108-659B-7-6	56	62.06	41.13	69.86	63.82	1.61	0.96	16.50
108-659B-8-1	56	64.16	38.75	63.26	61.55	1.65	1.02	24.00
108-659B-8-2	56	65.66	42.02	72.48	64.64	1.60	0.94	19.50
108-659B-8-3	56	67.16	43.07	75.67	65.60	1.58	0.91	18.00
108-659B-8-4	56	68.66	39.87	66.31	62.64	1.63	0.99	40.00
108-659B-8-5	56	69.88	42.51	73.93	65.08	1.59	0.93	24.00
108-659B-8-6	56	71.28	36.82	58.27	59.63	1.68	1.07	35.50
108-659B-9-1	56	73.66	40.56	68.24	63.29	1.62	0.97	42.50
108-659B-9-2	56	75.16	42.32	73.36	64.91	1.60	0.93	25.50
108-659B-9-3	56	76.66	42.75	74.67	65.31	1.59	0.92	20.00
108-659B-11-1	56	88.66	39.01	63.96	61.80	1.65	1.01	19.50
108-659B-11-2	56	90.11	43.25	76.22	65.76	1.58	0.91	27.00
108-659B-11-3	56	91.61	43.76	77.80	66.20	1.57	0.90	11.00
108-659B-11-4	56	93.00	39.69	65.81	62.46	1.63	0.99	16.00
108-659B-11-5	56	94.20	39.94	66.51	62.70	1.63	0.99	20.00

Table 6 (continued).

Core/ section	Interval (cm)	Depth (mbsf)	Wet-water content (%)	Dry-water content (%)	Porosity (%)	Wet-bulk density (g/cm^3)	Dry-bulk density (g/cm^3)	Vane shear strength (kPa)
108-659B-11-6	56	95.70	40.46	67.96	63.20	1.62	0.98	12.00
108-659B-12-1	56	98.16	35.03	83.91	57.78	1.71	1.12	35.00
108-659B-12-2	56	99.66	41.94	72.24	64.57	1.60	0.94	22.00
108-659B-12-3	56	101.16	42.61	74.24	65.18	1.59	0.92	13.00
108-659B-12-4	56	102.64	38.88	63.61	61.68	1.65	1.02	2.70
108-659B-12-5	56	104.14	41.67	71.43	64.32	1.60	0.95	16.00
108-659B-12-6	56	105.64	34.39	82.41	57.10	1.72	1.14	37.50
108-659B-13-1	56	107.66	36.15	56.61	58.95	1.69	1.09	39.00
108-659B-13-2	56	109.16	43.86	78.14	66.30	1.57	0.89	13.00
108-659B-13-3	56	110.66	41.55	71.08	64.21	1.61	0.95	25.00
108-659B-14-1	56	117.16	40.59	68.31	63.31	1.62	0.97	27.00
108-659B-14-2	56	118.63	39.86	66.27	62.62	1.63	0.99	17.00
108-659B-14-3	56	120.13	42.17	72.91	64.78	1.60	0.93	14.00
108-659B-14-4	56	121.63	42.14	72.83	64.75	1.60	0.92	15.00
108-659B-14-5	56	122.83	38.48	62.55	61.29	1.65	1.03	22.00
108-659B-14-6	56	124.33	34.83	53.45	57.58	1.71	1.12	46.00
108-659B-15-1	56	126.66	34.11	51.78	56.81	1.73	1.14	44.00
108-659B-15-2	56	128.03	35.26	54.46	58.02	1.71	1.11	44.00
108-659B-15-3	56	129.53	33.37	50.08	56.00	1.74	1.17	52.00
108-659B-15-4	56	131.03	37.73	60.59	60.55	1.67	1.05	23.00
108-659B-15-5	56	132.53	38.31	62.10	61.12	1.66	1.03	25.00
108-659B-15-6	56	134.03	38.70	63.13	61.50	1.65	1.02	21.00
108-659B-16-1	56	136.16	33.76	50.97	56.43	1.73	1.15	36.00
108-659B-16-2	56	137.59	37.42	59.80	60.24	1.67	1.05	37.00
108-659B-16-3	56	139.09	37.02	56.78	59.84	1.68	1.06	45.00
108-659B-16-4	56	140.59	36.01	56.27	58.81	1.69	1.09	21.00
108-659B-16-5	56	142.09	39.01	63.96	61.81	1.65	1.01	28.00
108-659B-16-6	56	143.51	38.53	62.68	61.34	1.65	1.02	22.50
108-659B-17-1	56	145.66	25.84	34.85	47.11	1.88	1.40	30.00
108-659B-17-2	56	147.10	36.84	56.33	59.65	1.68	1.07	31.00
108-659B-17-3	56	148.60	34.71	53.15	57.44	1.72	1.13	48.00
108-659B-17-4	56	150.10	37.94	61.13	60.75	1.66	1.04	38.00
108-659B-17-5	56	151.30	34.09	31.72	56.79	1.73	1.15	48.00
108-659B-17-6	56	152.73	33.32	49.97	55.95	1.74	1.17	58.00
108-659B-18-1	56	155.16	37.77	60.70	60.59	1.67	1.04	40.00
108-659B-18-2	56	156.50	37.70	60.51	60.52	1.67	1.05	43.00
108-659B-18-3	56	158.00	34.18	51.92	56.88	1.73	1.14	48.00
108-659B-18-4	56	159.50	35.65	55.40	58.43	1.70	1.10	26.00
108-659B-18-5	56	161.00	32.10	47.27	54.60	1.76	1.20	40.00
108-659B-19-1	56	164.66	35.27	54.48	58.03	1.71	1.11	45.00
108-659B-19-2	56	166.16	29.20	41.25	51.26	1.82	1.29	64.00
108-659B-19-3	56	167.66	36.12	56.54	58.92	1.69	1.09	33.00
108-659B-19-4	56	169.16	34.32	52.25	57.03	1.72	1.14	39.00
108-659B-19-5	56	170.66	31.48	45.94	53.91	1.77	1.22	49.00
108-659B-19-6	56	172.16	30.87	44.66	53.21	1.79	1.24	64.00
108-659B-20-1	56	174.16	28.79	40.44	50.77	1.82	1.30	45.50
108-659B-20-2	56	175.63	28.79	40.44	50.77	1.82	1.30	21.00
108-659B-20-3	56	177.13	24.55	32.55	45.43	1.91	1.45	126.63
108-659B-20-4	56	178.63	25.32	33.91	46.43	1.90	1.42	82.25
108-659B-21-1	56	183.66	28.46	39.78	50.37	1.83	1.32	122.50
108-659B-21-2	56	185.16	29.87	42.59	52.05	1.80	1.27	93.75
108-659B-21-3	56	186.66	28.88	40.61	50.88	1.82	1.30	77.50
108-659B-21-4	56	188.16	26.53	36.11	47.98	1.87	1.38	80.00
108-659B-21-5	48	189.58	28.60	40.06	50.54	1.83	1.31	87.50
108-659B-22-1	56	193.16	28.46	39.77	50.36	1.83	1.32	11.25
108-659B-22-2	56	194.66	27.91	38.72	49.70	1.84	1.33	170.00
108-659B-22-3	56	196.16	29.54	39.94	50.47	1.83	1.31	142.50
108-659B-22-4	56	197.66	26.41	35.89	47.83	1.87	1.38	165.00
108-659B-22-5	56	199.16	26.09	35.30	47.42	1.88	1.39	170.00

Table 7. Vane-shear-strength data for Hole 659A.

Core/ section	Interval (cm)	Depth (m)	Vane shear strength (kPa)
108-659A-1-1	56	0.56	1.0000
108-659A-1-2	56	2.06	2.0000
108-659A-1-3	56	3.56	1.5000
108-659A-1-4	56	5.06	1.0000
108-659A-1-5	56	6.56	19.0000
108-659A-2-1	56	8.36	11.5000
108-659A-2-2	56	9.86	12.0000
108-659A-2-3	56	11.36	15.0000
108-659A-2-4	56	12.86	13.5000
108-659A-2-5	56	14.36	18.5000
108-659A-3-1	60	17.90	11.0000
108-659A-3-2	56	19.36	22.0000
108-659A-3-3	56	20.86	19.0000
108-659A-3-4	56	22.36	16.5000
108-659A-3-5	56	23.86	22.0000
108-659A-3-6	56	25.36	31.0000
108-659A-4-1	56	27.36	20.0000
108-659A-4-2	56	28.84	23.0000
108-659A-4-3	56	30.34	24.5000
108-659A-4-4	56	31.84	25.5000
108-659A-5-1	56	36.86	11.0000
108-659A-5-2	56	38.36	13.5000
108-659A-5-3	51	39.81	15.0000
108-659A-5-4	56	41.36	25.0000
108-659A-5-5	56	42.86	10.0000
108-659A-5-6	56	44.36	18.0000
108-659A-7-1	56	55.86	30.0000
108-659A-7-2	56	57.34	19.5000
108-659A-7-3	20	58.48	20.5000
108-659A-7-4	56	60.34	23.5000
108-659A-7-5	56	61.84	30.5000
108-659A-7-6	56	63.34	39.5000
108-659A-8-1	59	65.39	13.0000
108-659A-8-2	56	66.58	18.0000
108-659A-8-3	54	68.06	26.0000
108-659A-8-4	56	69.58	28.0000
108-659A-8-5	56	71.08	22.5000
108-659A-8-6	56	72.58	24.0000
108-659A-9-1	56	74.86	18.0000
108-659A-9-2	56	76.36	22.5000
108-659A-9-3	56	77.86	35.0000
108-659A-9-4	56	79.36	27.5000
108-659A-9-5	56	80.86	25.5000
108-659A-9-6	56	82.36	22.5000
108-659A-10-1	56	84.36	21.5000
108-659A-10-2	56	85.83	22.5000
108-659A-10-3	56	87.33	7.0000
108-659A-10-4	56	88.83	17.0000
108-659A-10-5	56	90.33	18.0000
108-659A-10-6	56	91.83	20.0000
108-659A-11-1	56	93.86	30.0000
108-659A-11-2	56	95.28	29.0000
108-659A-11-3	56	96.76	8.0000
108-659A-11-4	56	98.06	14.0000
108-659A-11-5	56	99.56	30.0000
108-659A-12-1	56	103.22	24.0000

Table 7 (continued).

Core/ section	Interval (cm)	Depth (m)	Vane shear strength (kPa)
108-659A-13-1	56	112.86	4.0000
108-659A-13-2	56	114.36	4.0000
108-659A-13-3	56	115.86	16.0000
108-659A-13-4	56	117.36	3.0000
108-659A-13-5	56	118.86	6.0000
108-659A-13-6	68	120.19	29.0000
108-659A-14-1	56	122.36	24.0000
108-659A-14-2	56	123.86	24.0000
108-659A-14-3	56	125.36	28.0000
108-659A-14-4	56	126.86	38.0000
108-659A-14-5	56	128.36	26.0000
108-659A-15-1	56	131.86	8.0000
108-659A-15-2	56	133.32	30.0000
108-659A-15-3	56	134.78	36.0000
108-659A-15-4	56	136.28	40.0000
108-659A-15-5	56	137.78	36.5000
108-659A-16-1	60	141.40	4.0000
108-659A-16-2	56	142.86	30.5000
108-659A-16-3	56	144.36	30.0000
108-659A-16-4	56	145.86	30.0000
108-659A-16-5	56	147.36	40.5000
108-659A-17-1	56	150.86	41.0000
108-659A-17-2	56	152.23	42.5000
108-659A-17-3	56	153.68	34.5000
108-659A-17-4	56	155.18	28.0000
108-659A-17-5	56	156.68	55.0000
108-659A-20-1	55	179.35	41.0000
108-659A-20-2	56	180.86	40.0000
108-659A-20-3	56	182.36	73.0000
108-659A-20-4	56	183.86	35.0000
108-659A-20-5	56	185.36	98.0000
108-659A-20-6	56	186.86	63.0000
108-659A-21-3	85	192.05	36.0000
108-659A-22-1	56	198.36	42.0000
108-659A-22-2	56	199.86	60.0000
108-659A-22-3	56	201.36	90.0000
108-659A-22-4	56	202.86	23.0000
108-659A-23-1	65	207.95	80.0000
108-659A-23-2	56	209.34	57.0000
108-659A-23-3	76	211.04	61.0000
108-659A-23-4	56	212.34	84.0000
108-659A-23-5	74	213.74	80.0000
108-659A-23-6	36	214.86	97.5000
108-659A-24-1	51	217.31	55.0000
108-659A-24-2	71	218.92	56.0000
108-659A-25-1	58	226.88	70.0000
108-659A-25-2	56	228.29	78.0000
108-659A-25-3	56	229.79	80.0000
108-659A-25-4	51	231.24	69.0000
108-659A-25-5	47	232.70	60.0000
108-659A-27-1	65	245.95	65.0000
108-659A-27-2	56	247.36	55.0000
108-659A-27-3	51	248.81	43.0000
108-659A-27-4	61	250.41	57.0000
108-659A-27-5	51	251.71	63.0000
108-659A-27-6	51	252.93	47.0000

Table 8. Compressional-wave-velocity data for Site 659.

Core/ section	Interval (cm)	Depth (mbsf)	*P*-wave velocity (km/s)
108-659A-1-1	50	0.50	1.3200
108-659A-1-1	130	1.30	1.5400
108-659A-1-2	90	2.00	1.8300
108-659A-1-3	50	3.50	1.5400
108-659A-1-3	130	4.30	1.8300
108-659A-1-4	50	5.00	1.5300
108-659A-1-5	50	6.50	1.5200
108-659A-1-5	75	6.75	1.5400
108-659A-1-5	90	6.90	1.5300
108-659A-1-5	130	7.30	1.5200
108-659A-2-1	50	8.30	1.3200
108-659A-2-1	120	9.00	1.5200
108-659A-2-2	50	9.80	1.5100
108-659A-2-3	50	11.30	1.5100
108-659A-2-4	50	12.80	1.5000
108-659A-2-5	50	14.30	1.5200
108-659A-3-1	50	17.80	1.5500
108-659A-3-2	50	19.30	1.5500
108-659A-3-2	50	19.30	1.5500
108-659A-3-3	70	21.00	1.5200
108-659A-3-3	110	21.40	1.5300
108-659A-3-4	50	22.30	1.5300
108-659A-3-5	50	23.80	1.5300
108-659A-3-6	50	25.30	1.5300
108-659A-3-6	100	25.70	1.5300
108-659A-3-6	112	25.82	1.5700
108-659A-4-1	50	27.30	1.5400
108-659A-4-1	50	27.60	1.5200
108-659A-4-2	50	28.78	1.5300
108-659A-4-2	95	29.23	1.5500
108-659A-4-2	140	29.68	1.5400
108-659A-4-3	50	30.28	1.5300
108-659A-4-4	50	31.78	1.5300
108-659A-5-1	50	36.80	1.5400
108-659A-5-1	120	37.50	1.5500
108-659A-5-2	50	38.30	1.5400
108-659A-5-2	120	39.00	1.5500
108-659A-5-3	20	39.50	1.5300
108-659A-5-3	60	39.90	1.5500
108-659A-5-3	140	40.70	1.5400
108-659A-5-4	50	41.30	1.5400
108-659A-5-5	50	42.80	1.5200
108-659A-5-6	50	44.30	1.5400
108-659A-7-1	120	56.50	1.5600
108-659A-7-2	50	57.28	1.5500
108-659A-7-2	120	57.98	1.5400
108-659A-7-3	30	58.58	1.5500
108-659A-7-3	50	58.78	1.5300
108-659A-7-4	50	60.28	1.5400
108-659A-7-5	50	61.78	1.5400
108-659A-7-5	85	62.13	1.5600
108-659A-7-5	100	62.28	1.5400
108-659A-7-6	20	62.98	1.5300
108-659A-7-6	60	63.38	1.5600
108-659A-7-6	80	63.58	1.5300
108-659A-7-7	30	64.58	1.5400
108-659A-8-1	50	65.30	1.5300
108-659A-8-1	70	65.50	1.5500
108-659A-8-2	50	66.52	1.5300
108-659A-8-3	50	68.02	1.5500
108-659A-8-3	90	68.42	1.5300
108-659A-8-3	110	68.62	1.5500
108-659A-8-3	130	68.82	1.5300
108-659A-8-4	30	69.32	1.5500
108-659A-8-4	95	69.97	1.5200
108-659A-8-4	140	70.42	1.5500
108-659A-8-5	35	70.87	1.5300
108-659A-8-5	45	70.97	1.5500
108-659A-8-5	140	71.92	1.5300
108-659A-8-6	70	72.72	1.5400
108-659A-9-1	50	74.80	1.5400
108-659A-9-1	140	75.70	1.5600
108-659A-9-2	10	75.90	1.5700
108-659A-9-2	50	76.30	1.5300
108-659A-9-2	65	76.45	1.5800
108-659A-9-2	85	76.65	1.5300

Table 8 (continued).

Core/ section	Interval (cm)	Depth (mbsf)	*P*-wave velocity (km/s)
108-659A-9-3	20	77.50	1.5300
108-659A-9-3	50	77.80	1.5600
108-659A-9-3	70	78.00	1.5300
108-659A-9-3	140	78.70	1.5400
108-659A-9-4	20	79.00	1.5200
108-659A-9-4	30	79.10	1.5300
108-659A-9-4	60	79.40	1.5200
108-659A-9-4	90	79.70	1.5300
108-659A-9-5	40	80.70	1.5400
108-659A-9-5	50	80.80	1.5300
108-659A-9-5	140	81.70	1.5400
108-659A-9-6	50	82.30	1.5300
108-659A-10-1	110	84.90	1.5400
108-659A-10-2	20	85.47	1.5600
108-659A-10-2	40	85.67	1.5400
108-659A-10-2	70	85.97	1.5600
108-659A-10-2	100	86.27	1.5700
108-659A-10-2	115	86.42	1.5300
108-659A-10-3	30	87.07	1.5300
108-659A-10-3	50	87.27	1.5500
108-659A-10-3	60	87.37	1.5300
108-659A-10-3	90	87.67	1.5600
108-659A-10-3	110	87.87	1.5200
108-659A-10-3	140	88.17	1.5700
108-659A-10-4	30	88.57	1.5300
108-659A-10-4	60	88.87	1.5600
108-659A-10-4	90	89.07	1.5300
108-659A-10-4	120	89.47	1.5500
108-659A-10-4	140	89.67	1.5300
108-659A-10-5	50	90.27	1.5300
108-659A-10-6	60	91.87	1.5400
108-659A-11-1	50	93.80	1.5400
108-659A-11-1	70	94.00	1.5600
108-659A-11-1	130	94.60	1.5300
108-659A-11-2	30	95.02	1.5400
108-659A-11-2	45	95.17	1.5800
108-659A-11-2	50	95.22	1.5500
108-659A-11-2	95	95.67	1.5800
108-659A-11-2	140	96.12	1.5600
108-659A-11-4	10	97.60	1.5500
108-659A-11-4	35	97.85	1.5700
108-659A-11-4	60	98.10	1.5400
108-659A-11-4	95	98.45	1.5700
108-659A-11-4	110	98.60	1.5400
108-659A-11-4	140	98.90	1.5600
108-659A-11-5	50	99.50	1.5400
108-659A-11-5	130	100.30	1.5500
108-659A-11-6	35	100.85	1.5700
108-659A-12-1	60	103.26	1.5700
108-659A-12-1	90	103.56	1.6000
108-659A-12-1	120	103.86	1.5700
108-659A-13-1	50	112.80	1.5500
108-659A-13-2	20	114.00	1.5500
108-659A-13-2	50	114.30	1.5300
108-659A-13-3	20	115.50	1.5300
108-659A-13-3	80	116.10	1.5600
108-659A-13-3	110	116.40	1.5300
108-659A-13-3	140	116.70	1.5500
108-659A-13-4	20	117.00	1.5700
108-659A-13-4	50	117.30	1.5400
108-659A-13-4	75	117.55	1.5600
108-659A-13-4	90	117.70	1.5400
108-659A-13-4	140	118.20	1.5600
108-659A-13-5	10	118.40	1.5500
108-659A-13-5	90	119.20	1.5700
108-659A-13-5	105	119.35	1.5800
108-659A-13-5	120	119.50	1.5500
108-659A-13-6	25	119.93	1.5600
108-659A-13-6	40	120.08	1.5300
108-659A-13-6	70	120.21	1.5400
108-659A-13-6	75	120.26	1.6000
108-659A-13-6	80	120.31	1.5400
108-659A-13-6	120	120.71	1.5400
108-659A-13-6	130	120.81	1.5800
108-659A-13-7	20	121.21	1.5700
108-659A-14-1	50	122.30	1.5500
108-659A-14-1	80	122.60	1.5800

Table 8 (continued).

Core/ section	Interval (cm)	Depth (mbsf)	*P*-wave velocity (km/s)
108-659A-14-1	140	123.20	1.5400
108-659A-14-2	50	123.80	1.5600
108-659A-14-2	130	124.60	1.5800
108-659A-14-3	40	125.20	1.5900
108-659A-14-3	80	125.60	1.5500
108-659A-14-3	140	126.20	1.5700
108-659A-14-4	20	126.50	1.5800
108-659A-14-4	50	126.80	1.5500
108-659A-14-4	70	127.00	1.5700
108-659A-14-4	85	127.15	1.5400
108-659A-14-4	140	127.70	1.5800
108-659A-14-5	10	127.90	1.5400
108-659A-14-5	50	128.30	1.5500
108-659A-14-5	90	128.70	1.5400
108-659A-14-5	110	128.90	1.6000
108-659A-14-5	130	129.10	1.5400
108-659A-14-6	40	129.70	1.5500
108-659A-15-1	80	132.10	1.5400
108-659A-15-1	105	132.35	1.5800
108-659A-15-1	140	132.70	1.5400
108-659A-15-2	50	133.26	1.5500
108-659A-15-3	10	134.32	1.5800
108-659A-15-3	40	134.62	1.5400
108-659A-15-3	100	135.22	1.5800
108-659A-15-3	110	135.32	1.5400
108-659A-15-3	130	135.52	1.5800
108-659A-15-4	50	136.22	1.5500
108-659A-15-4	75	136.47	1.5900
108-659A-15-5	10	137.32	1.5400
108-659A-15-5	10	137.32	1.5400
108-659A-15-5	30	137.52	1.5700
108-659A-15-5	40	137.62	1.5400
108-659A-15-5	90	138.12	1.5900
108-659A-15-5	100	138.22	1.5400
108-659A-16-1	50	141.30	1.5700
108-659A-16-1	65	141.45	1.5400
108-659A-16-1	100	141.80	1.6000
108-659A-16-1	105	141.85	1.6000
108-659A-16-2	10	142.40	1.5500
108-659A-16-2	80	143.10	1.5900
108-659A-16-2	120	143.50	1.5400
108-659A-16-3	20	144.00	1.5400
108-659A-16-3	120	145.00	1.5500
108-659A-16-4	60	145.90	1.5400
108-659A-16-4	80	146.10	1.5700
108-659A-16-4	120	146.50	1.5600
108-659A-16-5	30	147.10	1.5900
108-659A-16-5	60	147.40	1.5400
108-659A-16-6	10	148.40	1.5700
108-659A-16-6	40	148.70	1.5500
108-659A-17-1	50	150.80	1.5500
108-659A-17-1	70	151.00	1.5900
108-659A-17-1	90	151.20	1.5500
108-659A-17-1	115	151.45	1.6200
108-659A-17-2	8	151.75	1.5900
108-659A-17-2	20	151.87	1.5400
108-659A-17-2	40	152.07	1.5800
108-659A-17-2	130	152.97	1.5400
108-659A-17-3	10	153.22	1.5400
108-659A-17-3	25	153.37	1.5800
108-659A-17-3	60	153.72	1.5500
108-659A-17-4	10	154.72	1.5500
108-659A-17-4	30	154.92	1.5800
108-659A-17-4	50	155.12	1.5400
108-659A-17-5	40	156.52	1.5500

Table 8 (continued).

Core/ section	Interval (cm)	Depth (mbsf)	*P*-wave velocity (km/s)
108-659A-17-5	68	156.80	1.5800
108-659A-17-5	90	157.02	1.5400
108-659A-17-5	115	157.27	1.5800
108-659A-17-5	120	157.42	1.5500
108-659A-20-1	10	178.90	1.5800
108-659A-20-1	40	179.20	1.6000
108-659A-20-2	20	180.50	1.5900
108-659A-20-2	45	180.75	1.6200
108-659A-20-2	55	180.85	1.5900
108-659A-20-2	65	180.95	1.6400
108-659A-20-2	80	181.10	1.5900
108-659A-20-2	85	181.15	1.6400
108-659A-20-2	100	181.30	1.5800
108-659A-20-2	140	181.70	1.5800
108-659A-20-3	20	182.00	1.6000
108-659A-20-3	35	182.15	1.6100
108-659A-20-3	45	182.25	1.5800
108-659A-20-3	70	182.50	1.6000
108-659A-20-3	110	182.90	1.5800
108-659A-20-3	125	183.05	1.6100
108-659A-20-4	15	183.45	1.6500
108-659A-20-4	30	183.60	1.5800
108-659A-20-4	70	184.00	1.6300
108-659A-20-4	85	184.15	1.5800
108-659A-20-4	95	184.25	1.6200
108-659A-20-4	100	184.30	1.5700
108-659A-20-4	120	184.50	1.6300
108-659A-20-4	140	184.70	1.5700
108-659A-20-5	20	185.00	1.5900
108-659A-20-5	55	185.35	1.6700
108-659A-20-5	70	185.50	1.5900
108-659A-20-5	115	185.95	1.6200
108-659A-20-5	120	186.00	1.5900
108-659A-20-5	140	186.20	1.6100
108-659A-20-6	10	186.40	1.6400
108-659A-20-6	20	186.50	1.6100
108-659A-20-7	10	187.90	1.6600
108-659A-20-7	30	188.10	1.6300
108-659A-21-1	50	188.80	1.5600
108-659A-21-2	80	190.60	1.5500
108-659A-21-3	70	191.90	1.5500
108-659A-21-3	85	192.05	1.6200
108-659A-22-1	10	197.90	1.6000
108-659A-22-1	90	198.70	1.6000
108-659A-22-1	105	198.85	1.6300
108-659A-22-1	125	199.05	1.6000
108-659A-22-1	140	199.20	1.6300
108-659A-22-2	20	199.50	1.6200
108-659A-22-3	50	201.30	1.6300
108-659A-22-4	20	202.50	1.6000
108-659A-22-4	60	202.90	1.6500
108-659A-22-4	85	203.15	1.5700
108-659A-22-4	105	203.35	1.6400
108-659A-22-4	125	203.55	1.6100
108-659A-22-5	10	203.90	1.6500
108-659A-22-5	35	204.15	1.5900
108-659A-23-1	35	207.65	1.5900
108-659A-23-1	125	208.55	1.6300
108-659A-23-2	10	208.88	1.6600
108-659A-32-2	50	209.28	1.6300
108-659A-23-2	90	209.68	1.6800
108-659A-23-2	115	209.93	1.6000
108-659A-23-3	70	210.98	1.6200
108-659A-23-3	130	211.58	1.6900
108-659A-23-4	70	212.48	1.6400

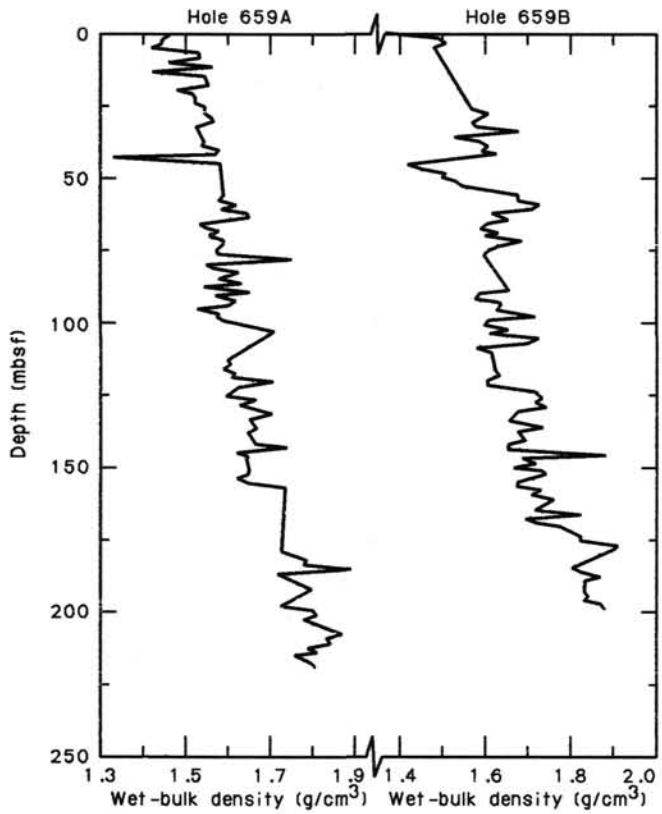

Figure 21. Wet-bulk-density profiles.

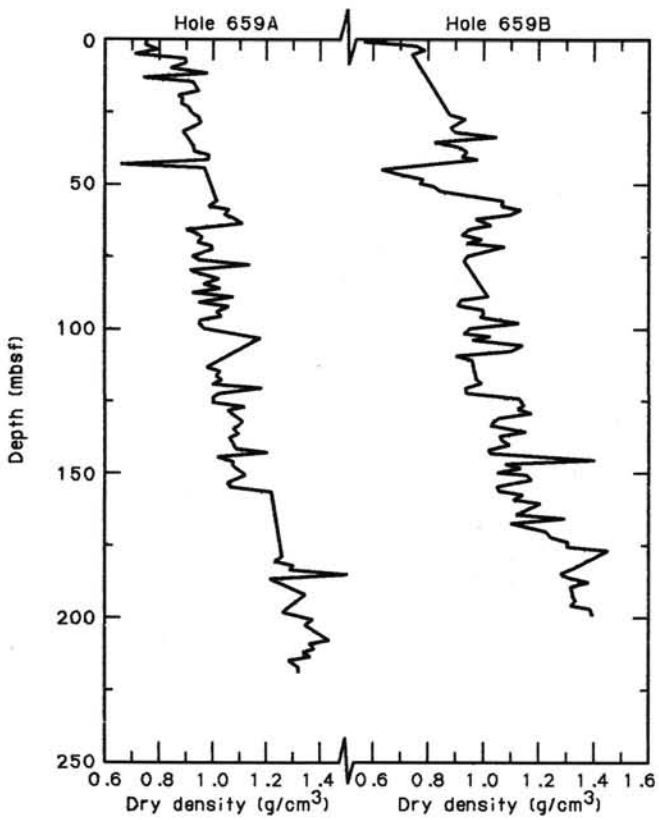

Figure 22. Dry-density profiles.

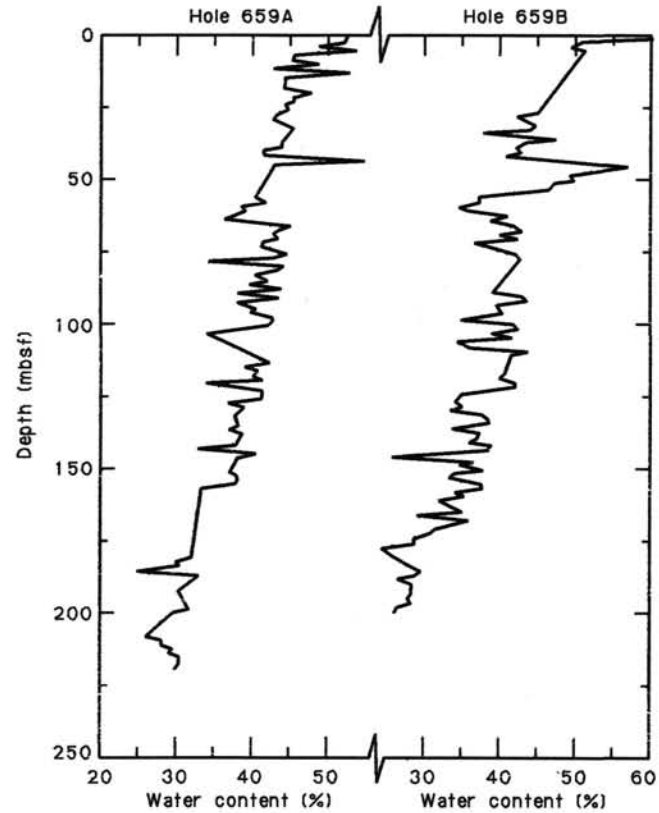

Figure 23. Water-content profiles.

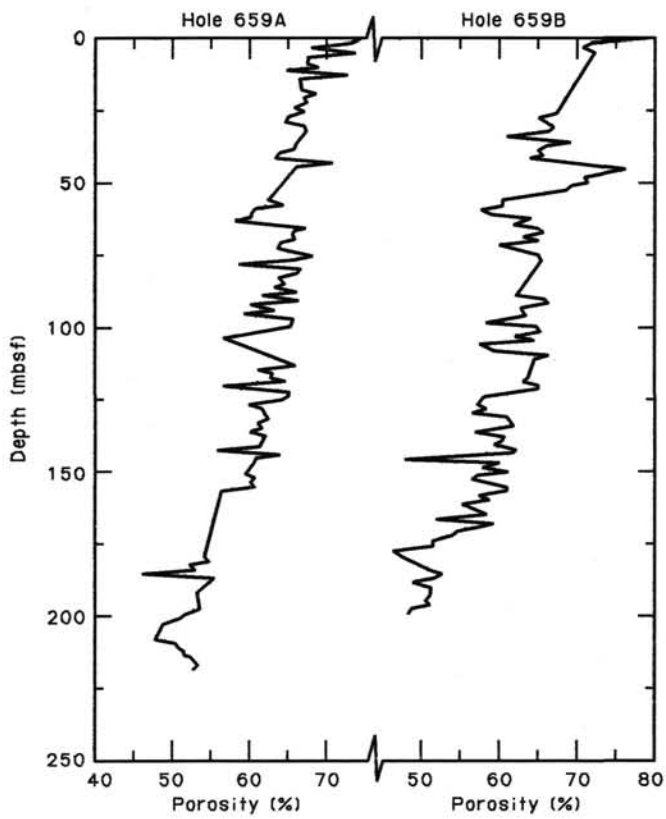

Figure 24. Porosity profiles.

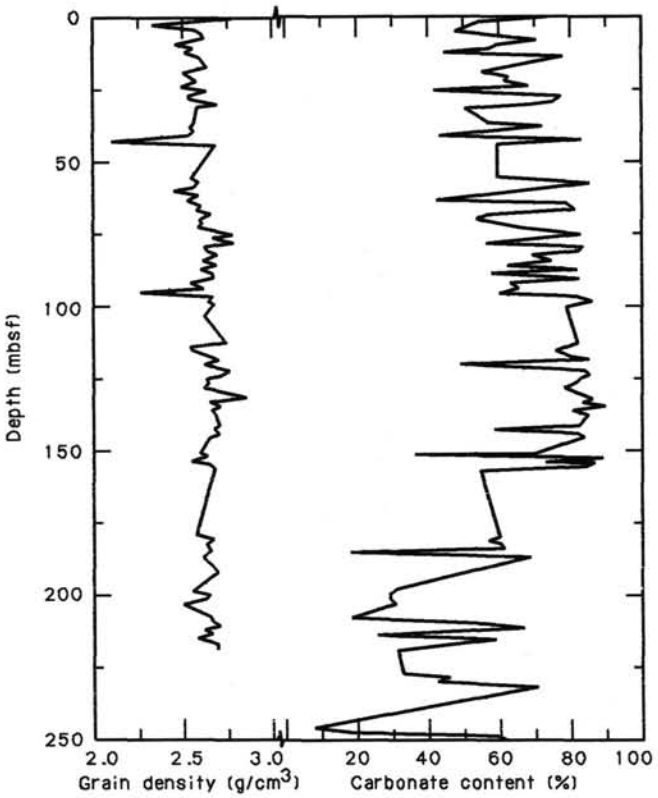

Figure 25. Grain-density and carbonate-content profiles for Hole 659A.

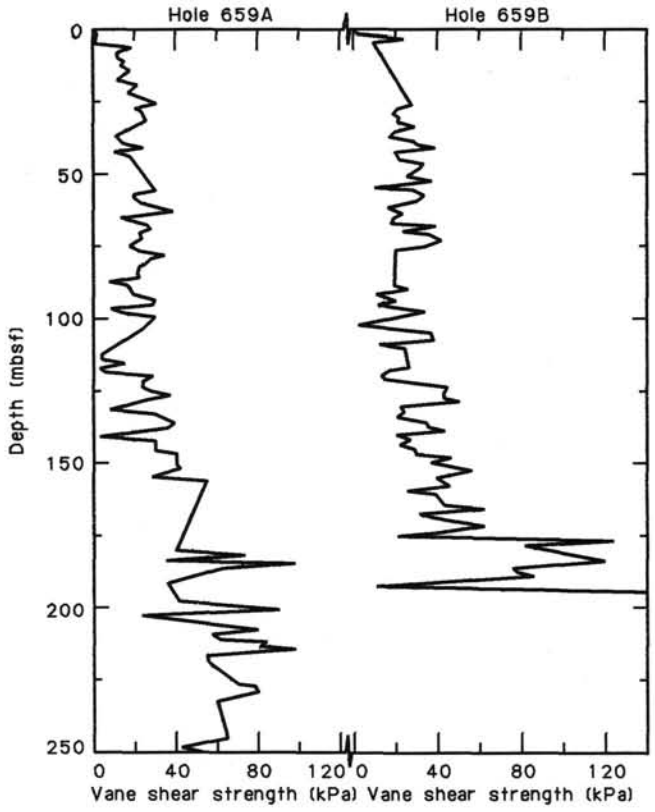

Figure 26. Vane-shear-strength profiles.

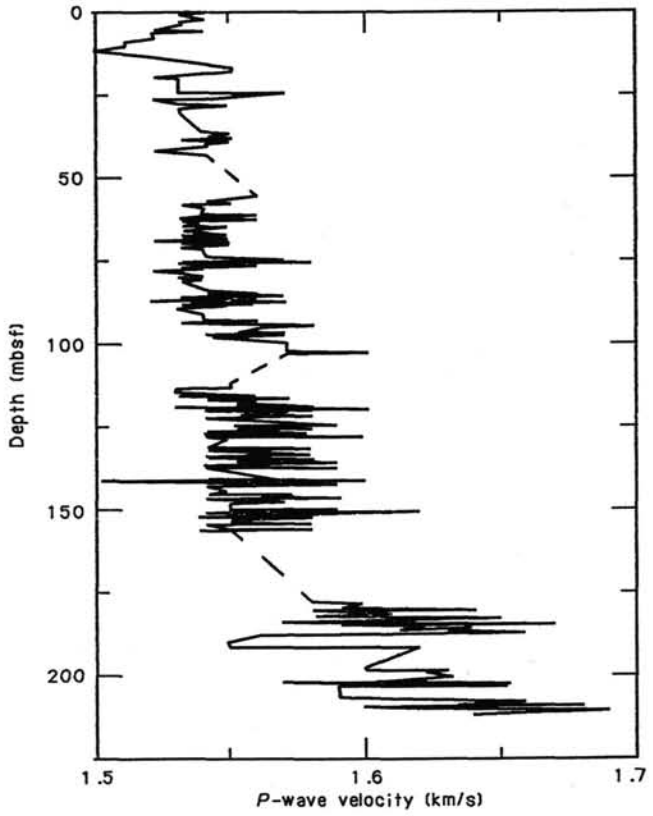

Figure 27. *P*-wave-logger velocity profile for Hole 659A.

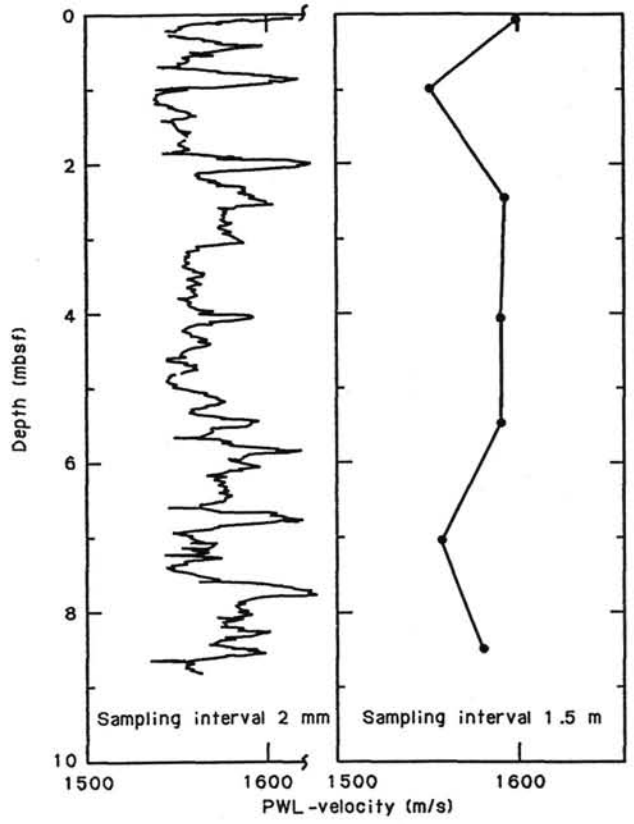

Figure 28. *P*-wave-velocity profile for Core 108-659B-19H.

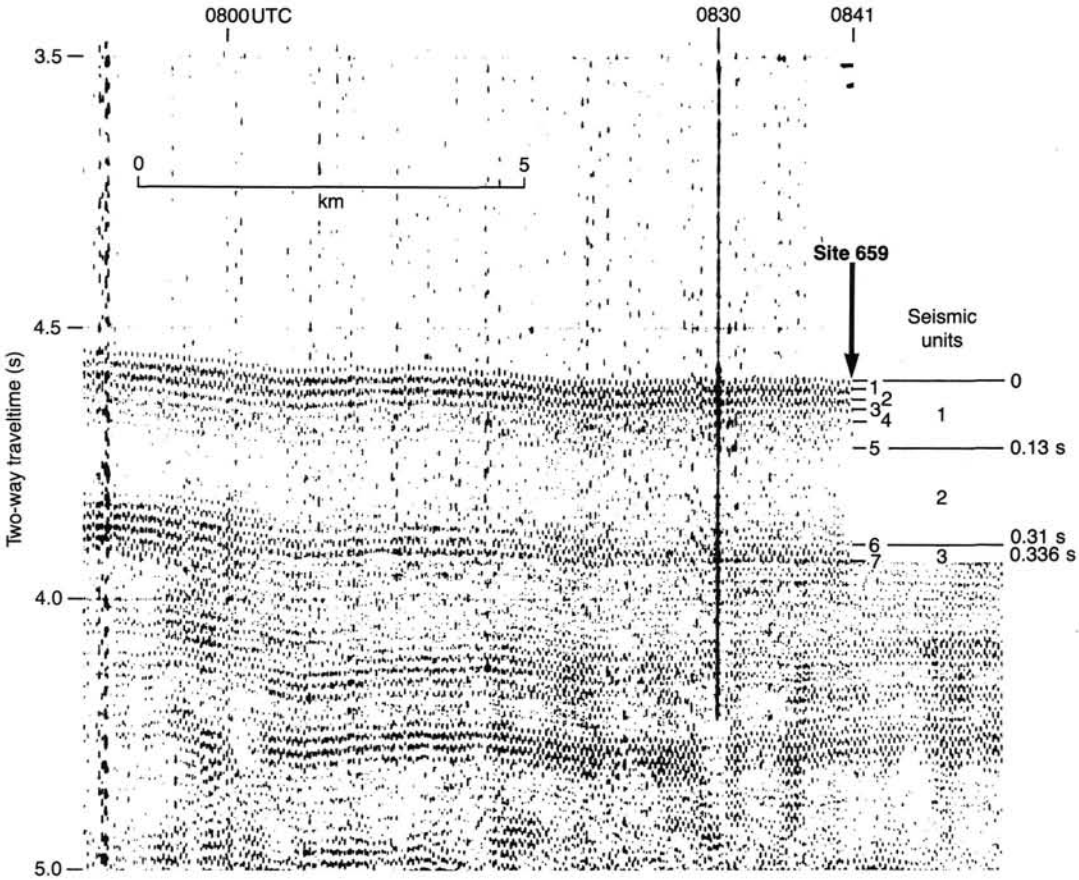

Figure 29. A 20- to 500-Hz reflection profile over Site 659 showing the seismic sequence described in the text and in Table 9.

Table 9. The 20- to 500-Hz seismic correlations at Site 659.

Base of seismic unit no.		Reflectors (sbsf)	Depth (m) relative to preceding reflector 1530 m/s	1550 m/s	1575 m/s	1650 m/s	Cumulative depth (mbsf)	Source	Age (Ma)	Lithologic unit
	1	0.0183	14.0				14.0			
	2	0.0366	14.0				28.0	Artifacts		
1	3	0.058	16.5				44.5	Interference of frequent $CaCO_3$ fluctuations		IA
	4	0.074	12.25				56.75			
	5	0.130 (weak)		43.5			100.25	Top of ± persistent high $CaCO_3$	3.3	IB + IIA
2		(0.290)			(126.0)		(226.0)			
	6	0.310				16.0	242.0	?Hiatus	18–23	IIB
3	7	0.336				22.0	264.0	?Oligocene/Miocene boundary		

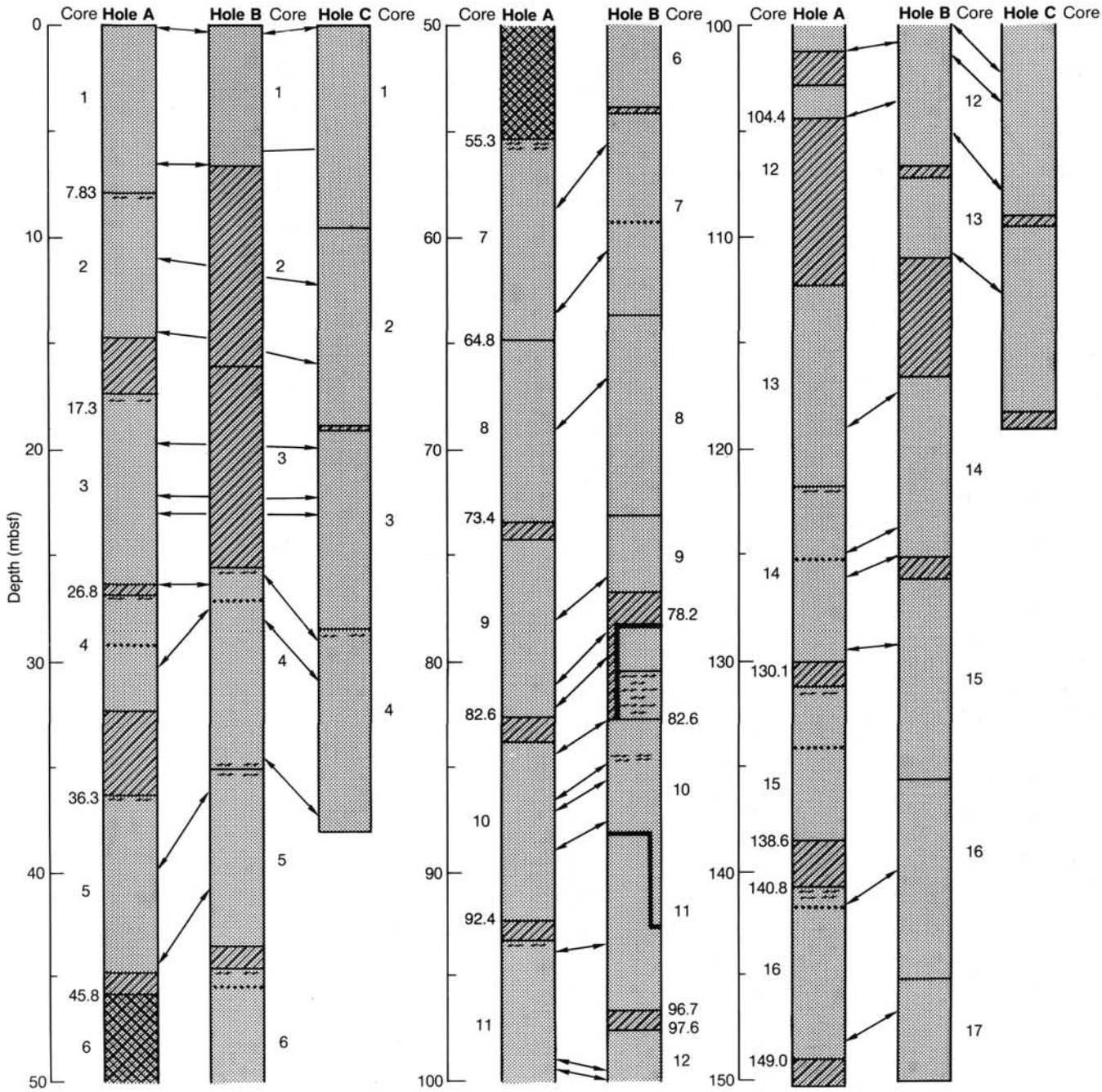

Figure 30. Depth correlation among Holes 659A, 659B, and 659C. Nominal depth below seafloor of penetration and core numbers appear along the graphs of the single holes.

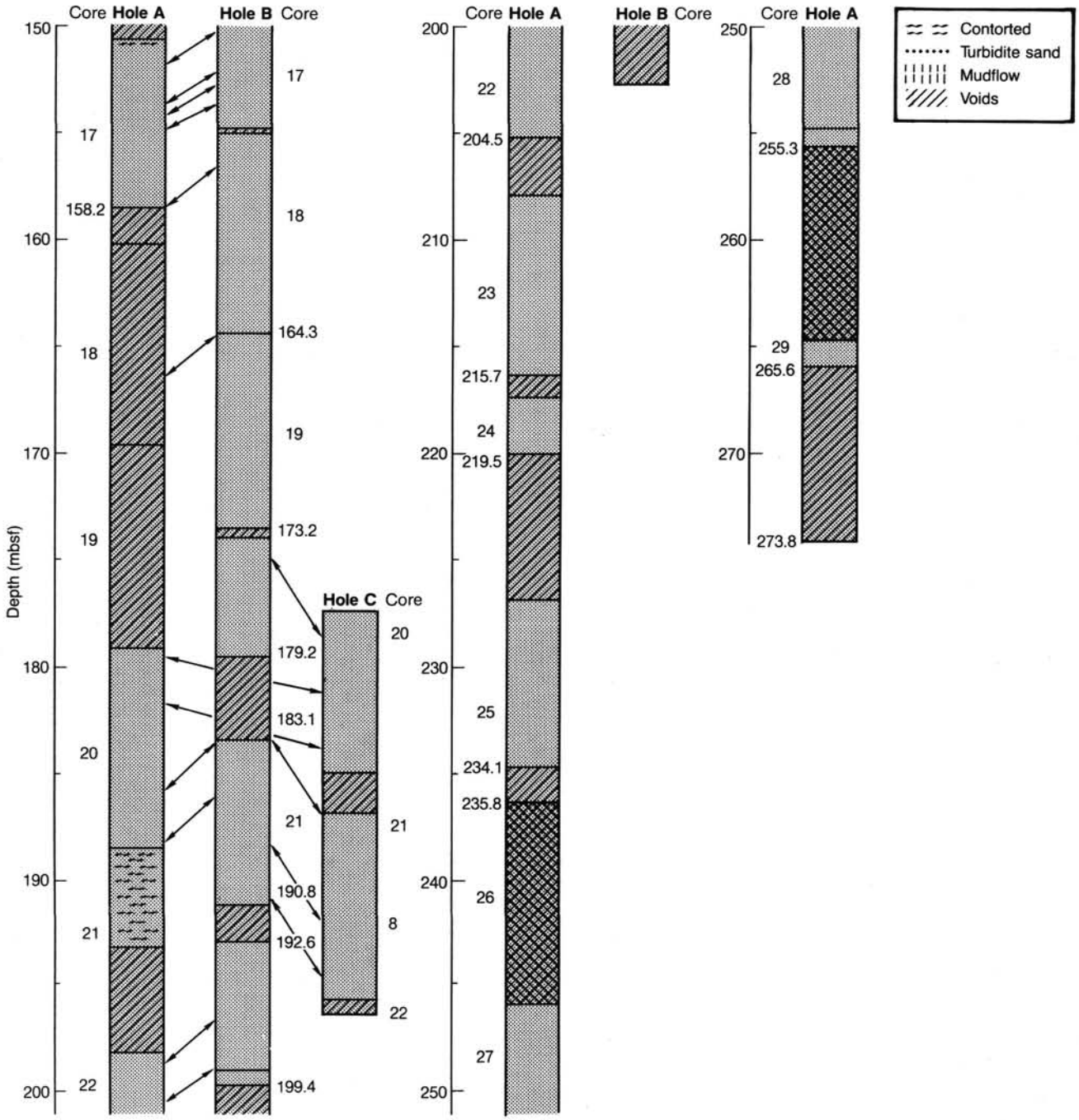

Figure 30 (continued).

Table 10. Composite-depth levels used to correlate cores from Hole 659A, 659B, and 659C.

Nominal depth (mbsf)			Composite depth (mbsf)
Hole 659A	Hole 659B	Hole 659C	
	0		0
0	0.25	0	0.25
	3.0	3.0	3.0
	5.9	5.9	5.9
6.5	6.5		6.5
11.0		12.1	11.0
14.3		15.8	14.3
19.6		19.9	19.6
22.2		22.25	22.2
23.0		23.0	23.0
26.3		26.3	26.3
	26.0	29.0	29.0
30.0	27.5		30.0
	28.0	30.75	30.5
	34.5	37.2	37.0
39.8	36.0		39.8
44.4	40.7		44.4
58.5	55.5		58.5
63.5	60.5		63.5
69.0	66.5		69.0
78.0	76.0		78.0
81.0	[a](82.9)		81.0
	[b]78.5		
82.2	(84.15)		82.2
	79.75		
84.5	(87.25)		84.5
	[b]82.85		
87.1	(90.0)		87.1
	[b]85.6		
89.0	(92.0)		89.0
	[b]87.6		
93.8	?93.5		93.8
98.8	99.5	102.0	98.8
99.4	100.0		99.4
101.25	100.75		100.25
	101.0	103.4	100.5
104.3	103.5		104.5
	104.75	107.5	105.75
	110.5	112.5	
119.0	117.25		119.0
124.4	123.2		124.4
126.0	125.0		125.0
129.5	129.2		129.5
141.5	140.0		141.5
148.0	146.5		148.0
151.5	149.75		151.5
153.25	151.75		153.25
154.5	153.25		154.5
158.0	156.2		158.0
	174.5	178.0	176.9
179.2		180.8	179.2
181.3		183.4	181.3
185.5	183.1	186.7	185.5
188.0	185.7		188.0
	188.0	191.5	190.3
	190.4	194.25	192.7
198.25	196.25		198.25
200.0	198.5		200.0

[a] ( ) = nominal depths in Core 108-659B-10H.
[b] Rearranged depths in Core 108-659B-10H, based on between-hole correlations.
Note: Composite-depth levels are mostly equal to depths in Hole 659A.

SITE 659 HOLE A CORE 1 H CORED INTERVAL 3071.2-3079.0 mbsl; 0-7.8 mbsf

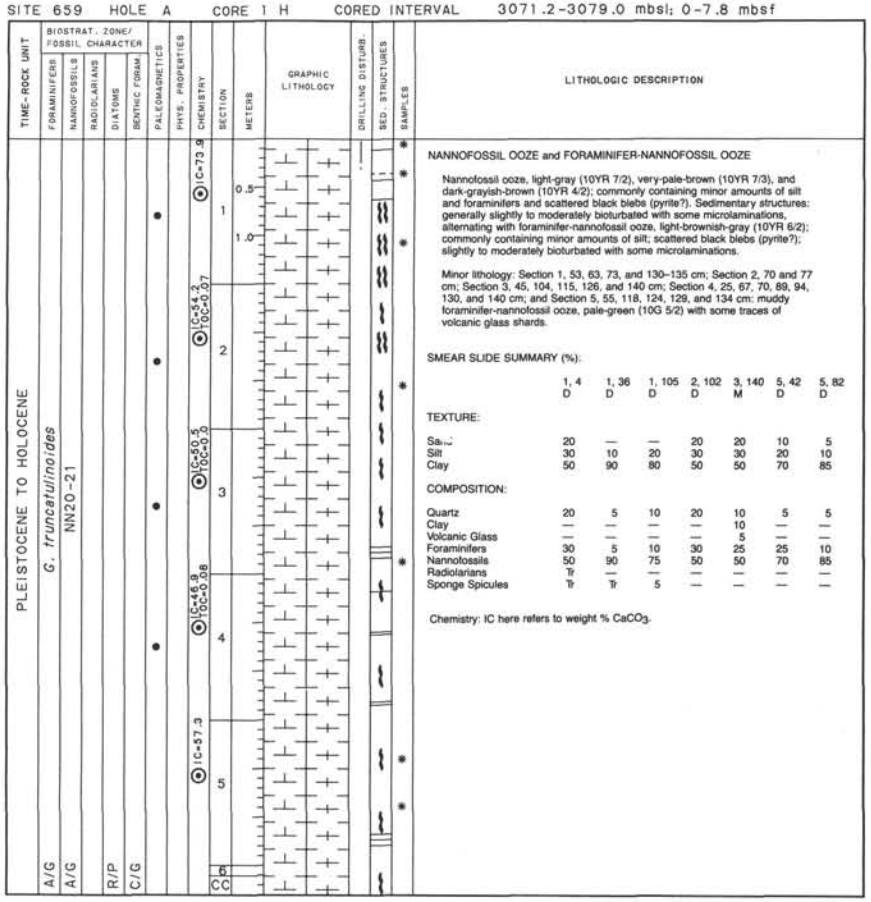

LITHOLOGIC DESCRIPTION

NANNOFOSSIL OOZE and FORAMINIFER-NANNOFOSSIL OOZE

Nannofossil ooze, light-gray (10YR 7/2), very-pale-brown (10YR 7/3), and dark-grayish-brown (10YR 4/2); commonly containing minor amounts of silt and foraminifers and scattered black blebs (pyrite?). Sedimentary structures: generally slightly to moderately bioturbated with some microlaminations, alternating with foraminifer-nannofossil ooze, light-brownish-gray (10YR 6/2); commonly containing minor amounts of silt; scattered black blebs (pyrite?); slightly to moderately bioturbated with some microlaminations.

Minor lithology: Section 1, 53, 63, 73, and 130–135 cm; Section 2, 70 and 77 cm; Section 3, 45, 104, 115, 126, and 140 cm; Section 4, 25, 67, 70, 89, 94, 130, and 140 cm; and Section 5, 55, 118, 124, 129, and 134 cm: muddy foraminifer-nannofossil ooze, pale-green (10G 5/2) with some traces of volcanic glass shards.

SMEAR SLIDE SUMMARY (%):

	1, 4 D	1, 36 D	1, 105 D	2, 102 D	3, 140 M	5, 42 D	5, 82 D
TEXTURE:							
Sand	20	—	—	20	20	10	5
Silt	30	10	20	30	30	20	10
Clay	50	90	80	50	50	70	85
COMPOSITION:							
Quartz	20	5	10	20	10	5	5
Clay	—	—	—	—	10	—	—
Volcanic Glass	—	—	—	—	5	—	—
Foraminifers	30	5	10	30	25	25	10
Nannofossils	50	90	75	50	50	70	85
Radiolarians	Tr	—	—	—	—	—	—
Sponge Spicules	Tr	Tr	5	—	—	—	—

Chemistry: IC here refers to weight % $CaCO_3$.

SITE 659 HOLE A CORE 2 H CORED INTERVAL 3079.0-3088.5 mbsl; 7.8-17.3 mbsf

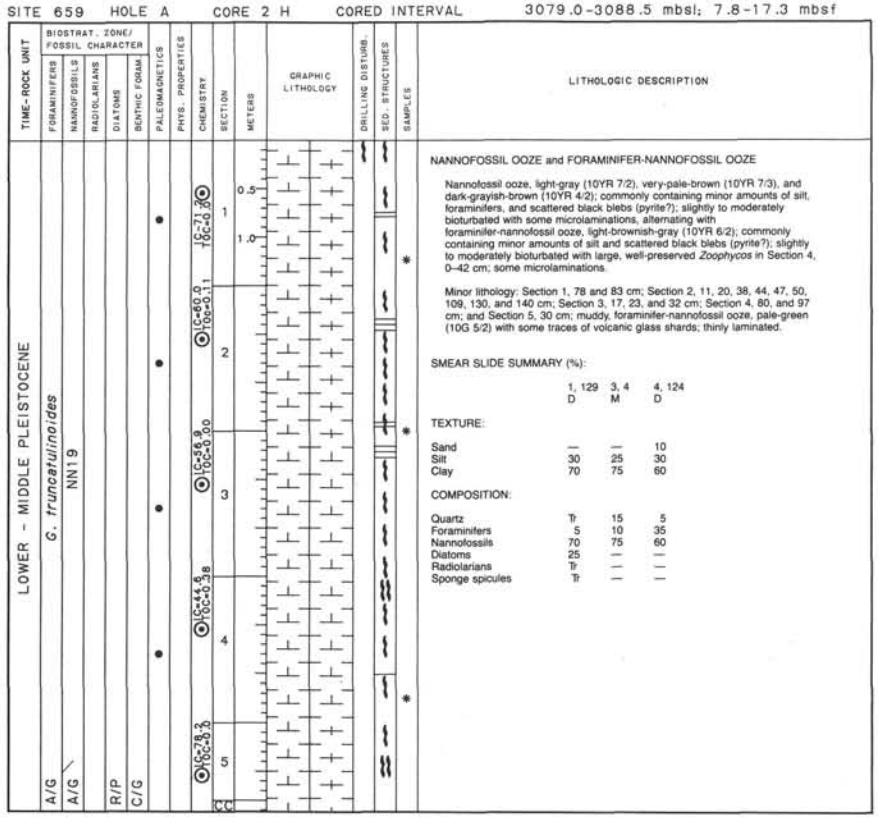

LITHOLOGIC DESCRIPTION

NANNOFOSSIL OOZE and FORAMINIFER-NANNOFOSSIL OOZE

Nannofossil ooze, light-gray (10YR 7/2), very-pale-brown (10YR 7/3), and dark-grayish-brown (10YR 4/2); commonly containing minor amounts of silt, foraminifers, and scattered black blebs (pyrite?); slightly to moderately bioturbated with some microlaminations, alternating with foraminifer-nannofossil ooze, light-brownish-gray (10YR 6/2); commonly containing minor amounts of silt and scattered black blebs (pyrite?); slightly to moderately bioturbated with large, well-preserved *Zoophycos* in Section 4, 0–42 cm; some microlaminations.

Minor lithology: Section 1, 78 and 83 cm; Section 2, 11, 20, 38, 44, 47, 50, 109, 130, and 140 cm; Section 3, 17, 23, and 32 cm; Section 4, 80, and 97 cm; and Section 5, 30 cm; muddy, foraminifer-nannofossil ooze, pale-green (10G 5/2) with some traces of volcanic glass shards; thinly laminated.

SMEAR SLIDE SUMMARY (%):

	1, 129 D	3, 4 M	4, 124 D
TEXTURE:			
Sand	—	—	10
Silt	30	25	30
Clay	70	75	60
COMPOSITION:			
Quartz	Tr	15	5
Foraminifers	5	10	35
Nannofossils	70	75	60
Diatoms	25	—	—
Radiolarians	Tr	—	—
Sponge spicules	Tr	—	—

SITE 659 HOLE A CORE 3 H CORED INTERVAL 3088.5-3098.0 mbsl; 17.3-26.8 mbsf

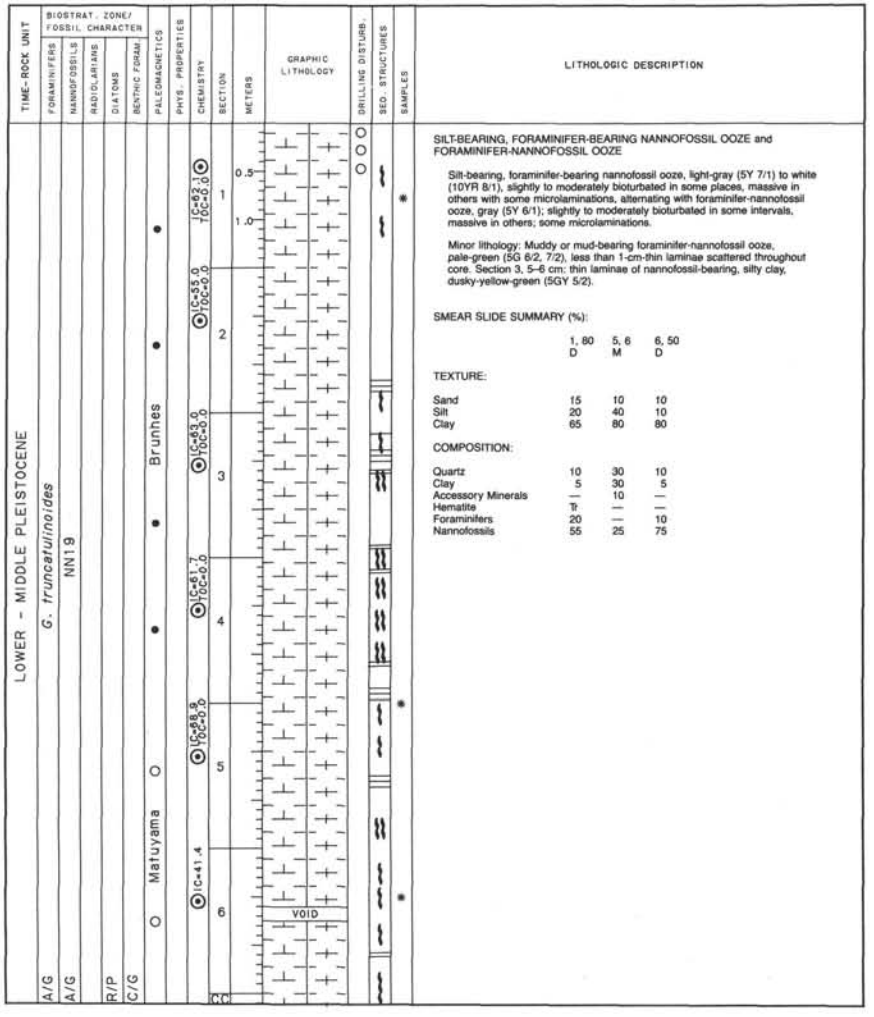

LITHOLOGIC DESCRIPTION

SILT-BEARING, FORAMINIFER-BEARING NANNOFOSSIL OOZE and FORAMINIFER-NANNOFOSSIL OOZE

Silt-bearing, foraminifer-bearing nannofossil ooze, light-gray (5Y 7/1) to white (10YR 8/1), slightly to moderately bioturbated in some places, massive in others with some microlaminations, alternating with foraminifer-nannofossil ooze, gray (5Y 6/1); slightly to moderately bioturbated in some intervals, massive in others; some microlaminations.

Minor lithology: Muddy or mud-bearing foraminifer-nannofossil ooze, pale-green (5G 6/2, 7/2), less than 1-cm-thin laminae scattered throughout core. Section 3, 5–6 cm: thin laminae of nannofossil-bearing, silty clay, dusky-yellow-green (5GY 5/2).

SMEAR SLIDE SUMMARY (%):

	1, 80 D	5, 6 M	6, 50 D
TEXTURE:			
Sand	15	10	10
Silt	20	40	10
Clay	65	80	80
COMPOSITION:			
Quartz	10	30	10
Clay	5	30	5
Accessory Minerals	—	10	—
Hematite	tr	tr	—
Foraminifers	20	—	10
Nannofossils	55	25	75

SITE 659 HOLE A CORE 4 H CORED INTERVAL 3098.0-3107.5 mbsl; 26.8-36.3 mbsf

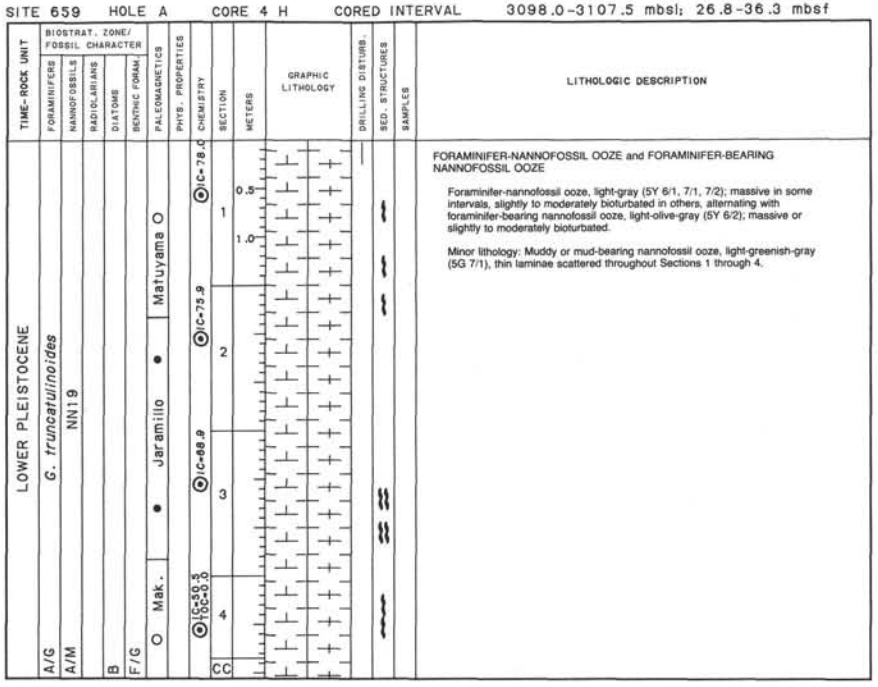

LITHOLOGIC DESCRIPTION

FORAMINIFER-NANNOFOSSIL OOZE and FORAMINIFER-BEARING NANNOFOSSIL OOZE

Foraminifer-nannofossil ooze, light-gray (5Y 6/1, 7/1, 7/2); massive in some intervals, slightly to moderately bioturbated in others, alternating with foraminifer-bearing nannofossil ooze, light-olive-gray (5Y 6/2); massive or slightly to moderately bioturbated.

Minor lithology: Muddy or mud-bearing nannofossil ooze, light-greenish-gray (5G 7/1), thin laminae scattered throughout Sections 1 through 4.

SITE 659 HOLE A CORE 5 H CORED INTERVAL 3107.5-3117.0 mbsl; 36.3-45.8 mbsf

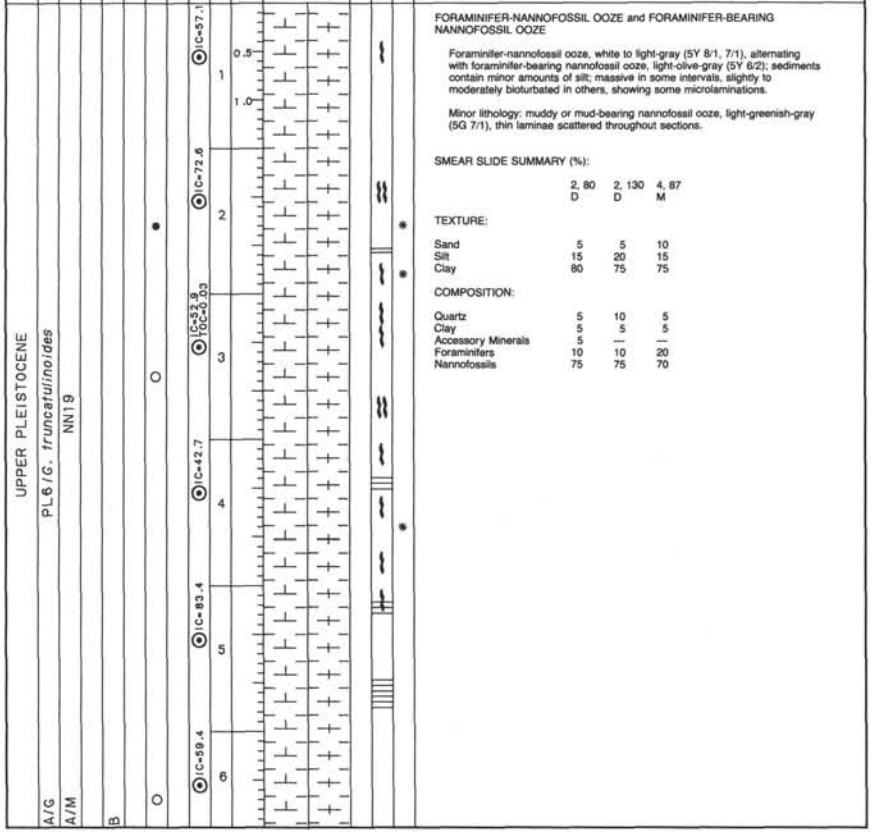

LITHOLOGIC DESCRIPTION

FORAMINIFER-NANNOFOSSIL OOZE and FORAMINIFER-BEARING NANNOFOSSIL OOZE

Foraminifer-nannofossil ooze, white to light-gray (5Y 8/1, 7/1), alternating with foraminifer-bearing nannofossil ooze, light-olive-gray (5Y 6/2); sediments contain minor amounts of silt; massive in some intervals, slightly to moderately bioturbated in others, showing some microlaminations.

Minor lithology: muddy or mud-bearing nannofossil ooze, light-greenish-gray (5G 7/1), thin laminae scattered throughout sections.

SMEAR SLIDE SUMMARY (%):

	2, 80 D	2, 130 D	4, 87 M
TEXTURE:			
Sand	5	5	10
Silt	15	20	15
Clay	80	75	75
COMPOSITION:			
Quartz	5	10	5
Clay	5	5	5
Accessory Minerals	5	—	—
Foraminifers	10	10	20
Nannofossils	75	75	70

CORE 6H NO RECOVERY

SITE 659 HOLE A CORE 7 H CORED INTERVAL 3126.5-3136.0 mbsl; 55.3-64.8 mbsf

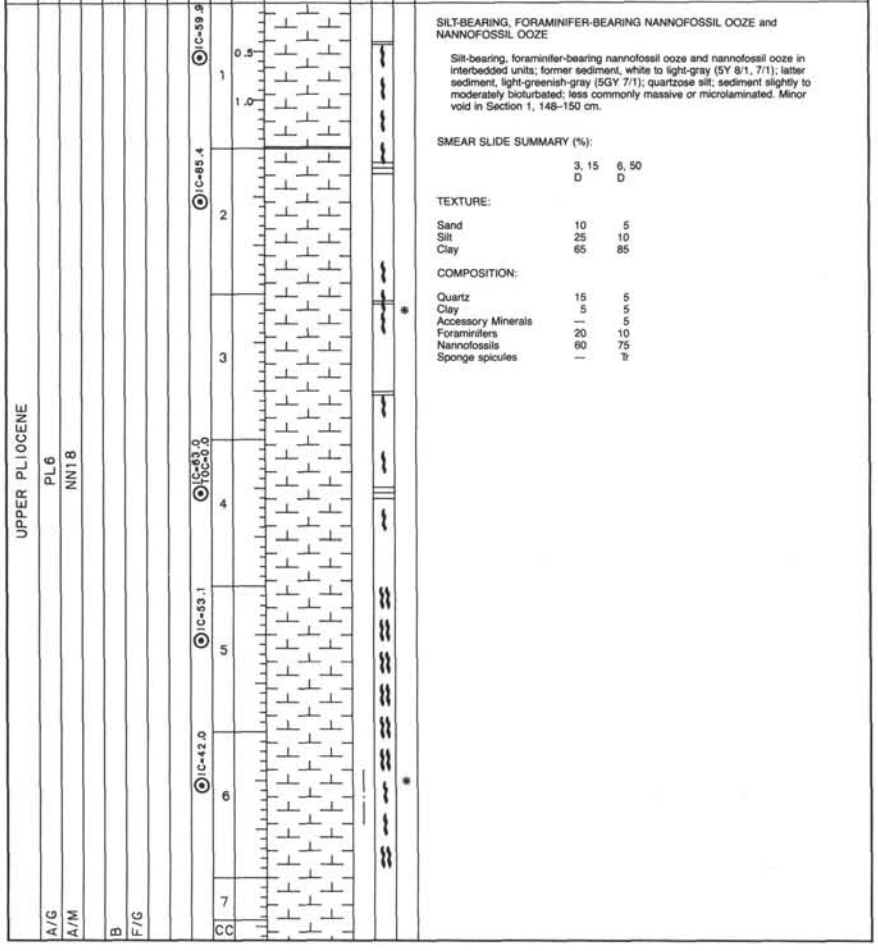

LITHOLOGIC DESCRIPTION

SILT-BEARING, FORAMINIFER-BEARING NANNOFOSSIL OOZE and NANNOFOSSIL OOZE

Silt-bearing, foraminifer-bearing nannofossil ooze and nannofossil ooze in interbedded units; former sediment, white to light-gray (5Y 8/1, 7/1); latter sediment, light-greenish-gray (5GY 7/1); quartzose silt; sediment slightly to moderately bioturbated; less commonly massive or microlaminated. Minor void in Section 1, 148–150 cm.

SMEAR SLIDE SUMMARY (%):

	3, 15 D	6, 50 D
TEXTURE:		
Sand	10	5
Silt	25	10
Clay	65	85
COMPOSITION:		
Quartz	15	5
Clay	5	5
Accessory Minerals	—	5
Foraminifers	20	10
Nannofossils	60	75
Sponge spicules	—	tr

SITE 659 HOLE A CORE 8 H CORED INTERVAL 3136.0-3145.5 mbsl; 64.8-74.3 mbsf

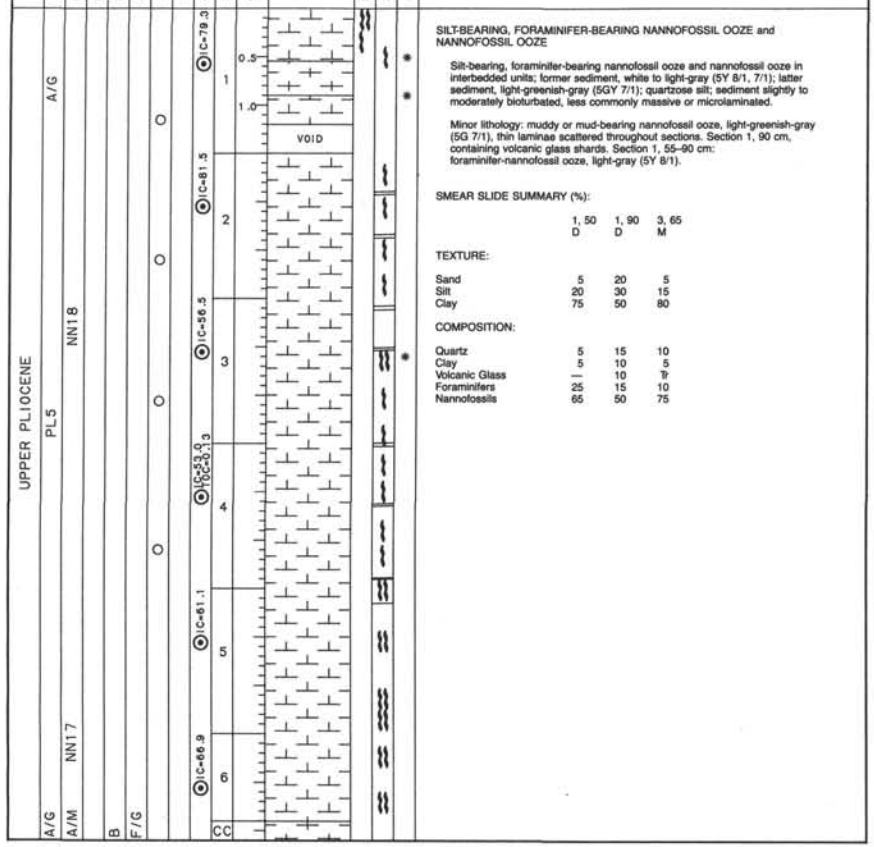

LITHOLOGIC DESCRIPTION

SILT-BEARING, FORAMINIFER-BEARING NANNOFOSSIL OOZE and NANNOFOSSIL OOZE

Silt-bearing, foraminifer-bearing nannofossil ooze and nannofossil ooze in interbedded units; former sediment, white to light-gray (5Y 8/1, 7/1); latter sediment, light-greenish-gray (5GY 7/1); quartzose silt; sediment slightly to moderately bioturbated, less commonly massive or microlaminated.

Minor lithology: muddy or mud-bearing nannofossil ooze, light-greenish-gray (5G 7/1), thin laminae scattered throughout sections. Section 1, 90 cm, containing volcanic glass shards. Section 1, 55–90 cm: foraminifer-nannofossil ooze, light-gray (5Y 8/1).

SMEAR SLIDE SUMMARY (%):

	1, 50 D	1, 90 D	3, 65 M
TEXTURE:			
Sand	5	20	5
Silt	20	30	15
Clay	75	50	80
COMPOSITION:			
Quartz	5	15	10
Clay	5	10	5
Volcanic Glass	—	10	Tr
Foraminifers	25	15	10
Nannofossils	65	50	75

SITE 659 HOLE A CORE 9 H CORED INTERVAL 3145.5-3155.0 mbsl; 74.3-85.8 mbsf

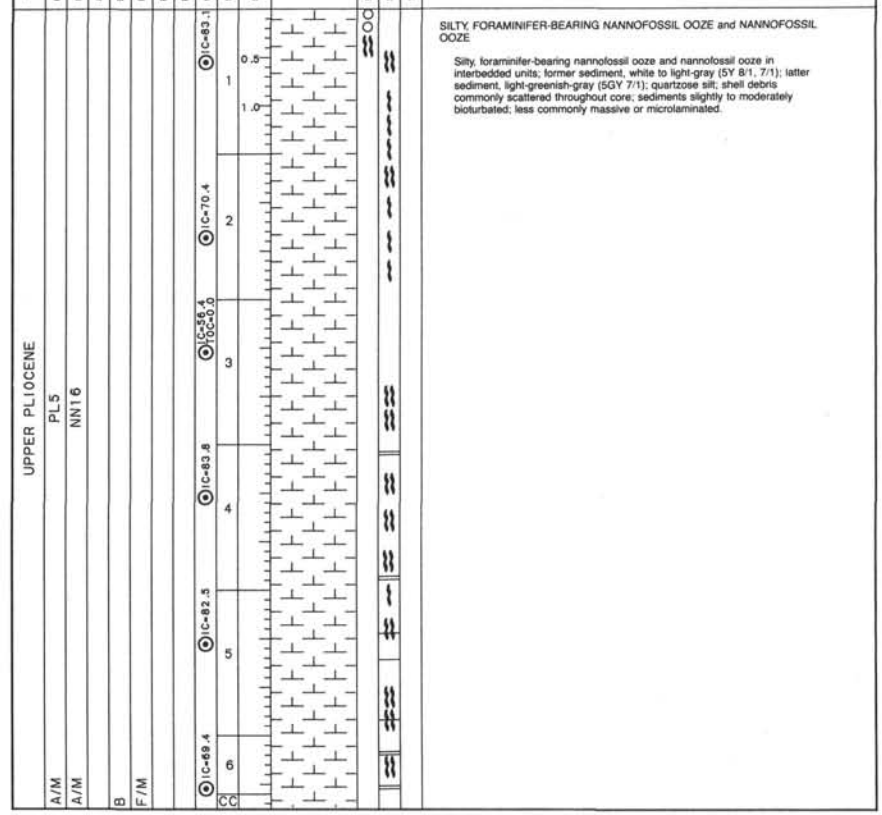

LITHOLOGIC DESCRIPTION

SILTY, FORAMINIFER-BEARING NANNOFOSSIL OOZE and NANNOFOSSIL OOZE

Silty, foraminifer-bearing nannofossil ooze and nannofossil ooze in interbedded units; former sediment, white to light-gray (5Y 8/1, 7/1); latter sediment, light-greenish-gray (5GY 7/1); quartzose silt; shell debris commonly scattered throughout core; sediments slightly to moderately bioturbated; less commonly massive or microlaminated.

SITE 659 HOLE A CORE 10 H CORED INTERVAL 3155.0-3164.5 mbsl; 83.8-93.3 mbsf

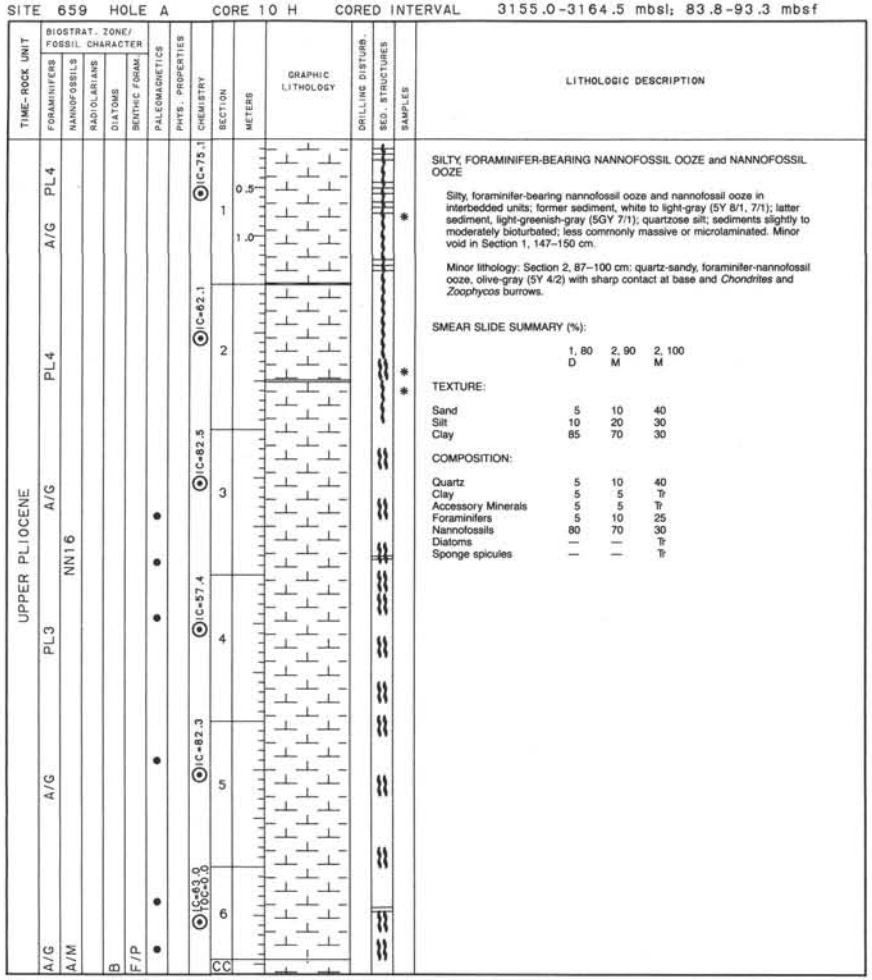

LITHOLOGIC DESCRIPTION

SILTY, FORAMINIFER-BEARING NANNOFOSSIL OOZE and NANNOFOSSIL OOZE

Silty, foraminifer-bearing nannofossil ooze and nannofossil ooze in interbedded units; former sediment, white to light-gray (5Y 8/1, 7/1); latter sediment, light-greenish-gray (5GY 7/1); quartzose silt; sediments slightly to moderately bioturbated; less commonly massive or microlaminated. Minor void in Section 1, 147–150 cm.

Minor lithology: Section 2, 87–100 cm: quartz-sandy, foraminifer-nannofossil ooze, olive-gray (5Y 4/2) with sharp contact at base and *Chondrites* and *Zoophycos* burrows.

SMEAR SLIDE SUMMARY (%):

	1, 80 D	2, 90 M	2, 100 M
TEXTURE:			
Sand	5	10	40
Silt	10	20	30
Clay	85	70	30
COMPOSITION:			
Quartz	5	10	40
Clay	5	5	Tr
Accessory Minerals	5	5	Tr
Foraminifers	5	10	25
Nannofossils	80	70	30
Diatoms	—	—	Tr
Sponge spicules	—	—	Tr

SITE 659 HOLE A CORE 11 H CORED INTERVAL 3164.5-3174.0 mbsl; 93.3-102.8 mbsf

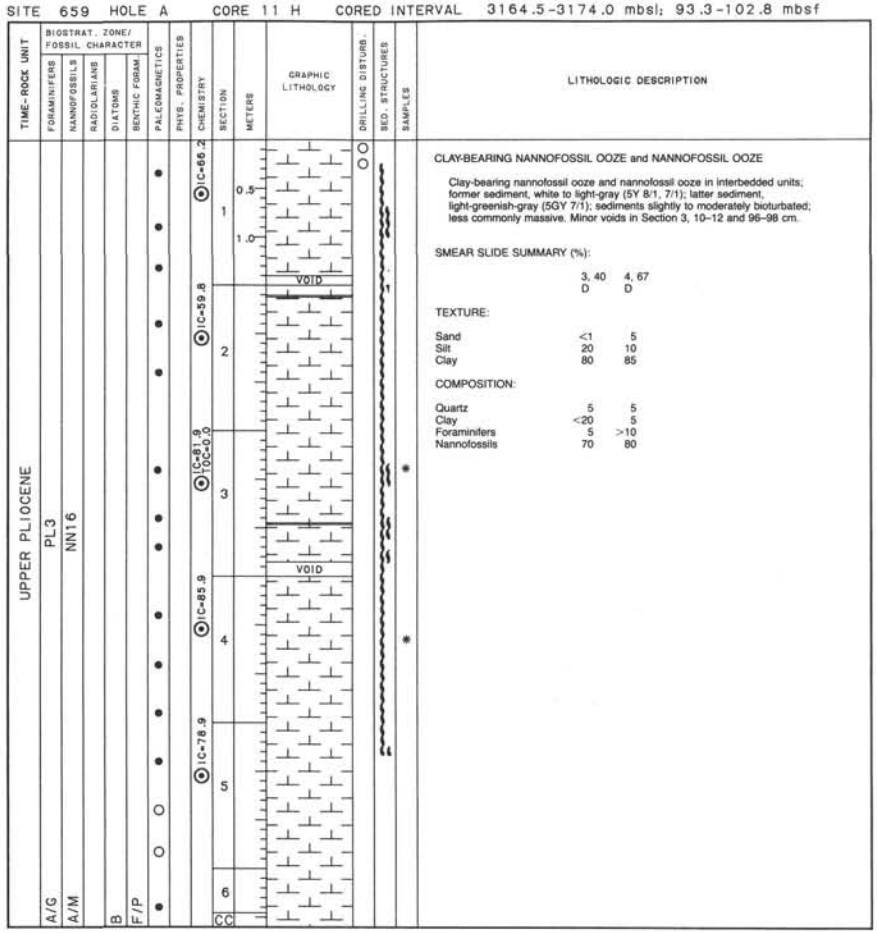

LITHOLOGIC DESCRIPTION

CLAY-BEARING NANNOFOSSIL OOZE and NANNOFOSSIL OOZE

Clay-bearing nannofossil ooze and nannofossil ooze in interbedded units; former sediment, white to light-gray (5Y 8/1, 7/1); latter sediment, light-greenish-gray (5GY 7/1); sediments slightly to moderately bioturbated; less commonly massive. Minor voids in Section 3, 10–12 and 96–98 cm.

SMEAR SLIDE SUMMARY (%):

	3, 40 D	4, 67 D
TEXTURE:		
Sand	<1	5
Silt	20	10
Clay	80	85
COMPOSITION:		
Quartz	5	5
Clay	<20	5
Foraminifers	5	>10
Nannofossils	70	80

SITE 659 HOLE A CORE 12 H CORED INTERVAL 3174.0-3183.5 mbsl; 102.8-112.3 mbsf

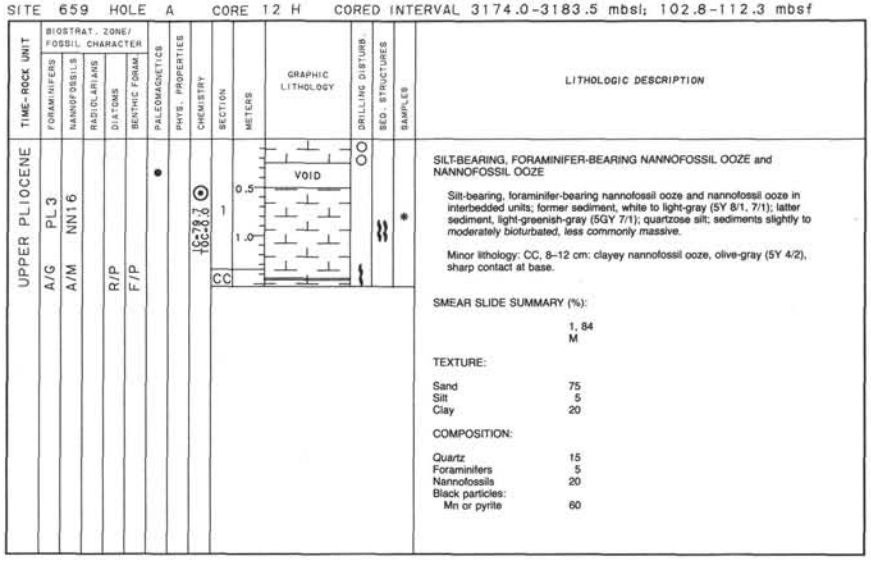

SILT-BEARING, FORAMINIFER-BEARING NANNOFOSSIL OOZE and NANNOFOSSIL OOZE

Silt-bearing, foraminifer-bearing nannofossil ooze and nannofossil ooze in interbedded units; former sediment, white to light-gray (5Y 8/1, 7/1); latter sediment, light-greenish-gray (5GY 7/1); quartzose silt; sediments slightly to moderately bioturbated, less commonly massive.

Minor lithology: CC, 8–12 cm: clayey nannofossil ooze, olive-gray (5Y 4/2), sharp contact at base.

SMEAR SLIDE SUMMARY (%):

	1, 84
	M
TEXTURE:	
Sand	75
Silt	5
Clay	20
COMPOSITION:	
Quartz	15
Foraminifers	5
Nannofossils	20
Black particles: Mn or pyrite	60

SITE 659 HOLE A CORE 13 H CORED INTERVAL 3183.5-3193.0 mbsl; 112.3-121.8 mbsf

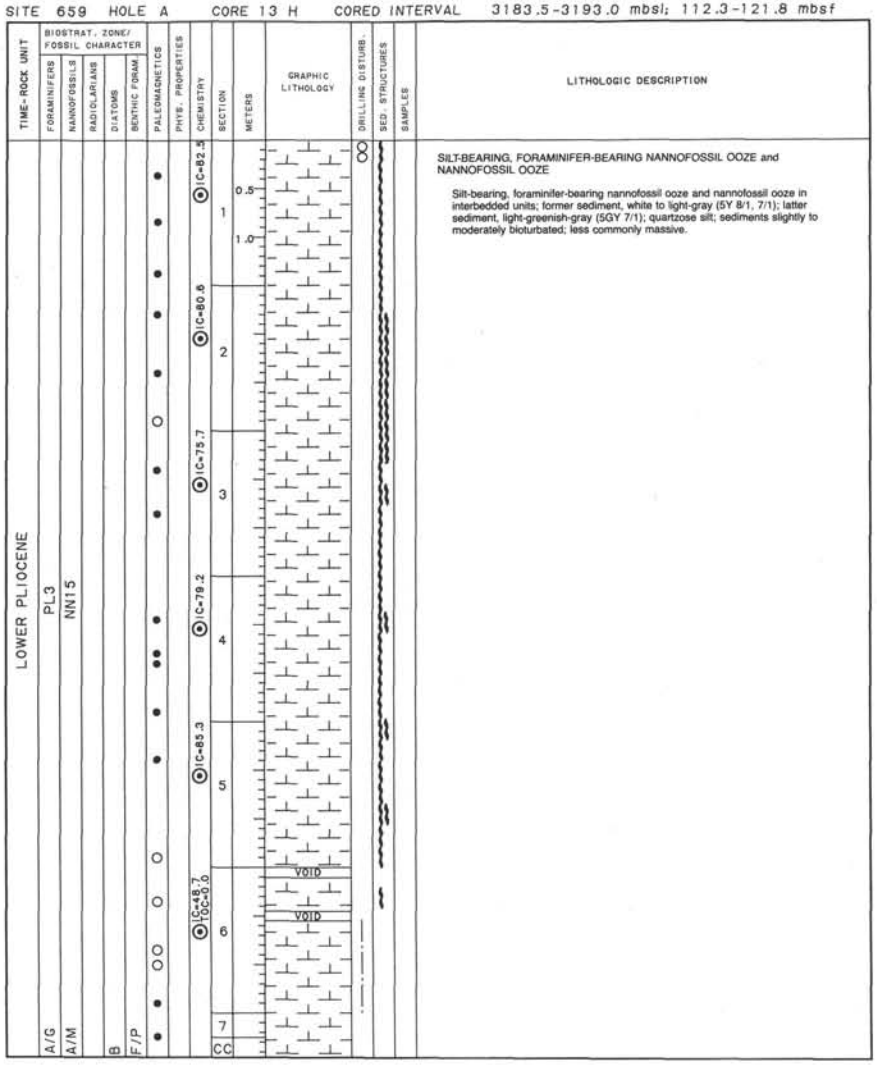

SILT-BEARING, FORAMINIFER-BEARING NANNOFOSSIL OOZE and NANNOFOSSIL OOZE

Silt-bearing, foraminifer-bearing nannofossil ooze and nannofossil ooze in interbedded units; former sediment, white to light-gray (5Y 8/1, 7/1); latter sediment, light-greenish-gray (5GY 7/1); quartzose silt; sediments slightly to moderately bioturbated; less commonly massive.

SITE 659 HOLE A CORE 14 H CORED INTERVAL 3193.0-3207.5 mbsl; 121.8-131.3 mbsf

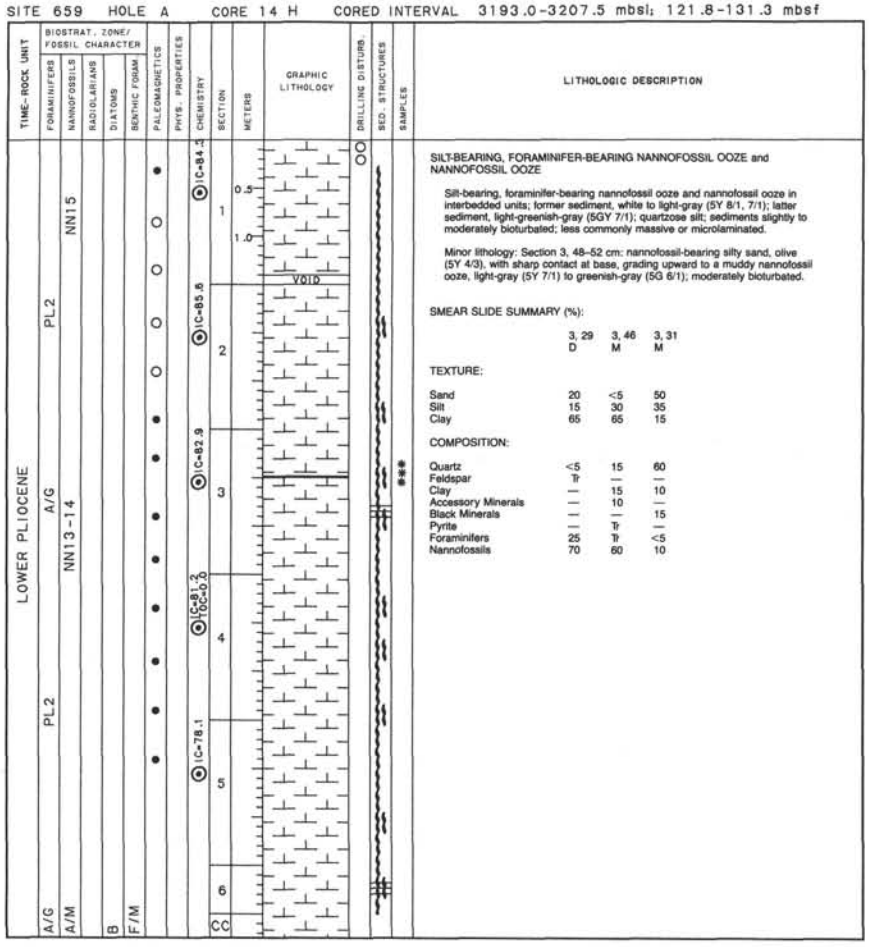

SILT-BEARING, FORAMINIFER-BEARING NANNOFOSSIL OOZE and NANNOFOSSIL OOZE

Silt-bearing, foraminifer-bearing nannofossil ooze and nannofossil ooze in interbedded units; former sediment, white to light-gray (5Y 8/1, 7/1); latter sediment, light-greenish-gray (5GY 7/1); quartzose silt; sediments slightly to moderately bioturbated; less commonly massive or microlaminated.

Minor lithology: Section 3, 48–52 cm: nannofossil-bearing silty sand, olive (5Y 4/3), with sharp contact at base, grading upward to a muddy nannofossil ooze, light-gray (5Y 7/1) to greenish-gray (5G 6/1); moderately bioturbated.

SMEAR SLIDE SUMMARY (%):

	3, 29 D	3, 46 M	3, 31 M
TEXTURE:			
Sand	20	<5	50
Silt	15	30	35
Clay	65	65	15
COMPOSITION:			
Quartz	<5	15	60
Feldspar	Tr	—	—
Clay	—	15	10
Accessory Minerals	—	10	—
Black Minerals	—	—	15
Pyrite	—	Tr	—
Foraminifers	25	Tr	<5
Nannofossils	70	60	10

SITE 659 HOLE A CORE 15 H CORED INTERVAL 3202.5-3212.0 mbsl; 131.3-140.8 mbsf

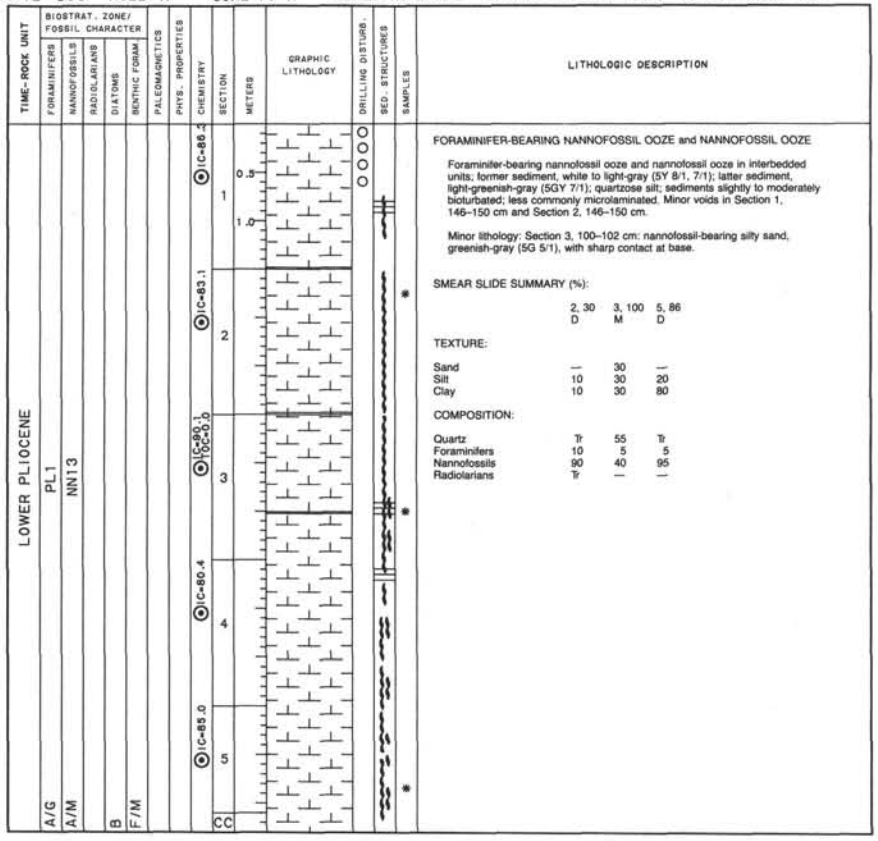

FORAMINIFER-BEARING NANNOFOSSIL OOZE and NANNOFOSSIL OOZE

Foraminifer-bearing nannofossil ooze and nannofossil ooze in interbedded units; former sediment, white to light-gray (5Y 8/1, 7/1); latter sediment, light-greenish-gray (5GY 7/1); quartzose silt; sediments slightly to moderately bioturbated; less commonly microlaminated. Minor voids in Section 1, 146–150 cm and Section 2, 146–150 cm.

Minor lithology: Section 3, 100–102 cm: nannofossil-bearing silty sand, greenish-gray (5G 5/1), with sharp contact at base.

SMEAR SLIDE SUMMARY (%):

	2, 30 D	3, 100 M	5, 86 D
TEXTURE:			
Sand	—	30	—
Silt	10	30	20
Clay	10	30	80
COMPOSITION:			
Quartz	Tr	55	Tr
Foraminifers	10	5	5
Nannofossils	90	40	95
Radiolarians	Tr	—	—

SITE 659 HOLE A CORE 16 H CORED INTERVAL 3212.0-3221.5 mbsl; 140.8-150.3 mbsf

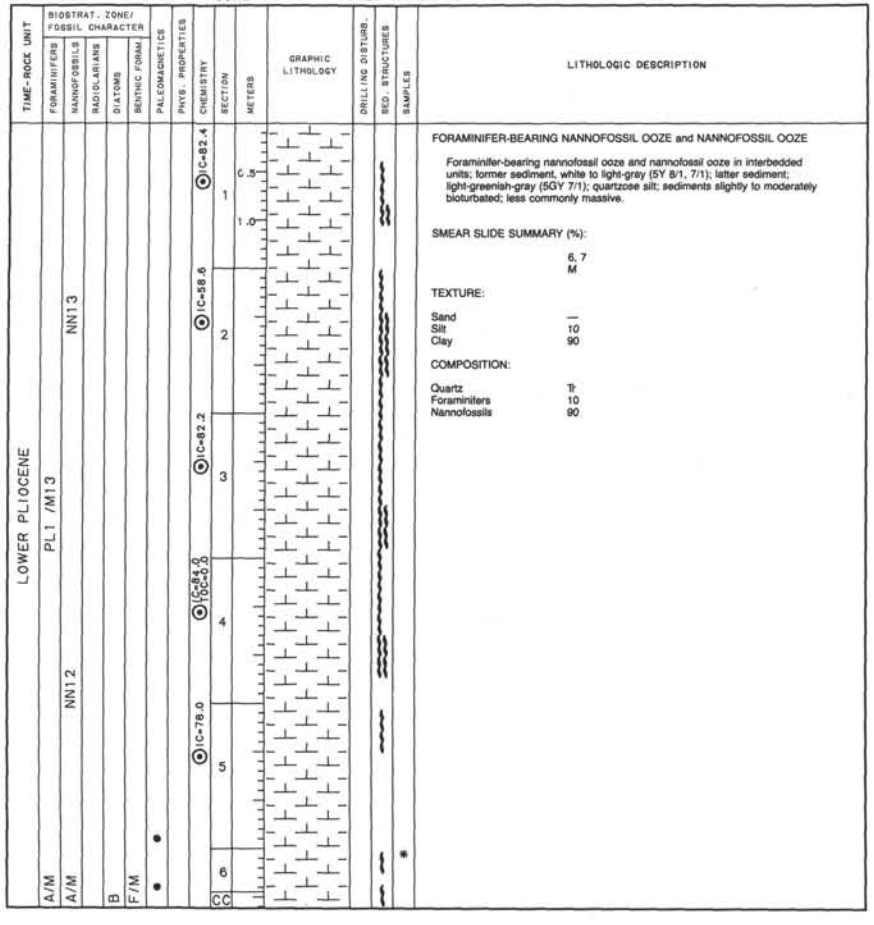

FORAMINIFER-BEARING NANNOFOSSIL OOZE and NANNOFOSSIL OOZE

Foraminifer-bearing nannofossil ooze and nannofossil ooze in interbedded units; former sediment, white to light-gray (5Y 8/1, 7/1); latter sediment; light-greenish-gray (5GY 7/1); quartzose silt; sediments slightly to moderately bioturbated; less commonly massive.

SMEAR SLIDE SUMMARY (%):

	6, 7 M
TEXTURE:	
Sand	—
Silt	10
Clay	90
COMPOSITION:	
Quartz	Tr
Foraminifers	10
Nannofossils	90

SITE 659 HOLE A CORE 17 H CORED INTERVAL 3221.5-3231.0 mbsl; 150.3-159.8 mbsf

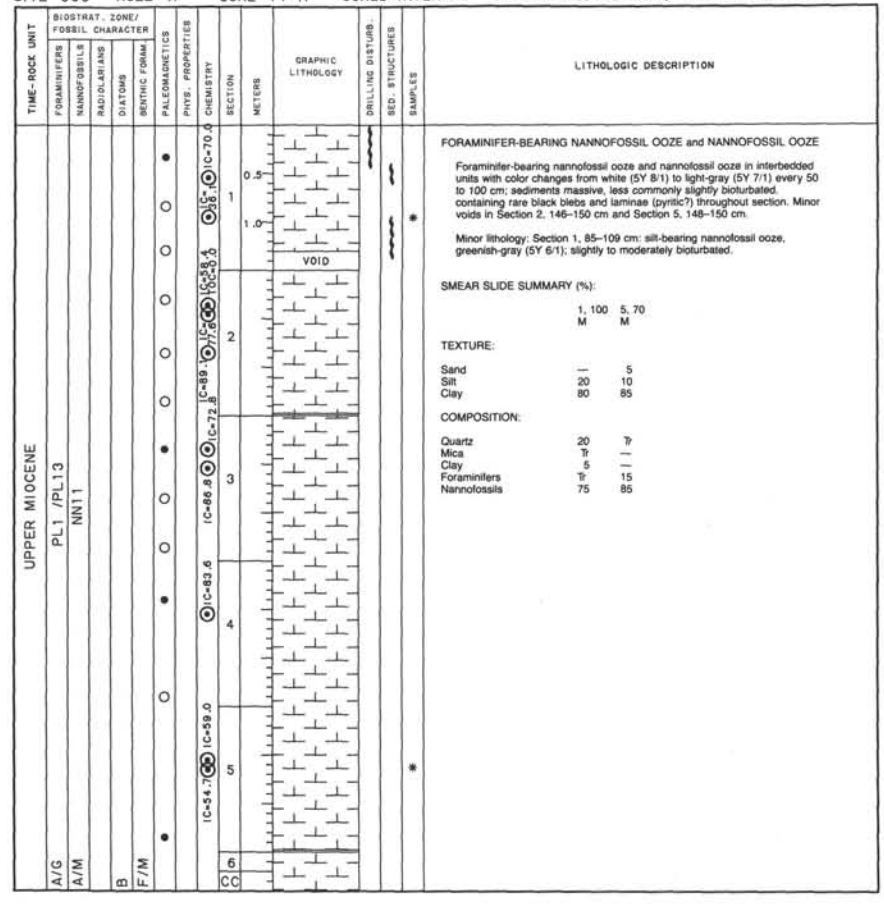

FORAMINIFER-BEARING NANNOFOSSIL OOZE and NANNOFOSSIL OOZE

Foraminifer-bearing nannofossil ooze and nannofossil ooze in interbedded units with color changes from white (5Y 8/1) to light-gray (5Y 7/1) every 50 to 100 cm; sediments massive, less commonly slightly bioturbated, containing rare black blebs and laminae (pyritic?) throughout section. Minor voids in Section 2, 146–150 cm and Section 5, 148–150 cm.

Minor lithology: Section 1, 85–109 cm: silt-bearing nannofossil ooze, greenish-gray (5Y 6/1); slightly to moderately bioturbated.

SMEAR SLIDE SUMMARY (%):

	1, 100 M	5, 70 M
TEXTURE:		
Sand	—	5
Silt	20	10
Clay	80	85
COMPOSITION:		
Quartz	20	Tr
Mica	Tr	—
Clay	5	—
Foraminifers	Tr	15
Nannofossils	75	85

CORE 18H NO RECOVERY

CORE 19H NO RECOVERY

SITE 659 HOLE A CORE 20 H CORED INTERVAL 3250.0-3259.5 mbsl; 178.8-188.3 mbsf

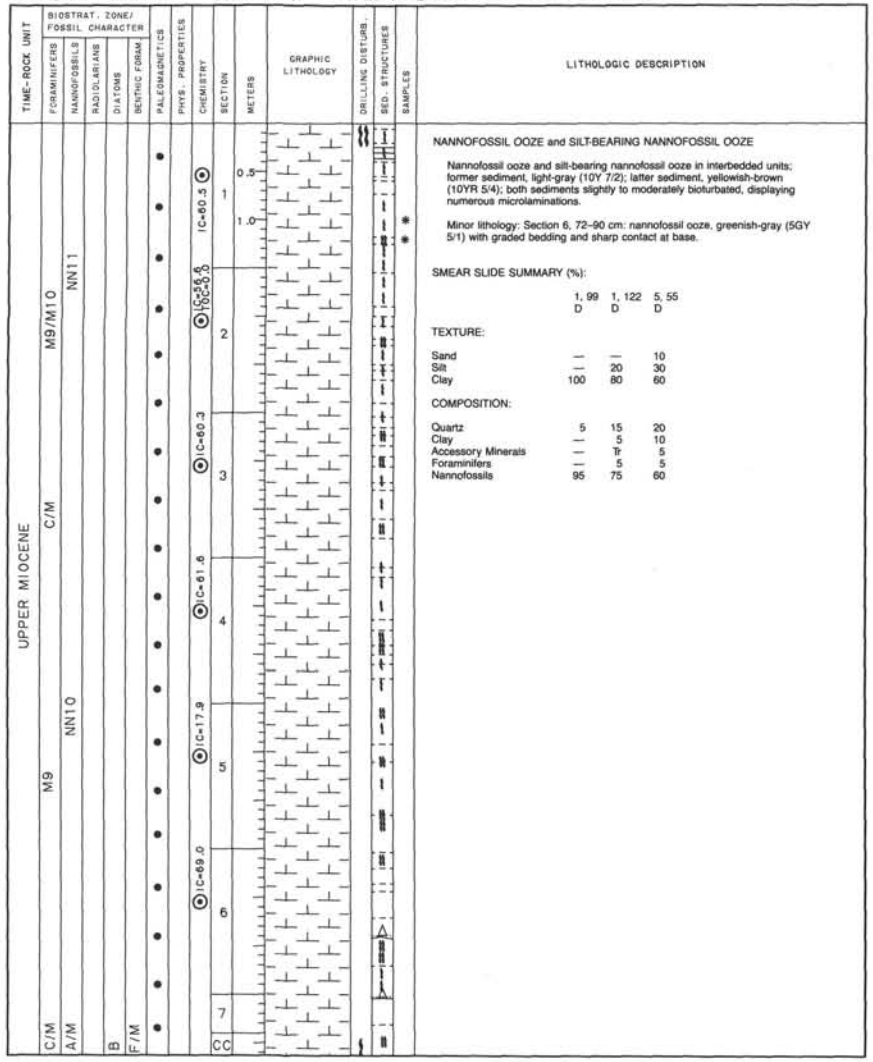

LITHOLOGIC DESCRIPTION

NANNOFOSSIL OOZE and SILT-BEARING NANNOFOSSIL OOZE

Nannofossil ooze and silt-bearing nannofossil ooze in interbedded units; former sediment, light-gray (10Y 7/2); latter sediment, yellowish-brown (10YR 5/4); both sediments slightly to moderately bioturbated, displaying numerous microlaminations.

Minor lithology: Section 6, 72–90 cm: nannofossil ooze, greenish-gray (5GY 5/1) with graded bedding and sharp contact at base.

SMEAR SLIDE SUMMARY (%):

	1, 99 D	1, 122 D	5, 55 D
TEXTURE:			
Sand	—	—	10
Silt	—	20	30
Clay	100	80	60
COMPOSITION:			
Quartz	5	15	20
Clay	—	5	10
Accessory Minerals	—	Tr	5
Foraminifers	—	5	5
Nannofossils	95	75	60

SITE 659 HOLE A CORE 21 X CORED INTERVAL 3259.5-3269.0 mbsl; 188.3-197.8 mbsf

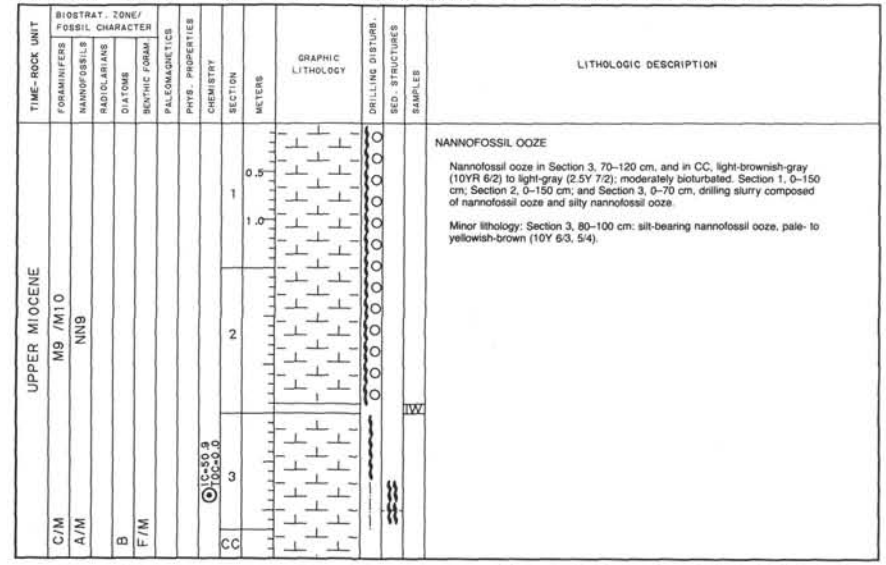

LITHOLOGIC DESCRIPTION

NANNOFOSSIL OOZE

Nannofossil ooze in Section 3, 70–120 cm, and in CC, light-brownish-gray (10YR 6/2) to light-gray (2.5Y 7/2); moderately bioturbated. Section 1, 0–150 cm; Section 2, 0–150 cm; and Section 3, 0–70 cm, drilling slurry composed of nannofossil ooze and silty nannofossil ooze.

Minor lithology: Section 3, 80–100 cm: silt-bearing nannofossil ooze, pale- to yellowish-brown (10Y 6/3, 5/4).

SITE 659 HOLE A CORE 22 X CORED INTERVAL 3269.0-3278.0 mbsl; 197.8-207.3 mbsf

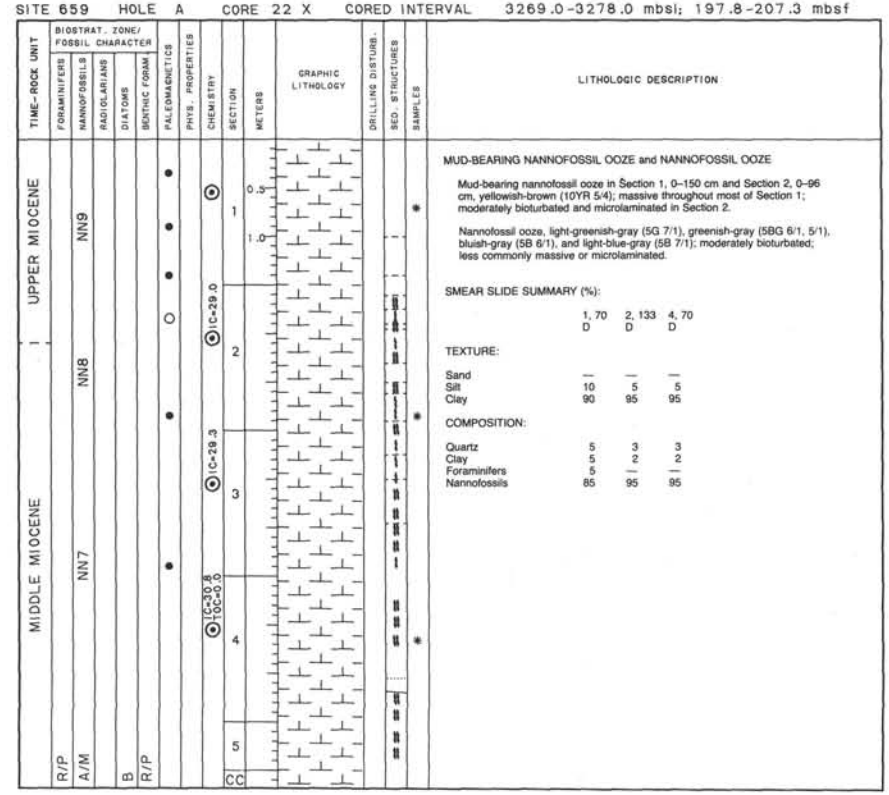

LITHOLOGIC DESCRIPTION

MUD-BEARING NANNOFOSSIL OOZE and NANNOFOSSIL OOZE

Mud-bearing nannofossil ooze in Section 1, 0–150 cm and Section 2, 0–96 cm, yellowish-brown (10YR 5/4); massive throughout most of Section 1; moderately bioturbated and microlaminated in Section 2.

Nannofossil ooze, light-greenish-gray (5G 7/1), greenish-gray (5BG 6/1, 5/1), bluish-gray (5B 6/1), and light-blue-gray (5B 7/1); moderately bioturbated; less commonly massive or microlaminated.

SMEAR SLIDE SUMMARY (%):

	1, 70 D	2, 133 D	4, 70 D
TEXTURE:			
Sand	—	—	—
Silt	10	5	5
Clay	90	95	95
COMPOSITION:			
Quartz	5	3	3
Clay	5	2	2
Foraminifers	5	—	—
Nannofossils	85	95	95

SITE 659 HOLE A CORE 23 X CORED INTERVAL 3278.5-3288.0 mbsl: 207.3-216.8 mbsf

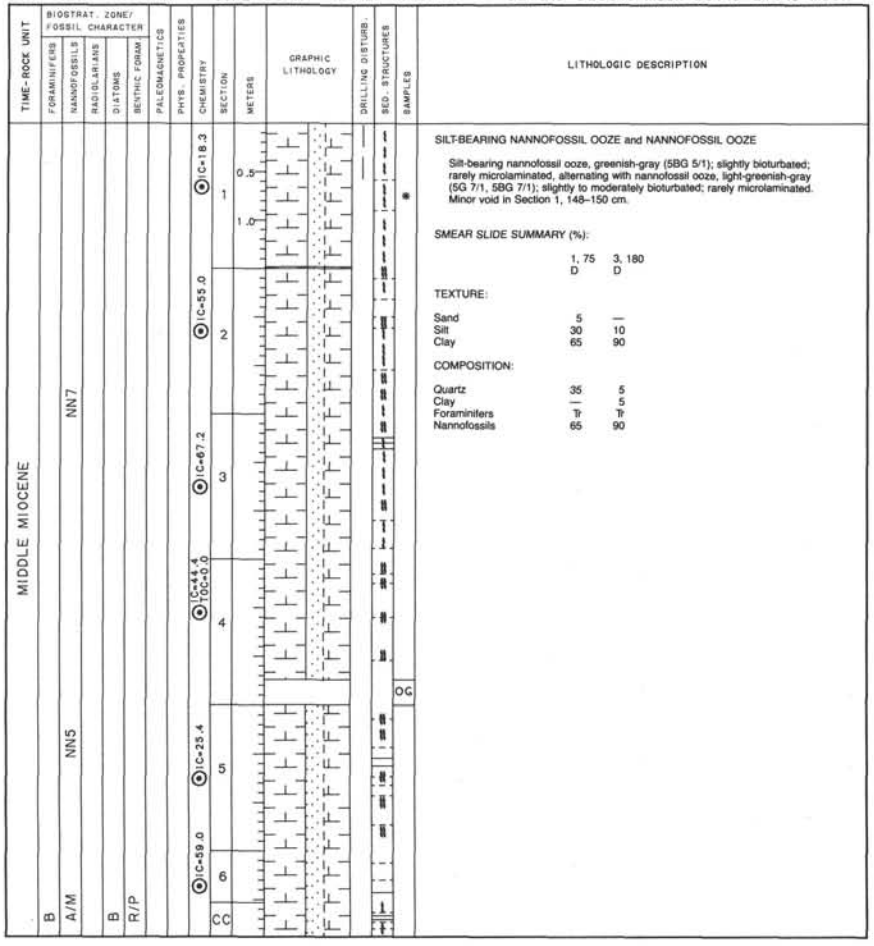

LITHOLOGIC DESCRIPTION

SILT-BEARING NANNOFOSSIL OOZE and NANNOFOSSIL OOZE

Silt-bearing nannofossil ooze, greenish-gray (5BG 5/1); slightly bioturbated; rarely microlaminated, alternating with nannofossil ooze, light-greenish-gray (5G 7/1, 5BG 7/1); slightly to moderately bioturbated; rarely microlaminated. Minor void in Section 1, 148–150 cm.

SMEAR SLIDE SUMMARY (%):

	1, 75 D	3, 180 D
TEXTURE:		
Sand	5	—
Silt	30	10
Clay	65	90
COMPOSITION:		
Quartz	35	5
Clay	—	5
Foraminifers	Tr	Tr
Nannofossils	65	90

SITE 659 HOLE A CORE 24 X CORED INTERVAL 3288.0-3297.5 mbsl: 216.8-226.3 mbsf

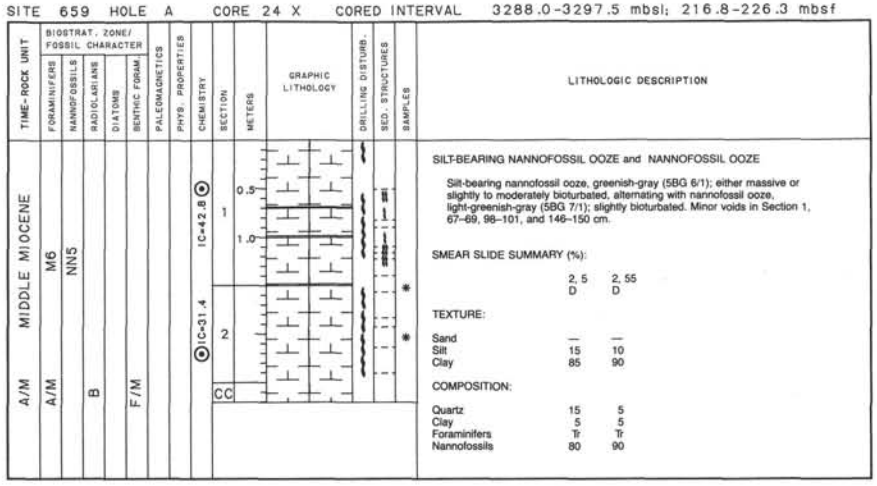

LITHOLOGIC DESCRIPTION

SILT-BEARING NANNOFOSSIL OOZE and NANNOFOSSIL OOZE

Silt-bearing nannofossil ooze, greenish-gray (5BG 6/1); either massive or slightly to moderately bioturbated, alternating with nannofossil ooze, light-greenish-gray (5BG 7/1); slightly bioturbated. Minor voids in Section 1, 67–69, 98–101, and 146–150 cm.

SMEAR SLIDE SUMMARY (%):

	2, 5 D	2, 55 D
TEXTURE:		
Sand	—	—
Silt	15	10
Clay	85	90
COMPOSITION:		
Quartz	15	5
Clay	5	5
Foraminifers	Tr	Tr
Nannofossils	80	90

SITE 659 HOLE A CORE 25 X CORED INTERVAL 3297.5-3302.0 mbsl; 226.3-235.8 mbsf

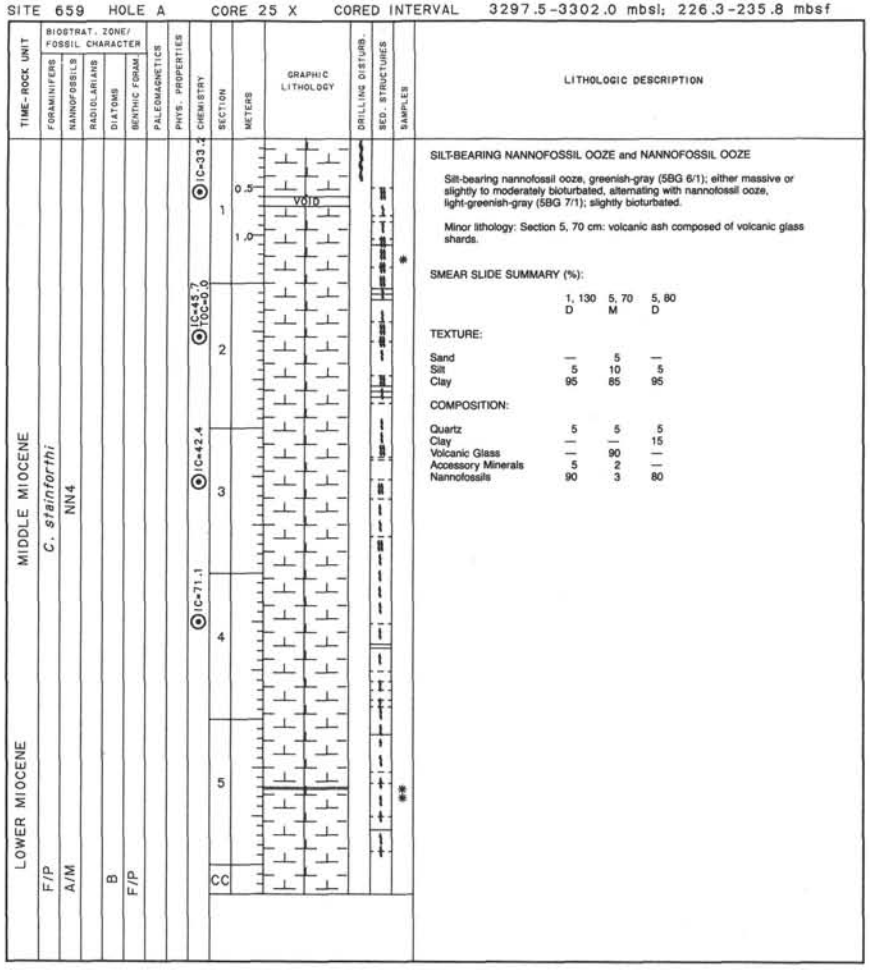

LITHOLOGIC DESCRIPTION

SILT-BEARING NANNOFOSSIL OOZE and NANNOFOSSIL OOZE

Silt-bearing nannofossil ooze, greenish-gray (5BG 6/1); either massive or slightly to moderately bioturbated, alternating with nannofossil ooze, light-greenish-gray (5BG 7/1); slightly bioturbated.

Minor lithology: Section 5, 70 cm: volcanic ash composed of volcanic glass shards.

SMEAR SLIDE SUMMARY (%):

	1, 130 D	5, 70 M	5, 80 D
TEXTURE:			
Sand	—	5	—
Silt	5	10	5
Clay	95	85	95
COMPOSITION:			
Quartz	5	5	5
Clay	—	—	15
Volcanic Glass	—	90	—
Accessory Minerals	5	2	—
Nannofossils	90	3	80

CORE 26X NO RECOVERY

SITE 659 HOLE A CORE 27 X CORED INTERVAL 3316.5-3326.0 mbsl; 245.3-254.8 mbsf

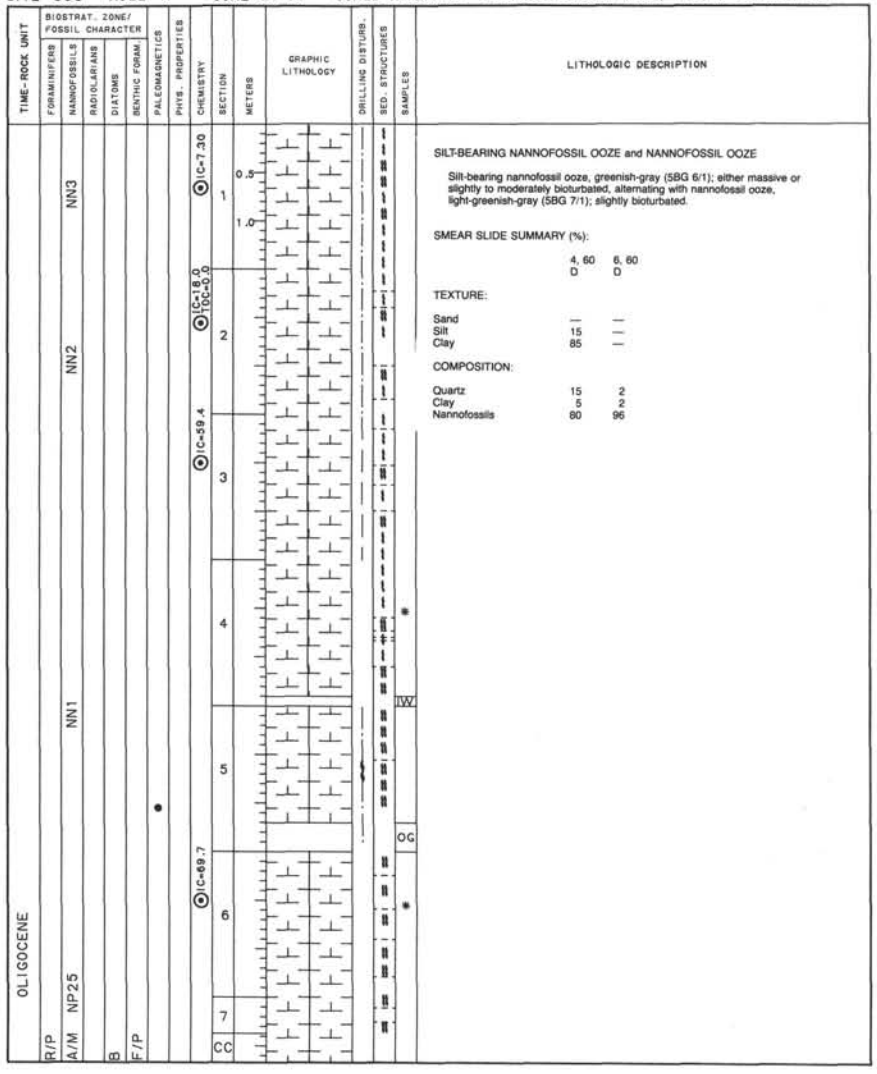

LITHOLOGIC DESCRIPTION

SILT-BEARING NANNOFOSSIL OOZE and NANNOFOSSIL OOZE

Silt-bearing nannofossil ooze, greenish-gray (5BG 6/1); either massive or slightly to moderately bioturbated, alternating with nannofossil ooze, light-greenish-gray (5BG 7/1); slightly bioturbated.

SMEAR SLIDE SUMMARY (%):

	4, 60 D	6, 60 D
TEXTURE:		
Sand	—	—
Silt	15	—
Clay	85	—
COMPOSITION:		
Quartz	15	2
Clay	5	2
Nannofossils	80	96

SITE 659 HOLE A CORE 28 X CORED INTERVAL 3326.0-3338.5 mbsl; 254.8-264.3 mbsf

TIME-ROCK UNIT	BIOSTRAT. ZONE/ FOSSIL CHARACTER: FORAMINIFERS	NANNOFOSSILS	RADIOLARIANS	DIATOMS	BENTHIC FORAM	PALEOMAGNETICS	PHYS. PROPERTIES	CHEMISTRY	SECTION	METERS	GRAPHIC LITHOLOGY	DRILLING DISTURB.	SED. STRUCTURES	SAMPLES	LITHOLOGIC DESCRIPTION
OLIGOCENE	B	A/P NP25		B	B				1, CC						SILT-BEARING NANNOFOSSIL OOZE Silt-bearing nannofossil ooze, gray (5Y 6/1); slightly bioturbated.

SITE 659 HOLE A CORE 29 X CORED INTERVAL 3335.5-3345.0 mbsl; 264.3-279.8 mbsf

TIME-ROCK UNIT	BIOSTRAT. ZONE/ FOSSIL CHARACTER: FORAMINIFERS	NANNOFOSSILS	RADIOLARIANS	DIATOMS	BENTHIC FORAM	PALEOMAGNETICS	PHYS. PROPERTIES	CHEMISTRY	SECTION	METERS	GRAPHIC LITHOLOGY	DRILLING DISTURB.	SED. STRUCTURES	SAMPLES	LITHOLOGIC DESCRIPTION
	B	B		B	B				1, CC	0.5				*	SILTY NANNOFOSSIL OOZE Silty nannofossil ooze, greenish-gray (5BG 5/1); slightly bioturbated. SMEAR SLIDE SUMMARY (%): 1, 40 D TEXTURE: Sand —; Silt 25; Clay 75 COMPOSITION: Quartz 20; Clay 5; Accessory Minerals 5; Nannofossils 70

SITE 659 HOLE B CORE 1 H CORED INTERVAL 3073.4-3080.0 mbsl; 0-6.60 mbsf

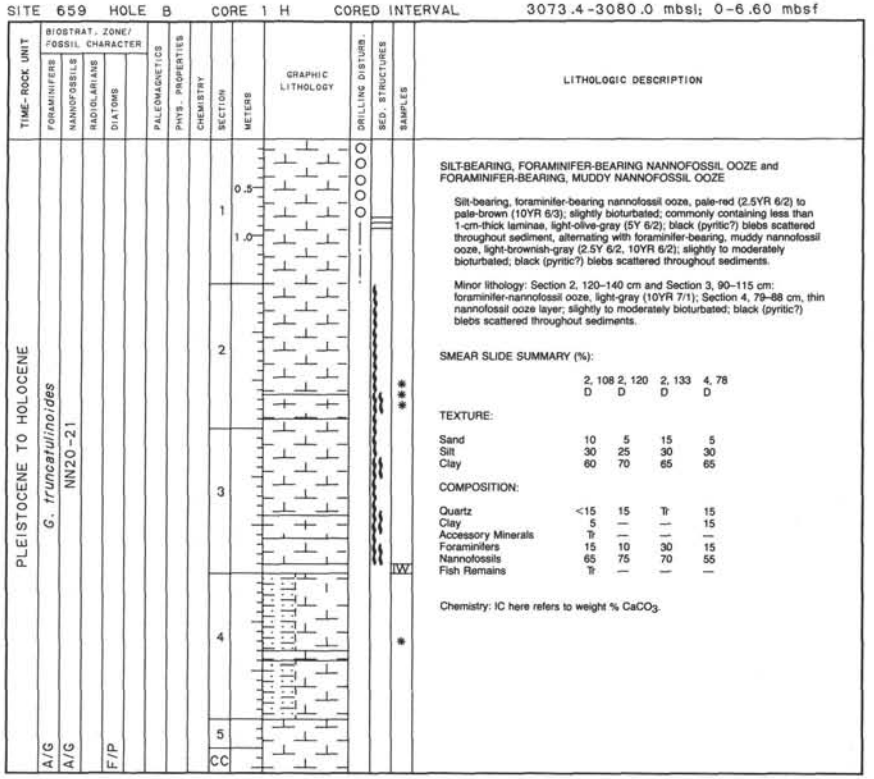

LITHOLOGIC DESCRIPTION

SILT-BEARING, FORAMINIFER-BEARING NANNOFOSSIL OOZE and FORAMINIFER-BEARING, MUDDY NANNOFOSSIL OOZE

Silt-bearing, foraminifer-bearing nannofossil ooze, pale-red (2.5YR 6/2) to pale-brown (10YR 6/3); slightly bioturbated; commonly containing less than 1-cm-thick laminae, light-olive-gray (5Y 6/2); black (pyritic?) blebs scattered throughout sediment, alternating with foraminifer-bearing, muddy nannofossil ooze, light-brownish-gray (2.5Y 6/2, 10YR 6/2); slightly to moderately bioturbated; black (pyritic?) blebs scattered throughout sediments.

Minor lithology: Section 2, 120–140 cm and Section 3, 90–115 cm: foraminifer-nannofossil ooze, light-gray (10YR 7/1); Section 4, 79–88 cm, thin nannofossil ooze layer; slightly to moderately bioturbated; black (pyritic?) blebs scattered throughout sediments.

SMEAR SLIDE SUMMARY (%):

	2, 108 D	2, 120 D	2, 133 D	4, 78 D
TEXTURE:				
Sand	10	5	15	5
Silt	30	25	30	30
Clay	60	70	65	65
COMPOSITION:				
Quartz	<15	15	Tr	15
Clay	5	—	—	15
Accessory Minerals	Tr	—	—	—
Foraminifers	15	10	30	15
Nannofossils	65	75	70	55
Fish Remains	Tr	—	—	—

Chemistry: IC here refers to weight % $CaCO_3$.

CORE 2H NO RECOVERY

CORE 3H NO RECOVERY

SITE 659 HOLE B CORE 4 H CORED INTERVAL 3099.0-3108.5 mbsl; 25.6-35.10 mbsf

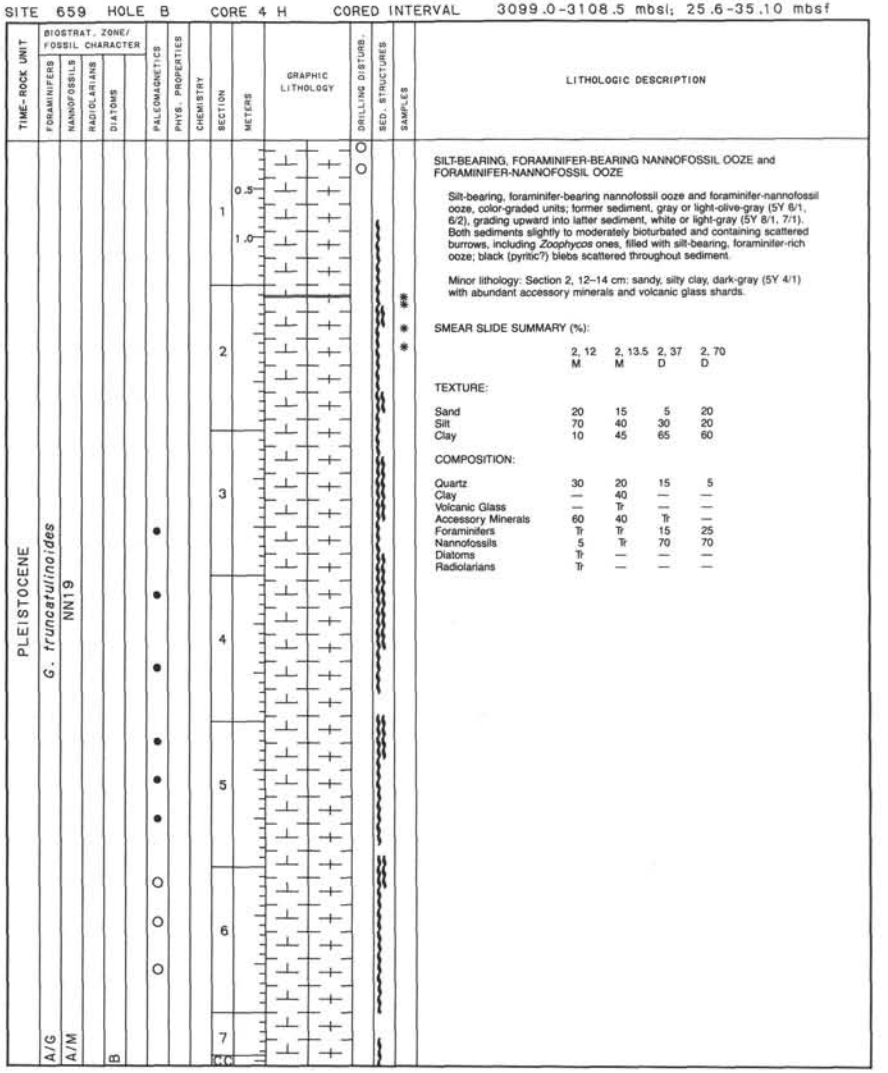

LITHOLOGIC DESCRIPTION

SILT-BEARING, FORAMINIFER-BEARING NANNOFOSSIL OOZE and FORAMINIFER-NANNOFOSSIL OOZE

Silt-bearing, foraminifer-bearing nannofossil ooze and foraminifer-nannofossil ooze, color-graded units; former sediment, gray or light-olive-gray (5Y 6/1, 6/2), grading upward into latter sediment, white or light-gray (5Y 8/1, 7/1). Both sediments slightly to moderately bioturbated and containing scattered burrows, including *Zoophycos* ones, filled with silt-bearing, foraminifer-rich ooze; black (pyritic?) blebs scattered throughout sediment.

Minor lithology: Section 2, 12–14 cm: sandy, silty clay, dark-gray (5Y 4/1) with abundant accessory minerals and volcanic glass shards.

SMEAR SLIDE SUMMARY (%):

	2, 12 M	2, 13.5 M	2, 37 D	2, 70 D
TEXTURE:				
Sand	20	15	5	20
Silt	70	40	30	20
Clay	10	45	65	60
COMPOSITION:				
Quartz	30	20	15	5
Clay	—	40	—	—
Volcanic Glass	—	Tr	—	—
Accessory Minerals	60	40	Tr	—
Foraminifers	Tr	Tr	15	25
Nannofossils	5	Tr	70	70
Diatoms	Tr	—	—	—
Radiolarians	Tr	—	—	—

SITE 659 HOLE B CORE 5 H CORED INTERVAL 3108.5-3118.0 mbsl; 35.10-44.60 mbsf

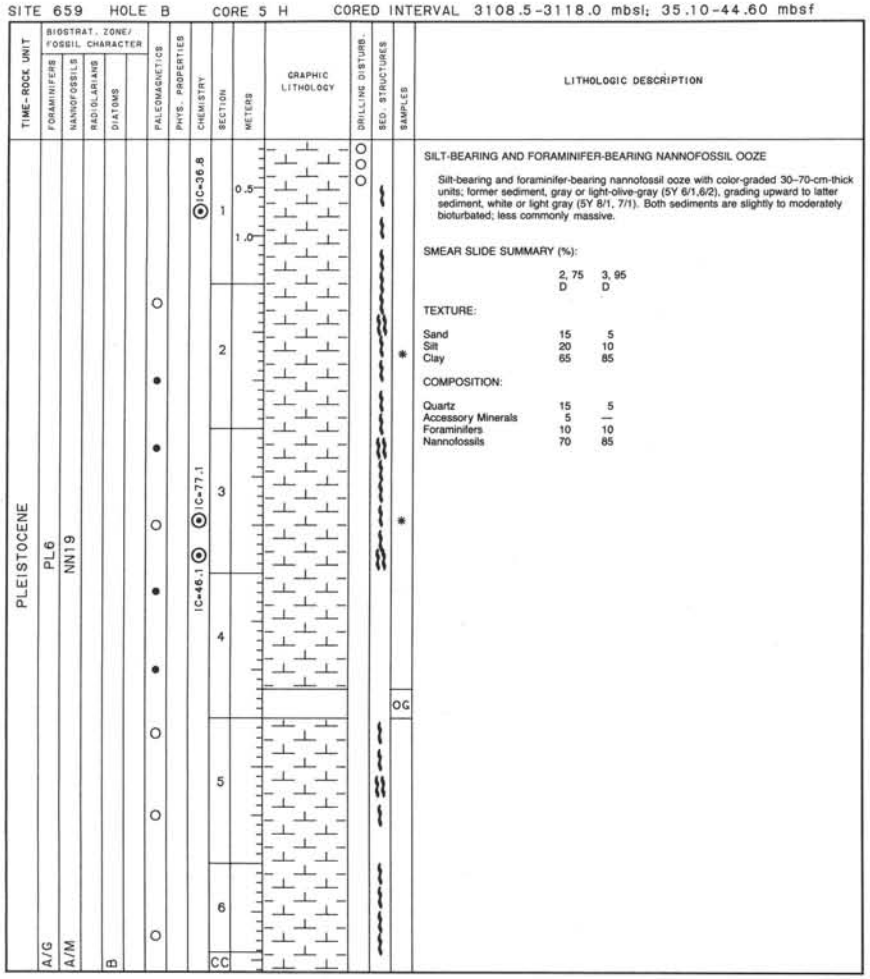

LITHOLOGIC DESCRIPTION

SILT-BEARING AND FORAMINIFER-BEARING NANNOFOSSIL OOZE

Silt-bearing and foraminifer-bearing nannofossil ooze with color-graded 30–70-cm-thick units; former sediment, gray or light-olive-gray (5Y 6/1,6/2), grading upward to latter sediment, white or light gray (5Y 8/1, 7/1). Both sediments are slightly to moderately bioturbated; less commonly massive.

SMEAR SLIDE SUMMARY (%):

	2, 75	3, 95
	D	D
TEXTURE:		
Sand	15	5
Silt	20	10
Clay	65	85
COMPOSITION:		
Quartz	15	5
Accessory Minerals	5	—
Foraminifers	10	10
Nannofossils	70	85

SITE 659 HOLE B CORE 6 H CORED INTERVAL 3118.0-3127.5 mbsl; 44.6-54.1 mbsf

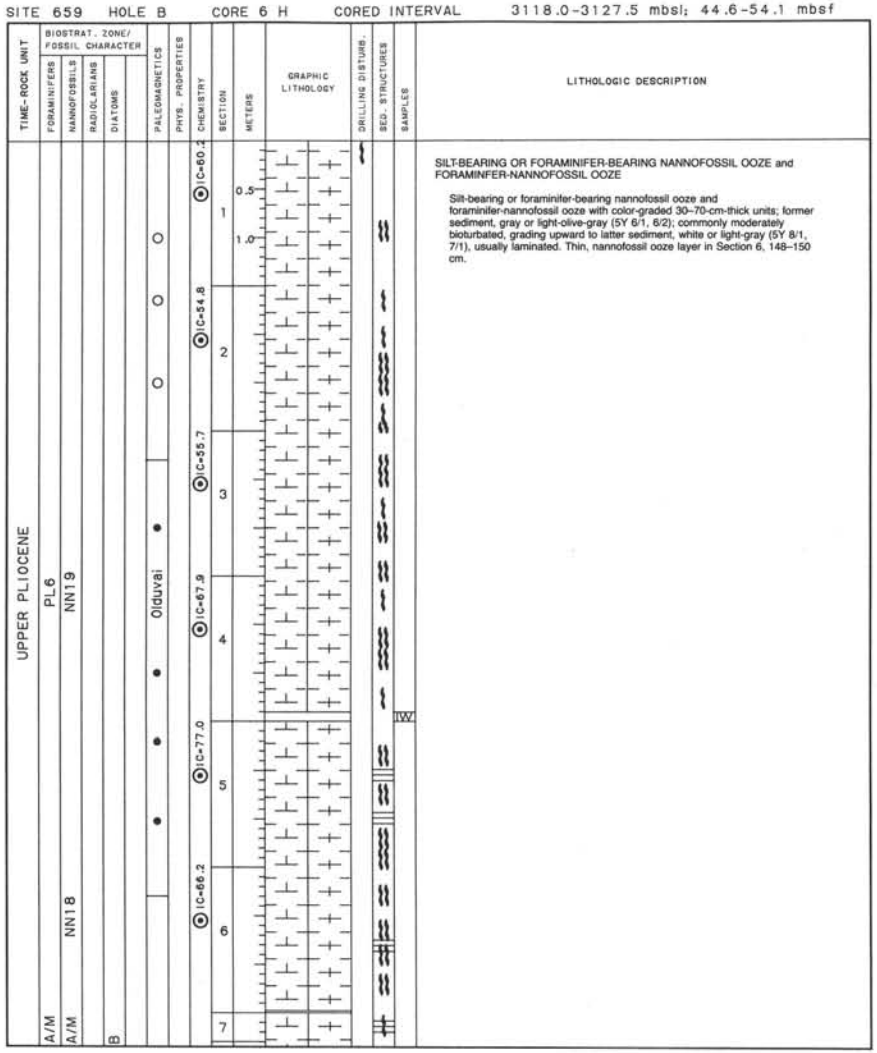

LITHOLOGIC DESCRIPTION

SILT-BEARING OR FORAMINIFER-BEARING NANNOFOSSIL OOZE and FORAMINFER-NANNOFOSSIL OOZE

Silt-bearing or foraminifer-bearing nannofossil ooze and foraminifer-nannofossil ooze with color-graded 30–70-cm-thick units; former sediment, gray or light-olive-gray (5Y 6/1, 6/2); commonly moderately bioturbated, grading upward to latter sediment, white or light-gray (5Y 8/1, 7/1), usually laminated. Thin, nannofossil ooze layer in Section 6, 148–150 cm.

SITE 659 HOLE B CORE 7 H CORED INTERVAL 3127.5-3137.0 mbsl; 54.1-63.6 mbsf

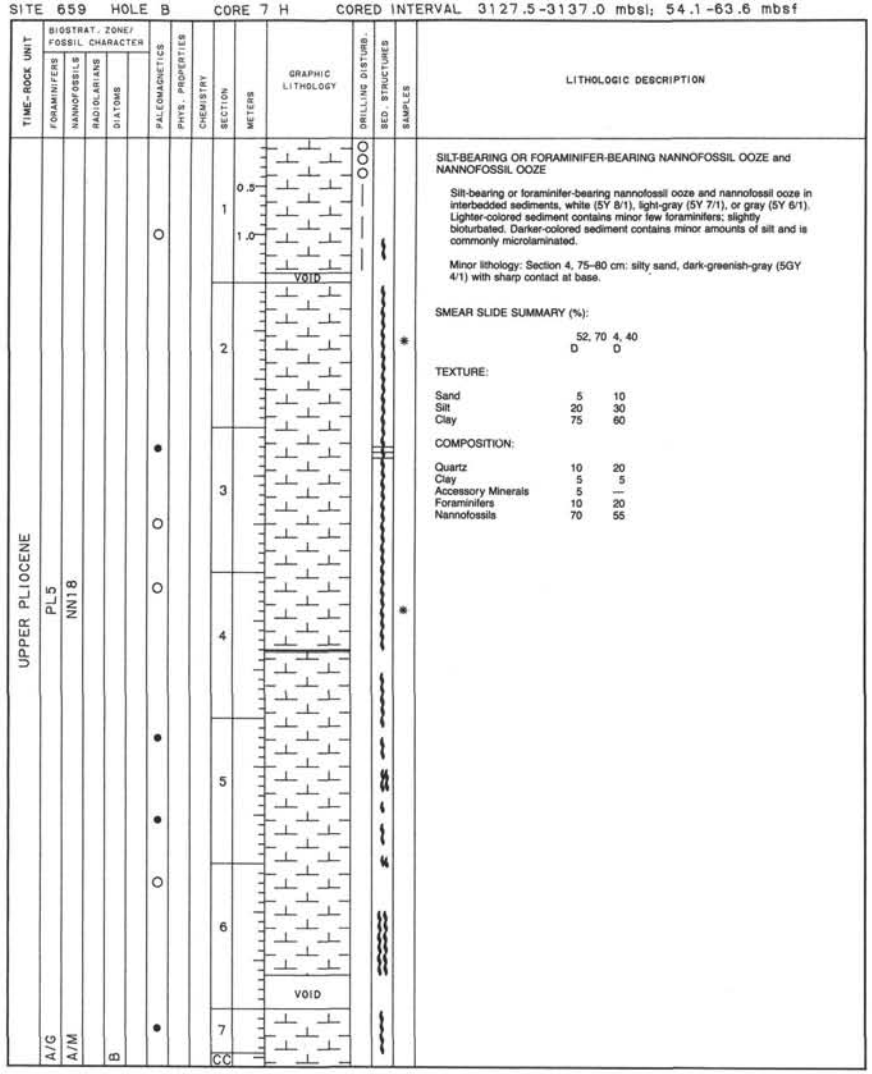

LITHOLOGIC DESCRIPTION

SILT-BEARING OR FORAMINIFER-BEARING NANNOFOSSIL OOZE and NANNOFOSSIL OOZE

Silt-bearing or foraminifer-bearing nannofossil ooze and nannofossil ooze in interbedded sediments, white (5Y 8/1), light-gray (5Y 7/1), or gray (5Y 6/1). Lighter-colored sediment contains minor few foraminifers; slightly bioturbated. Darker-colored sediment contains minor amounts of silt and is commonly microlaminated.

Minor lithology: Section 4, 75–80 cm: silty sand, dark-greenish-gray (5GY 4/1) with sharp contact at base.

SMEAR SLIDE SUMMARY (%):

	52, 70 D	4, 40 D
TEXTURE:		
Sand	5	10
Silt	20	30
Clay	75	60
COMPOSITION:		
Quartz	10	20
Clay	5	5
Accessory Minerals	5	1
Foraminifers	10	20
Nannofossils	70	55

SITE 659 HOLE B CORE 8 H CORED INTERVAL 3137.0-3146.5 mbsl; 63.6-73.1 mbsf

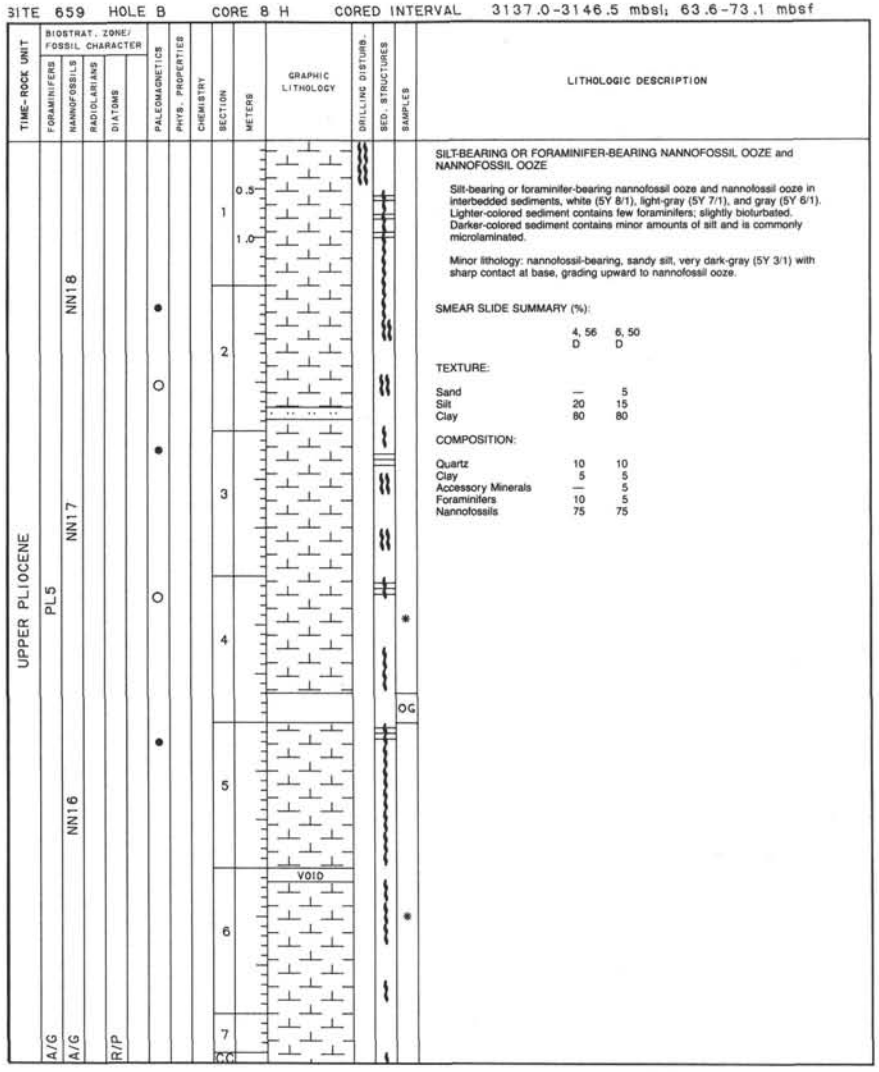

LITHOLOGIC DESCRIPTION

SILT-BEARING OR FORAMINIFER-BEARING NANNOFOSSIL OOZE and NANNOFOSSIL OOZE

Silt-bearing or foraminifer-bearing nannofossil ooze and nannofossil ooze in interbedded sediments, white (5Y 8/1), light-gray (5Y 7/1), and gray (5Y 6/1). Lighter-colored sediment contains few foraminifers; slightly bioturbated. Darker-colored sediment contains minor amounts of silt and is commonly microlaminated.

Minor lithology: nannofossil-bearing, sandy silt, very dark-gray (5Y 3/1) with sharp contact at base, grading upward to nannofossil ooze.

SMEAR SLIDE SUMMARY (%):

	4, 56 D	6, 50 D
TEXTURE:		
Sand	—	5
Silt	20	15
Clay	80	80
COMPOSITION:		
Quartz	10	10
Clay	5	5
Accessory Minerals	—	5
Foraminifers	10	5
Nannofossils	75	75

SITE 659 HOLE B CORE 9 H CORED INTERVAL 3146.5-3156.0 mbsl; 73.1-82.6 mbsf

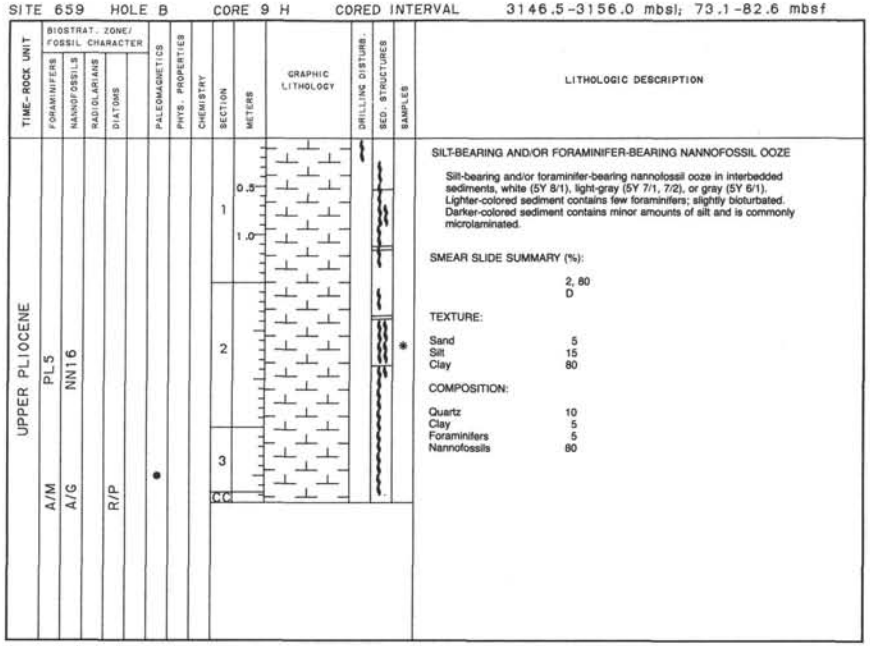

LITHOLOGIC DESCRIPTION

SILT-BEARING AND/OR FORAMINIFER-BEARING NANNOFOSSIL OOZE

Silt-bearing and/or foraminifer-bearing nannofossil ooze in interbedded sediments, white (5Y 8/1), light-gray (5Y 7/1, 7/2), or gray (5Y 6/1). Lighter-colored sediment contains few foraminifers; slightly bioturbated. Darker-colored sediment contains minor amounts of silt and is commonly microlaminated.

SMEAR SLIDE SUMMARY (%):

	2, 80
	D
TEXTURE:	
Sand	5
Silt	15
Clay	80
COMPOSITION:	
Quartz	10
Clay	5
Foraminifers	5
Nannofossils	80

SITE 659 HOLE B CORE 10 H CORED INTERVAL 3156.0-3161.5 mbsl; 82.6-88.1 mbsf

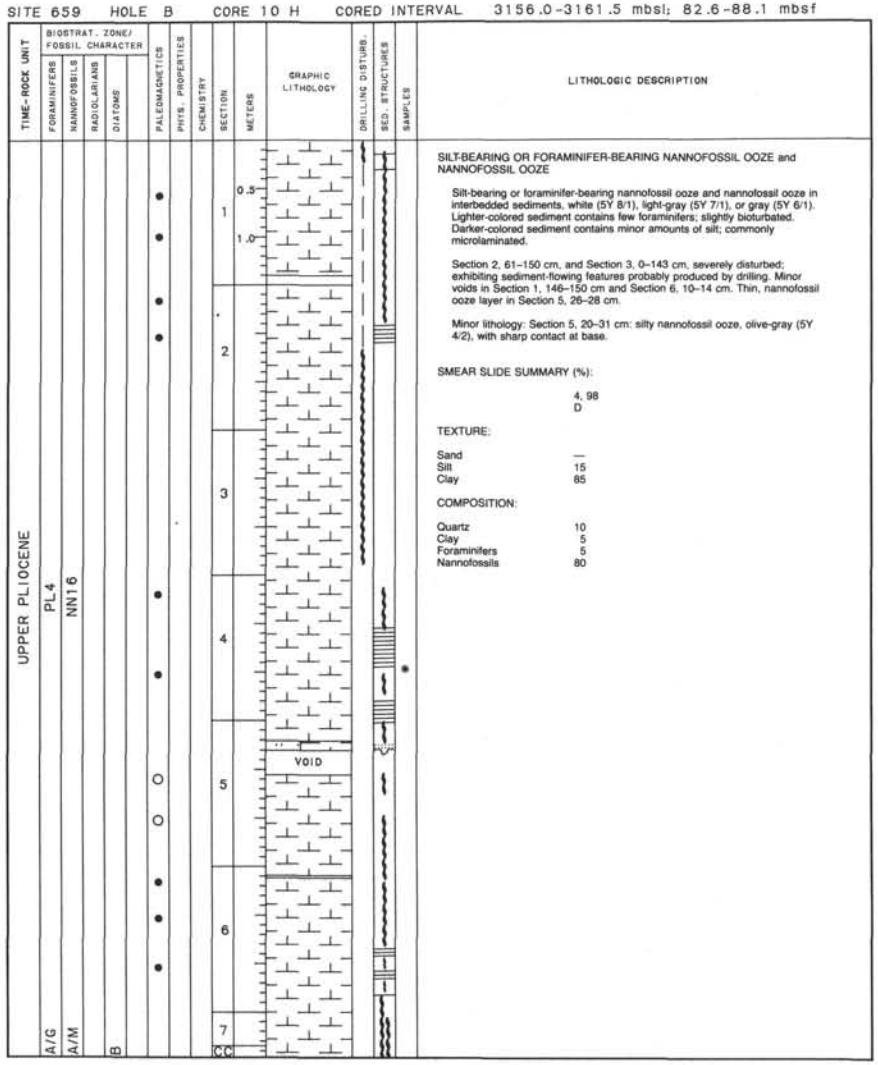

LITHOLOGIC DESCRIPTION

SILT-BEARING OR FORAMINIFER-BEARING NANNOFOSSIL OOZE and NANNOFOSSIL OOZE

Silt-bearing or foraminifer-bearing nannofossil ooze and nannofossil ooze in interbedded sediments, white (5Y 8/1), light-gray (5Y 7/1), or gray (5Y 6/1). Lighter-colored sediment contains few foraminifers; slightly bioturbated. Darker-colored sediment contains minor amounts of silt; commonly microlaminated.

Section 2, 61–150 cm, and Section 3, 0–143 cm, severely disturbed; exhibiting sediment-flowing features probably produced by drilling. Minor voids in Section 1, 146–150 cm and Section 6, 10–14 cm. Thin, nannofossil ooze layer in Section 5, 26–28 cm.

Minor lithology: Section 5, 20–31 cm: silty nannofossil ooze, olive-gray (5Y 4/2), with sharp contact at base.

SMEAR SLIDE SUMMARY (%):

	4, 98
	D
TEXTURE:	
Sand	—
Silt	15
Clay	85
COMPOSITION:	
Quartz	10
Clay	5
Foraminifers	5
Nannofossils	80

SITE 659 HOLE B CORE 11 H CORED INTERVAL 3161.5-3171.0 mbsl; 88.1-97.6 mbsf

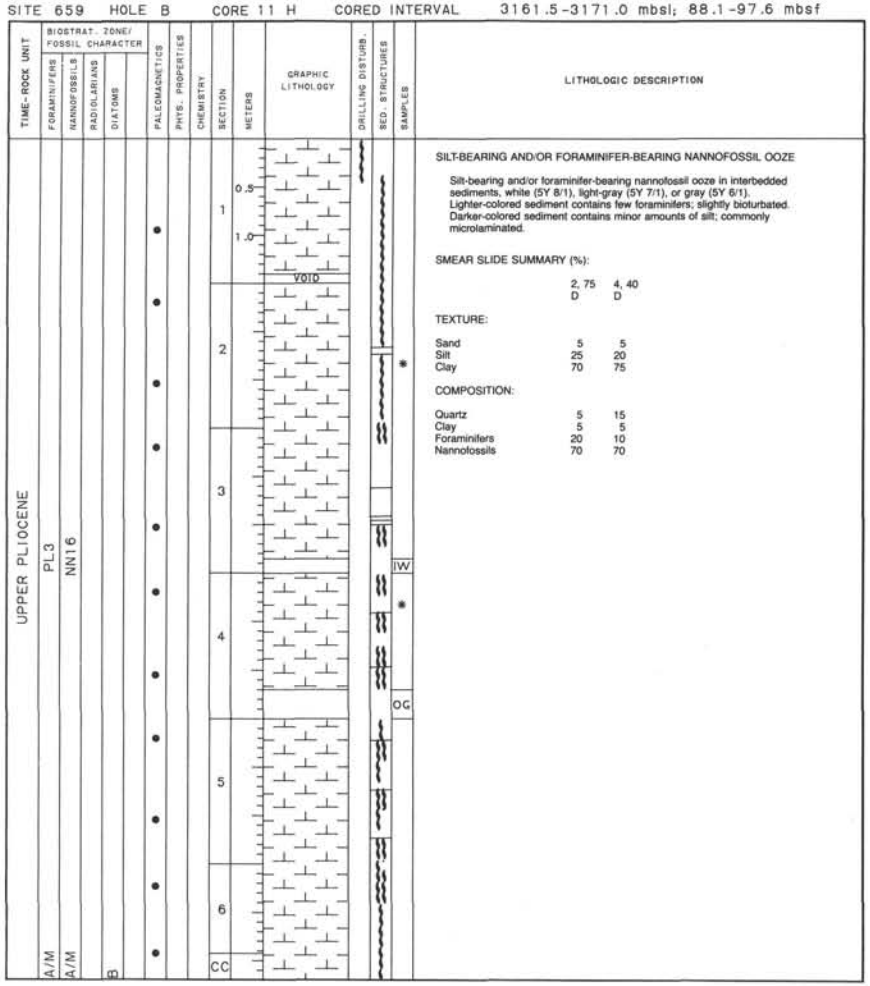

LITHOLOGIC DESCRIPTION

SILT-BEARING AND/OR FORAMINIFER-BEARING NANNOFOSSIL OOZE

Silt-bearing and/or foraminifer-bearing nannofossil ooze in interbedded sediments, white (5Y 8/1), light-gray (5Y 7/1), or gray (5Y 6/1). Lighter-colored sediment contains few foraminifers; slightly bioturbated. Darker-colored sediment contains minor amounts of silt; commonly microlaminated.

SMEAR SLIDE SUMMARY (%):

	2, 75 D	4, 40 D
TEXTURE:		
Sand	5	5
Silt	25	20
Clay	70	75
COMPOSITION:		
Quartz	5	15
Clay	5	5
Foraminifers	20	10
Nannofossils	70	70

SITE 659 HOLE B CORE 12 H CORED INTERVAL 3171.0-3180.5 mbsl; 97.6-107.1 mbsf

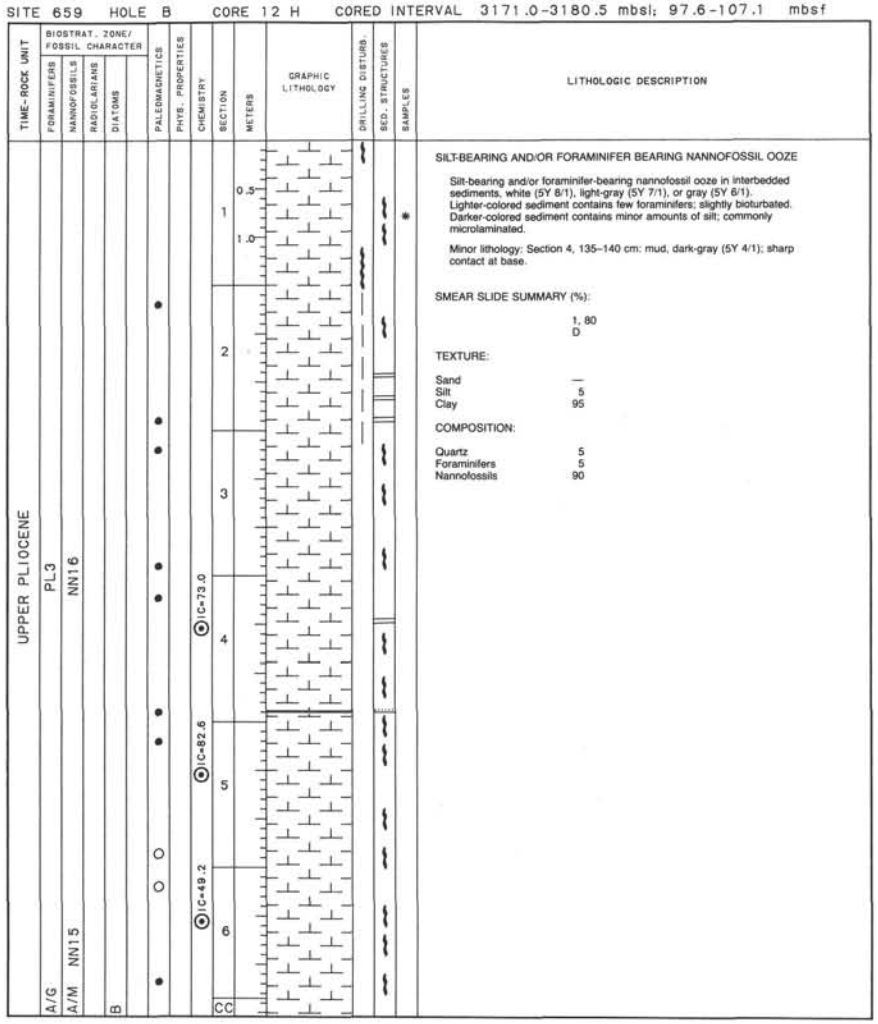

LITHOLOGIC DESCRIPTION

SILT-BEARING AND/OR FORAMINIFER BEARING NANNOFOSSIL OOZE

Silt-bearing and/or foraminifer-bearing nannofossil ooze in interbedded sediments, white (5Y 8/1), light-gray (5Y 7/1), or gray (5Y 6/1). Lighter-colored sediment contains few foraminifers; slightly bioturbated. Darker-colored sediment contains minor amounts of silt; commonly microlaminated.

Minor lithology: Section 4, 135–140 cm: mud, dark-gray (5Y 4/1); sharp contact at base.

SMEAR SLIDE SUMMARY (%):

	1, 80 D
TEXTURE:	
Sand	—
Silt	5
Clay	95
COMPOSITION:	
Quartz	5
Foraminifers	5
Nannofossils	90

SITE 659 HOLE B CORE 13 H CORED INTERVAL 3180.5-3190.0 mbsl; 102.1-116.6 mbsf

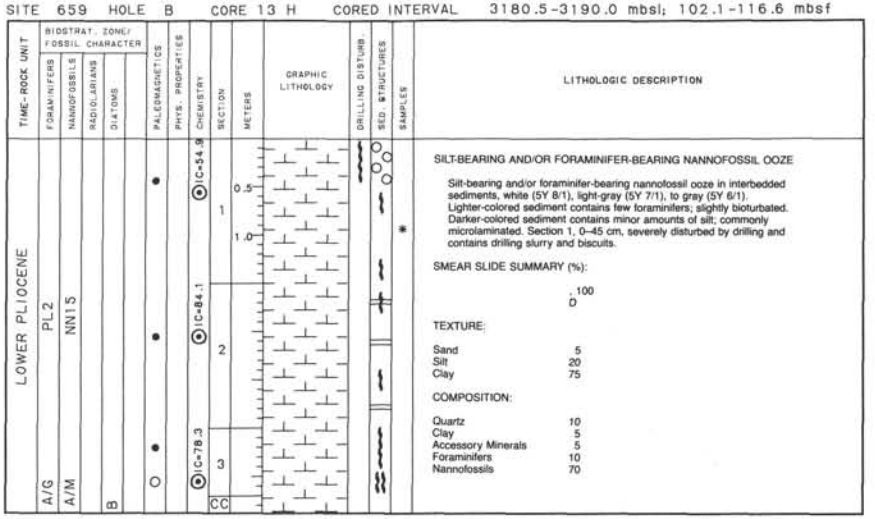

SILT-BEARING AND/OR FORAMINIFER-BEARING NANNOFOSSIL OOZE

Silt-bearing and/or foraminifer-bearing nannofossil ooze in interbedded sediments, white (5Y 8/1), light-gray (5Y 7/1), to gray (5Y 6/1). Lighter-colored sediment contains few foraminifers; slightly bioturbated. Darker-colored sediment contains minor amounts of silt; commonly microlaminated. Section 1, 0–45 cm, severely disturbed by drilling and contains drilling slurry and biscuits.

SMEAR SLIDE SUMMARY (%):

	100
	D
TEXTURE:	
Sand	5
Silt	20
Clay	75
COMPOSITION:	
Quartz	10
Clay	5
Accessory Minerals	5
Foraminifers	10
Nannofossils	70

SITE 659 HOLE B CORE 14 H CORED INTERVAL 3190.0-3199.5 mbsl; 116.6-120.1 mbsf

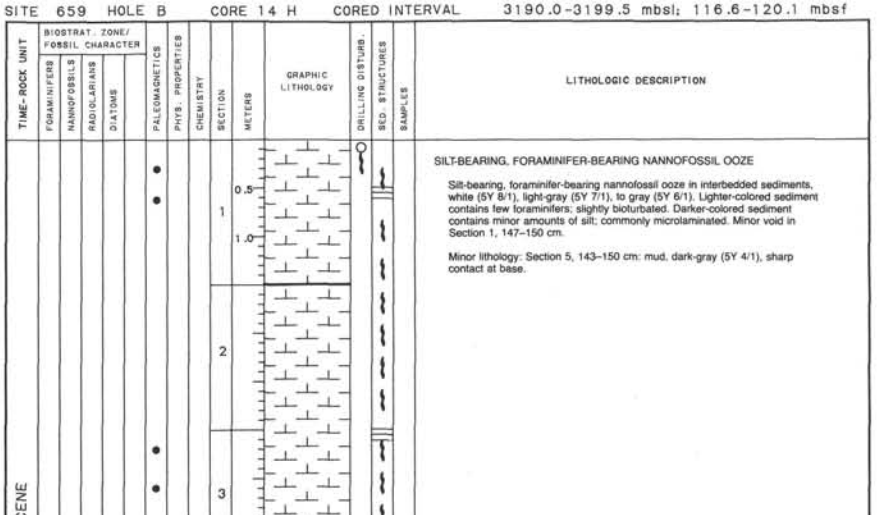

SILT-BEARING, FORAMINIFER-BEARING NANNOFOSSIL OOZE

Silt-bearing, foraminifer-bearing nannofossil ooze in interbedded sediments, white (5Y 8/1), light-gray (5Y 7/1), to gray (5Y 6/1). Lighter-colored sediment contains few foraminifers; slightly bioturbated. Darker-colored sediment contains minor amounts of silt; commonly microlaminated. Minor void in Section 1, 147–150 cm.

Minor lithology: Section 5, 143–150 cm: mud, dark-gray (5Y 4/1), sharp contact at base.

SITE 659 HOLE B CORE 15 H CORED INTERVAL 3199.5-3209.0 mbsl; 126.1-135.6 mbsf

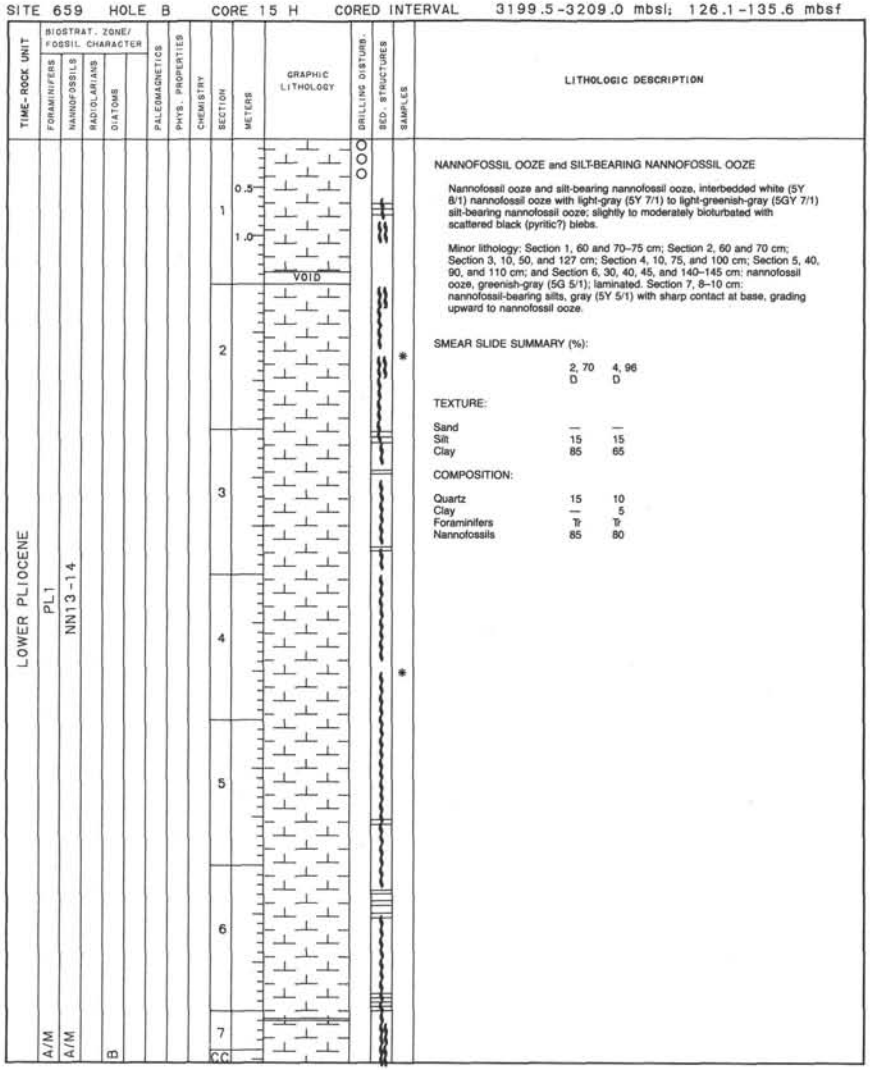

NANNOFOSSIL OOZE and SILT-BEARING NANNOFOSSIL OOZE

Nannofossil ooze and silt-bearing nannofossil ooze, interbedded white (5Y 8/1) nannofossil ooze with light-gray (5Y 7/1) to light-greenish-gray (5GY 7/1) silt-bearing nannofossil ooze; slightly to moderately bioturbated with scattered black (pyritic?) blebs.

Minor lithology: Section 1, 60 and 70–75 cm; Section 2, 60 and 70 cm; Section 3, 10, 50, and 127 cm; Section 4, 10, 75, and 100 cm; Section 5, 40, 90, and 110 cm; and Section 6, 30, 40, 45, and 140–145 cm: nannofossil ooze, greenish-gray (5G 5/1); laminated. Section 7, 8–10 cm: nannofossil-bearing silts, gray (5Y 5/1) with sharp contact at base, grading upward to nannofossil ooze.

SMEAR SLIDE SUMMARY (%):

	2, 70 D	4, 96 D
TEXTURE:		
Sand	—	—
Silt	15	15
Clay	85	85
COMPOSITION:		
Quartz	15	10
Clay	—	5
Foraminifers	Tr	Tr
Nannofossils	85	80

SITE 659 HOLE B CORE 16 H CORED INTERVAL 3209.0-3218.5 mbsl; 135.6-145.1 mbsf

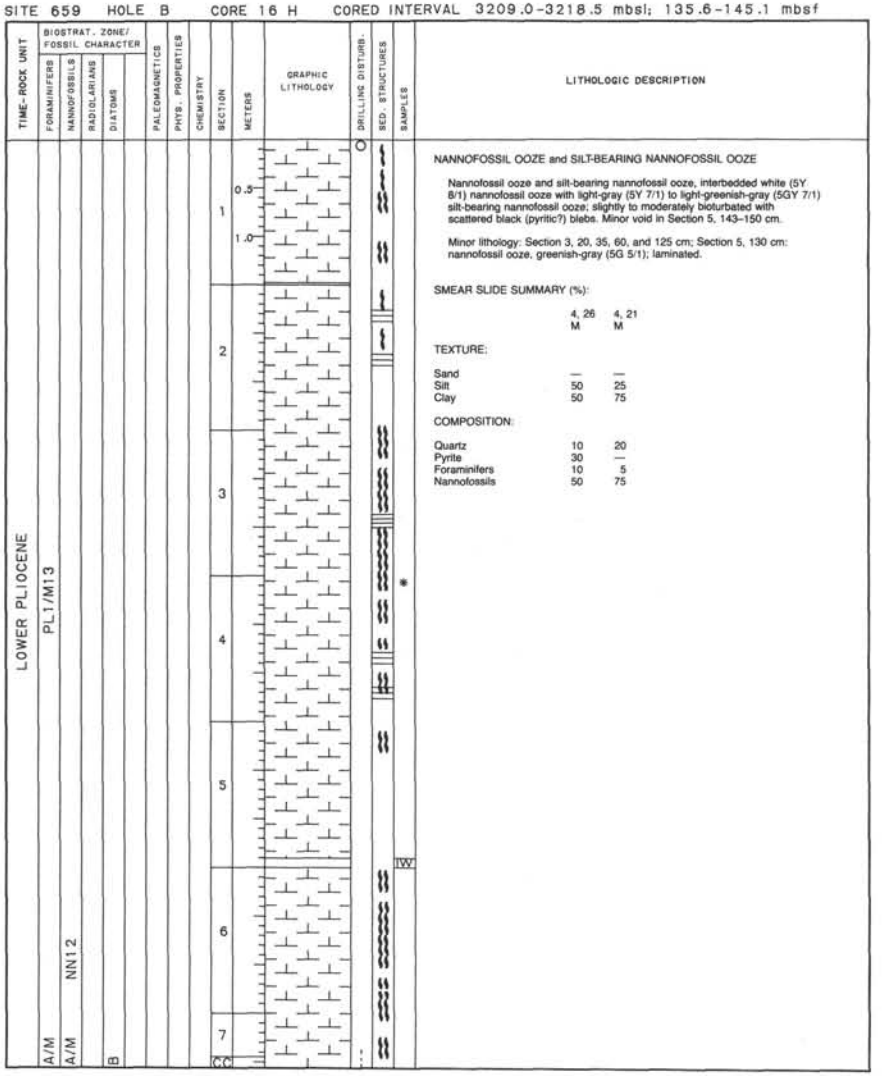

NANNOFOSSIL OOZE and SILT-BEARING NANNOFOSSIL OOZE

Nannofossil ooze and silt-bearing nannofossil ooze, interbedded white (5Y 8/1) nannofossil ooze with light-gray (5Y 7/1) to light-greenish-gray (5GY 7/1) silt-bearing nannofossil ooze; slightly to moderately bioturbated with scattered black (pyritic?) blebs. Minor void in Section 5, 143–150 cm.

Minor lithology: Section 3, 20, 35, 60, and 125 cm; Section 5, 130 cm: nannofossil ooze, greenish-gray (5G 5/1); laminated.

SMEAR SLIDE SUMMARY (%):

	4, 26 M	4, 21 M
TEXTURE:		
Sand	—	—
Silt	50	25
Clay	50	75
COMPOSITION:		
Quartz	10	20
Pyrite	30	—
Foraminifers	10	5
Nannofossils	50	75

SITE 659 HOLE B CORE 17 H CORED INTERVAL 3218.5-3228.0 mbsl; 145.1-154.6 mbsf

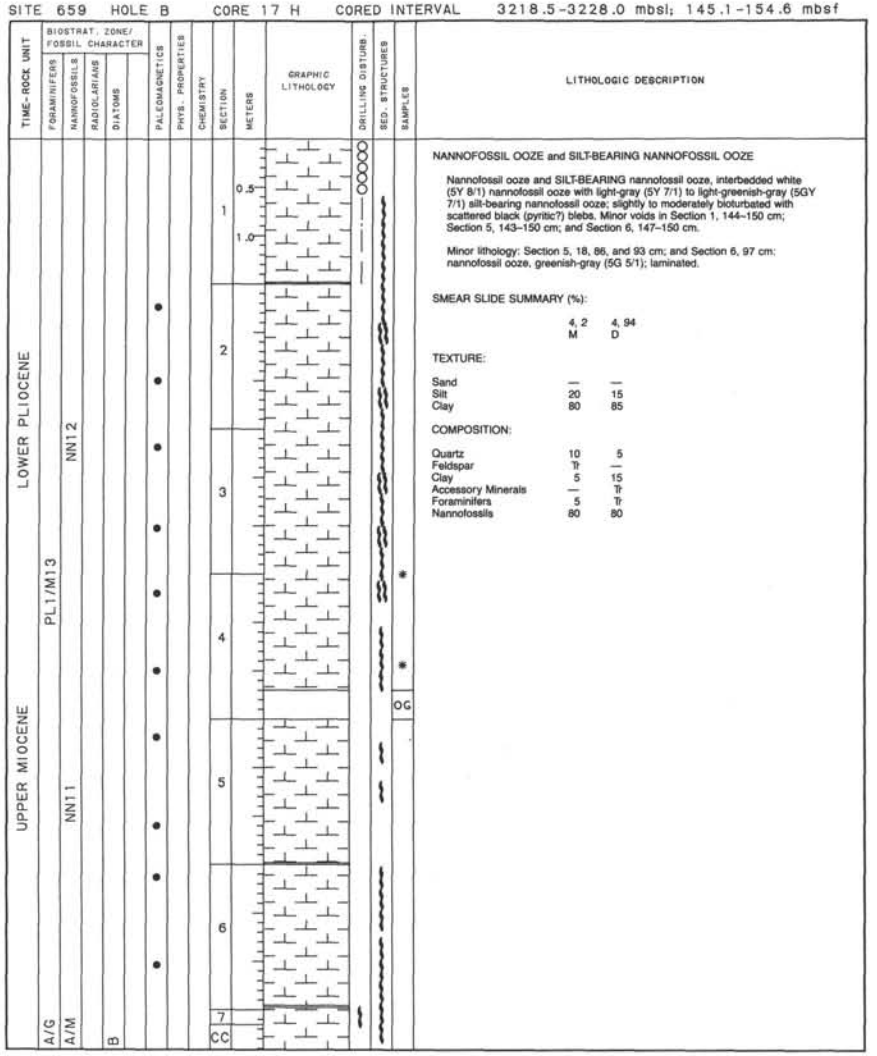

NANNOFOSSIL OOZE and SILT-BEARING NANNOFOSSIL OOZE

Nannofossil ooze and SILT-BEARING nannofossil ooze, interbedded white (5Y 8/1) nannofossil ooze with light-gray (5Y 7/1) to light-greenish-gray (5GY 7/1) silt-bearing nannofossil ooze; slightly to moderately bioturbated with scattered black (pyritic?) blebs. Minor voids in Section 1, 144–150 cm; Section 5, 143–150 cm; and Section 6, 147–150 cm.

Minor lithology: Section 5, 18, 86, and 93 cm; and Section 6, 97 cm: nannofossil ooze, greenish-gray (5G 5/1); laminated.

SMEAR SLIDE SUMMARY (%):

	4, 2 M	4, 94 D
TEXTURE:		
Sand	—	—
Silt	20	15
Clay	80	85
COMPOSITION:		
Quartz	10	5
Feldspar	Tr	—
Clay	5	15
Accessory Minerals	—	Tr
Foraminifers	5	Tr
Nannofossils	80	80

SITE 659 HOLE B CORE 18 H CORED INTERVAL 3228.0-3237.5 mbsl; 154.6-164.1 mbsf

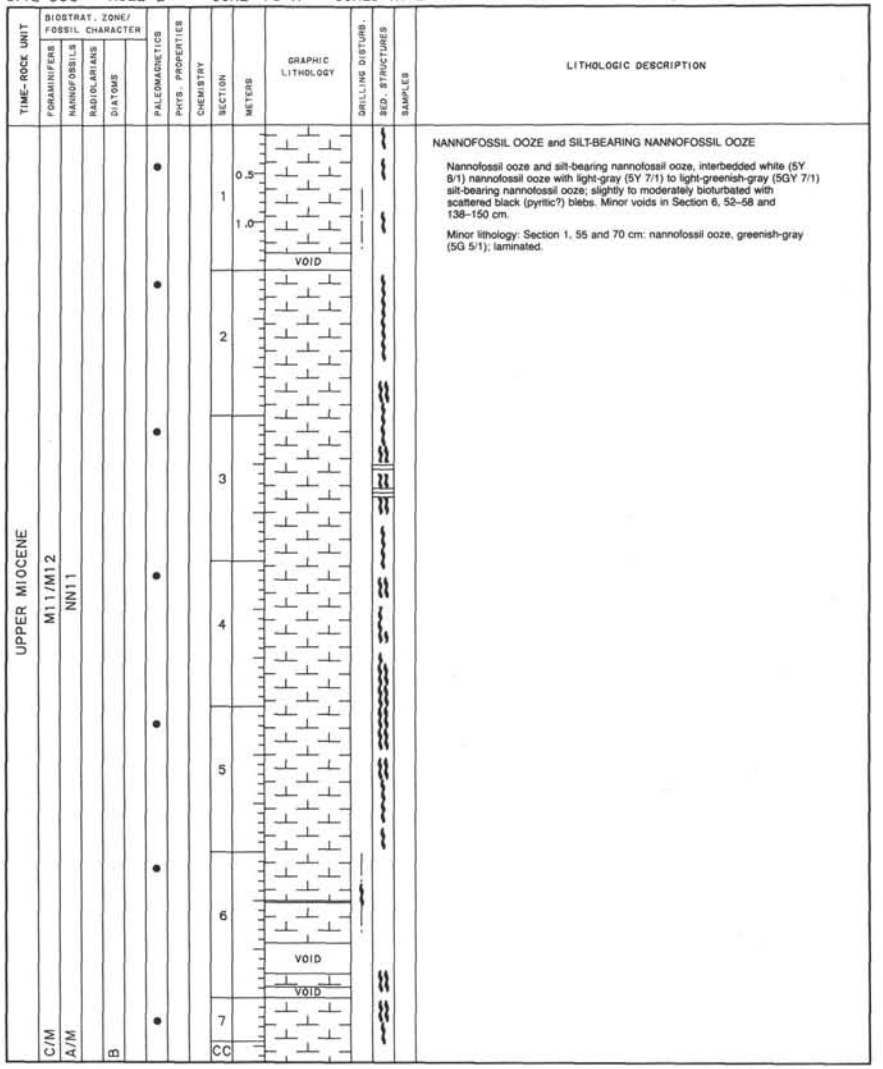

NANNOFOSSIL OOZE and SILT-BEARING NANNOFOSSIL OOZE

Nannofossil ooze and silt-bearing nannofossil ooze, interbedded white (5Y 8/1) nannofossil ooze with light-gray (5Y 7/1) to light-greenish-gray (5GY 7/1) silt-bearing nannofossil ooze; slightly to moderately bioturbated with scattered black (pyritic?) blebs. Minor voids in Section 6, 52–58 and 138–150 cm.

Minor lithology: Section 1, 55 and 70 cm: nannofossil ooze, greenish-gray (5G 5/1); laminated.

SITE 659 HOLE B CORE 19 H CORED INTERVAL 3237.5-3247.0 mbsl; 164.1-173.6 mbsf

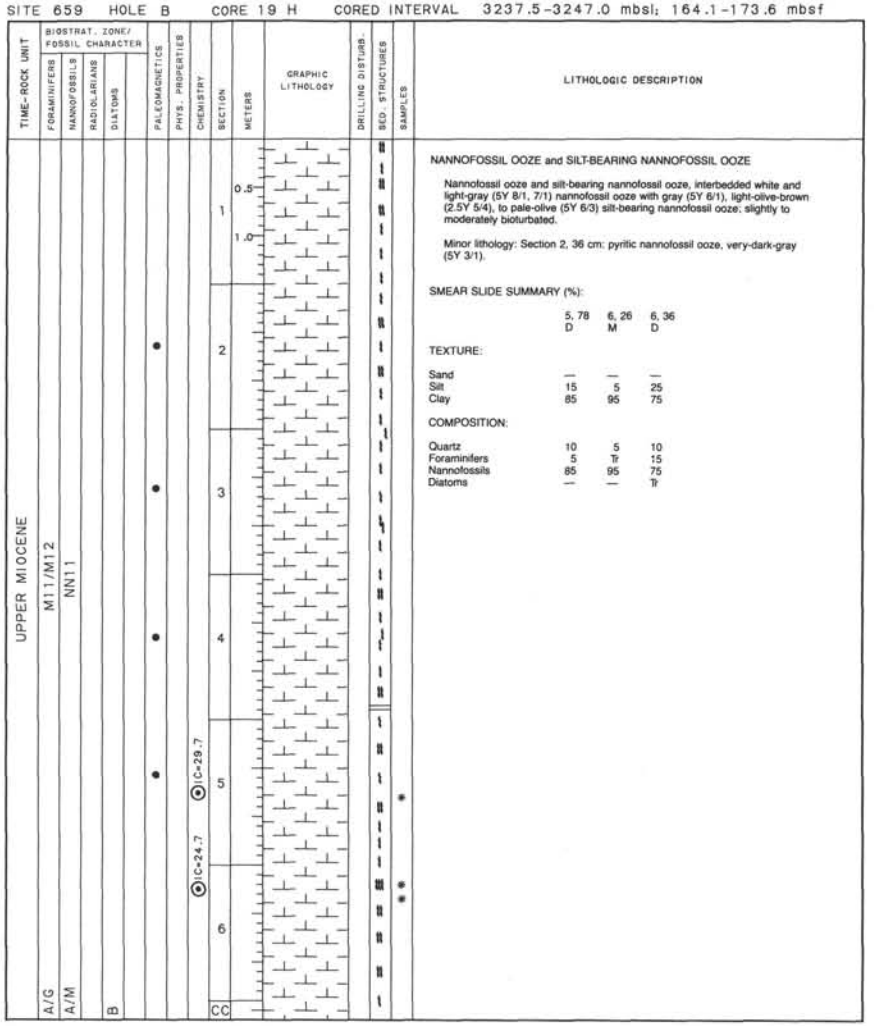

LITHOLOGIC DESCRIPTION

NANNOFOSSIL OOZE and SILT-BEARING NANNOFOSSIL OOZE

Nannofossil ooze and silt-bearing nannofossil ooze, interbedded white and light-gray (5Y 8/1, 7/1) nannofossil ooze with gray (5Y 6/1), light-olive-brown (2.5Y 5/4), to pale-olive (5Y 6/3) silt-bearing nannofossil ooze; slightly to moderately bioturbated.

Minor lithology: Section 2, 36 cm: pyritic nannofossil ooze, very-dark-gray (5Y 3/1).

SMEAR SLIDE SUMMARY (%):

	5, 78 D	6, 26 M	6, 36 D
TEXTURE:			
Sand	—	—	—
Silt	15	5	25
Clay	85	95	75
COMPOSITION:			
Quartz	10	5	10
Foraminifers	5	Tr	15
Nannofossils	85	95	75
Diatoms	—	—	Tr

SITE 659 HOLE B CORE 20 H CORED INTERVAL 3247.0-3256.5 mbsl; 173.6-183.1 mbsf

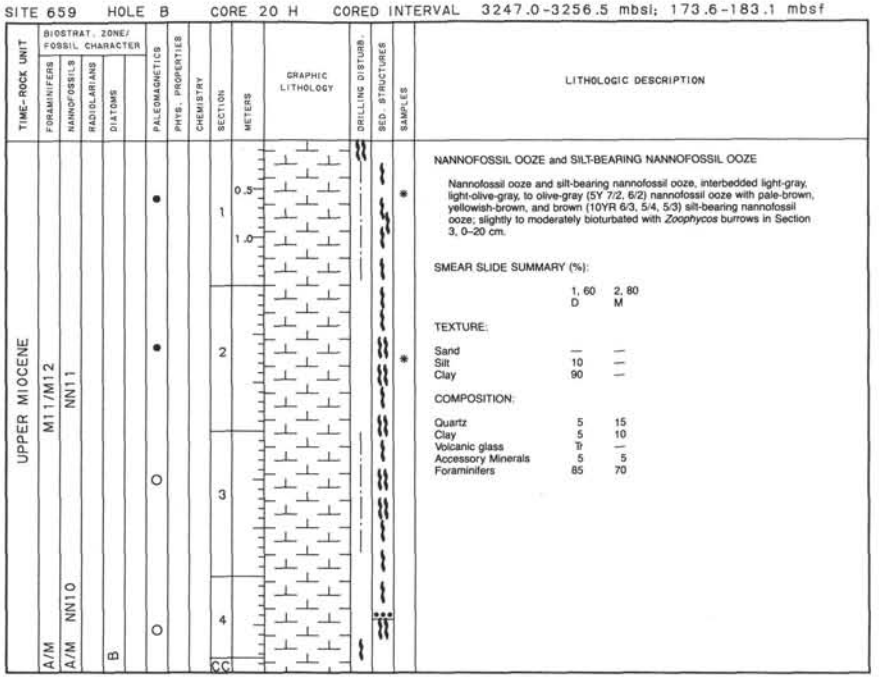

LITHOLOGIC DESCRIPTION

NANNOFOSSIL OOZE and SILT-BEARING NANNOFOSSIL OOZE

Nannofossil ooze and silt-bearing nannofossil ooze, interbedded light-gray, light-olive-gray, to olive-gray (5Y 7/2, 6/2) nannofossil ooze with pale-brown, yellowish-brown, and brown (10YR 6/3, 5/4, 5/3) silt-bearing nannofossil ooze; slightly to moderately bioturbated with *Zoophycos* burrows in Section 3, 0–20 cm.

SMEAR SLIDE SUMMARY (%):

	1, 60 D	2, 80 M
TEXTURE:		
Sand	—	—
Silt	10	—
Clay	90	—
COMPOSITION:		
Quartz	5	15
Clay	5	10
Volcanic glass	Tr	—
Accessory Minerals	5	5
Foraminifers	85	70

SITE 659 HOLE B CORE 21 H CORED INTERVAL 3256.5-3266.0 mbsl; 183.1-192.6 mbsf

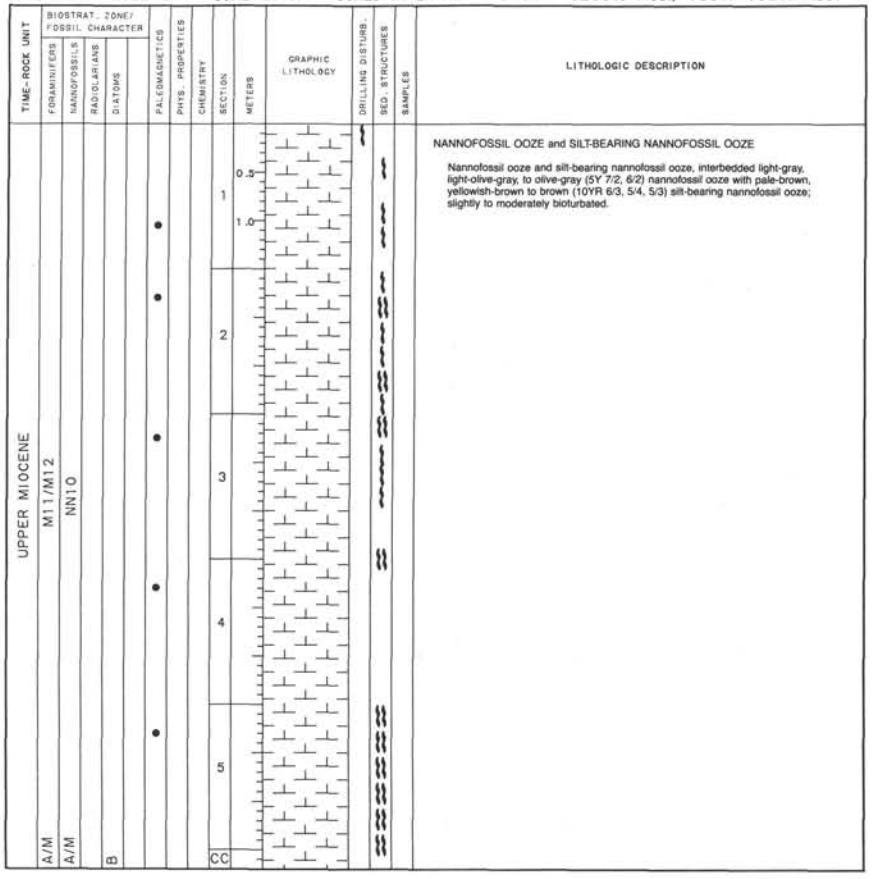

LITHOLOGIC DESCRIPTION

NANNOFOSSIL OOZE and SILT-BEARING NANNOFOSSIL OOZE

Nannofossil ooze and silt-bearing nannofossil ooze, interbedded light-gray, light-olive-gray, to olive-gray (5Y 7/2, 6/2) nannofossil ooze with pale-brown, yellowish-brown to brown (10YR 6/3, 5/4, 5/3) silt-bearing nannofossil ooze; slightly to moderately bioturbated.

SITE 659 HOLE B CORE 22 H CORED INTERVAL 3266.0-3275.5 mbsl; 192.6-202.1 mbsf

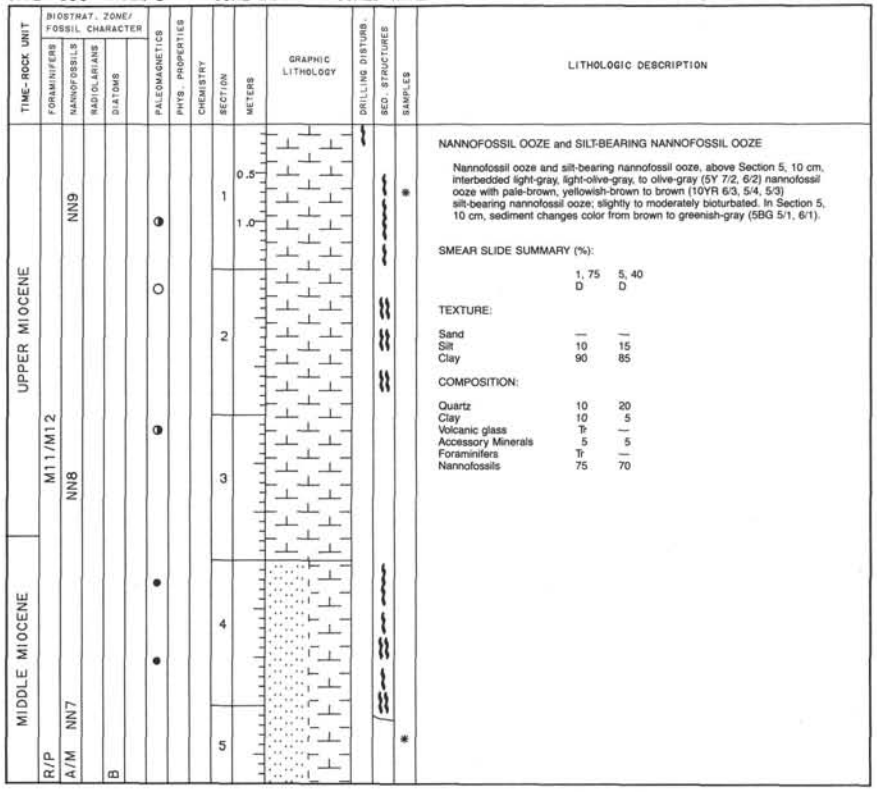

LITHOLOGIC DESCRIPTION

NANNOFOSSIL OOZE and SILT-BEARING NANNOFOSSIL OOZE

Nannofossil ooze and silt-bearing nannofossil ooze, above Section 5, 10 cm, interbedded light-gray, light-olive-gray, to olive-gray (5Y 7/2, 6/2) nannofossil ooze with pale-brown, yellowish-brown to brown (10YR 6/3, 5/4, 5/3) silt-bearing nannofossil ooze; slightly to moderately bioturbated. In Section 5, 10 cm, sediment changes color from brown to greenish-gray (5BG 5/1, 6/1).

SMEAR SLIDE SUMMARY (%):

	1, 75	5, 40
	D	D
TEXTURE:		
Sand	—	—
Silt	10	15
Clay	90	85
COMPOSITION:		
Quartz	10	20
Clay	10	5
Volcanic glass	Tr	—
Accessory Minerals	5	5
Foraminifers	Tr	—
Nannofossils	75	70

SITE 659 HOLE C CORE 1 H CORED INTERVAL 3070.5-3080.0 mbsl; 0-9.5 mbsf

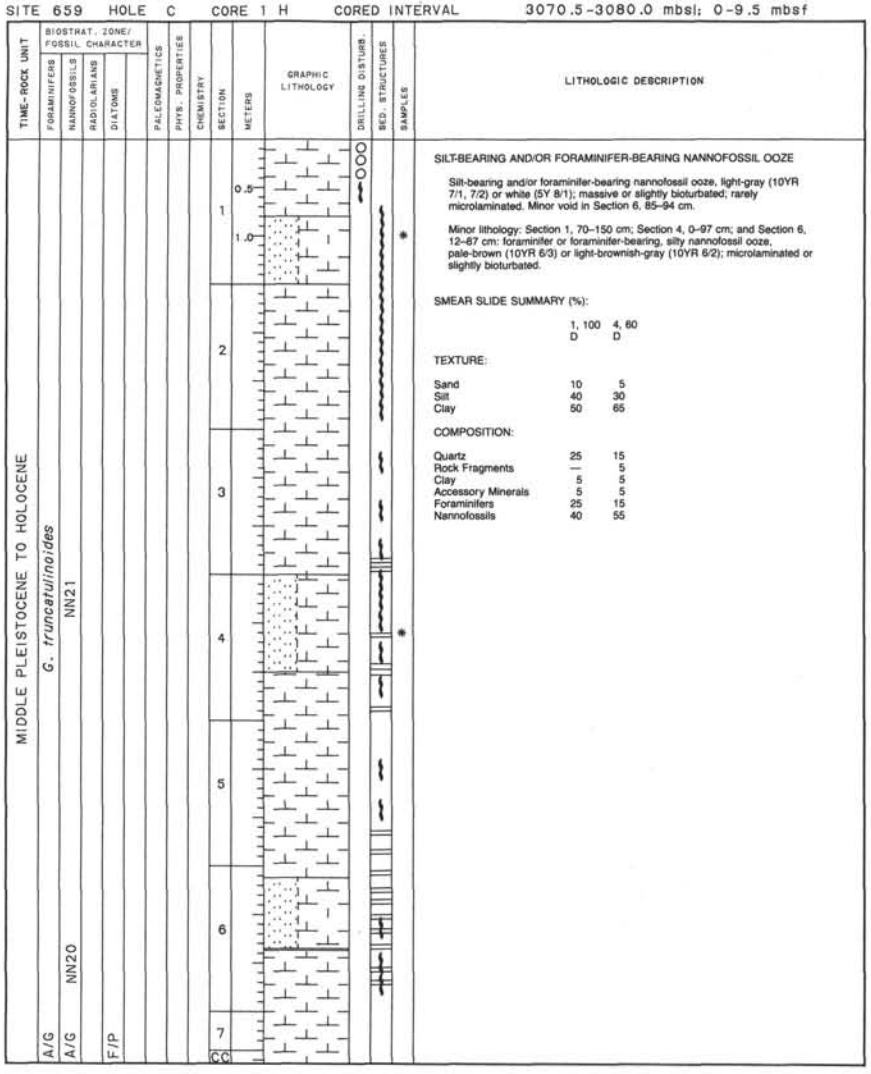

LITHOLOGIC DESCRIPTION

SILT-BEARING AND/OR FORAMINIFER-BEARING NANNOFOSSIL OOZE

Silt-bearing and/or foraminifer-bearing nannofossil ooze, light-gray (10YR 7/1, 7/2) or white (5Y 8/1); massive or slightly bioturbated; rarely microlaminated. Minor void in Section 6, 85–94 cm.

Minor lithology: Section 1, 70–150 cm; Section 4, 0–97 cm; and Section 6, 12–87 cm: foraminifer or foraminifer-bearing, silty nannofossil ooze, pale-brown (10YR 6/3) or light-brownish-gray (10YR 6/2); microlaminated or slightly bioturbated.

SMEAR SLIDE SUMMARY (%):

	1, 100 D	4, 60 D
TEXTURE:		
Sand	10	5
Silt	40	30
Clay	50	65
COMPOSITION:		
Quartz	25	15
Rock Fragments	—	5
Clay	5	5
Accessory Minerals	5	5
Foraminifers	25	15
Nannofossils	40	55

SITE 659 HOLE C CORE 2 H CORED INTERVAL 3080.0-3089.5 mbsl; 9.5-19.0 mbsf

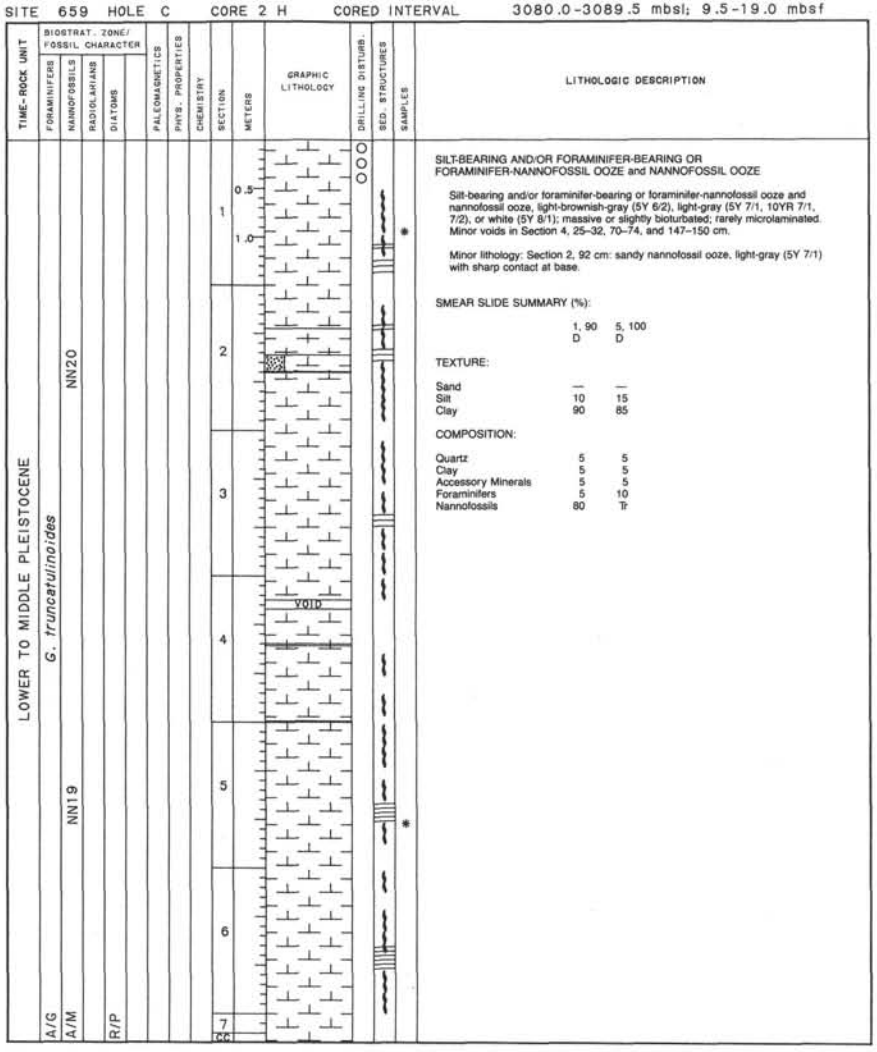

LITHOLOGIC DESCRIPTION

SILT-BEARING AND/OR FORAMINIFER-BEARING OR FORAMINIFER-NANNOFOSSIL OOZE and NANNOFOSSIL OOZE

Silt-bearing and/or foraminifer-bearing or foraminifer-nannofossil ooze and nannofossil ooze, light-brownish-gray (5Y 6/2), light-gray (5Y 7/1, 10YR 7/1, 7/2), or white (5Y 8/1); massive or slightly bioturbated; rarely microlaminated. Minor voids in Section 4, 25–32, 70–74, and 147–150 cm.

Minor lithology: Section 2, 92 cm: sandy nannofossil ooze, light-gray (5Y 7/1) with sharp contact at base.

SMEAR SLIDE SUMMARY (%):

	1, 90 D	5, 100 D
TEXTURE:		
Sand	—	—
Silt	10	15
Clay	90	85
COMPOSITION:		
Quartz	5	5
Clay	5	5
Accessory Minerals	5	5
Foraminifers	5	10
Nannofossils	80	Tr

SITE 659 HOLE C CORE 3 H CORED INTERVAL 3089.5-3099.0 mbsl; 19.0-28.5 mbsf

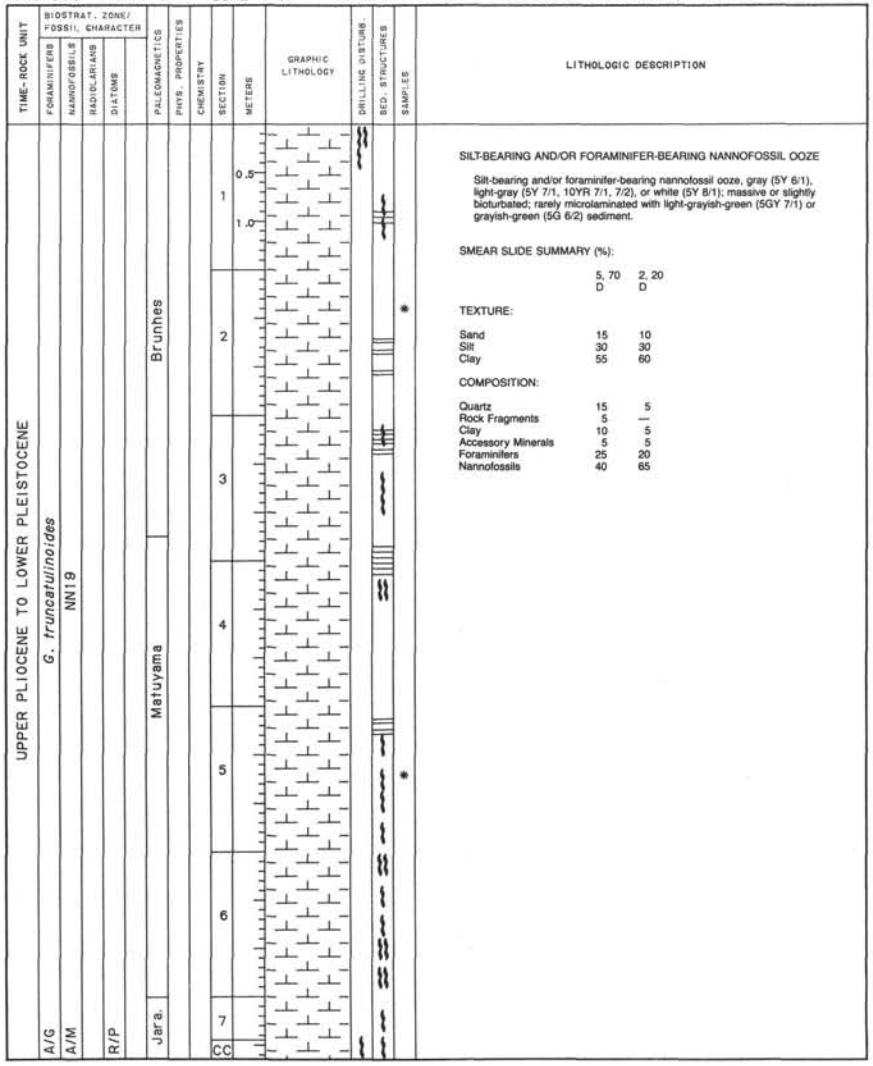

LITHOLOGIC DESCRIPTION

SILT-BEARING AND/OR FORAMINIFER-BEARING NANNOFOSSIL OOZE

Silt-bearing and/or foraminifer-bearing nannofossil ooze, gray (5Y 6/1), light-gray (5Y 7/1, 10YR 7/1, 7/2), or white (5Y 8/1); massive or slightly bioturbated; rarely microlaminated with light-grayish-green (5GY 7/1) or grayish-green (5G 6/2) sediment.

SMEAR SLIDE SUMMARY (%):

	5, 70 D	2, 20 D
TEXTURE:		
Sand	15	10
Silt	30	30
Clay	55	60
COMPOSITION:		
Quartz	15	5
Rock Fragments	5	—
Clay	10	5
Accessory Minerals	5	5
Foraminifers	25	20
Nannofossils	40	65

SITE 659 HOLE C CORE 4 H CORED INTERVAL 3099.0-3108.5 mbsl; 28.5-38.0 mbsf

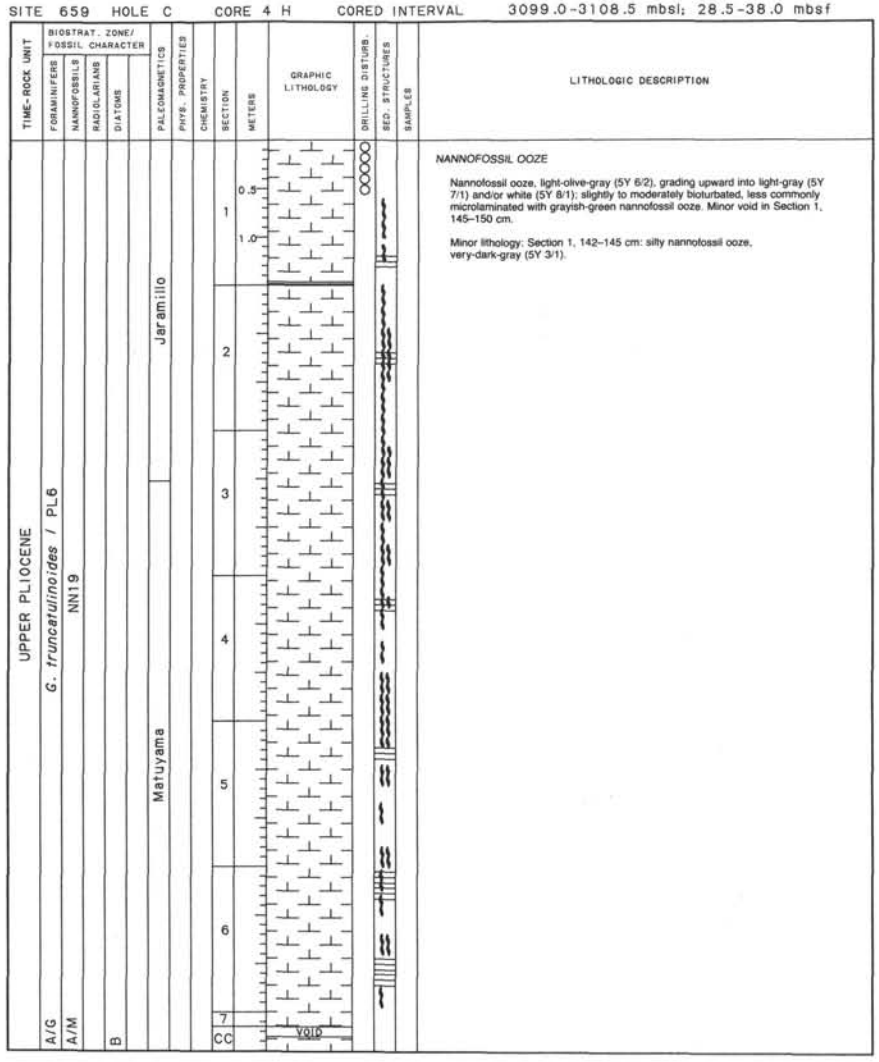

LITHOLOGIC DESCRIPTION

NANNOFOSSIL OOZE

Nannofossil ooze, light-olive-gray (5Y 6/2), grading upward into light-gray (5Y 7/1) and/or white (5Y 8/1); slightly to moderately bioturbated, less commonly microlaminated with grayish-green nannofossil ooze. Minor void in Section 1, 145–150 cm.

Minor lithology: Section 1, 142–145 cm: silty nannofossil ooze, very-dark-gray (5Y 3/1).

SITE 659 HOLE C CORE 5 H CORED INTERVAL 3108.5-3118.0 mbsl; 100.0-109.5 mbsf

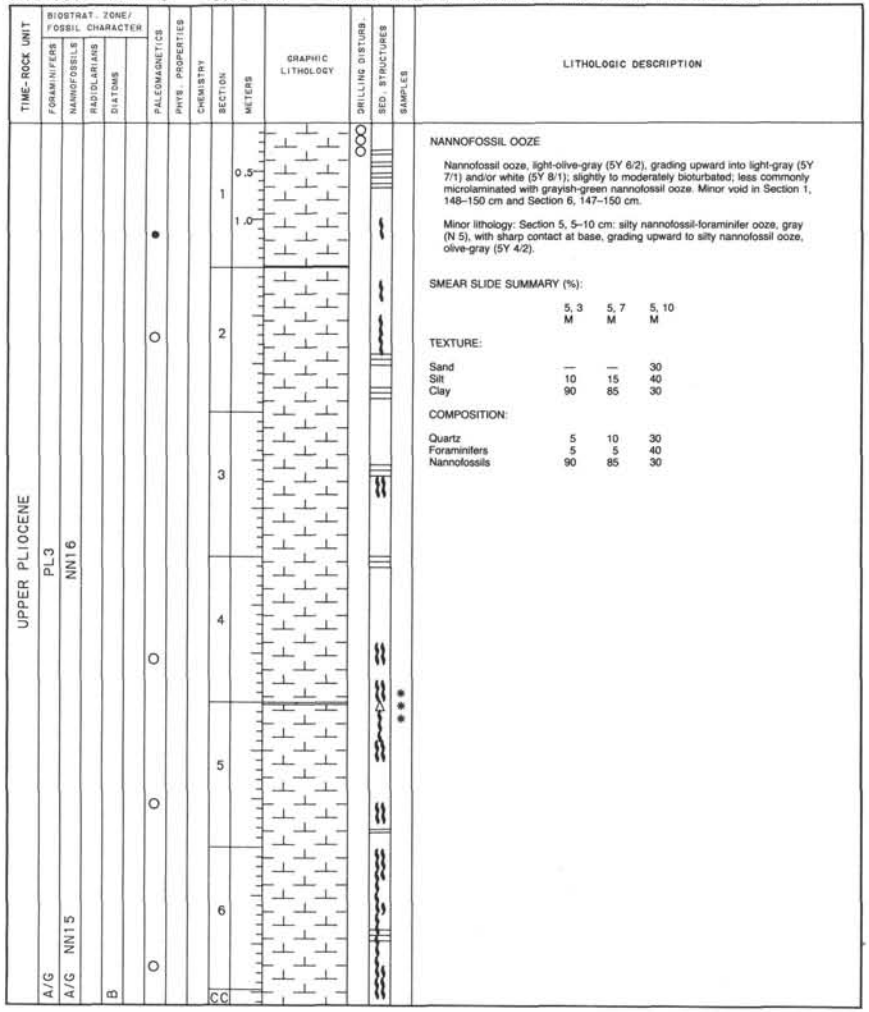

LITHOLOGIC DESCRIPTION

NANNOFOSSIL OOZE

Nannofossil ooze, light-olive-gray (5Y 6/2), grading upward into light-gray (5Y 7/1) and/or white (5Y 8/1); slightly to moderately bioturbated; less commonly microlaminated with grayish-green nannofossil ooze. Minor void in Section 1, 148–150 cm and Section 6, 147–150 cm.

Minor lithology: Section 5, 5–10 cm: silty nannofossil-foraminifer ooze, gray (N 5), with sharp contact at base, grading upward to silty nannofossil ooze, olive-gray (5Y 4/2).

SMEAR SLIDE SUMMARY (%):

	5, 3 M	5, 7 M	5, 10 M
TEXTURE:			
Sand	—	—	30
Silt	10	15	40
Clay	90	85	30
COMPOSITION:			
Quartz	5	10	30
Foraminifers	5	5	40
Nannofossils	90	85	30

SITE 659 HOLE C CORE 6 H CORED INTERVAL 3118.0-3127.5 mbsl; 109.5-119.0 mbsf

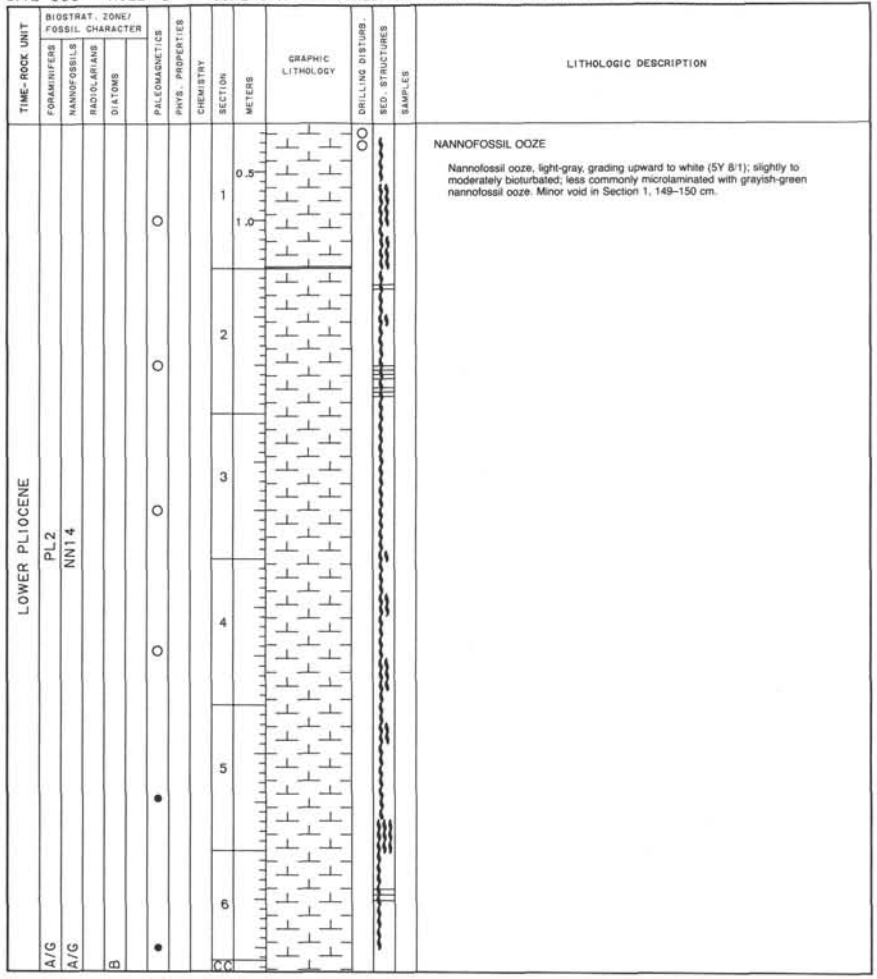

LITHOLOGIC DESCRIPTION

NANNOFOSSIL OOZE

Nannofossil ooze, light-gray, grading upward to white (5Y 8/1); slightly to moderately bioturbated; less commonly microlaminated with grayish-green nannofossil ooze. Minor void in Section 1, 149–150 cm.

SITE 659 HOLE C CORE 7 H CORED INTERVAL 3127.5-3137.0 mbsl; 177.0-186.5 mbsf

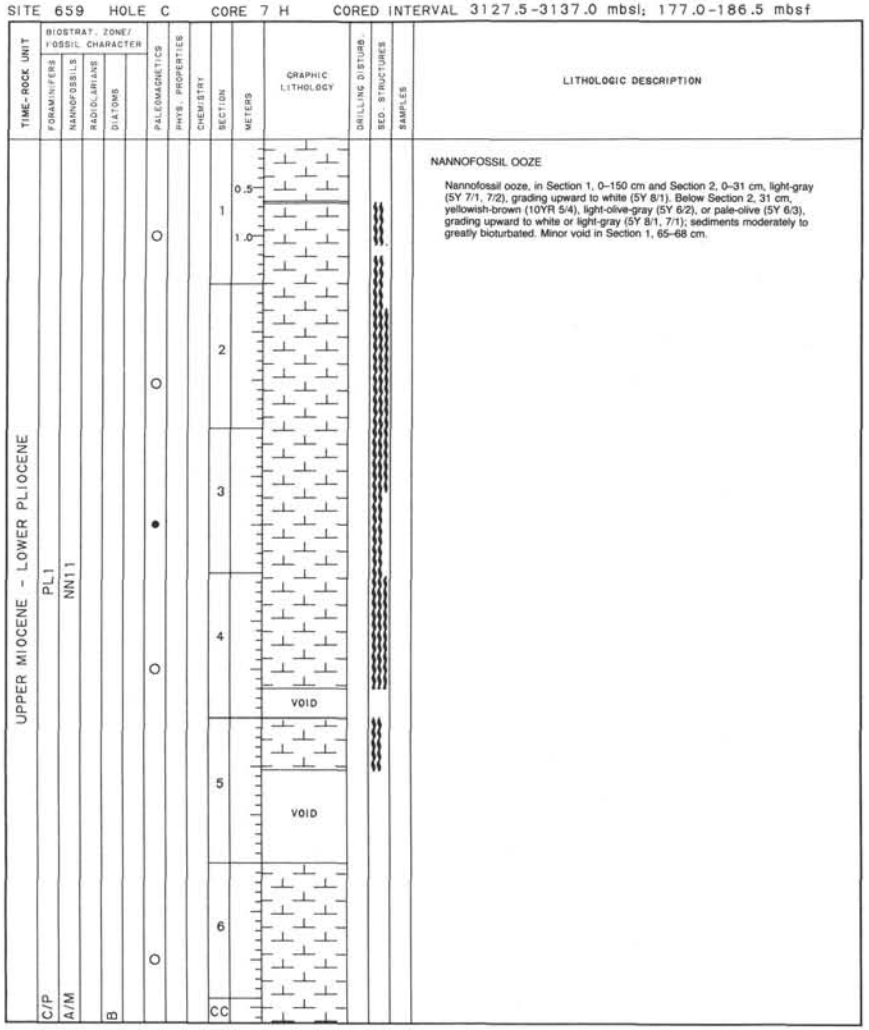

SITE 659 HOLE C CORE 8 H CORED INTERVAL 3137.0-3146.5 mbsl; 3146.5 mbsf

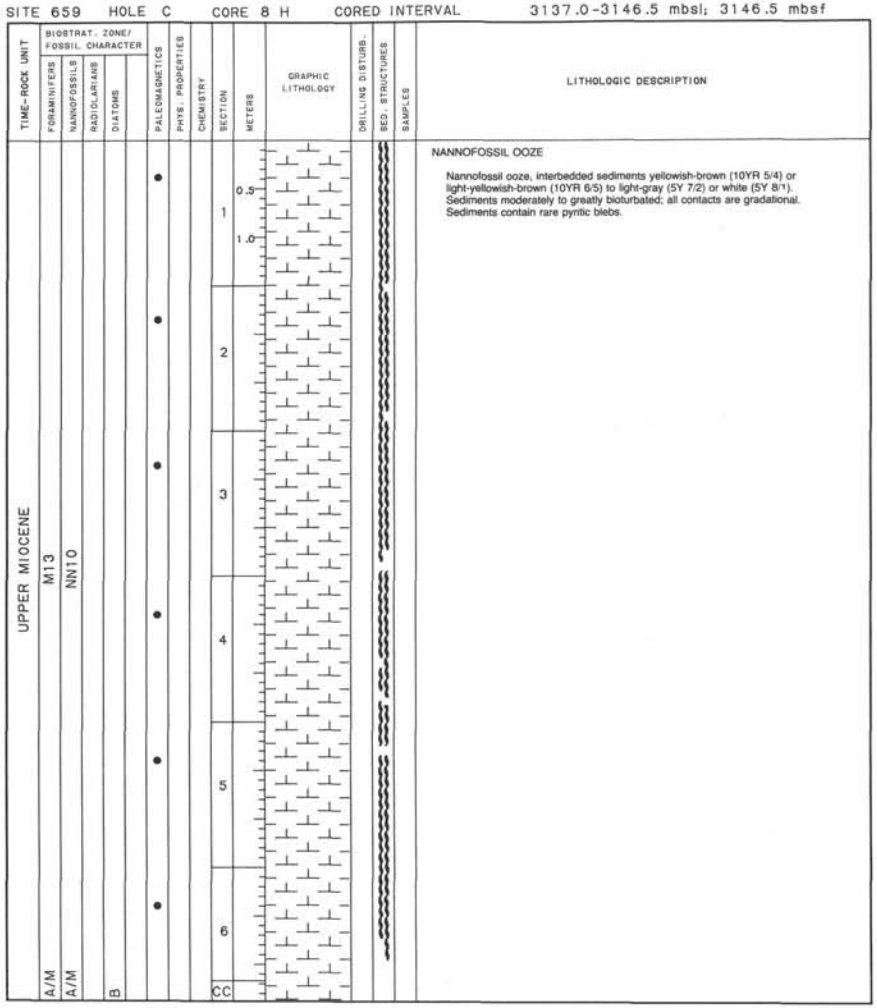

SITE 659 (HOLE A)

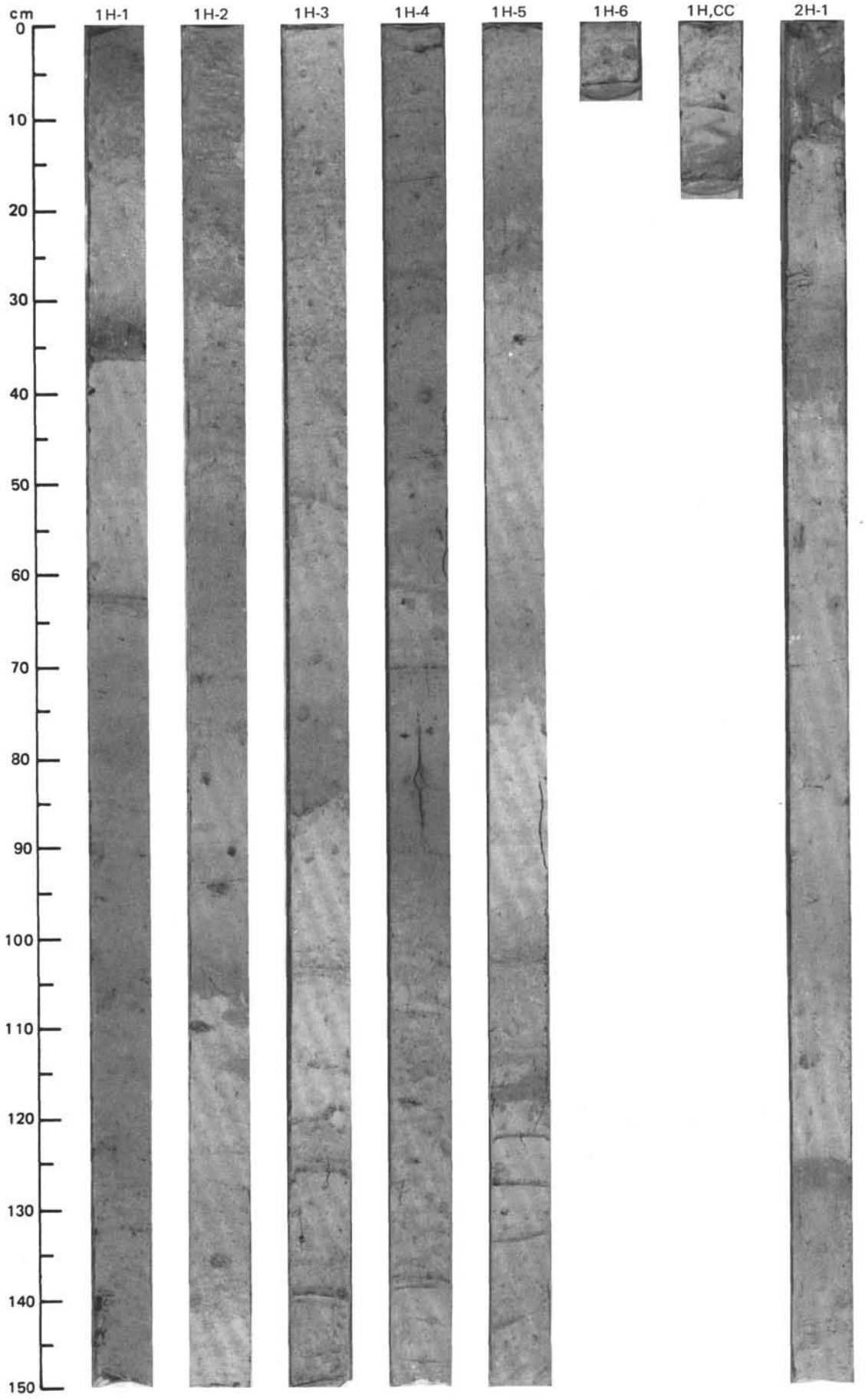

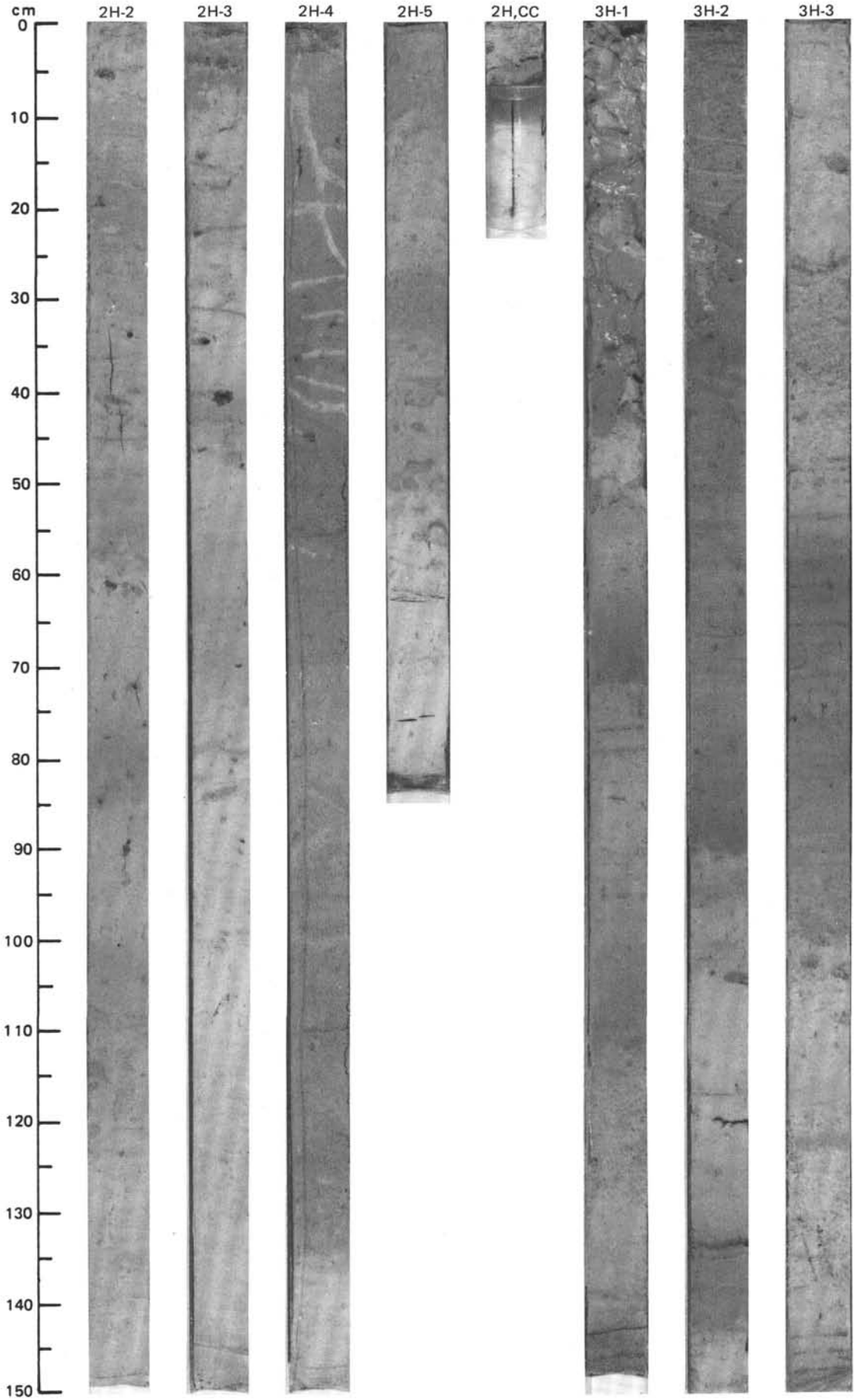
cm
0
10
20
30
40
50
60
70
80
90
100
110
120
130
140
150
2H-2
2H-3
2H-4
2H-5
2H,CC
3H-1
3H-2
3H-3

SITE 659 (HOLE A)

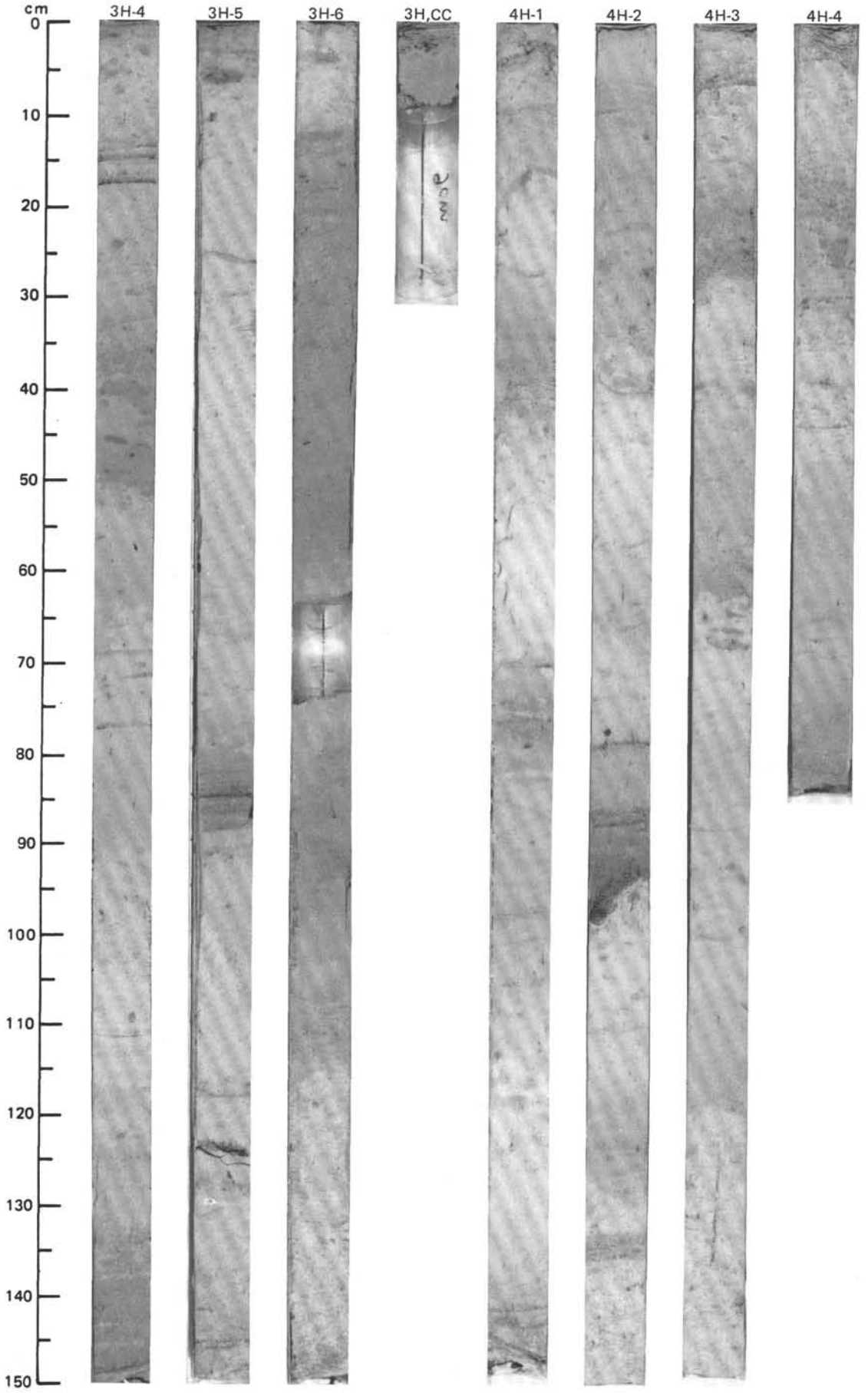

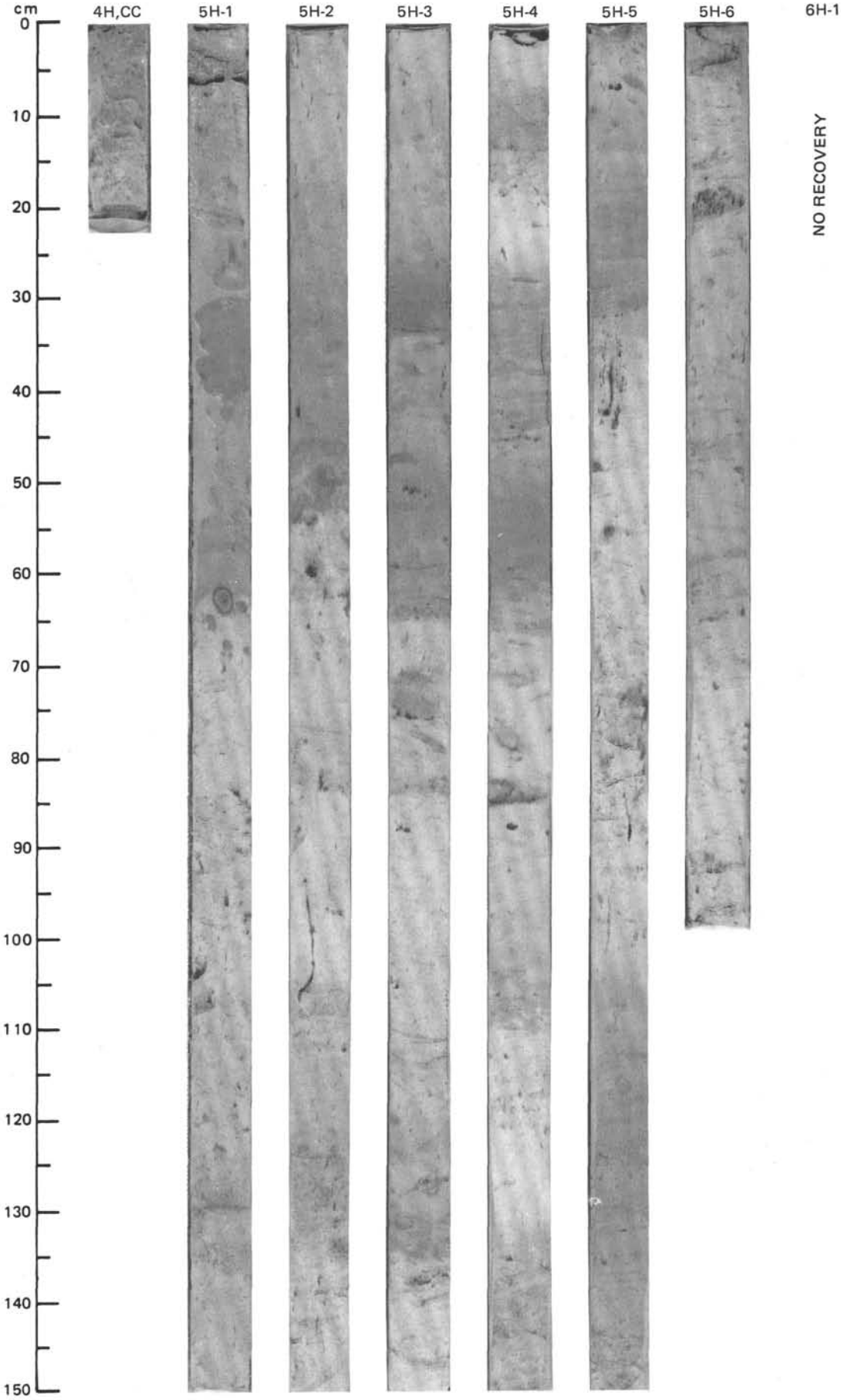
cm
0
10
20
30
40
50
60
70
80
90
100
110
120
130
140
150
4H,CC
5H-1
5H-2
5H-3
5H-4
5H-5
5H-6
6H-1
NO RECOVERY

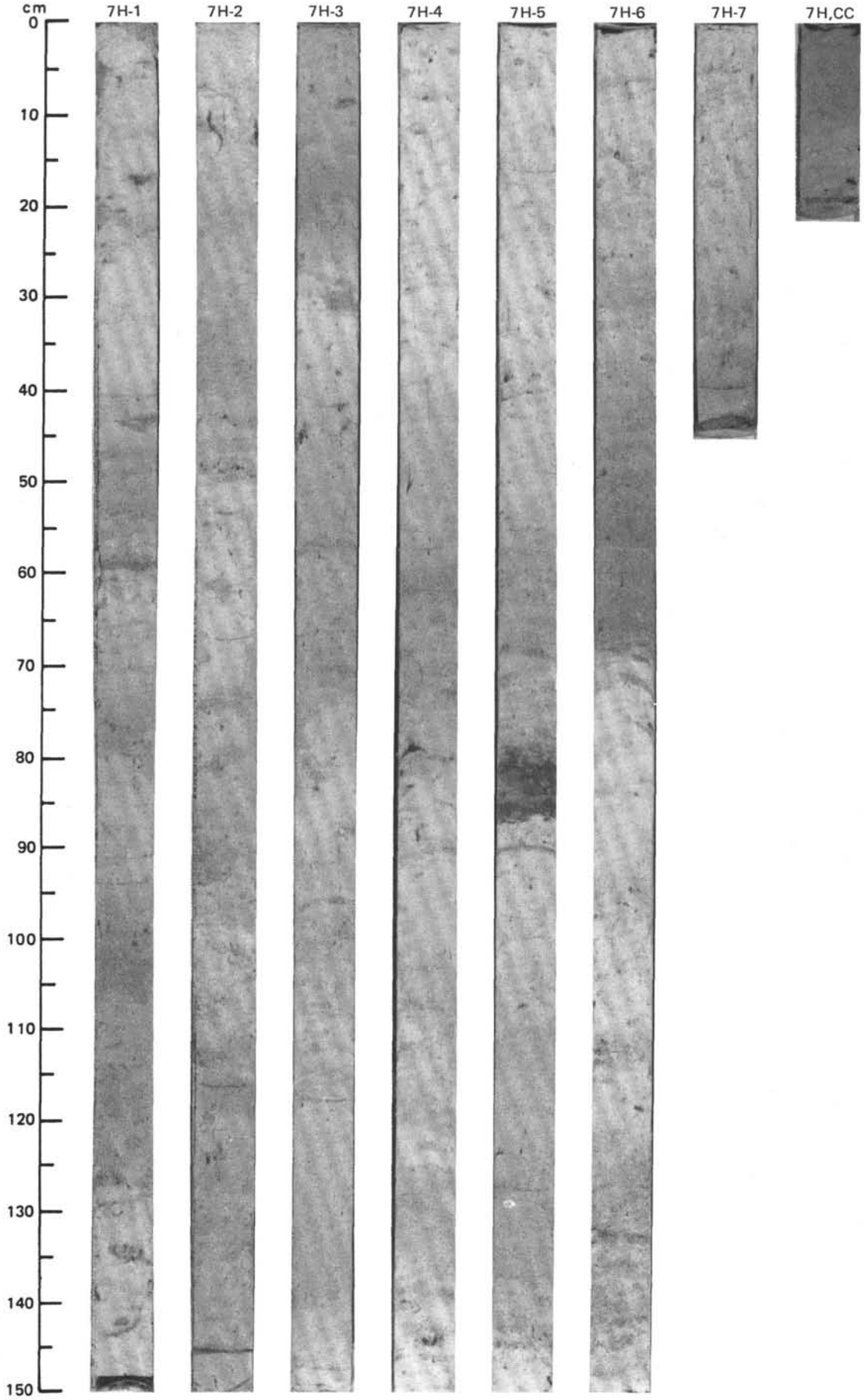
cm
0
10
20
30
40
50
60
70
80
90
100
110
120
130
140
150
7H-1
7H-2
7H-3
7H-4
7H-5
7H-6
7H-7
7H,CC

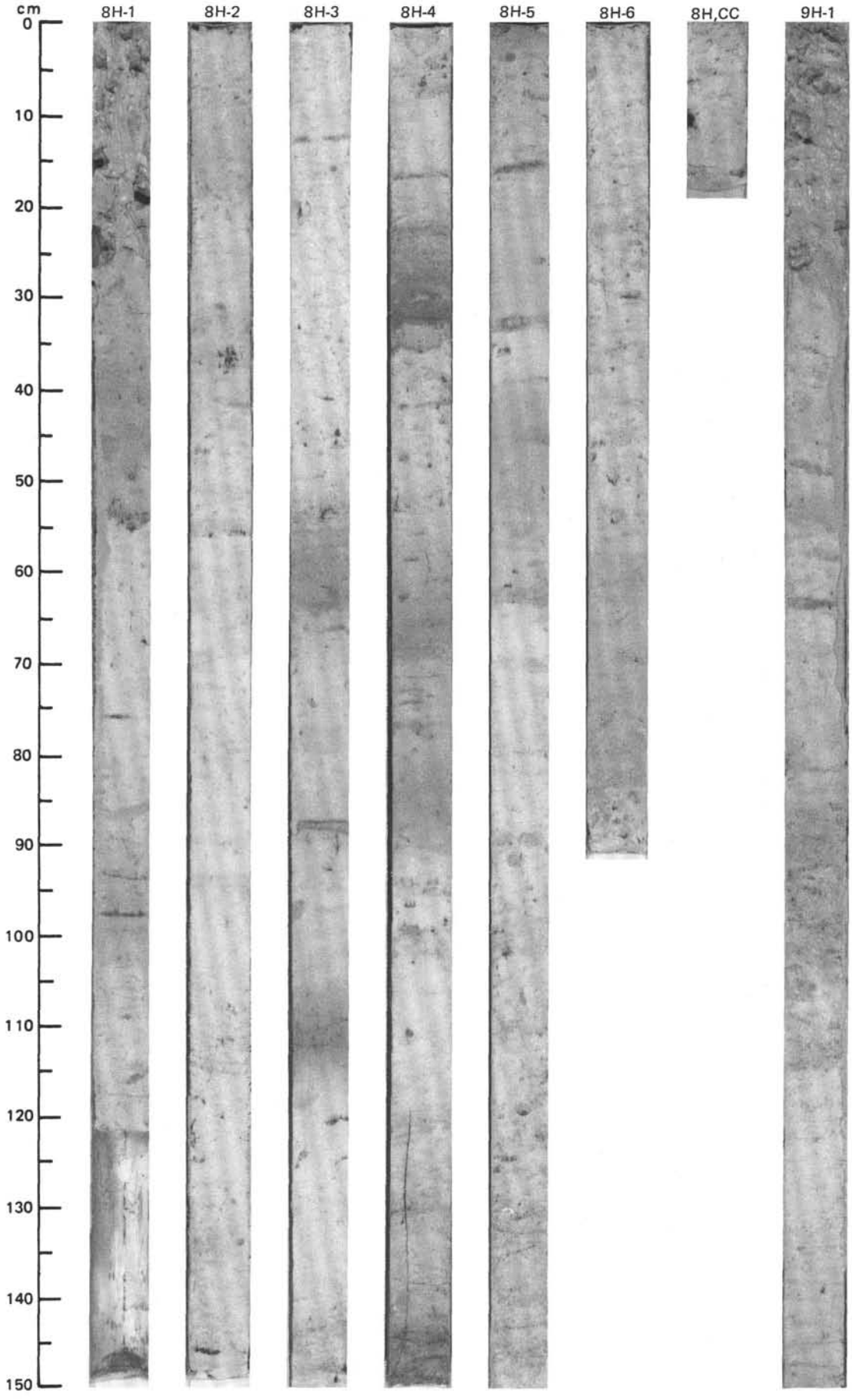
cm
0
10
20
30
40
50
60
70
80
90
100
110
120
130
140
150
8H-1
8H-2
8H-3
8H-4
8H-5
8H-6
8H,CC
9H-1

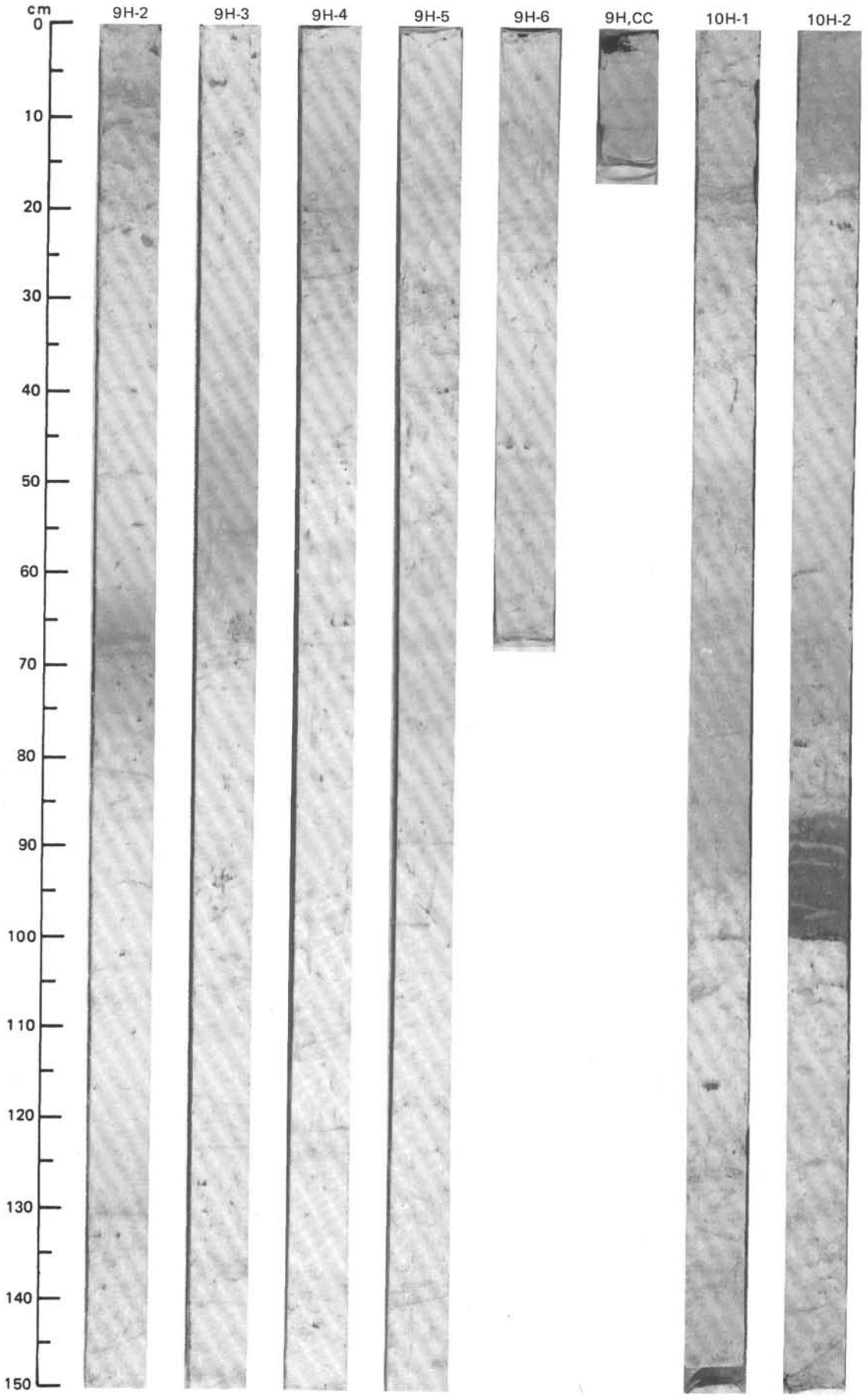
cm
0
10
20
30
40
50
60
70
80
90
100
110
120
130
140
150
9H-2
9H-3
9H-4
9H-5
9H-6
9H,CC
10H-1
10H-2

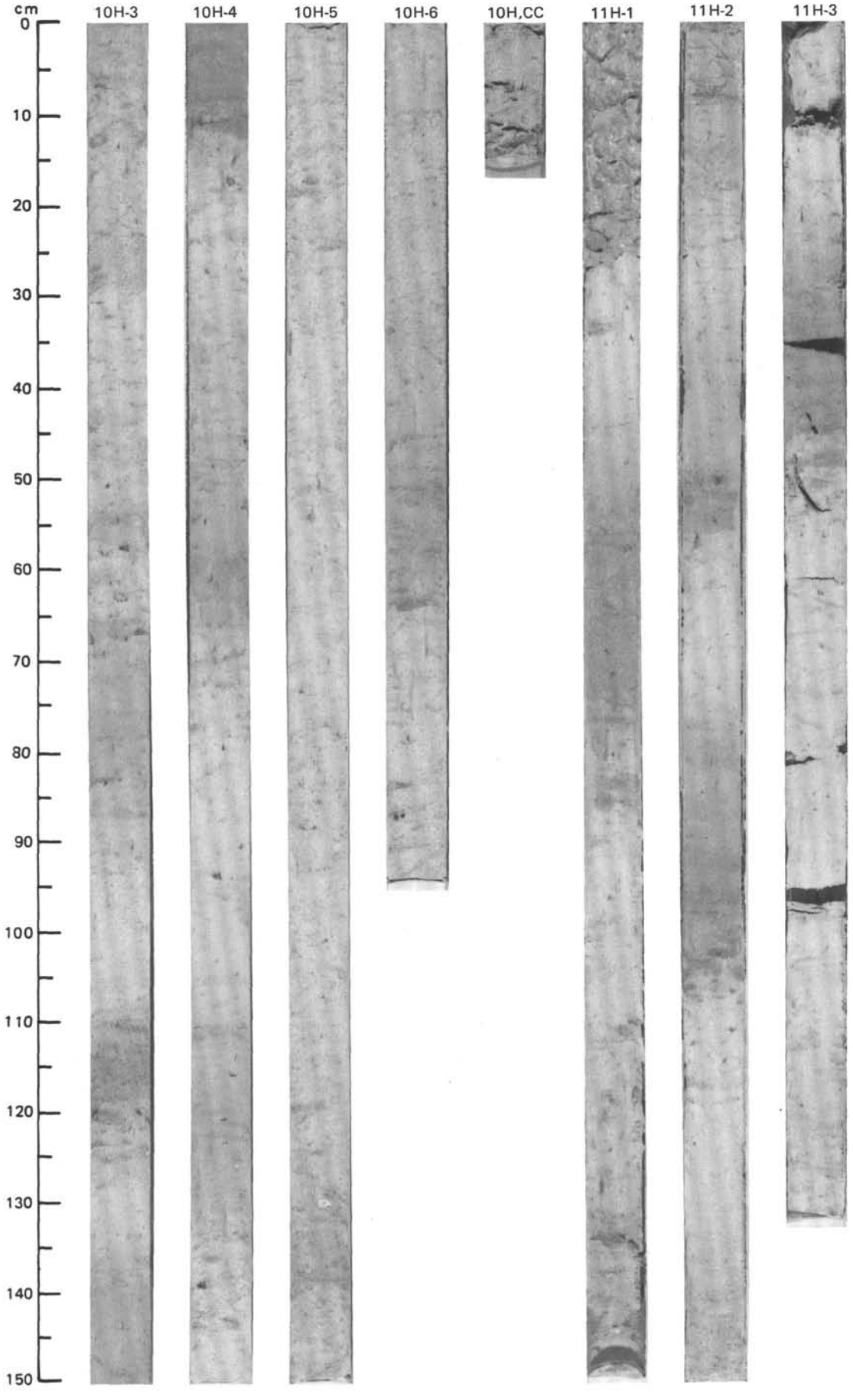
cm
0
10
20
30
40
50
60
70
80
90
100
110
120
130
140
150
10H-3
10H-4
10H-5
10H-6
10H,CC
11H-1
11H-2
11H-3

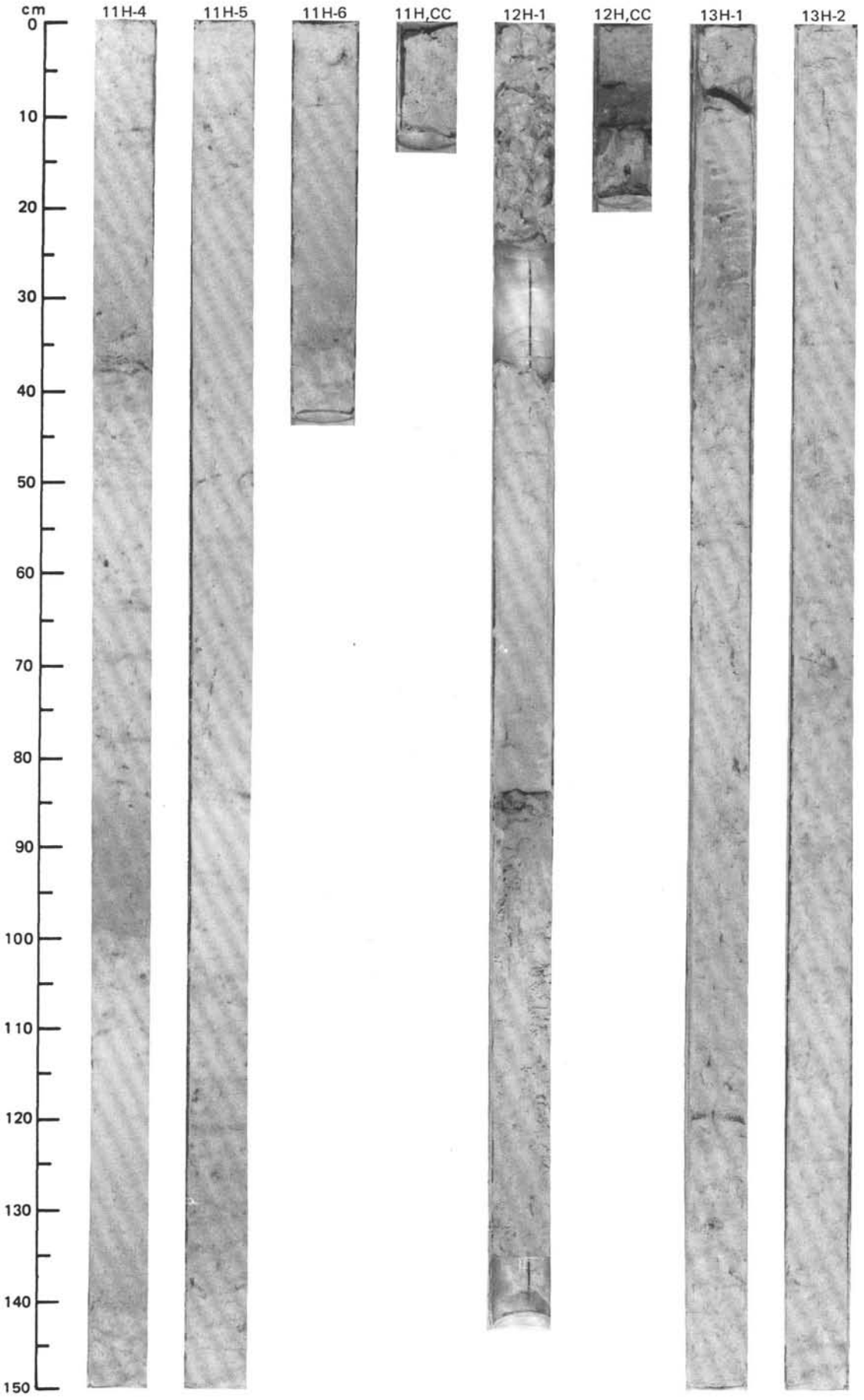
cm
0
10
20
30
40
50
60
70
80
90
100
110
120
130
140
150
11H-4
11H-5
11H-6
11H,CC
12H-1
12H,CC
13H-1
13H-2

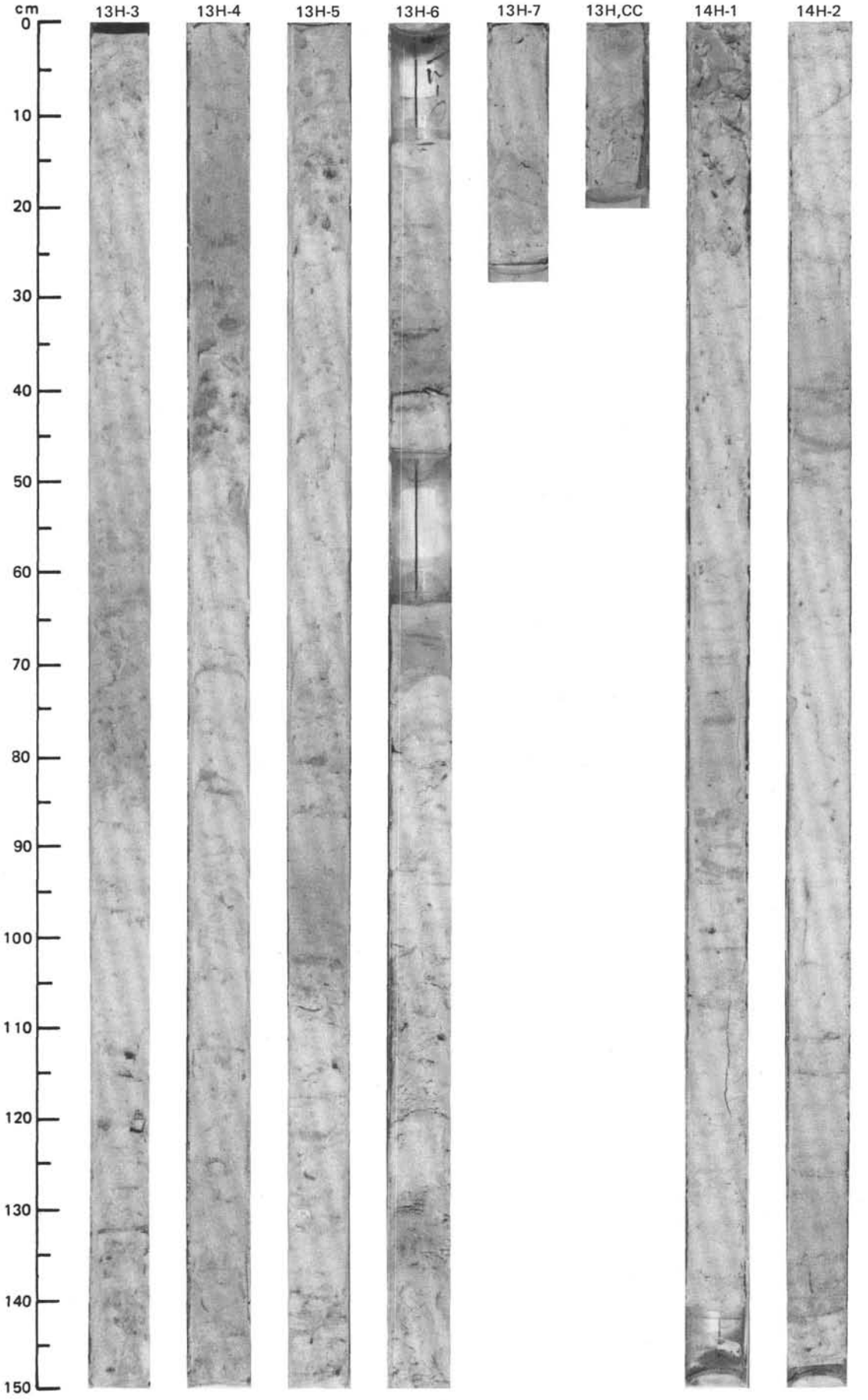
cm
0
10
20
30
40
50
60
70
80
90
100
110
120
130
140
150
13H-3
13H-4
13H-5
13H-6
13H-7
13H,CC
14H-1
14H-2

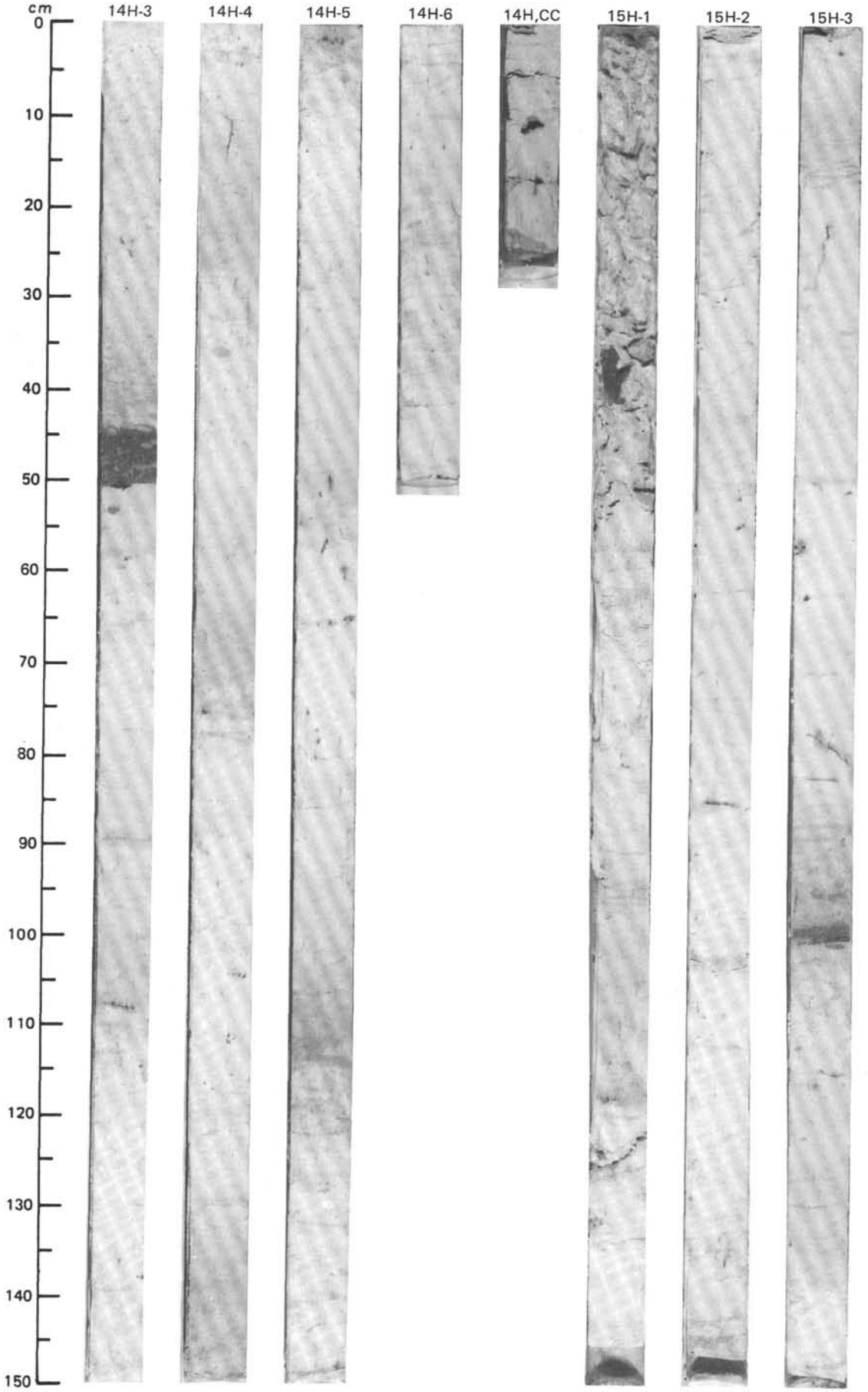
cm
0
10
20
30
40
50
60
70
80
90
100
110
120
130
140
150
14H-3
14H-4
14H-5
14H-6
14H,CC
15H-1
15H-2
15H-3

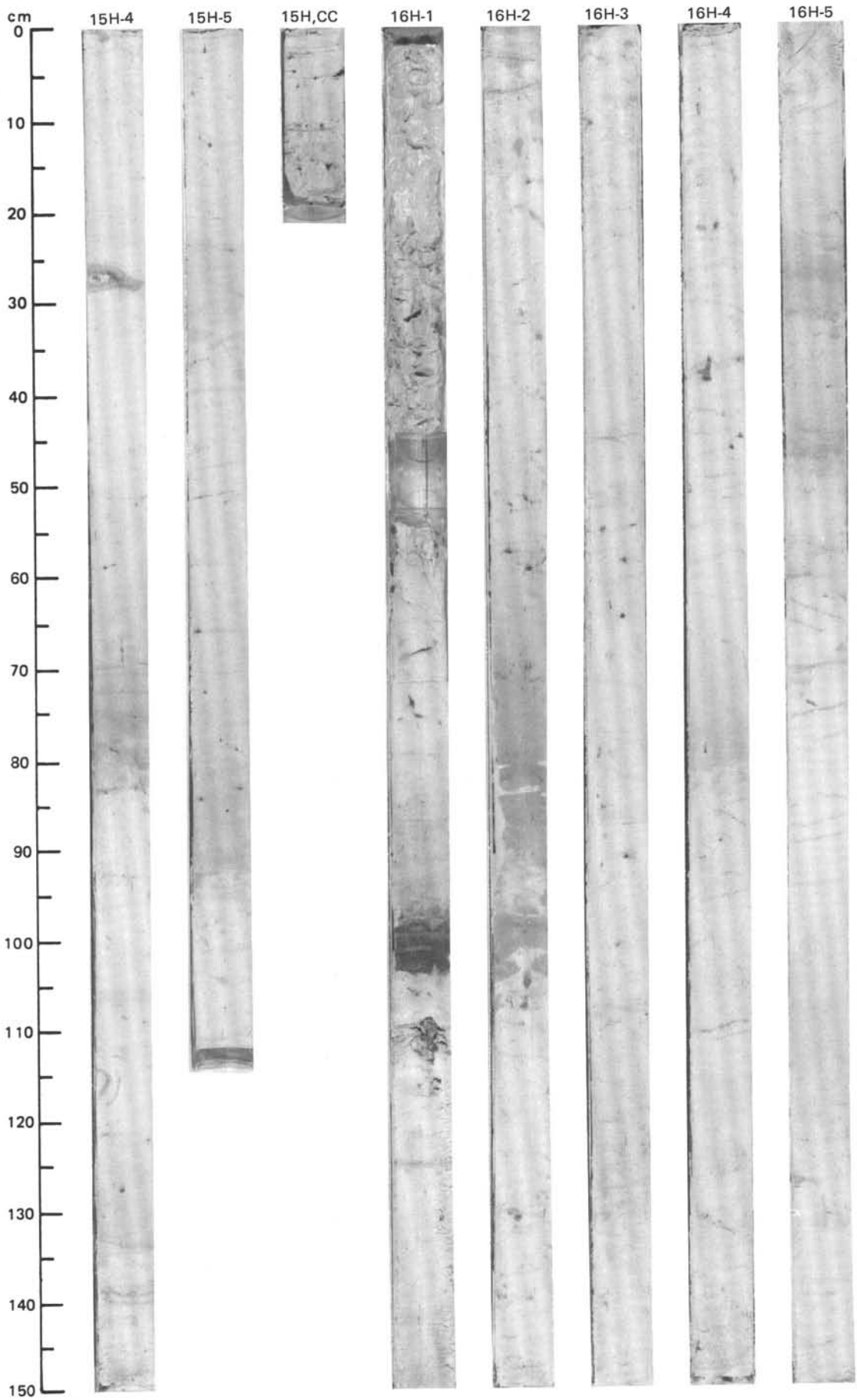
cm
0
10
20
30
40
50
60
70
80
90
100
110
120
130
140
150
15H-4
15H-5
15H,CC
16H-1
16H-2
16H-3
16H-4
16H-5

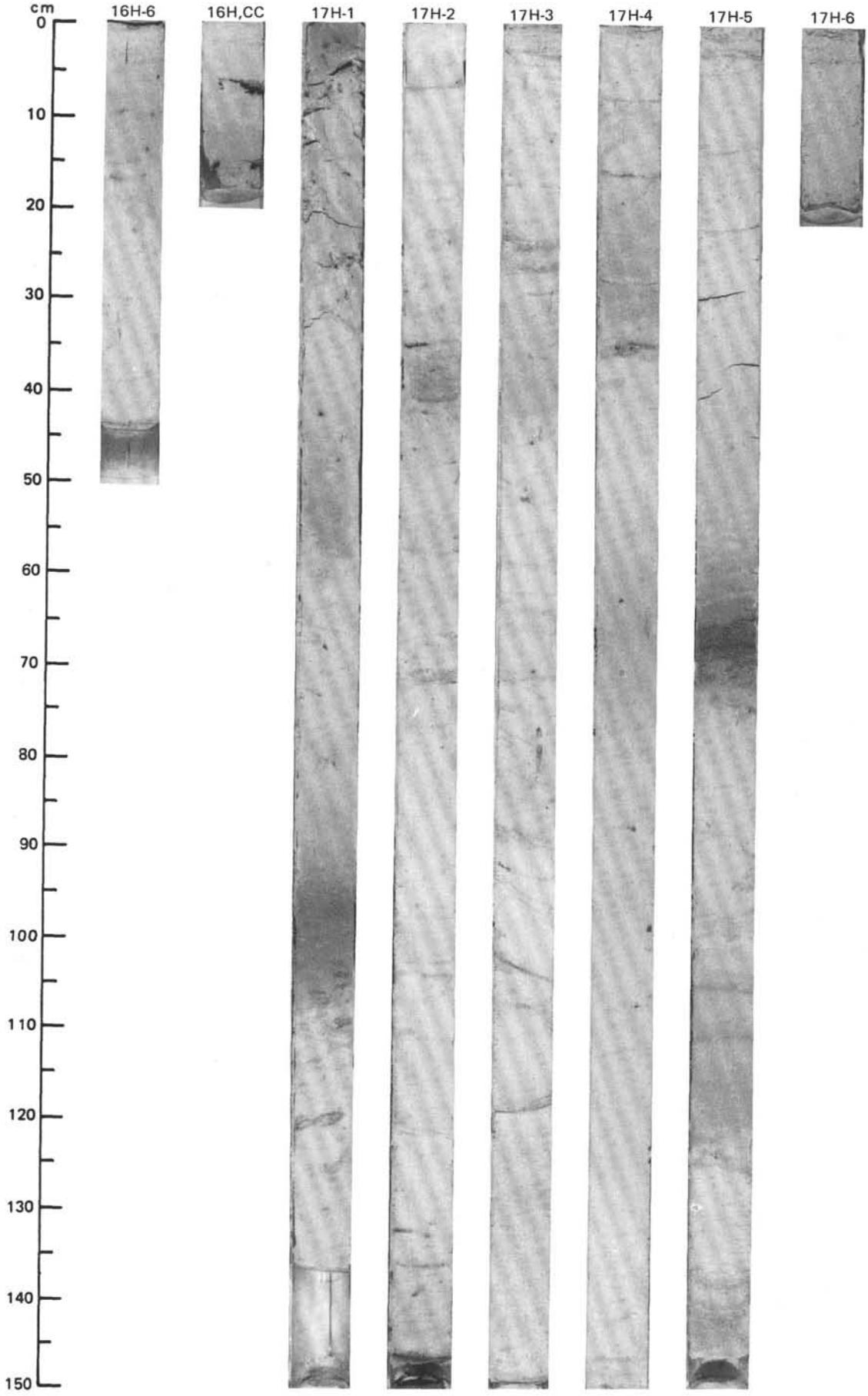
cm
0
10
20
30
40
50
60
70
80
90
100
110
120
130
140
150
16H-6
16H,CC
17H-1
17H-2
17H-3
17H-4
17H-5
17H-6

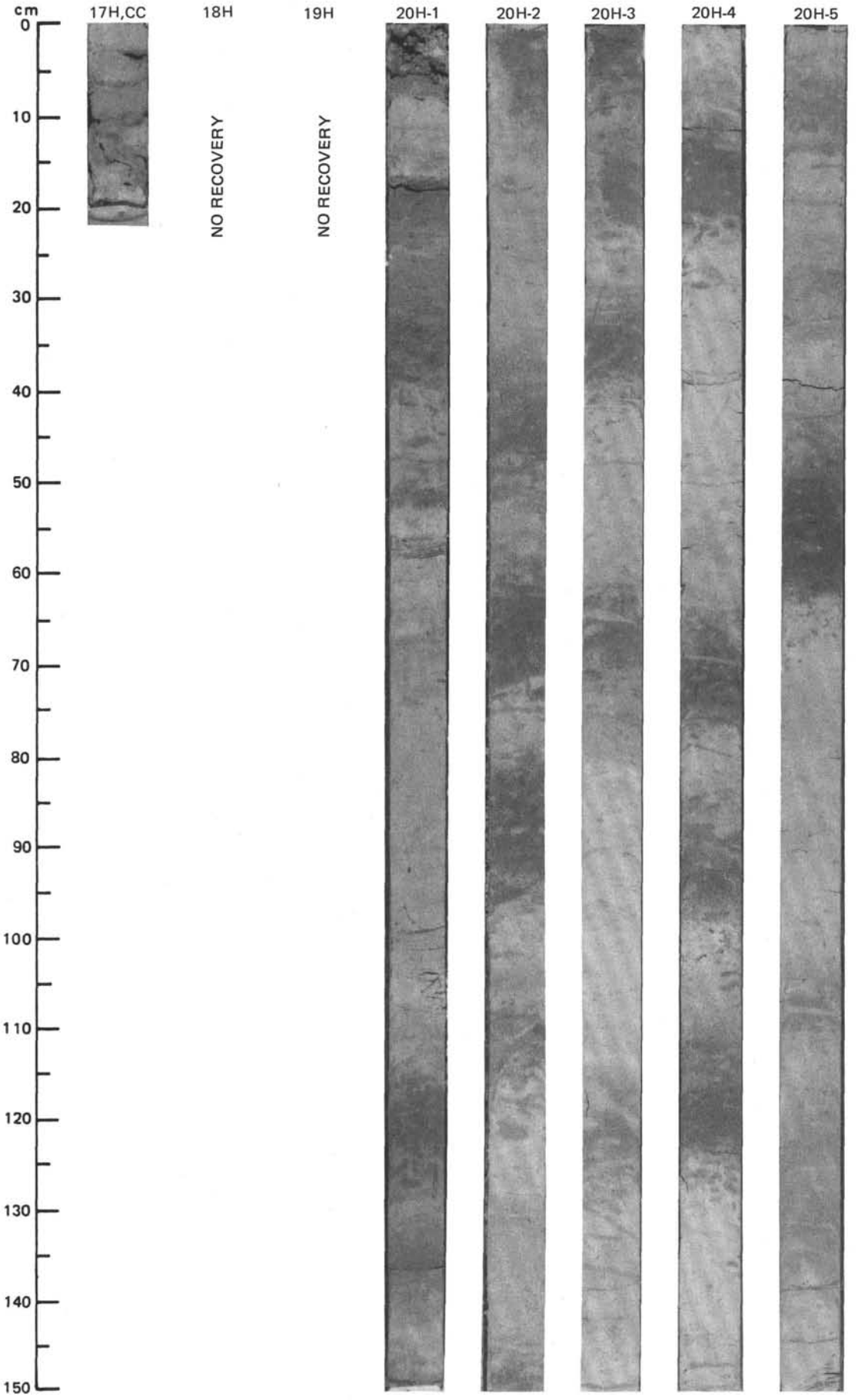
cm
0
10
20
30
40
50
60
70
80
90
100
110
120
130
140
150
17H,CC
18H
NO RECOVERY
19H
NO RECOVERY
20H-1
20H-2
20H-3
20H-4
20H-5

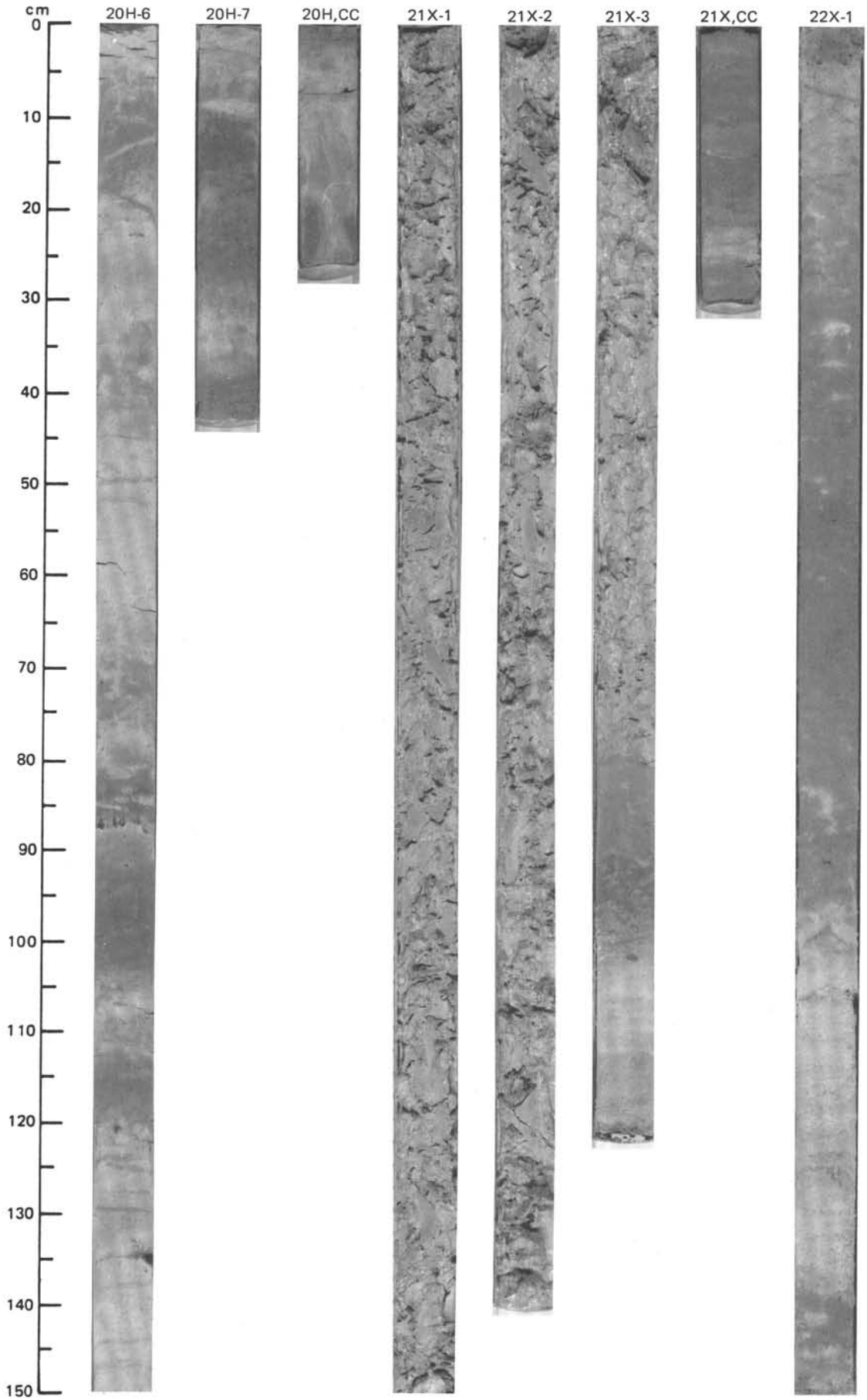
cm
0
10
20
30
40
50
60
70
80
90
100
110
120
130
140
150
20H-6
20H-7
20H,CC
21X-1
21X-2
21X-3
21X,CC
22X-1

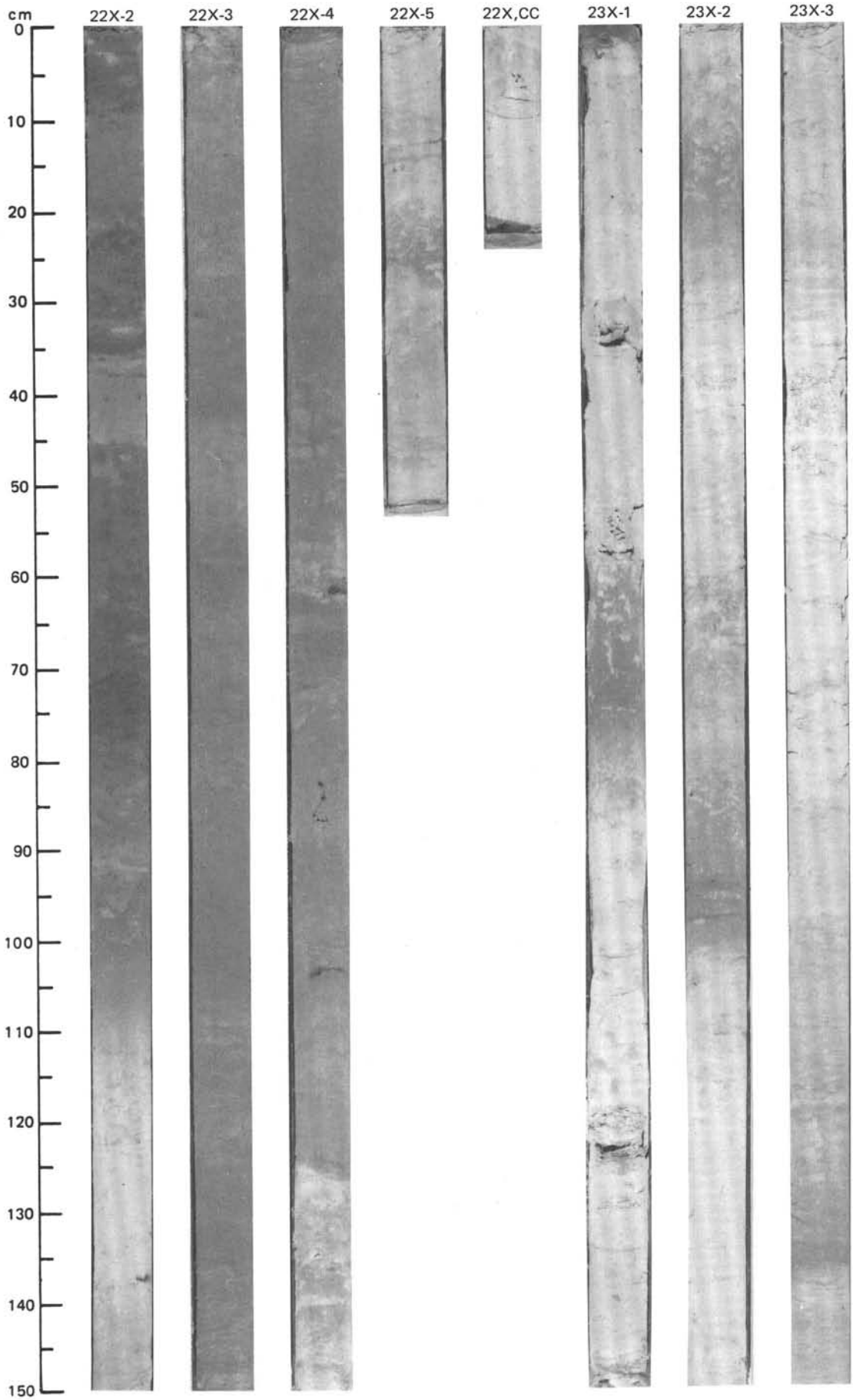
cm
0
10
20
30
40
50
60
70
80
90
100
110
120
130
140
150
22X-2
22X-3
22X-4
22X-5
22X,CC
23X-1
23X-2
23X-3

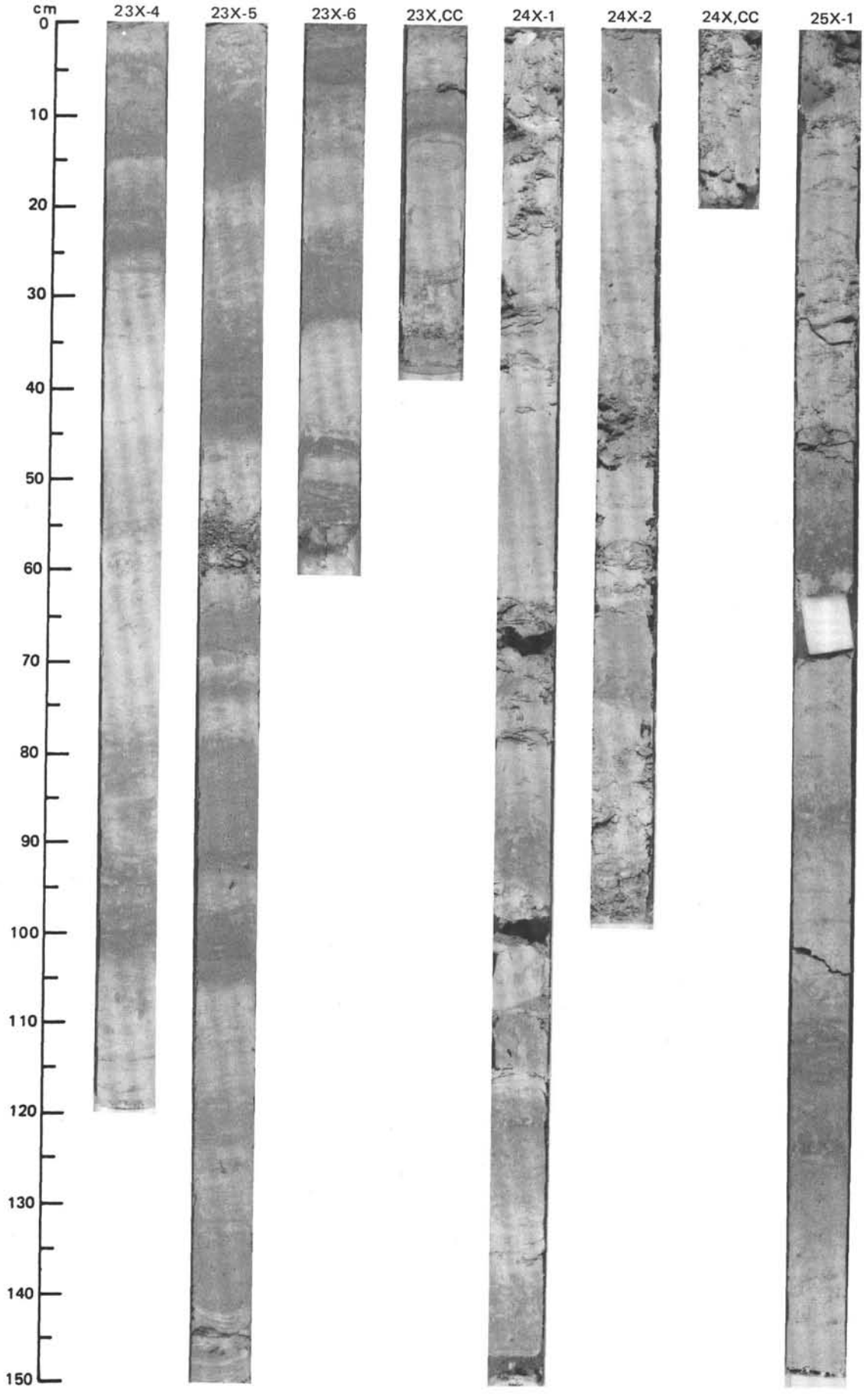
cm
0
10
20
30
40
50
60
70
80
90
100
110
120
130
140
150
23X-4
23X-5
23X-6
23X,CC
24X-1
24X-2
24X,CC
25X-1

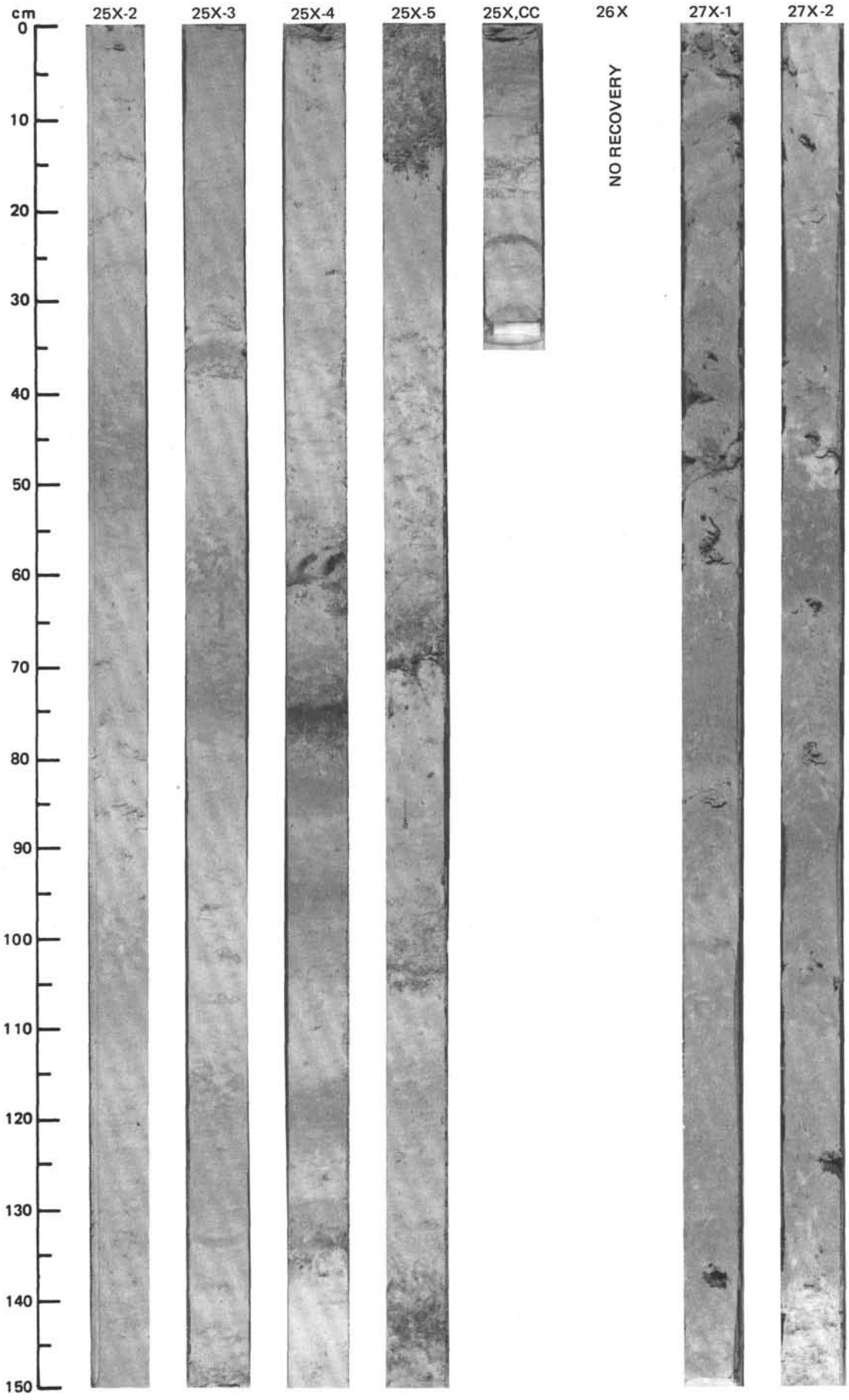
cm
0
10
20
30
40
50
60
70
80
90
100
110
120
130
140
150
25X-2
25X-3
25X-4
25X-5
25X,CC
26X
NO RECOVERY
27X-1
27X-2

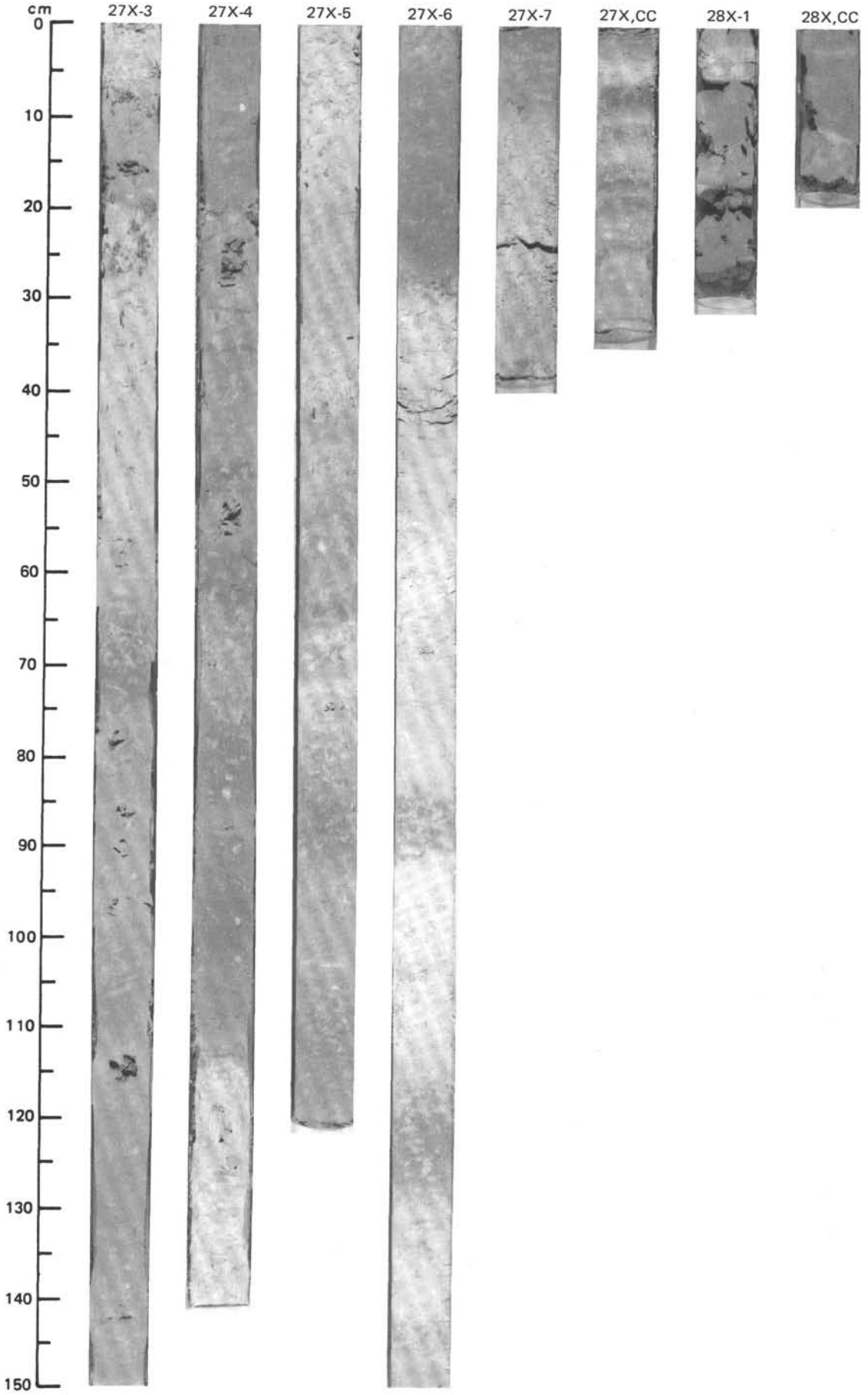
cm
0
10
20
30
40
50
60
70
80
90
100
110
120
130
140
150
27X-3
27X-4
27X-5
27X-6
27X-7
27X,CC
28X-1
28X,CC

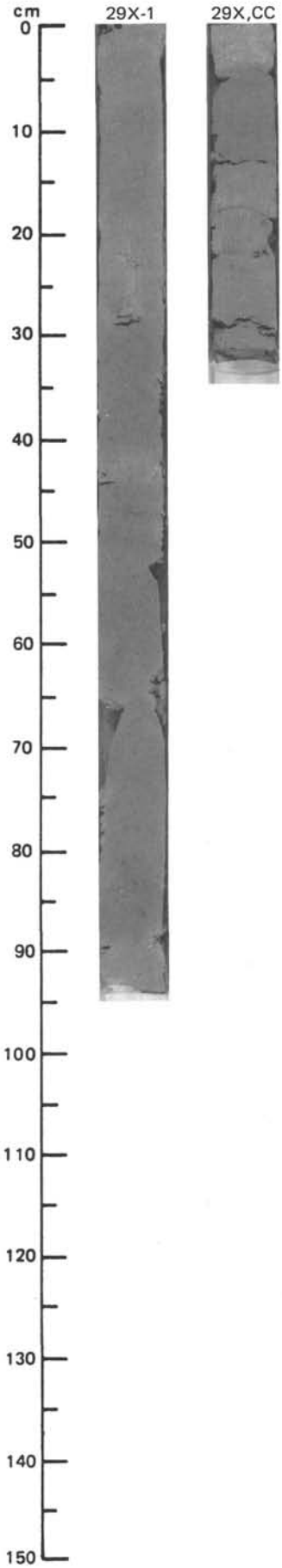
cm
29X-1
29X,CC
0
10
20
30
40
50
60
70
80
90
100
110
120
130
140
150

SITE 659 (HOLE B)

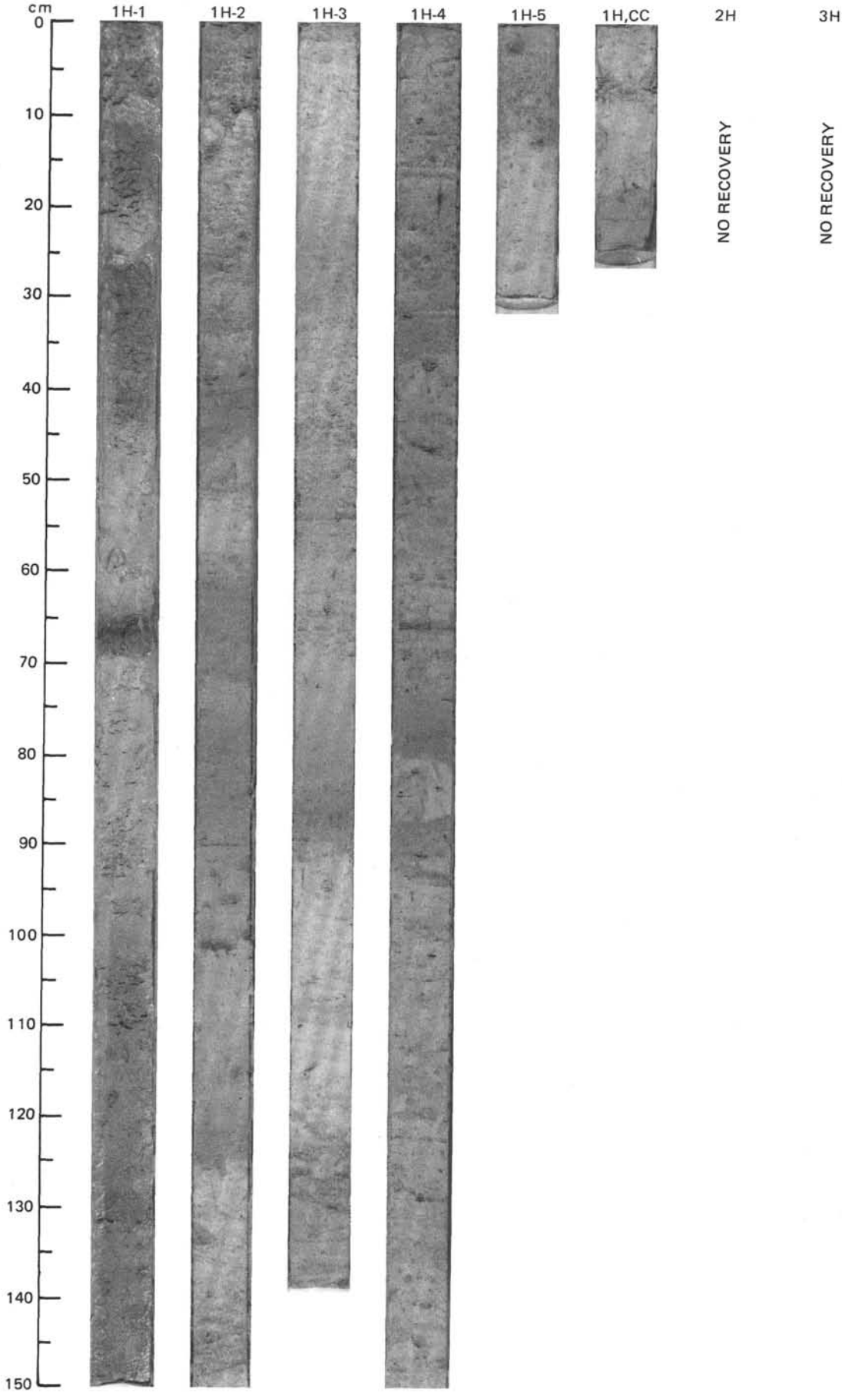

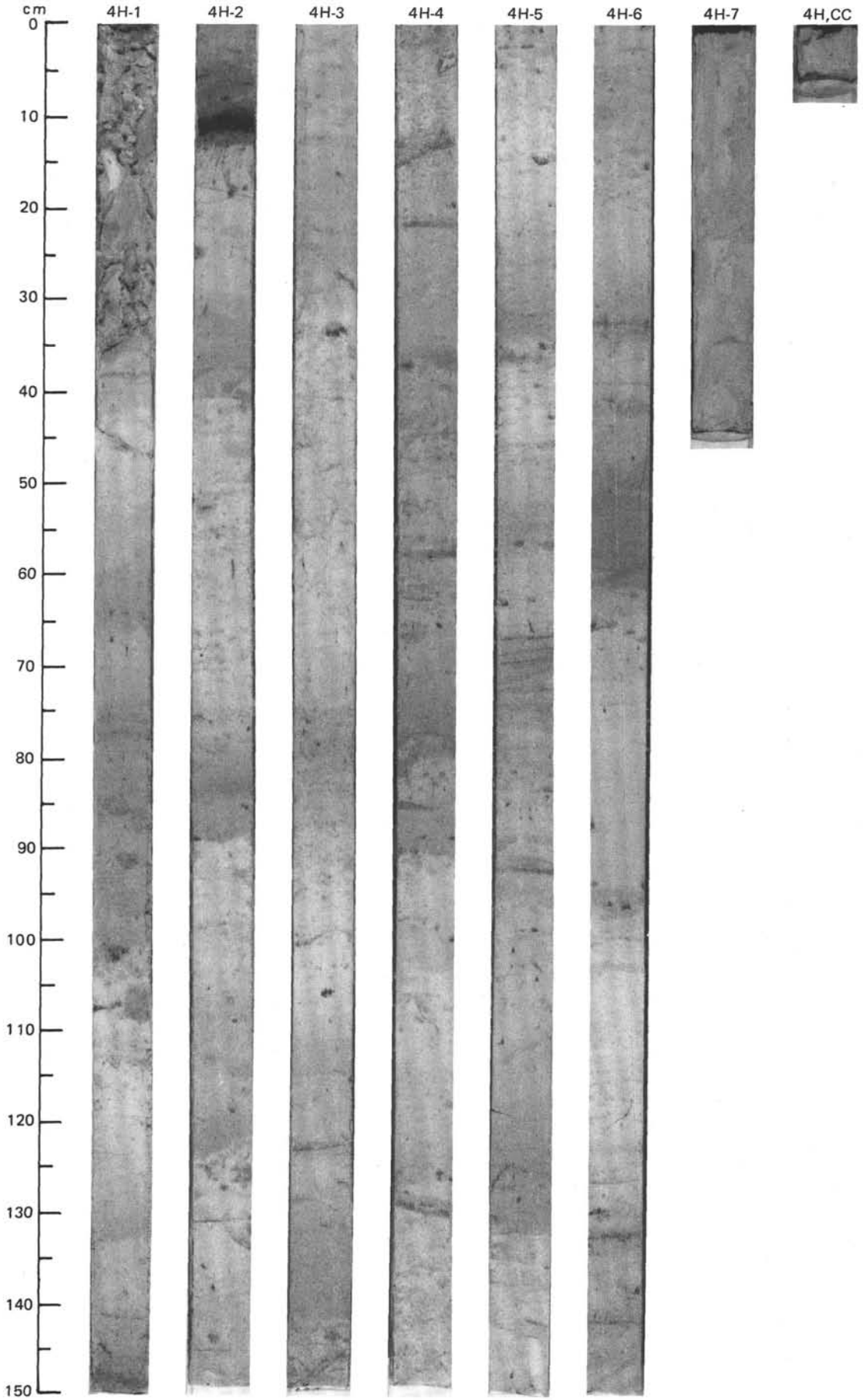
cm
0
10
20
30
40
50
60
70
80
90
100
110
120
130
140
150
4H-1
4H-2
4H-3
4H-4
4H-5
4H-6
4H-7
4H,CC

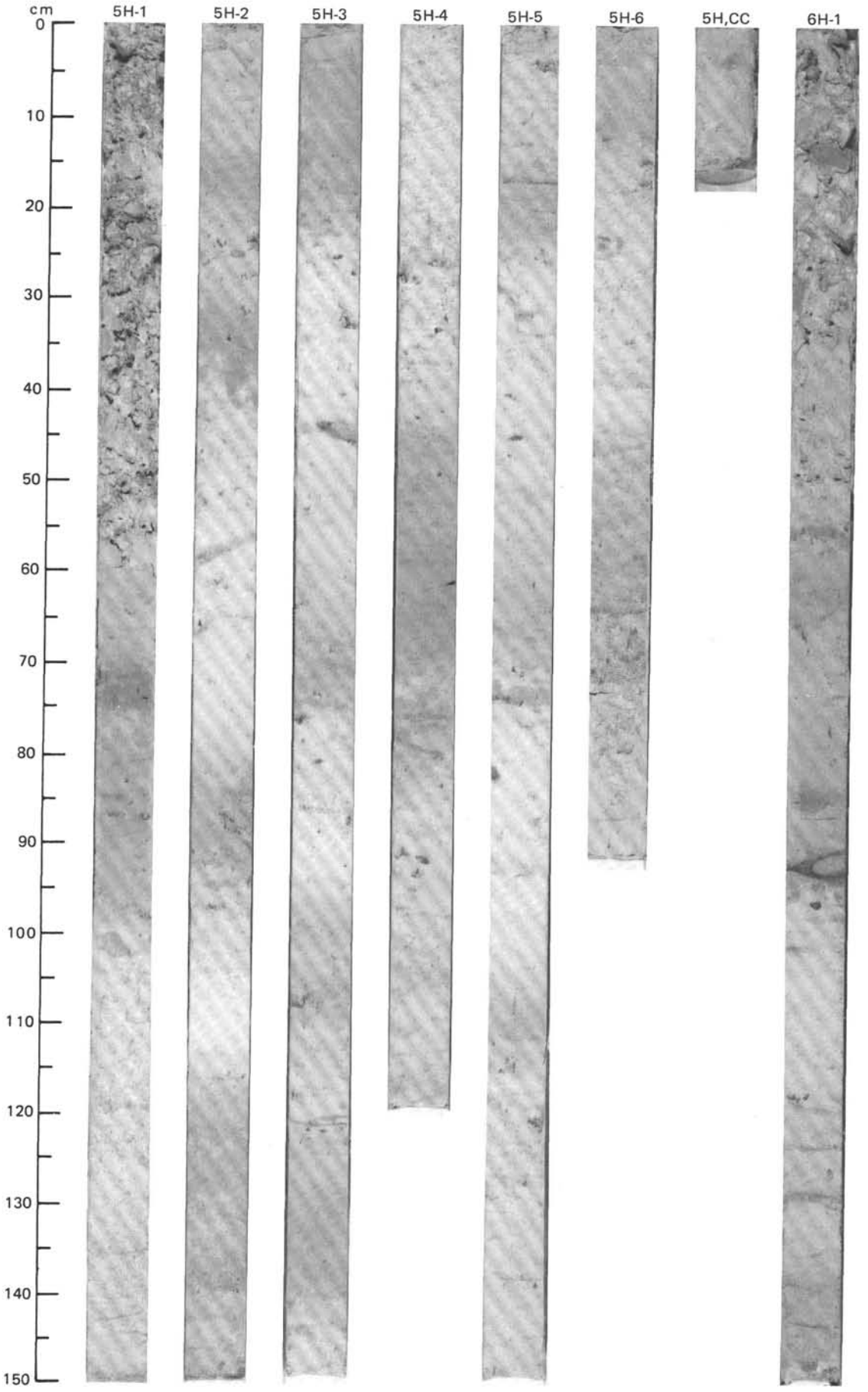
cm
0
10
20
30
40
50
60
70
80
90
100
110
120
130
140
150
5H-1
5H-2
5H-3
5H-4
5H-5
5H-6
5H,CC
6H-1

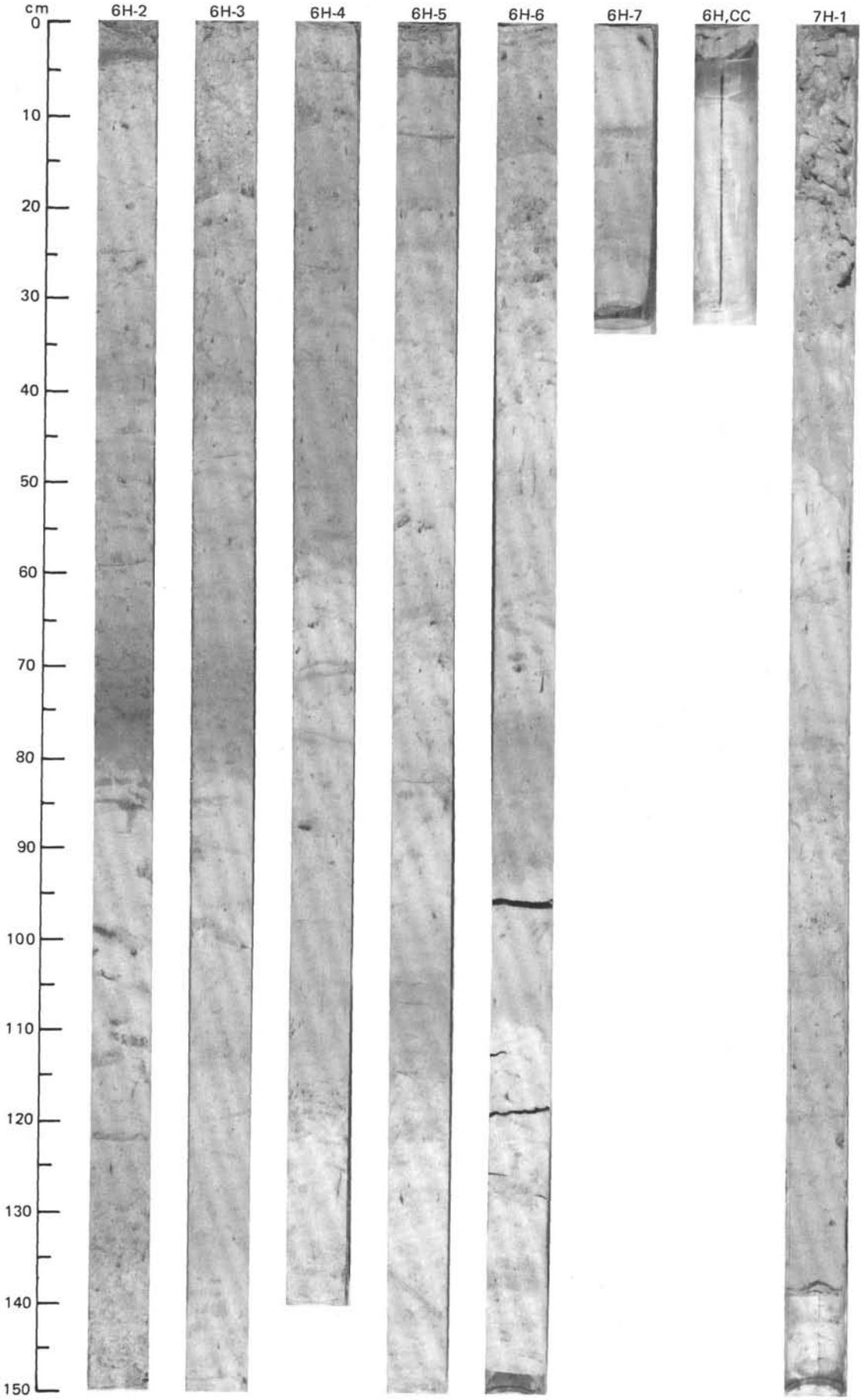
cm
0
10
20
30
40
50
60
70
80
90
100
110
120
130
140
150
6H-2
6H-3
6H-4
6H-5
6H-6
6H-7
6H,CC
7H-1

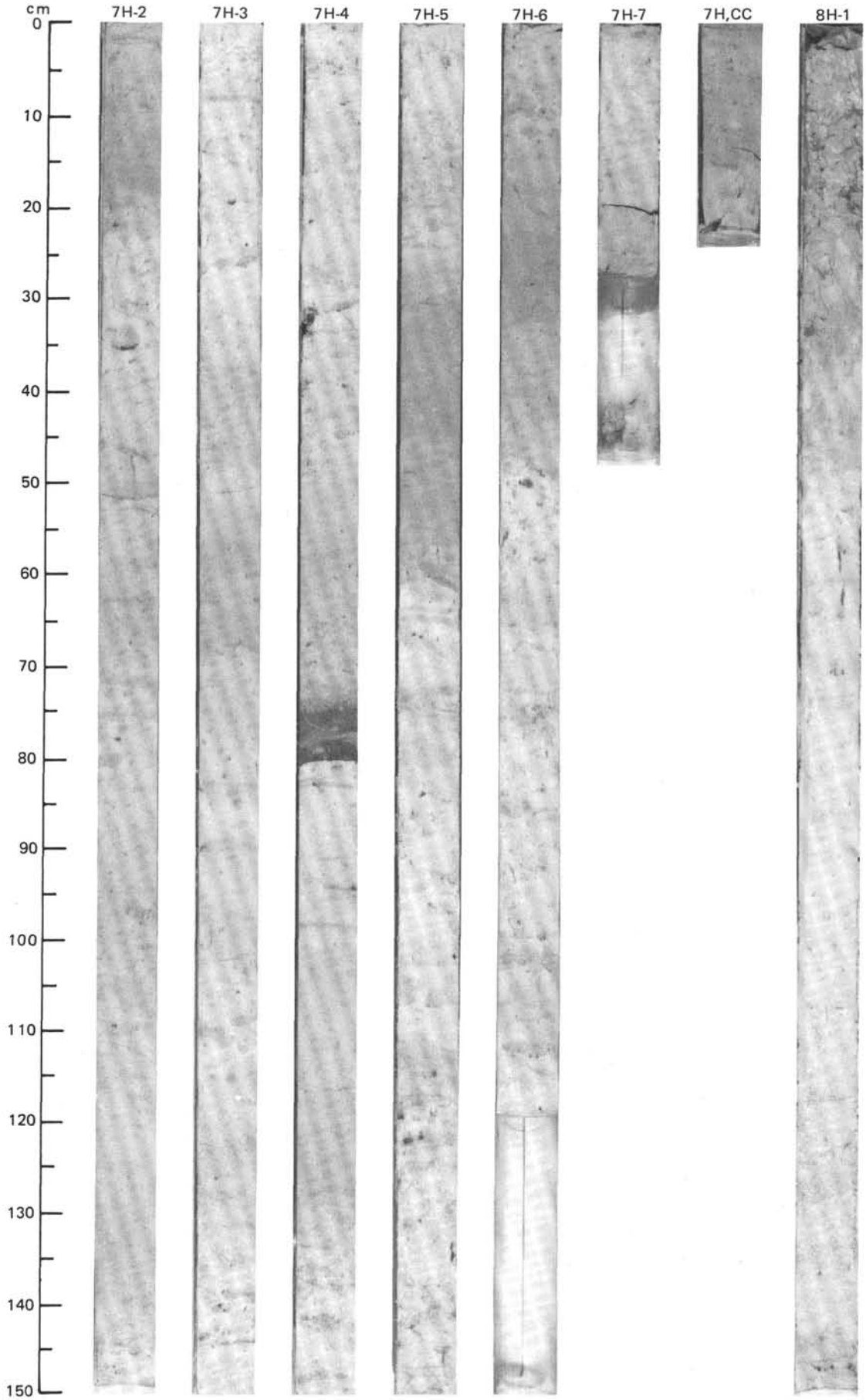
cm
0
10
20
30
40
50
60
70
80
90
100
110
120
130
140
150
7H-2
7H-3
7H-4
7H-5
7H-6
7H-7
7H,CC
8H-1

cm
0
10
20
30
40
50
60
70
80
90
100
110
120
130
140
150
8H-2
8H-3
8H-4
8H-5
8H-6
8H-7
8H,CC
9H-1

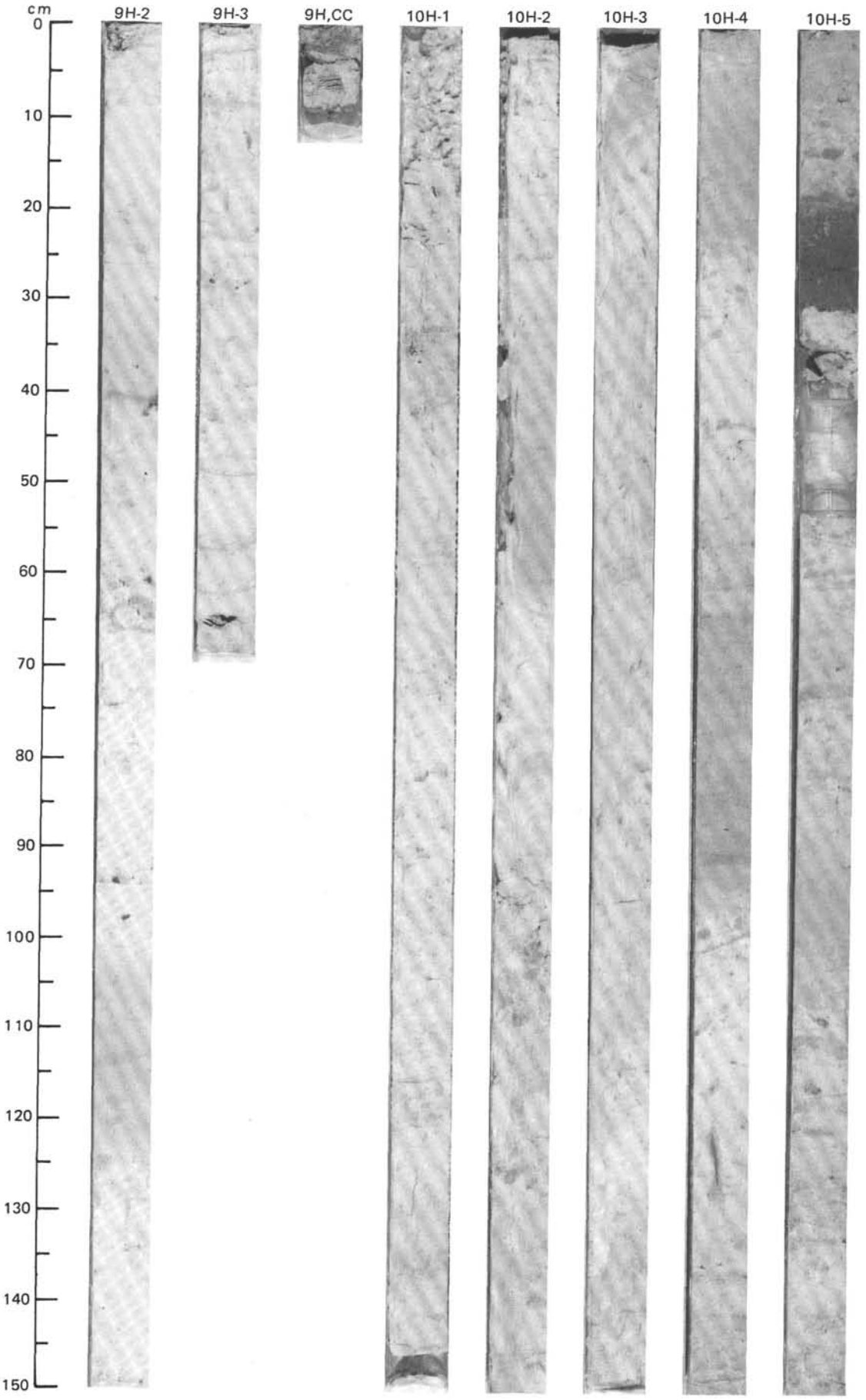
cm
0
10
20
30
40
50
60
70
80
90
100
110
120
130
140
150
9H-2
9H-3
9H,CC
10H-1
10H-2
10H-3
10H-4
10H-5

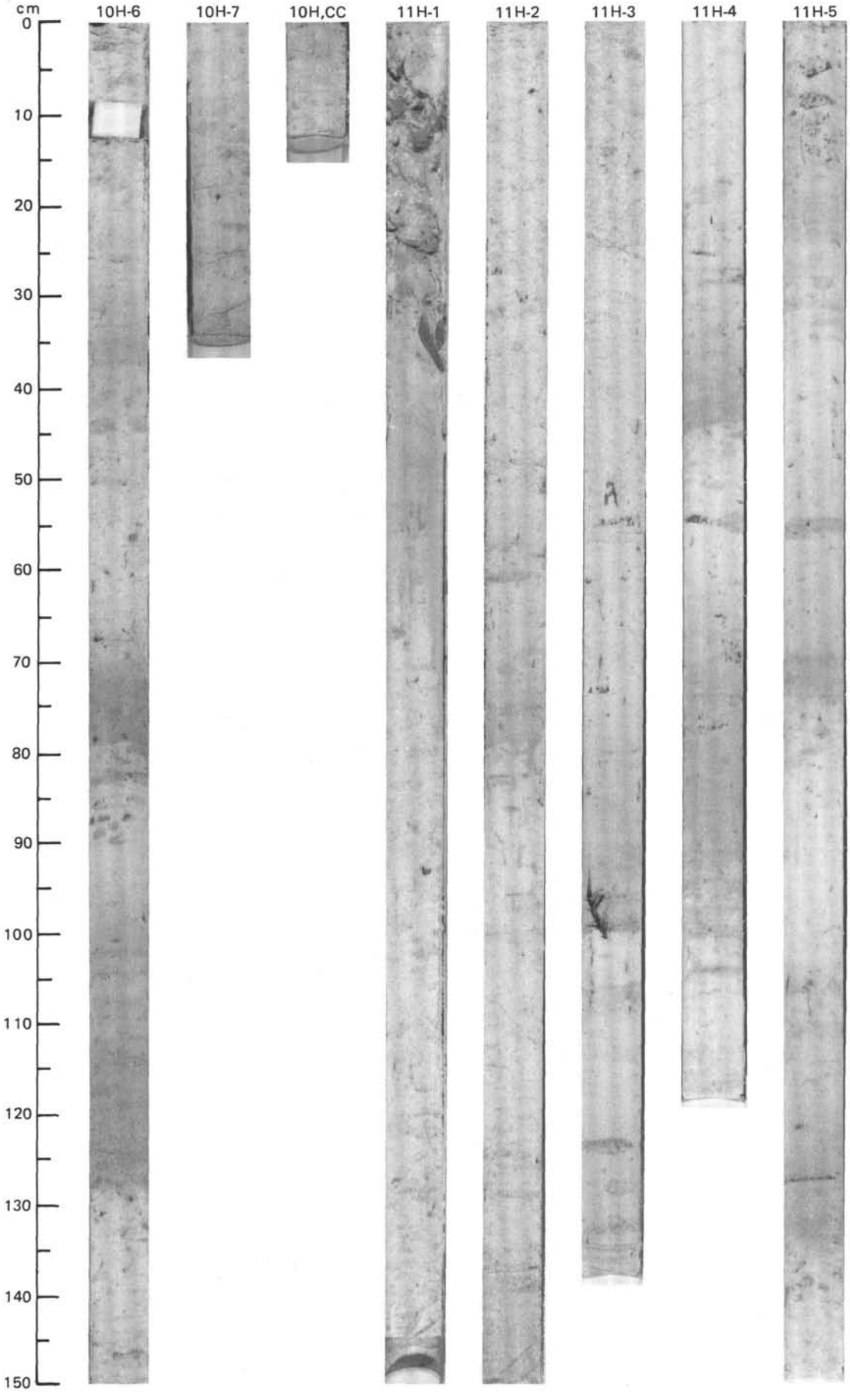
cm
0
10
20
30
40
50
60
70
80
90
100
110
120
130
140
150
10H-6
10H-7
10H,CC
11H-1
11H-2
11H-3
11H-4
11H-5

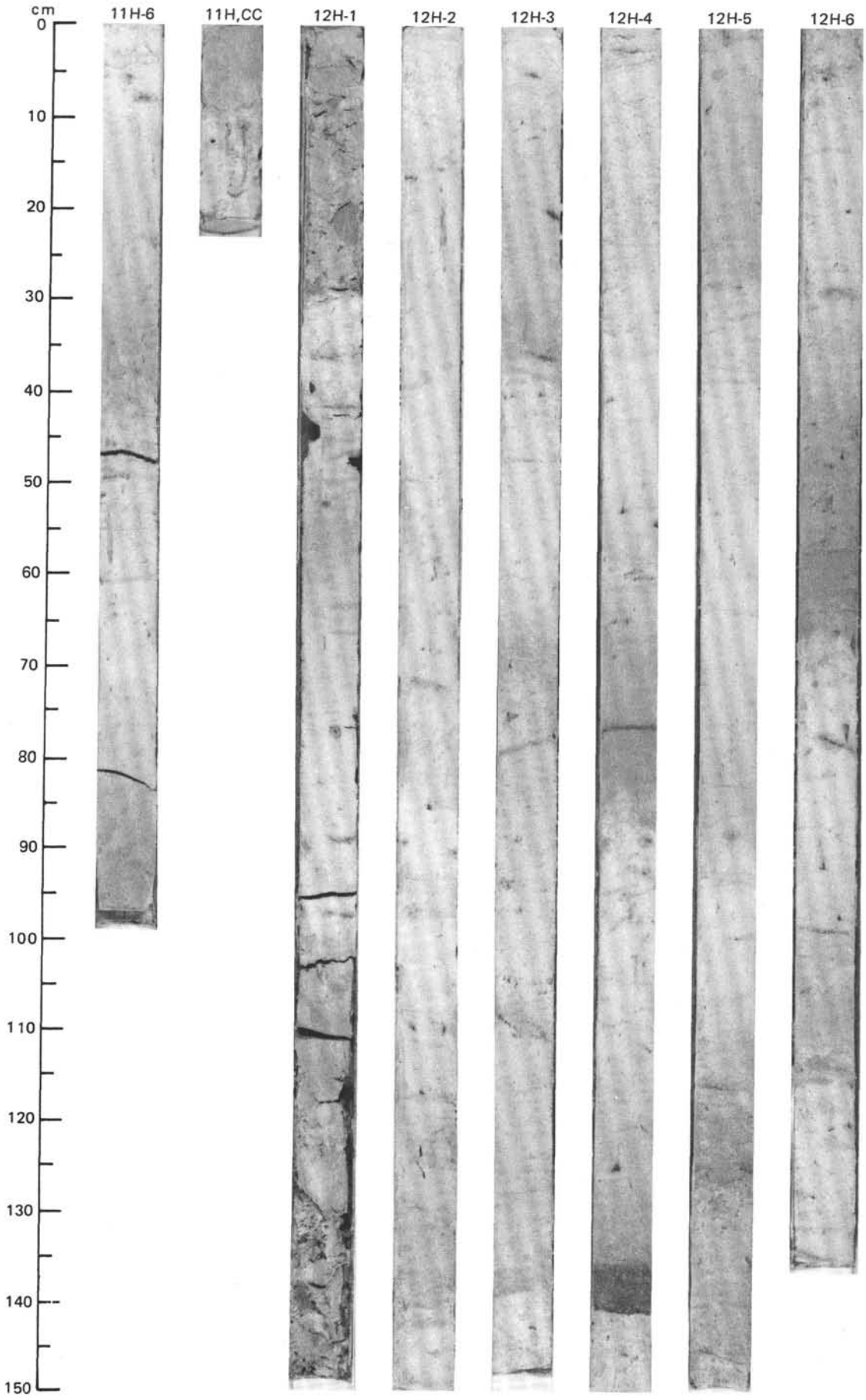
cm
0
10
20
30
40
50
60
70
80
90
100
110
120
130
140
150
11H-6
11H,CC
12H-1
12H-2
12H-3
12H-4
12H-5
12H-6

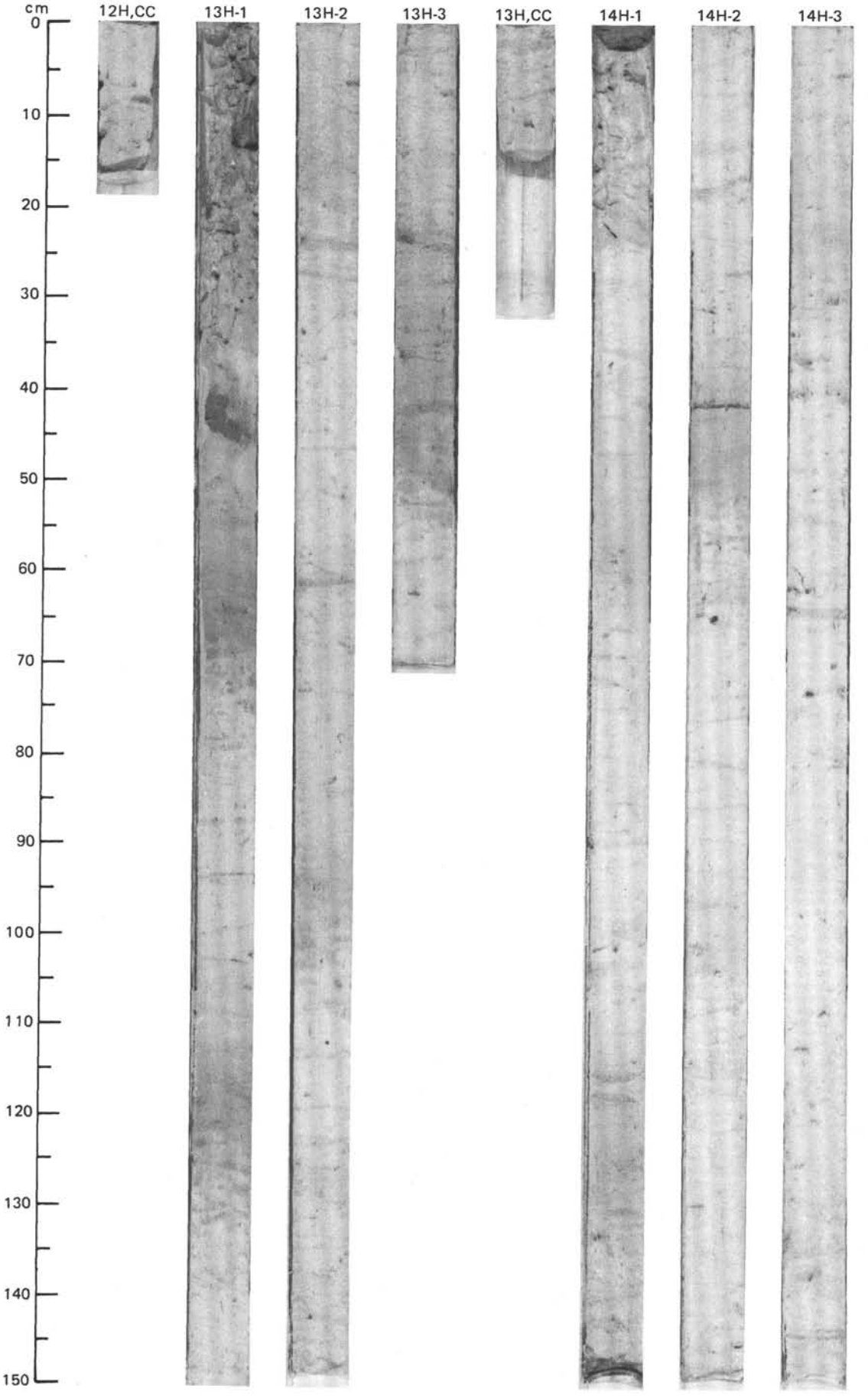
cm
0
10
20
30
40
50
60
70
80
90
100
110
120
130
140
150
12H,CC
13H-1
13H-2
13H-3
13H,CC
14H-1
14H-2
14H-3

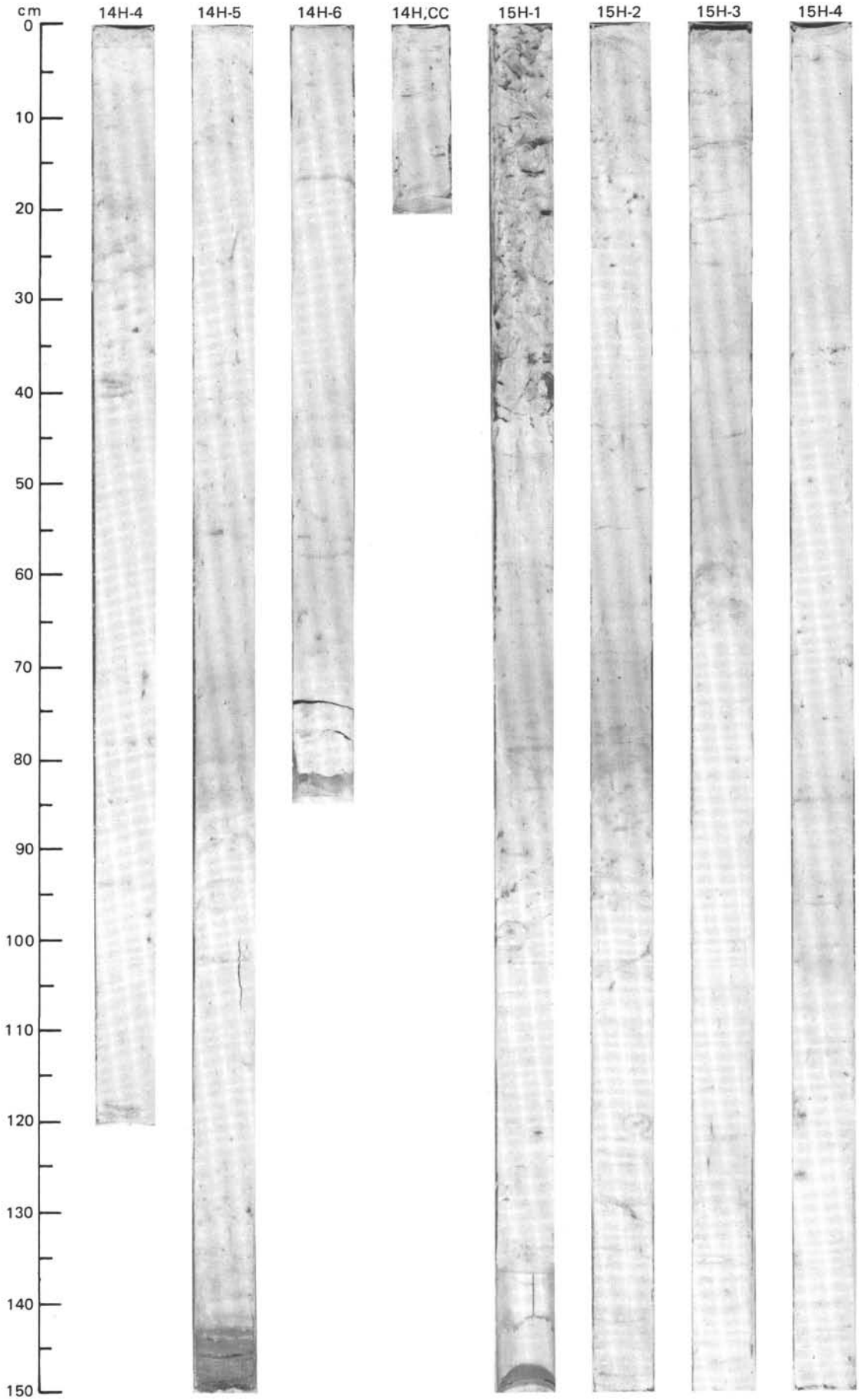
cm
0
10
20
30
40
50
60
70
80
90
100
110
120
130
140
150
14H-4
14H-5
14H-6
14H,CC
15H-1
15H-2
15H-3
15H-4

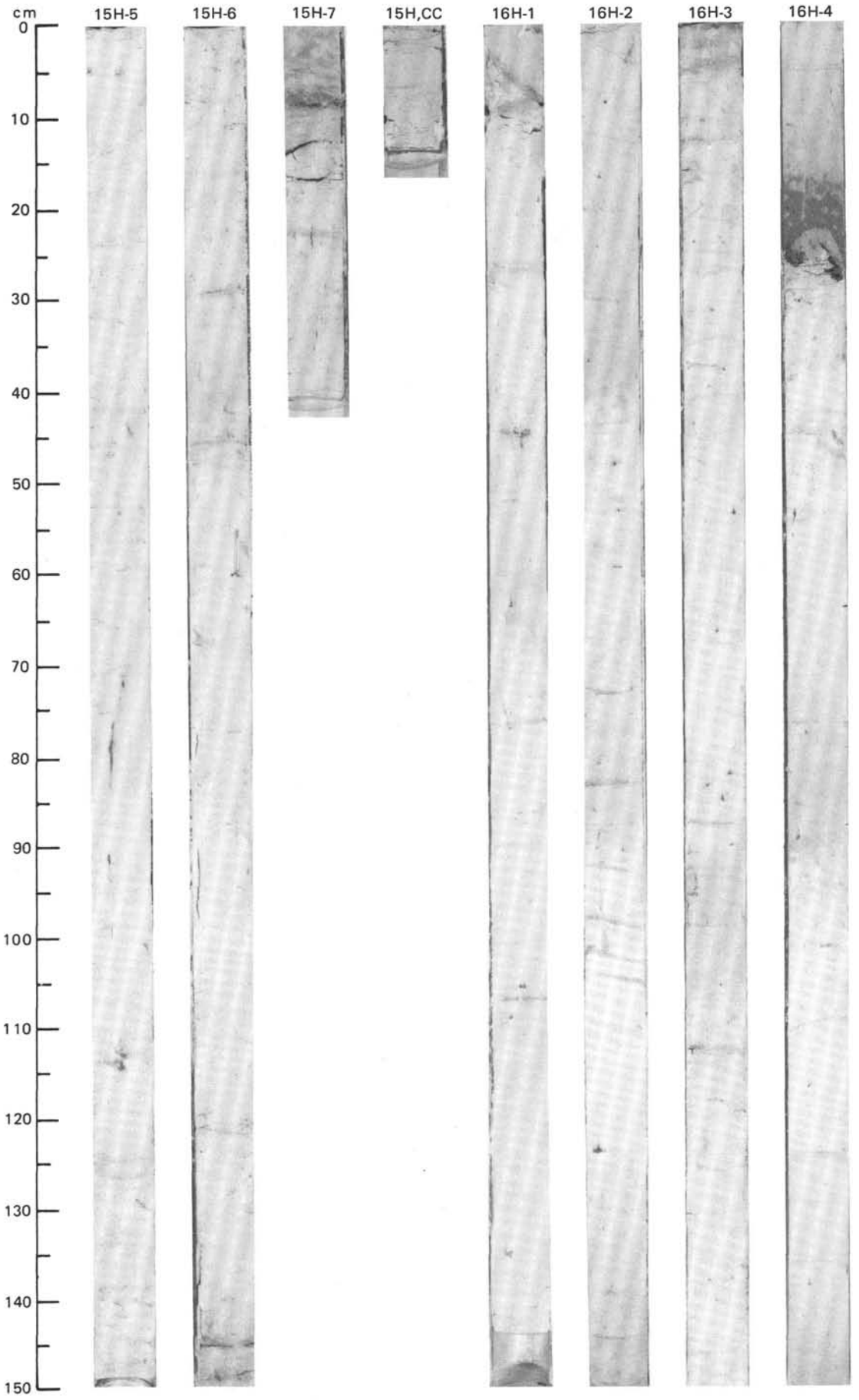
cm
0
10
20
30
40
50
60
70
80
90
100
110
120
130
140
150
15H-5
15H-6
15H-7
15H,CC
16H-1
16H-2
16H-3
16H-4

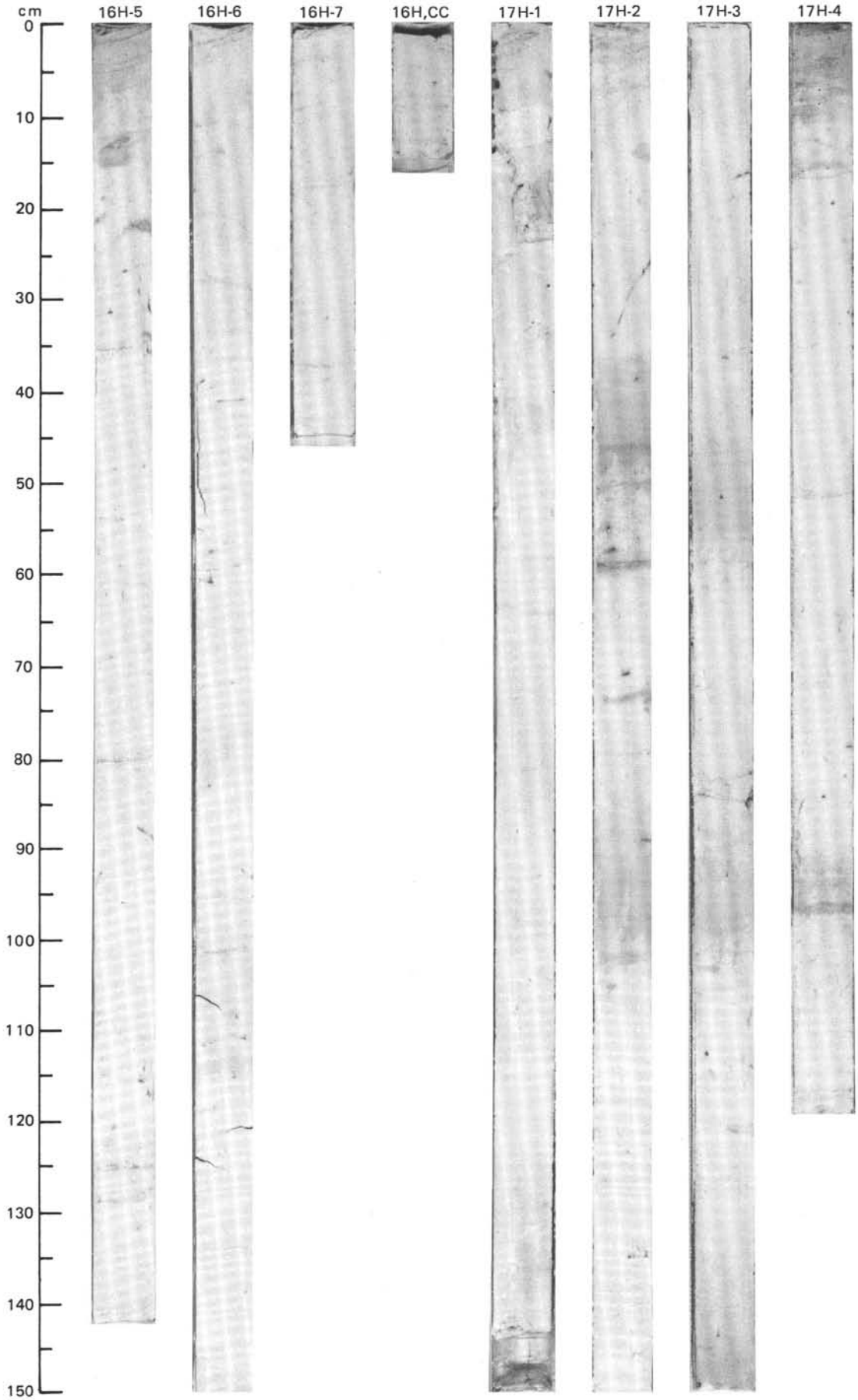
cm
0
10
20
30
40
50
60
70
80
90
100
110
120
130
140
150
16H-5
16H-6
16H-7
16H,CC
17H-1
17H-2
17H-3
17H-4

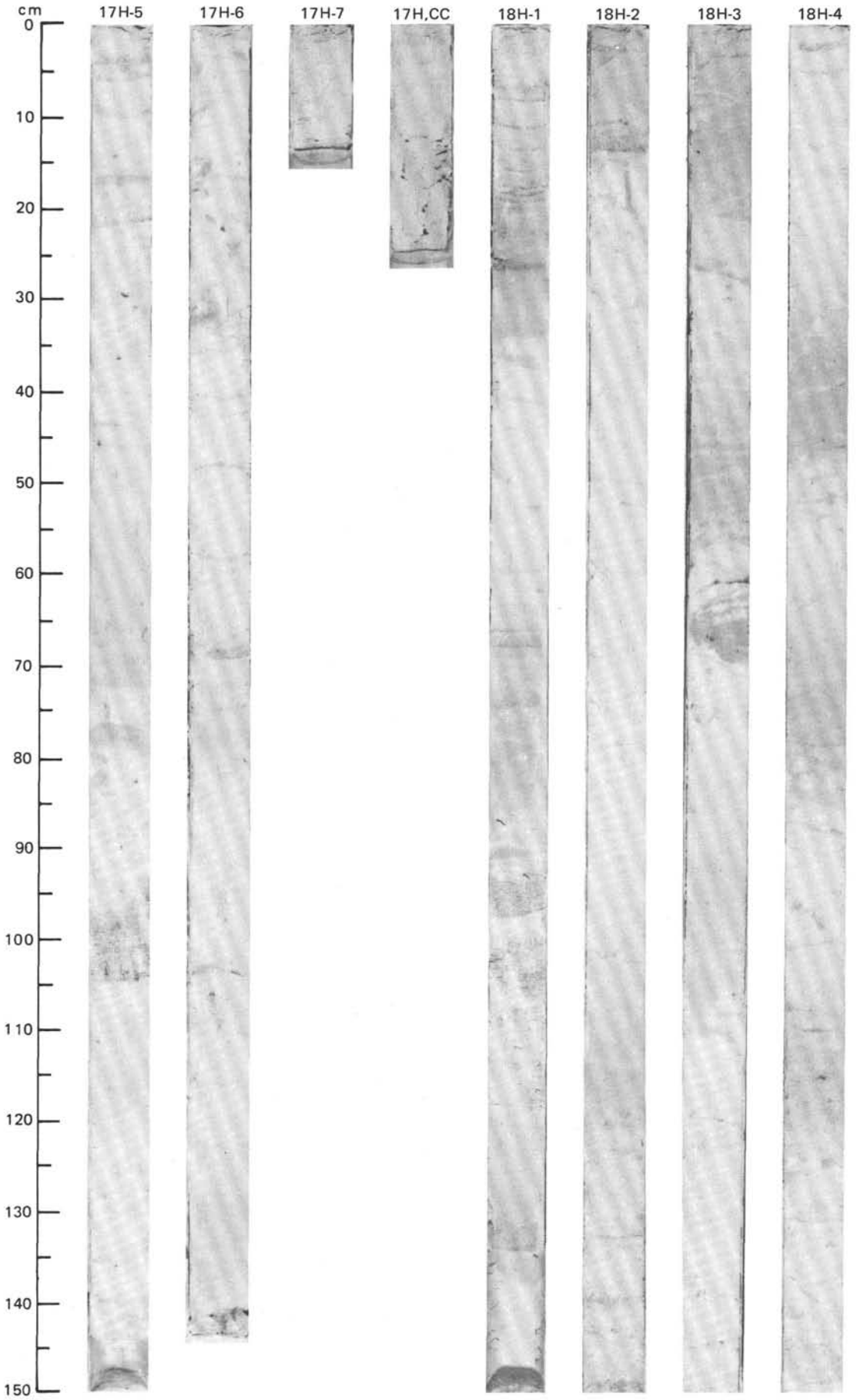
cm
0
10
20
30
40
50
60
70
80
90
100
110
120
130
140
150
17H-5
17H-6
17H-7
17H,CC
18H-1
18H-2
18H-3
18H-4

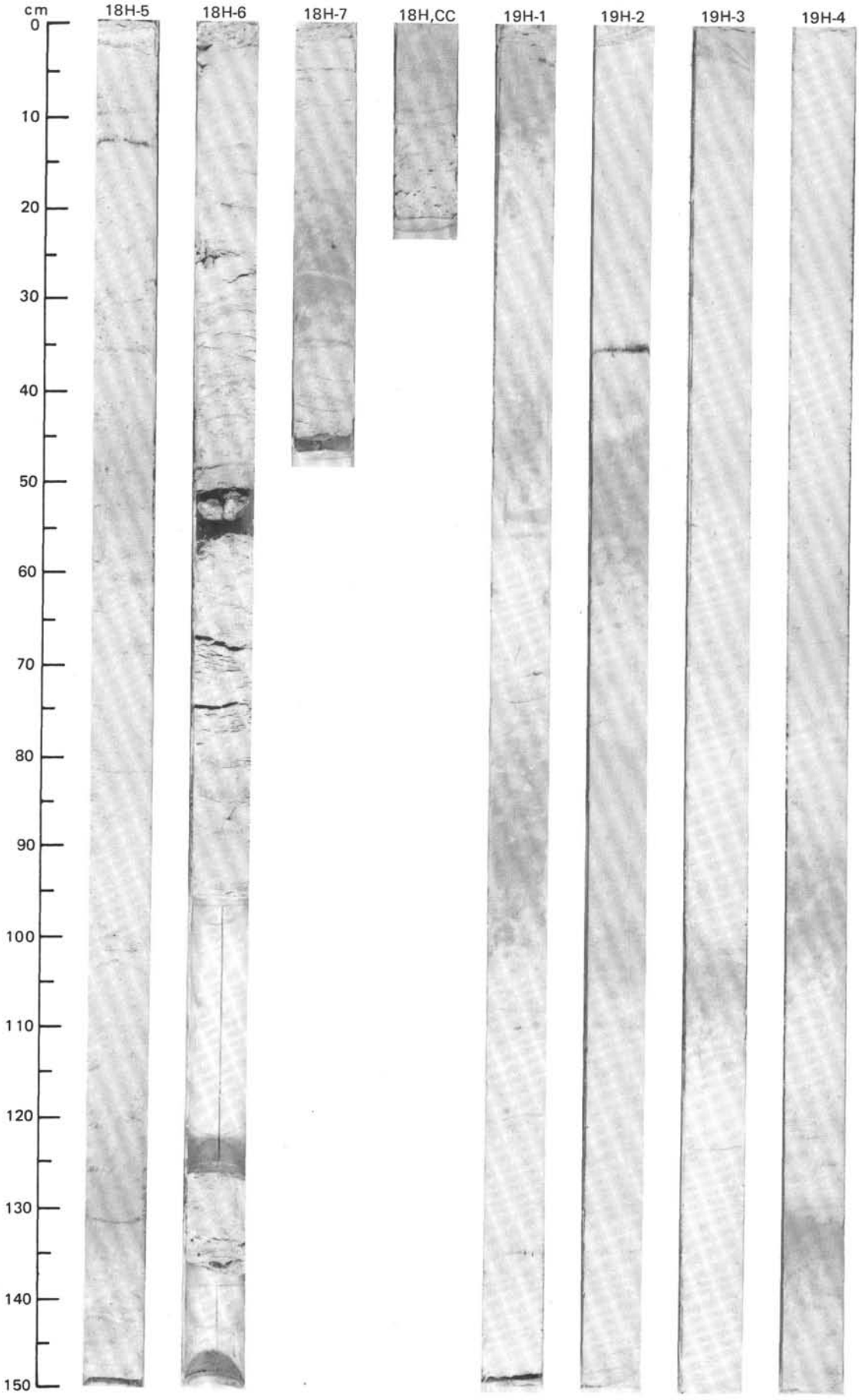
cm
0
10
20
30
40
50
60
70
80
90
100
110
120
130
140
150
18H-5
18H-6
18H-7
18H,CC
19H-1
19H-2
19H-3
19H-4

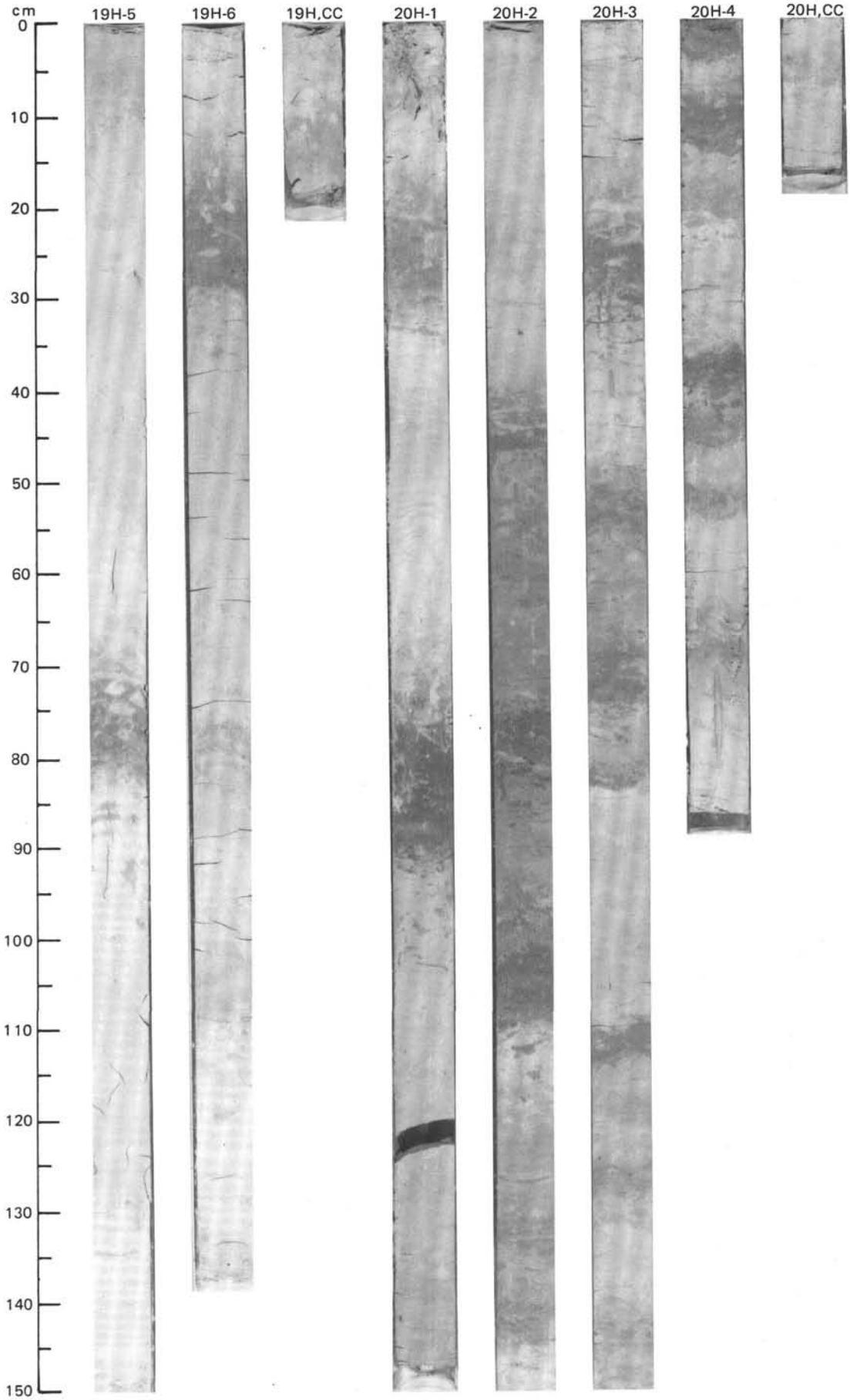
cm
0
10
20
30
40
50
60
70
80
90
100
110
120
130
140
150
19H-5
19H-6
19H,CC
20H-1
20H-2
20H-3
20H-4
20H,CC

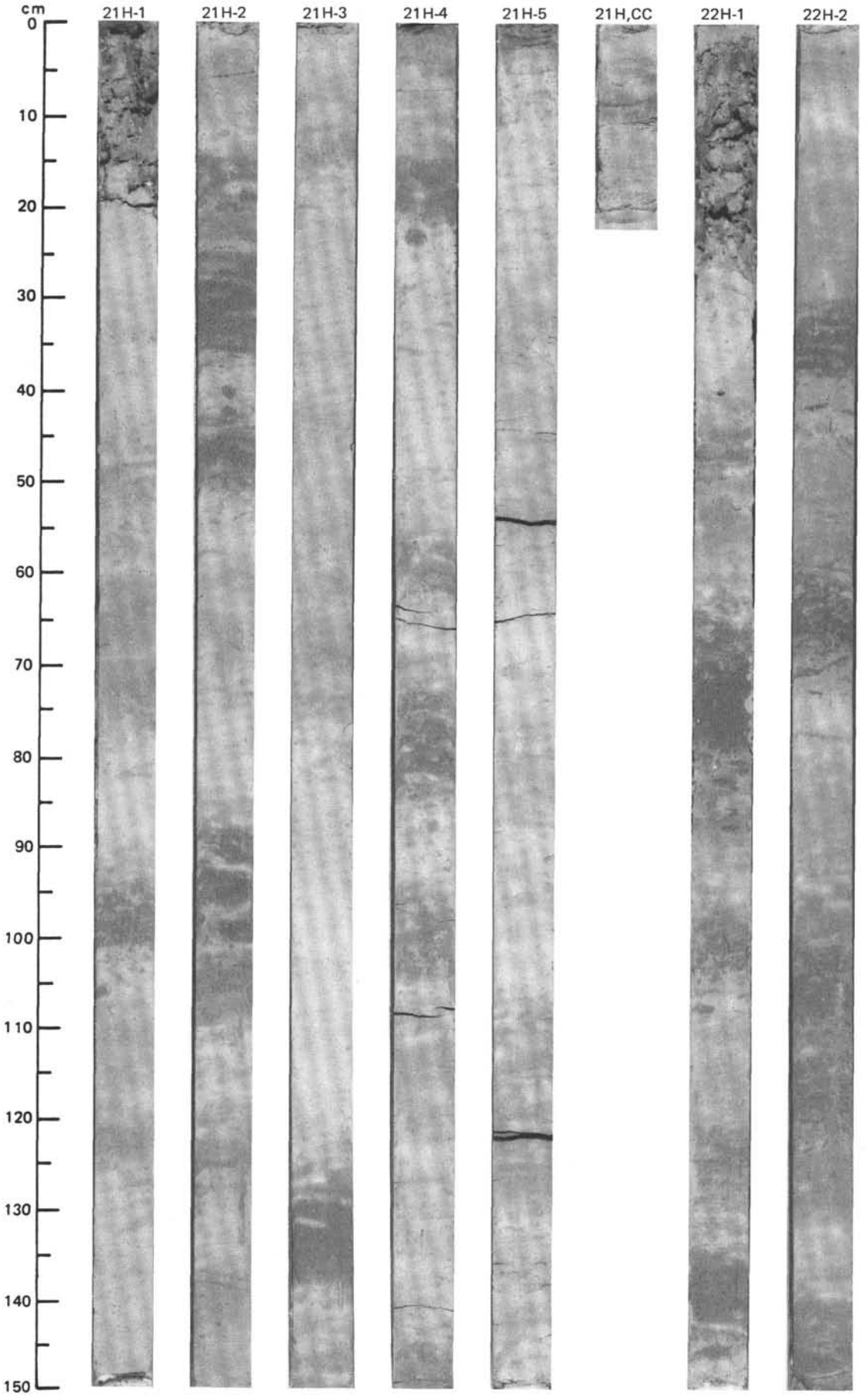
cm
0
10
20
30
40
50
60
70
80
90
100
110
120
130
140
150
21H-1
21H-2
21H-3
21H-4
21H-5
21H,CC
22H-1
22H-2

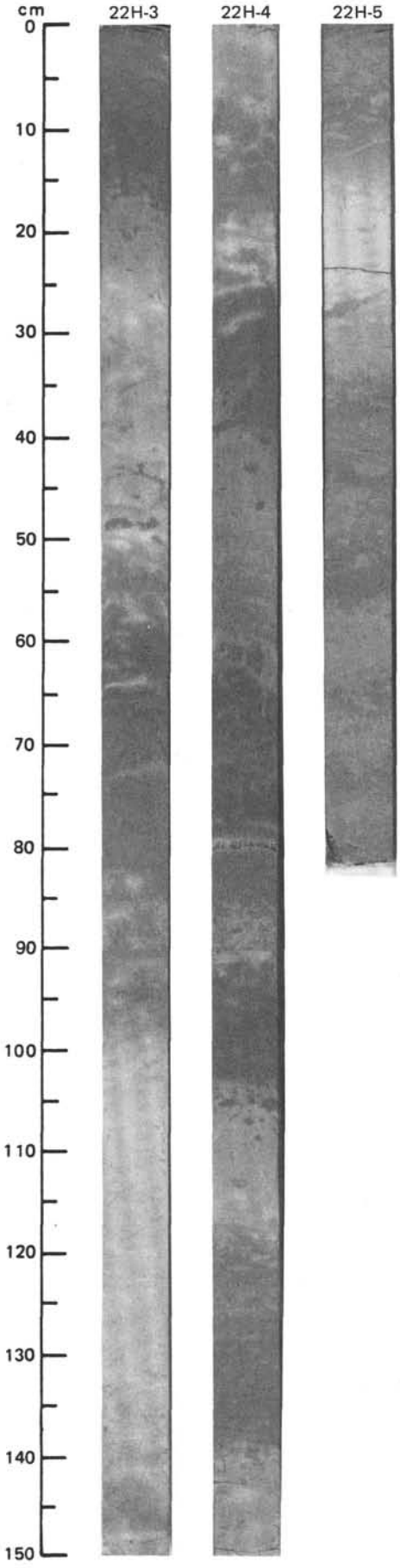
cm
22H-3
22H-4
22H-5
0
10
20
30
40
50
60
70
80
90
100
110
120
130
140
150

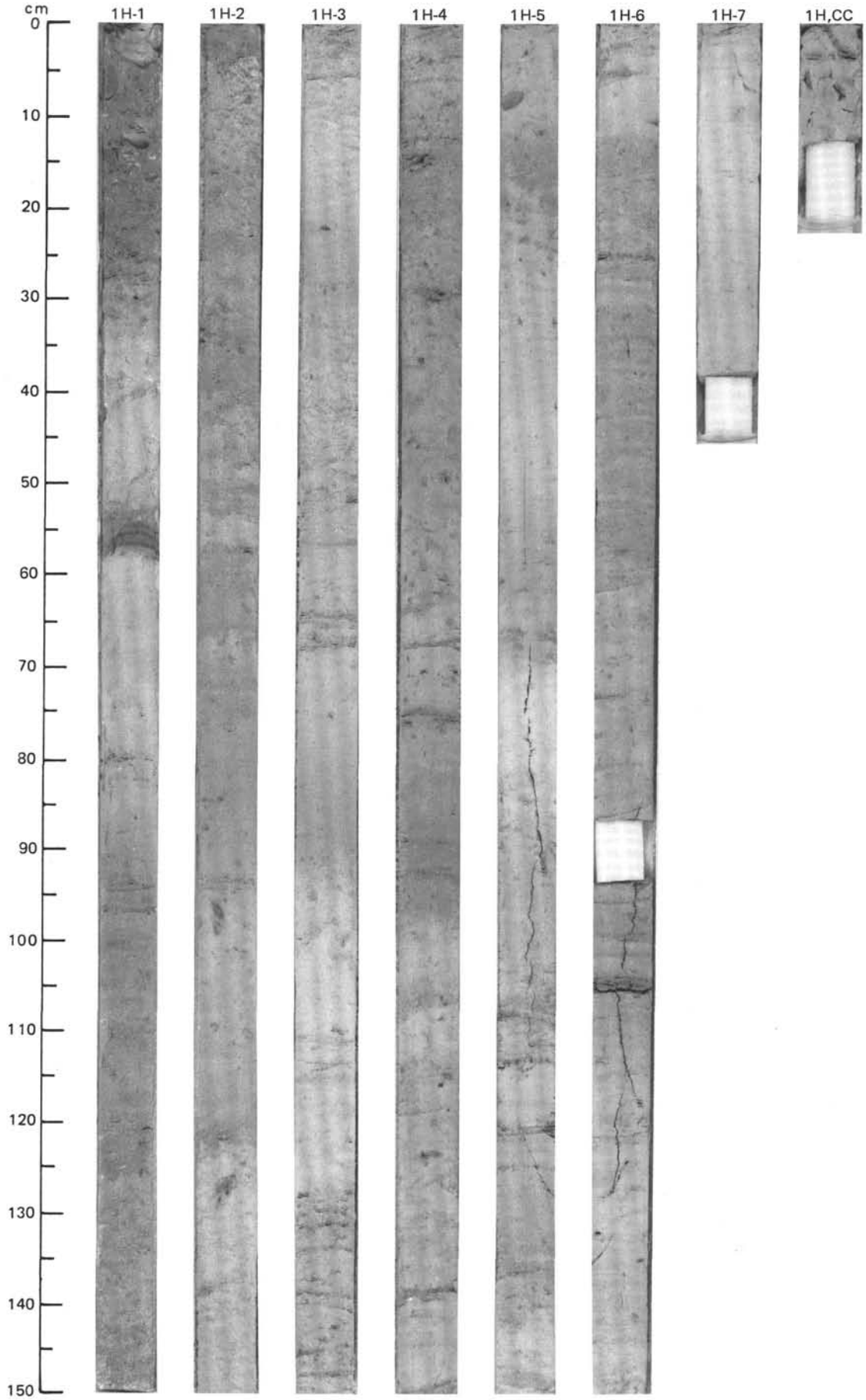
cm
0
10
20
30
40
50
60
70
80
90
100
110
120
130
140
150
1H-1
1H-2
1H-3
1H-4
1H-5
1H-6
1H-7
1H,CC

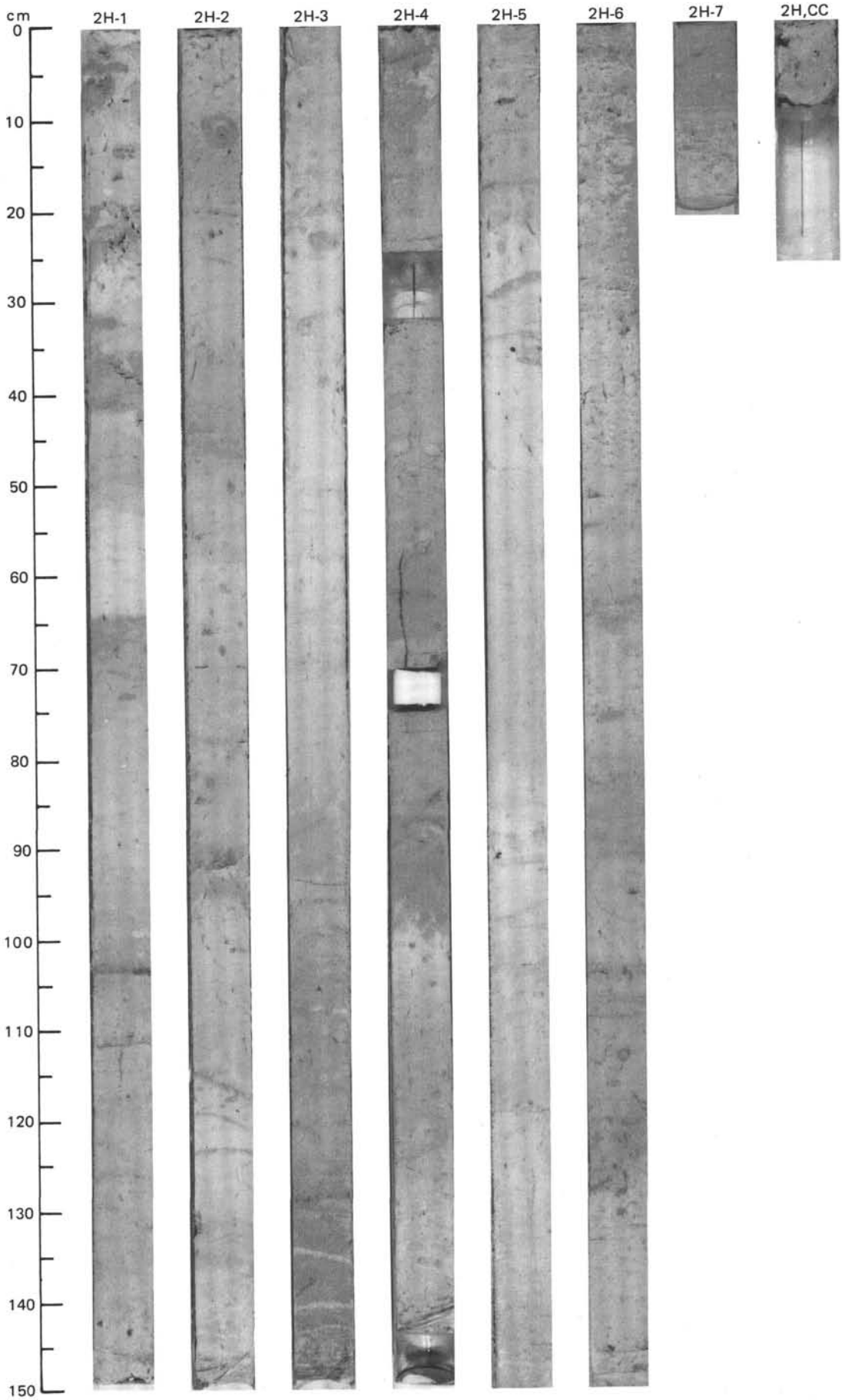
cm
0
10
20
30
40
50
60
70
80
90
100
110
120
130
140
150
2H-1
2H-2
2H-3
2H-4
2H-5
2H-6
2H-7
2H,CC

SITE 659 (HOLE C)

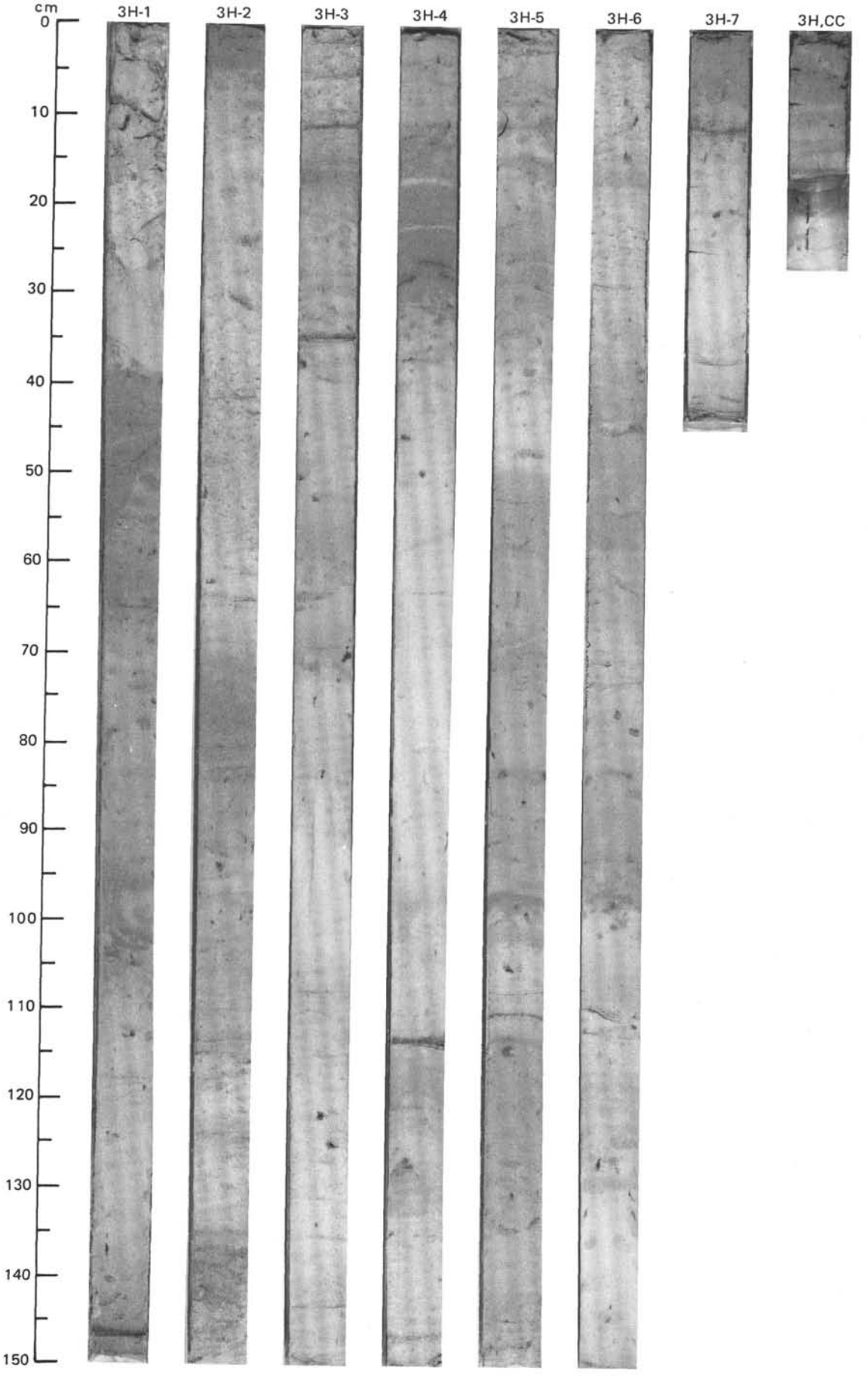

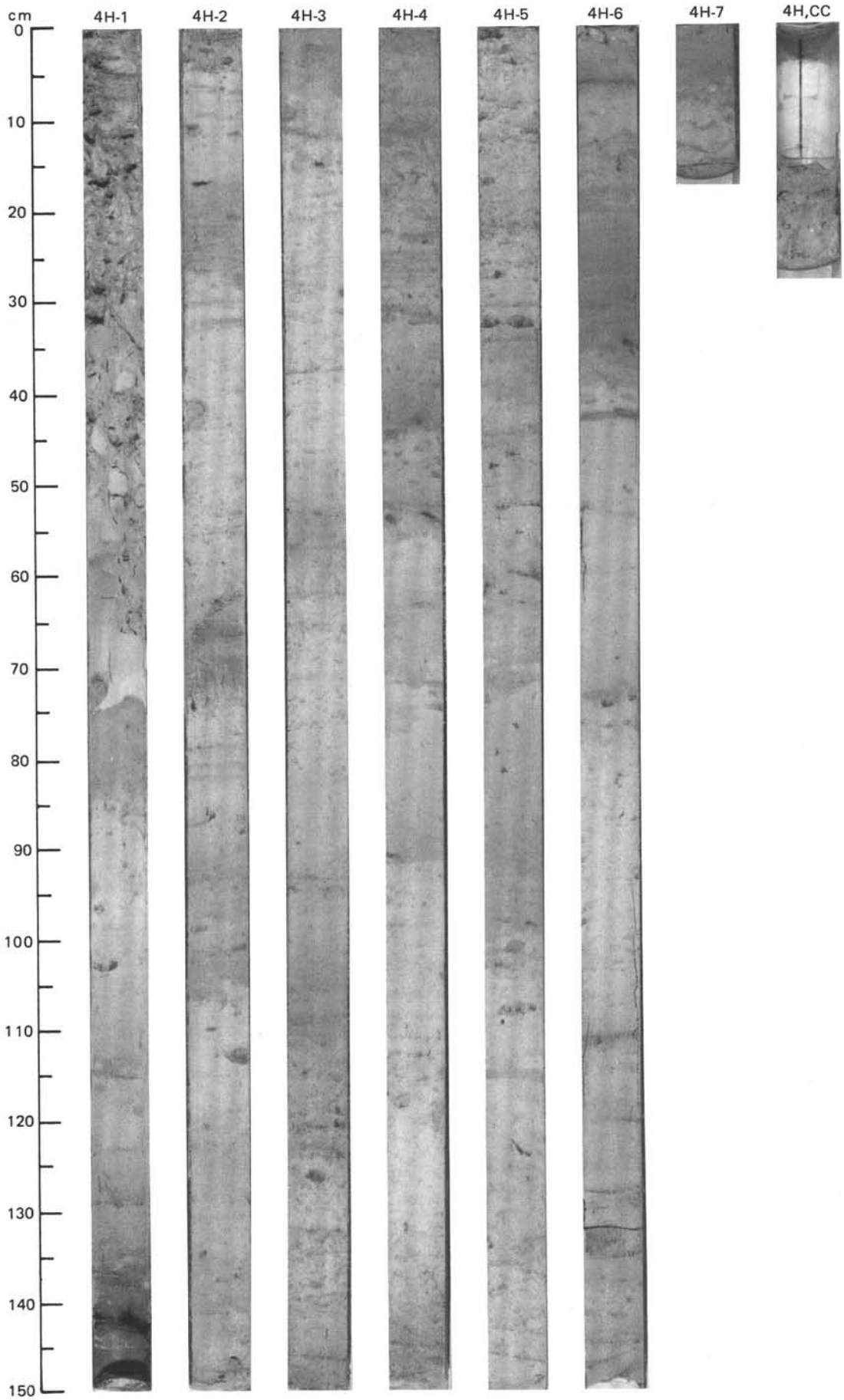
cm
0
10
20
30
40
50
60
70
80
90
100
110
120
130
140
150
4H-1
4H-2
4H-3
4H-4
4H-5
4H-6
4H-7
4H,CC

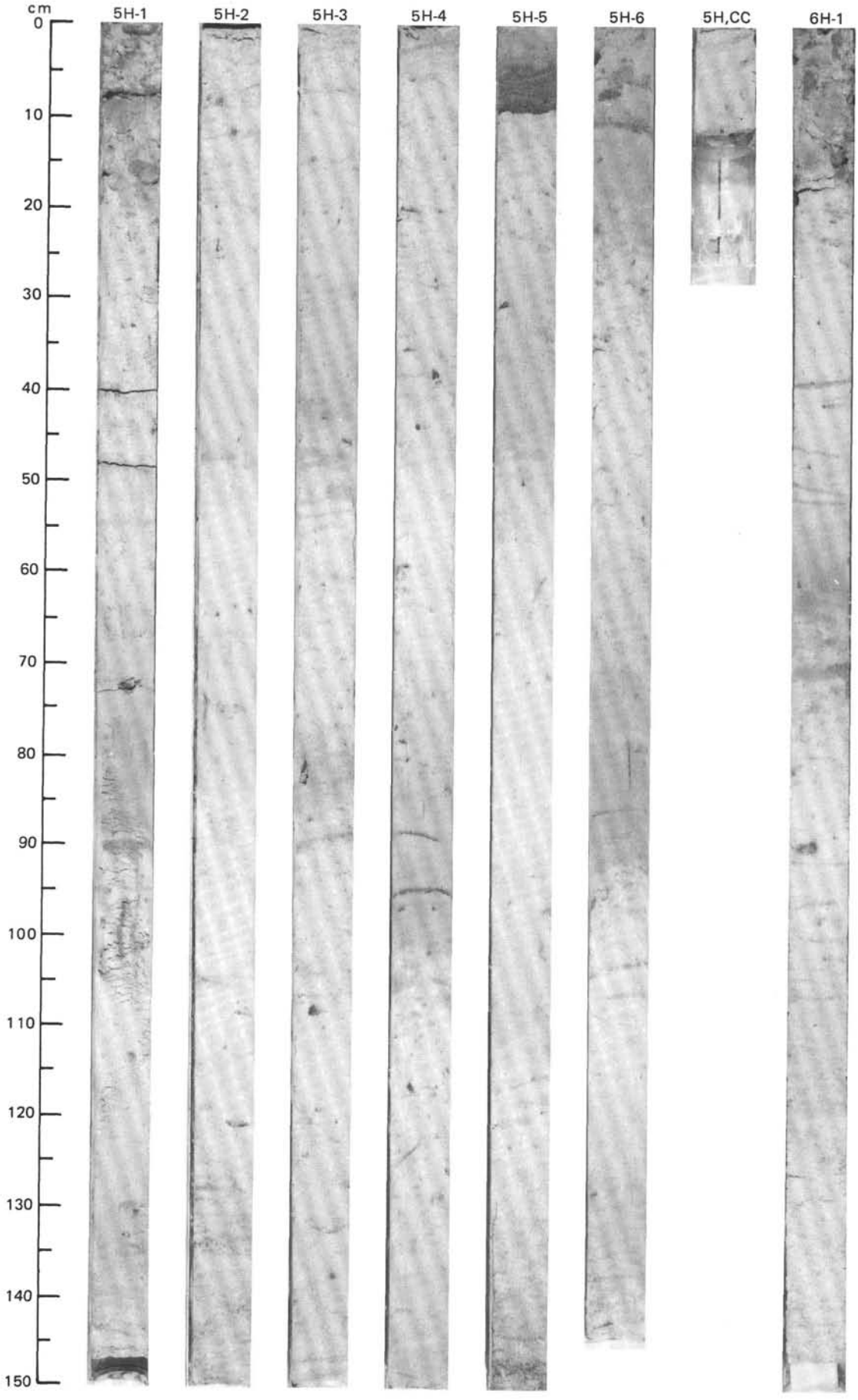
cm
0
10
20
30
40
50
60
70
80
90
100
110
120
130
140
150
5H-1
5H-2
5H-3
5H-4
5H-5
5H-6
5H,CC
6H-1

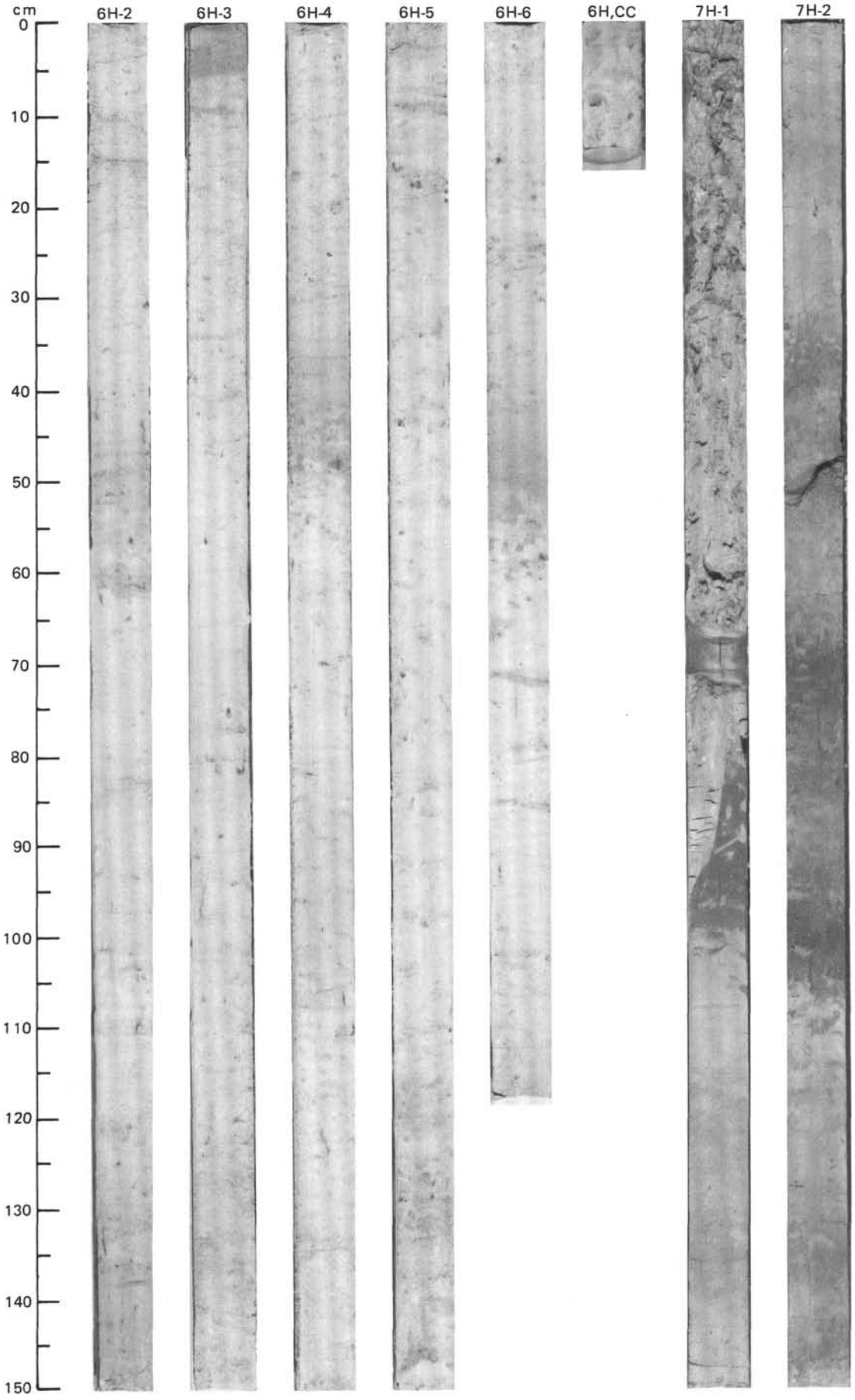
cm
0
10
20
30
40
50
60
70
80
90
100
110
120
130
140
150
6H-2
6H-3
6H-4
6H-5
6H-6
6H,CC
7H-1
7H-2

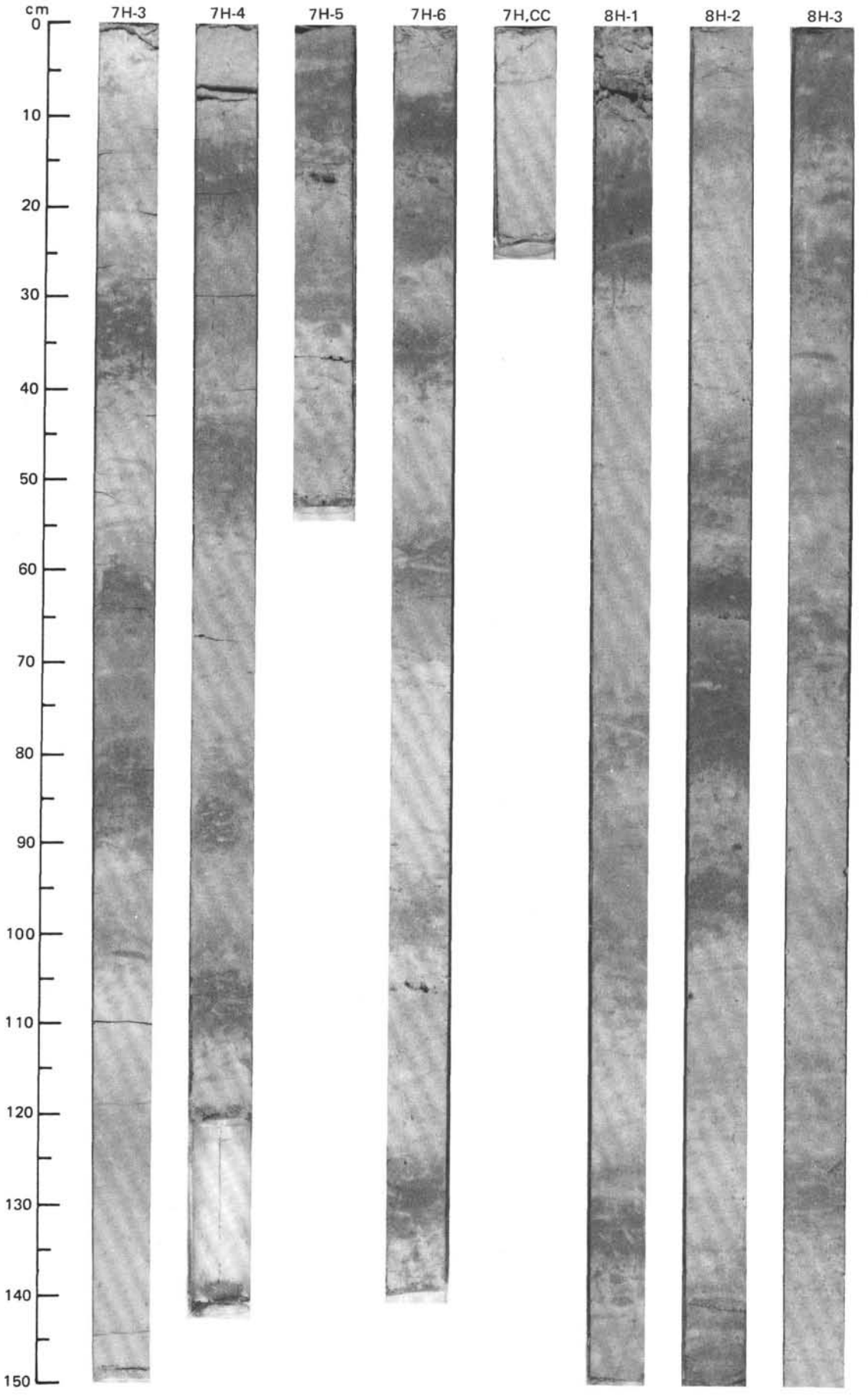
cm
0
10
20
30
40
50
60
70
80
90
100
110
120
130
140
150
7H-3
7H-4
7H-5
7H-6
7H,CC
8H-1
8H-2
8H-3

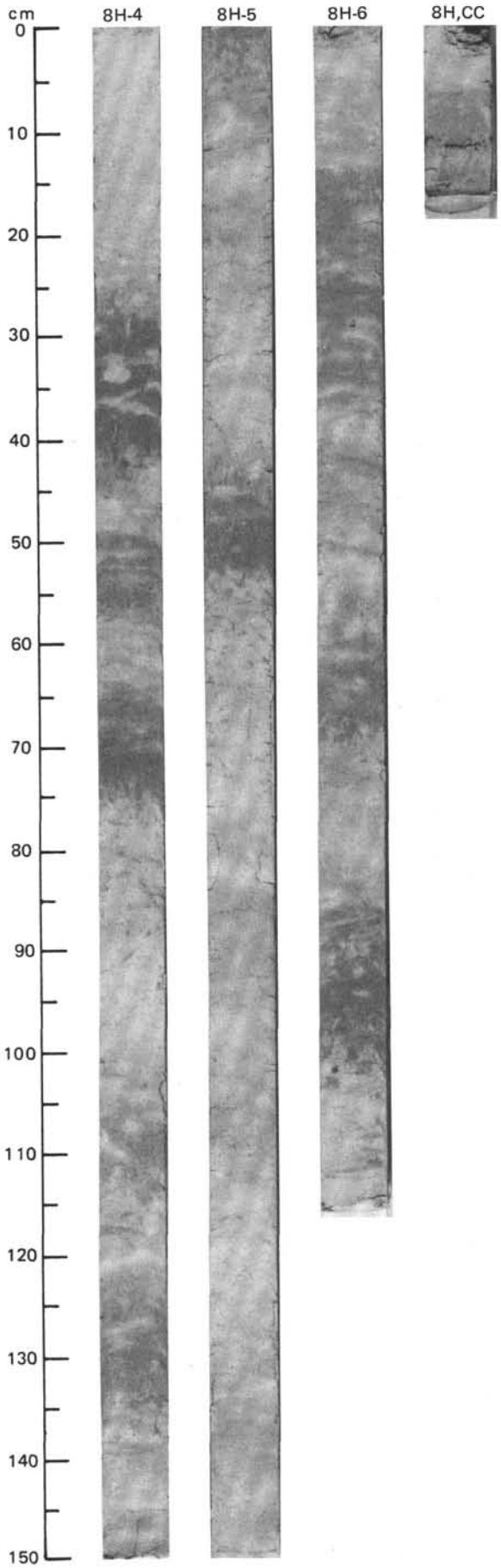
cm
8H-4
8H-5
8H-6
8H,CC
0
10
20
30
40
50
60
70
80
90
100
110
120
130
140
150